The development of biosensors based on functional nucleic acids

Inauguraldisseration

zur

Erlangung des akademischen Grades eines

Doktors der Naturwissenschaften (Dr. rer. nat.)

der

Mathematisch-Naturwissenschaftlichen Fakultät

der

Universität Greifswald

vorgelegt von

Claudia Nübel

geboren am 11. April 1984

in Soest

Greifswald, Juli 2017

Dekan:	Prof. Dr. Werner Weitschies
1. Gutachter:	Prof. Dr. Sabine Müller
2. Gutachter:	Prof. Dr. Ulrich Hahn
Tag der Promotion	08.12.2017

"*How do you find a very small needle in a very large haystack? This proverbial problem is often used in conjunction with accomplishing a nearly impossible feat, and usually with a negative connotation to discourage attempts to such an endeavor*."

From Jijakli et al., The in vitro selection World [1]

Der praktische Teil dieser Arbeit wurde im Zeitraum von August 2011 bis Juli 2016 unter Anleitung von Frau Prof. Dr. Sabine Müller an der Universtität Greifswald durchgeführt. Die QCM-Experimente wurden in den Laboren von Sony Europe Limited, Zweigniederlassung Deutschland, Stuttgart Technology Center, durchgeführt.

Content

Abbreviations 11

1 Introduction 13

2 Investigation of RNA Aptamers for TNFα 17

2.1 Aptamers and Other Affinity Tools 17

2.2 Endonucleolytic Nucleic Acids 20

2.3 Modular Aptazymes 21

2.3.1 RNA Aptamers for a Modular Aptazyme for TNFα 22

2.3.2 Significance of the Results for the Construction of a Modular Aptazyme for TNFα 28

3 Simultaneous *In Vitro* Selection of Aptamer and Catalytic Function 31

3.1 *In Vitro* Selection of Functional Nucleic Acids 31

3.2 The *In Vitro* Selection of an Aptazyme for TNFalpha 33

3.2.1 Design and Synthesis of the DNA Library for TNFα 33

3.2.2 *In Vitro* Selection Strategy 34

3.2.3 The *In Vitro* Selection Process 37

3.2.4 *In Vitro* Selection of an Aptazyme for Creatinine 46

3.3 The Simultaneous *In Vitro* Selection – Discussion 48

4 Combination of *In Vitro* Selection and Rational Design 51

4.1 A New Approach for the Development of a Biosensor 51

4.2 Investigation of the 17E-DNAzyme's Catalytic Activity 60

4.2.1 Cleavage Assays with the 17E-DNAzyme 62

4.2.2 Identification of Cleavage Products of the 17E DNAzyme 66

4.3 Rational Design and Validation of the 17E-DNAzyme Inhibitor 67

4.3.1 Proof of Principle with a Trans-Cleaving System 70

4.4 *In Vitro* Selection with a Supporting Regulatory Unit 73

4.4.1 Step 1: *In Vitro* Selection of the Aptamer Part 73

4.4.2 Binding Assay 82

4.4.3 Step 2: *In Vitro* Selection of the Aptazyme 87

4.4.4 Biacore (SPR) Measurements of the Potential Streptavidin Aptamers 98

4.4.5 Sanger-Sequencing of the Binding Pool 99

4.5 Concluding Discussion of the Combination of *In Vitro* Selection and Rational Design 101

4.5.1 Analysis of the 17E-DNAzyme's Cleavage Activity 101

4.5.2 Rational Design and *In Vitro* Selection 102

5 Summary and Outlook 107

6 Materials and Methods 109

6.1 Buffers and Solutions 109

6.2 Proteins and Reagents, Kits and Accessory 109

6.3 Enzymes 110

6.4 Devices 111

6.5 Software 111

6.6 Basic Methods 112

6.6.1 NanoDrop (UV/Vis-spectroscopy) 112

6.6.2 Ethanol Precipitation 112

6.6.3 Butanol Precipitation 112

6.6.4 Gel filtration/ Size Exclusion Chromatography 113

6.6.5 Purification on Silica Columns 113

6.6.6 Native PAGE 113

6.6.7 Denaturing PAGE 114

6.6.8 Native Agarose Electrophoresis 114

6.6.9 Sample Preparation for Gel Electrophoresis 114

6.6.10 Gel elution A 114

6.6.11 Gel elution B 115

6.6.12 Phenol-Chloroform Extraction 115

6.6.13 Reactions in Thermal Cycler: PCR and Other Enzymatic Reactions 115

6.7 Synthesis of Aptamer Sequences 115

6.8 QCM Experiments 116

6.8.1 QCM Data Evaluation 116

6.9 SPR Measurements of RNA Aptamers 117

  6.9.1 SPR Data Evaluation 117

6.10 ELISA of TNFalpha 118

6.11 Extension Reaction of the Library (section 3.2.1) 118

6.12 General Application of TNFα 118

6.13 Working with Magnetic Beads 118

6.14 Binding of the Library to the Streptavidin Magnetic Beads (3.2.2) 119

6.15 Process of the Initial *in Vitro* Selection Experiment (section 3.2.3) 119

6.16 Emulsion PCR 121

6.17 Synthesis and Deprotection of the DNA-library 121

6.18 ATTO Labelling 122

6.19 Cleavage Reactions with DNAzymes 122

6.20 Alkaline Lysis of DNAzymes or Substrate Strands 122

6.21 MALDI-TOF Analysis of Nucleic Acids 122

6.22 Klenow Reaction 123

6.23 Cleavage Activity of the Library (4.4.1) 123

6.24 Phosphorylation of PD1 123

6.25 λ-Exonuclease Digestion 124

6.26 Process of the *In Vitro* Selection Part 1 (4.4.1) 124

6.27 General PCR Composition and Programs 125

6.28 Electrophoretic Mobility Shift Assay (EMSA) 127

6.29 NaOH Digestion after SRλ 127

6.30 Anion exchange chromatography for Cleavage Assay 127

6.31 Process of the *In Vitro* Selection on Beads Part 2 (4.4.3) 127

6.32 SPR measurements of Streptavidin Aptamers 128

  6.32.1 SPR Data Evaluation 129

6.33 Cloning, Expression, and Sequencing 129

  6.33.1 Overnight Culture 129

  6.33.2 Preparation of Chemically-Competent E. coli TG1 Cells 129

6.33.3 Transformation of Plasmid DNA in Chemically-Competent E. coli TG1 Cells 129

6.33.4 TOPO-TA Cloning 130

6.33.5 Isolation of the Plasmid-DNA 130

6.33.6 Sequencing 130

Table of Figures 131

Table of Tables 135

References 137

Appendix I

Sequences of the Oligonucleotides II

Zusammenfassung und Ausblick V

Danksagung VII

Fold-out: Figure 59 and Figure 60 IX

Fold-out: Figure 62 and Figure 61 X

Lebenslauf XI

Publikationen XII

Abbreviations

ATP	adenosine triphosphate
AU	absorbance units
bp	base pair
BSA	bovine serum albumin
CAGR	compound annual growth rate
CuAAC	CuI catalyzed [3+2] azide-alkyne cycloaddition
cv	column volume
CPG	controlled pore glass
DARPins	designed ankyrin repeat proteins
denat.	denaturing
DMSO	dimethyl sulfoxide
DMT	dimethoxytrityl
DNA	deoxyribonucleic acid
dsDNA	double-stranded DNA
DTT	dithiothreitol
EA-C	enzyme activator catalytic domain
EA-S	enzyme activator substrate domain
EDTA	ethylenediaminetetraacetic acid
EI-C	enzyme inhibitor catalytic domain
EI-S	enzyme inhibitor substrate domain
ELISA	enzyme-linked immunosorbent assay
ELONA	enzyme-linked oligonucleotide assay
ePCR	emulsionPCR
EtBr	ethidium bromide
FDA	US food and drug administration
FMN	flavin mononucleotide
FRET	förster resonance energy transfer
fw	forward
HEPES	4-(2-hydroxyethyl)-1-piperazineethanesulfonic acid
HIV	human immunodeficiency virus
hsDNA	herring sperm DNA
IgG	immunoglobulin G
IP-RP-HPLC	ion pair-reverse phase-high performance liquid chromatography
LB	(gel) loading buffer
LB denat	denaturing gel loading buffer
LB nat	native gel loading buffer
MALDI-TOF	matrix-assisted laser desorption/ionization time-of-flight

(m)Ab	(monoclonal) antibody
MES	2-(N-morpholino)ethane sulfonic acid
mto	multiple turnover
NA	nucleic acid
NC	negative control of PCR reaction, referring to a reaction without template DNA
nt	nucleotides
P	primer
PAA	polyacrylamide
pAbs	polyclonal antibodies
PAGE	polyacrylamide gel electrophoresis
PBS	phosphate buffered saline
PBS	phosphate buffered saline
PCR	polymerase chain reaction
PEG	polyethyleneglycol
QCM	quartz crystal microbalance
rev	reverse
RNA	ribonucleic acid
RNAi	RNA interference
RU	resonance units
SD	standard deviation
SELEX	systematic evolution of ligands by exponential enrichment
siRNA	small interfering RNA
SMB	streptavidin magnetic beads
SPR	surface plasmon resonance
SR	selection round
ssDNA	single-stranded DNA
sto	single turnover
TBDMS	*tert*-butyldimethylsilyl
TEAAc	triethylammonium acetate
TNFa	tumor necrosis factor alpha
TRIS	*tris*(hydroxymethyl)aminomethane
tRNA	transfer RNA
UV/Vis	ultraviolet/visible light
VEGF	vascular endothelial growth factor

1 Introduction

Nucleic acids, such as ribonucleic acid (RNA) and deoxyribonucleic acid (DNA), not only hold the information of life but also have diverse functions, and play crucial roles in regulation and catalysis. Therefore, nucleic acids are much more than the storage of genetic information and its transporter. It was great news when it was found that natural occurring RNA can catalyze self-cleavage.[2, 3] This discovery was ground breaking for the nucleic acid research. For a large part of its functions, nucleic acid does not need another molecule but itself. It is regulating (RNA interference, riboswitches), it is cleaving and ligating itself, it recognizes itself and other molecules.[4-9] Research on nucleic acids has advanced by biologists, chemists, mathematicians, computer scientist, and physicians, and found various applications in the fields of molecular biology, diagnostics, therapy, nanotechnology, and analytics.

It may be assumed that most of the nucleic acid researchers learned the immense potential and variability of this class of organic polymers not earlier than university classes. Nucleic acids in everyday life are still known as for only carrying the information of life. This may be because nucleic acid tools are still not the most straightforward ones. In 2003, Scott Silverman titled his review "Rube Goldberg goes (ribo)nuclear? Molecular switches and sensors made from RNA".[10] This title speaks for itself. However, there is more than an academic reason to work with nucleic acids. The organic polymers can be easily synthesized economically by means of chemical and/or enzymatic synthesis. They are relatively stable and for many applications, reusable. It was discovered that it is possible to artificially reconstruct and create their ability to recognize other molecules, as nature impressively shows with riboswitches and protein-binding nucleic acids. The aptamers, DNA and RNA molecules that specifically recognize and bind other molecules can be developed in the lab. The corresponding process is called Systematic Evolution of Ligands by EXponential enrichment (SELEX). The resulting aptamer-analyte interactions show low constants of dissociation (nanomolar to the picomolar range) and high specificity.[11] Aptamers were developed for instance for molecules like ethanolamine or acetylcholine,[12, 13] large protein complexes like thrombin,[14] or even entire cells.[15, 16]

The scope of this work is in the field of biosensing. This field has developed into a highly active research area. Biosensing is powerful and interesting because assays based on biomolecules are often more specific than conventional analytical assays, and therefore can be applied without sample processing. The most popular biomolecules in this field are antibodies. Aptamers, however, hold several advantages over antibodies such as easiness of its production, production cost, stability, and reusability. Various aptamers (DNA and RNA) and related species were developed for drugs, allergens, heavy metals, antibiotics, proteins, toxins and as recognition elements in sensors.[17-31] However, a recognition element alone does not make a sensor where an output element is needed. For aptamer-based sensors, various output and detection methods were developed. There are optical sensing methods, using fluorescent nucleotide analogs,[32] fluorescence-quencher pairs,[33] polythiophenes,[34], or gold nanoparticles.[35] Furthermore, electrochemical methods,[36-38] or piezoelectric methods were applied.[39, 40] Of special interest are the methods that amplify the detected signal, as it was done by coupling the polymerase chain reaction (PCR) to the detection event and using the horseradish-peroxidase-mimicking DNAzyme for the detection of thrombin.[41-43] In conventional assays, the recognition and the detection must be based on specific chemical or physical characteristics of the analyte to be detected, or the analyte has to be previously specifically labeled. For example, in a reversed phase-high performance liquid chromatography-based assay, the analyte is recognized by its specific retention time, and it has to be UV (ultraviolet) active for optical detection. That means, in the designated sample, the specific lipophilicity and UV activity of the analyte have to be the unique features. However, biosensors can be designed modularly, and different analytes with different or similar characteristics can be detected in parallel using different output signals. This modular assembly moreover, allows for the construction of real multi-detection platforms.[44]

The power of biosensors offers great opportunities for the biomarker development and the clinical diagnostic. Fast, specific and reliable readout of potential biomarkers is strongly simplifying their discovery and improves the diagnostics, therefore enabling for more immediate and targeted medical treatment of the patient. An interesting group of analytes is, for instance, the cytokines. Cytokines, a large group of proteins, are part of the innate immune system and they play an important role in inflammatory reactions.[45] Their concentration in tissues and body fluids is an indicator for the inflammation status of an organism. Therefore, they are of special interest in drug development and clinical diagnostics.[46] Another interesting group of molecules for physicians are the metabolites. The concentration of various metabolites in urine indicates the condition of the kidney. Acute kidney injury is an important cause of morbidity and mortality after surgeries. It is supposed that the treatment could be improved by faster analysis of important biomarkers, like creatinine.[47]

The need for biosensing was the motivation of this work and it was aimed to develop a biosensor based on functional nucleic acids. For specific recognition of the analyte, an aptamer was used. Furthermore, the ability of nucleic acids to perform multiple turnover cleavage reactions was exploited to enhance the signal of recognition and to lower the detection limit. In a preceding work, a modular RNA system for the detection of tumor necrosis factor alpha (TNFa) was tested which turned out to be not functional. In order to find and to understand the reason for failure, the RNA system was investigated more closely in the present work. For different reasons, afterward, it was decided to continue the work with a DNAzyme and it was not followed the strictly modular approach. The work with TNFα and creatinine as model analytes revealed that with the approach of choice, no general method was going to be developed. This was the reason, to develop a new and different method with streptavidin as a model analyte. This work presents valuable results for the development of biosensors based on nucleic acids, applying *in vitro* selection and rational design.

2 Investigation of RNA Aptamers for TNFα

2.1 Aptamers and Other Affinity Tools

Aptamers are nucleic acids that are capable of specifically binding to other molecules. Ellington and Szostak defined the term *aptamer* in 1990.[48] They selected ligands for different organic dyes from a pool of randomized RNA (N = 100). In parallel, Tuerk and Gold did a similar experiment and developed RNA aptamers toward bacterial T4 DNA Polymerase. They titled the procedure SELEX – Systematic evolution of ligands by exponential enrichment.[49] However, they did not work with a long randomized domain but varied only eight nucleotides in the RNA-loop binding to the protein. Four selection rounds resulted in two predominant sequences, one of them was the wild-type sequence, and the other varied in four nucleotides. This experiment demonstrates the advantage of *in vitro* selection over site-directed mutagenesis. A similar result would have been reached using this strategy, but with a considerable higher effort. In theory, 4^8 single mutants had to be individually synthesized to generate the same pool as in the SELEX-experiment. Until now, a large number of aptamers were developed. Small molecules like ethanolamine or acetylcholine,[12, 13], large protein complexes,[14] or cells[15, 16] served as targets for SELEX (Figure 1).

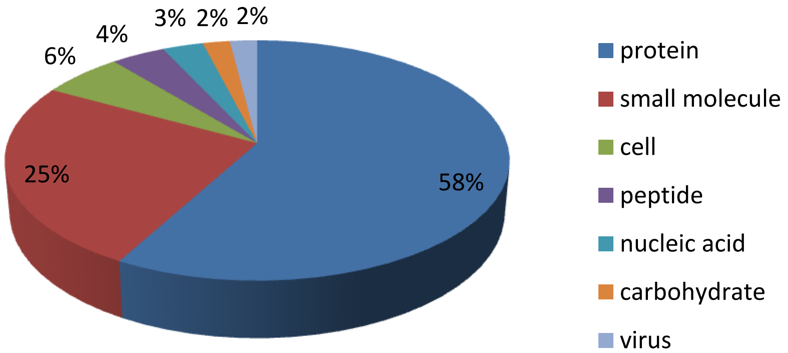

Figure 1. The proportion of aptamers by their target that were selected for binding to different targets by SELEX from 1997 to 2013. 569 targets in 492 SELEX experiments. [50]

There are many examples in nature that nucleic acids can bind to other molecules: DNA-binding proteins, cytokines, growth factors, DNA polymerases, transcription factors, and riboswitches. Intramolecular structures like hairpin loops, bulges, loops of G-quadruplexes, and pseudo-knots support the binding to the ligand.[51] The average surface area of the contact domain of an aptamer is about 300-400 Å^2 (roughly the same as the antigen recognition area of antibodies).[51, 52] The binding is often companied by induced fit and therefore, aptamers may be used as molecular beacons for detection of the binding event.[53-55] Such structural changes are exploited for electrochemical detection.[25] Vice versa, these detection methods can be used to investigate the structural changes. The characteristics of aptamers further enable their use as small, reusable sensors and for affinity purification of proteins without a tag. They were applied for the separation of chiral compounds and proteins for therapeutic use.[56, 57] A prominent example for aptamers in use is the drug Pegaptanib (PEGylated aptamer inhibitor).[58] Furthermore, aptamers can be used for targeted drug delivery. For example, a siRNA-aptamer chimera was designed to bind to a receptor on the target cell. Then, the uptake of the drug happens by endocytosis via a specific aptamer receptor interaction. The drug is then released from the endosome to enter the RNAi pathway, which leads to the silencing of target genes.[59-61]

Aptamers are not the only available affinity tools. There are antibodies, inorganic matrices, and DARPins. The undeniably best-known affinity tools are the antibodies and it has to be admitted that 25 years of research on aptamers did not enhance the capabilities of aptamers to remarkably overtake antibodies. Antibodies are the most used tools in diagnostics (ELISA, Western-Blot), purification, and therapeutics. The pregnancy test that is on the market for about 40 years is based on monoclonal antibodies (mAbs). It detects the hCG (human chorionic gonadotropin). In 2004, the first rapid test for HIV in oral fluids was approved by the FDA.[62] Furthermore, there are few examples of antibodies as therapeutics; about 30 mAbs are FDA approved.[63] PFIZER marketed the above mentioned Pegaptanib as Macugen® in Germany, but they took it from the market because of its lower potency compared to other drugs; e.g. Ranibizumab (Lucentis®, Genentech), which is a monoclonal antibody fragment.[64] mAbs are prepared by immunization of animals or by a screening of recombinant, synthetic libraries as reviewed in Hoogenboom 2005.[65] Production of antibodies often involves high cost (high molecular mass, disulfide bonds, glycosylation). Their production in simple microbial hosts is not possible. Instead, human cell lines are needed, which makes the cultivation complex and cost-intensive. In contrast, other affinity tools can be produced without the use of higher living organisms. For instance, the inorganic matrices that were forgotten for a large period: The method of production was originally published in 1949. Therein, a polymer is built in the presence of a target molecule that is afterward extracted.[66, 67] Also without the need to use living organisms for their production, but located in the biological field, the polypeptides (monobodies) represent another affinity tool. They are developed by the molecular display.[68, 69] Another prominent tool are the DARPins (Designed Ankyrin Repeat Proteins).[70, 71] DARPins and monobodies share a structural feature with mABs: the well-conserved rigid scaffold at which variable domains are positioned. This stiffness is discussed to be an advantage over nucleic acid affinity tools. Nucleic acids are much more flexible, and therefore more entropy is lost by binding in comparison to ligand binding to protein affinity tools. However, this point of discussion can be as well considered from the other side, and for the same reason, it is supposed that RNA might be the better affinity tool than DNA. RNA has a more flexible structure compared to DNA; therefore it should have a broader range of potential target molecules. This circumstance does not implicate less specificity. It has to be understood in the manner that minimal sequence changes in RNA might let to remarkable changes in secondary structure. The inherent disadvantage of RNA is its instability towards the omnipresent RNases, but this problem is overcome by modifications. Overall, nucleic acid affinity tools are more stable toward harsh temperature, pH and salt conditions than antibodies and peptides. They are reusable, and their immobilization on surfaces is easy. Furthermore, an assay that is comparable to ELISA (enzyme-linked immunosorbent assay) was developed: The ELONA (enzyme-linked oligonucleotide assay).[72] Another advantage of nucleic acid tools is the capability for multiplex detection. Multiplexing in antibody-based methods is difficult because of cross-reactivity of secondary antibodies, which are required for enhanced sensitivity. A sophisticated method for a multiplex proteomic approach was worked out for aptamers. In this assay, the aptamers are biotinylated by a photocleavable linker. After specific binding of the individual aptamers to proteins in a mixture, the aptamer-protein complexes bind to streptavidin magnetic beads, and unbound protein is washed out. In the next step, the proteins are biotinylated, and the photocleavable bond is cleaved. The biotinylated proteins are captured with streptavidin coated beads. The aptamers are eluted and used for hybridization on a microarray, this way giving proteomic information.[44] Finally, it should be mentioned that the patent situation for aptamers is clearer than for antibodies.[73] In 1999 GILEAD SCIENCE INC. acquired many patents related to general aptamer-selection strategies and of many individual aptamers. Now, ARCHEMIX holds the only license to use the aptamers for therapeutic applications and SOMAMERS for diagnostic applications.[63, 74, 75] However, the control of aptamer intellectual property by two major players often is a hurdle for academic and commercial organizations.

To sum up, antibodies are the market leader. Their application is established, and they are well understood. The other three mentioned affinity tools hold great potential; however, more research has to be done to improve their potential. It is imaginable that the rediscovered inorganic matrices will play a role in material sciences. Affinity tools made *in vitro* out of oligopeptides or oligonucleotides have a broad application range. Its great advantage is that they are prepared *in vitro* and that every thinkable function is possible to select, even if in some cases just in theory until now. One the other hand, antibodies are mainly made by nature and being as good as nature indeed is difficult, it requires a huge research effort.

2.2 Endonucleolytic Nucleic Acids

The present work deals with endonucleolytic RNA and DNA that can cleave a single ribonucleotide bond. These species are used for various purposes in diverse variants in laboratories dealing with functional nucleic acids. They can be a tool to cut RNA specifically in different applications and can be used in SELEX experiments. Their mechanism was studied extensively and is well understood. The cleavage (Figure 2) of RNA basically happens uncatalyzed. The 2'-OH group can attack the phosphate in the phosphodiester linkage and break this linkage by the formation of a cyclic phosphate. The rate constant for this transesterification reaction is $\approx 10^{-8}$ min^{-1} (pH 7.0, 250 mM K^+, 5 mM Mg^{2+}, 23 °C).[76] The enzymatic catalysis of the transesterification by ribonuclease A has a maximum rate constant of $\approx 8 \times 10^4$ min^{-1}.[76, 77] The small hydrolytic ribozymes' rate enhancement is not higher than $\approx 10^9$-fold (rate constant ≈ 10 min^{-1}). This variance in catalytic efficiency is reasoned by the different use and combination of catalytic strategies. There are four possible strategies to promote the transesterification reaction (Figure 2): the in-line nucleophilic attack (α catalysis),[78] neutralization of the negative charge of a nonbridging phosphate oxygen (β catalysis),[79] deprotonation of the 2'-hydroxyl group (γ catalysis),[76] and neutralization of negative charge on the 5'-oxygen atom (δ catalysis),[79].[80] That means ribozymes put the bond to be cleaved in a structural surrounding stabilizing the transition state and provide groups that support acid-base catalysis. These catalytically essential groups can be nucleobases or dehydrated water from the water shell of cations.[81-90]

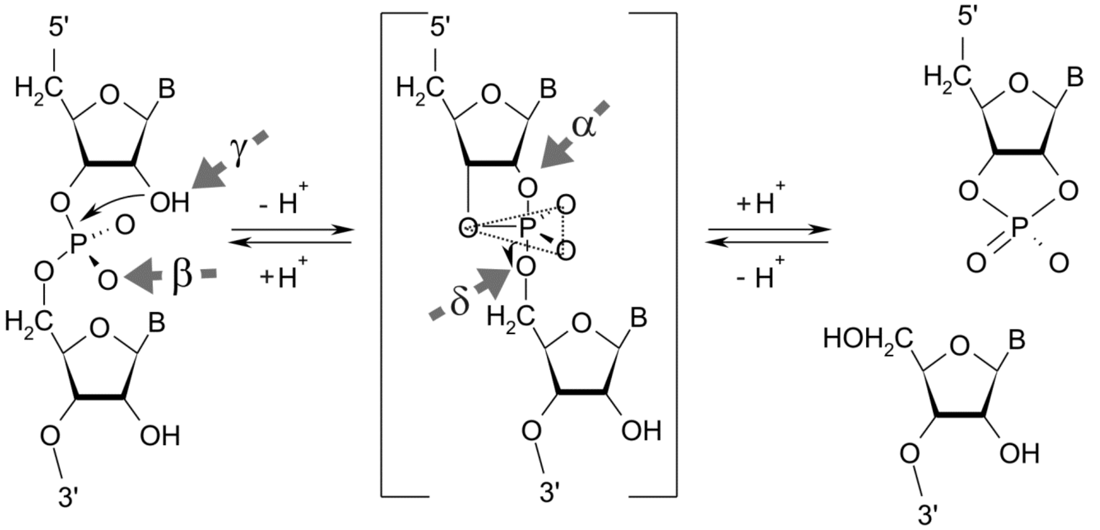

Figure 2. Mechanism of hydrolytic cleavage of a phosphodiester bond in RNA. α, β, γ, δ indicate the working points for the four different catalytic strategies.

The mechanism of transesterification of the RNA-cleaving DNAzymes is at least similar to that of the ribozymes. Like the ribozymes they bind their substrate strand by base-pairing and cleave it at a designated site. The substrate is either an all-RNA strand or a DNA-RNA hybride. However, at the site of the cleavage, a ribonucleotide must be present.[91, 92] Indeed there are DNA-cleaving DNAzymes, but these species use a different mechanism.[93, 94]

2.3 Modular Aptazymes

The word aptazyme is a combination of the words aptamer and enzyme: aptazymes are nucleic acids combining catalytic activity and aptamer function (Figure 3).

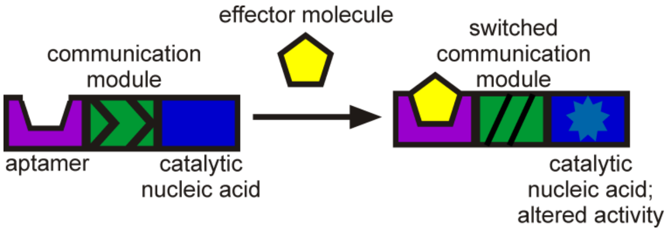
effector molecule
communication module
aptamer
catalytic nucleic acid
switched communication module
catalytic nucleic acid; altered activity

Figure 3. Schematic illustration of an aptazyme.

Similar to allosteric enzymes, these catalysts are able to respond to the binding of an effector molecule with altered activity. The mediation of the binding information can happen in different ways. A very direct way is to exploit base pairing to capture or to release sequences that are essential for catalytic activity, as presented in the first work referring to an aptazyme in 1995. The researchers extended the hammerhead ribozyme with an inhibitor strand. The effector molecule was an oligonucleotide, which was complementary to the inhibitor strand, and therefore was able to regulate the hammerhead ribozyme's activity allosterically.[95] However, the era of the really modular switches started two years later with the ATP-sensitive hammerhead ribozyme.[96] An aptamer was linked by a small four-base pair stem to the hammerhead ribozyme and the construct was catalytically active in the absence of ATP. In the presence of ATP, the catalytic rate was reduced by 180-fold, but no effect on activity was observed in the presence of dATP or adenosine. Figure 3 illustrates the general assembly of a modular aptazyme. Further studies with the FMN, flavin, doxycyclin, and theophylline aptamers as well resulted in switchable modular aptazymes.[29, 97, 98] It was even possible to combine a ribozyme with two aptamers (theophylline and FMN), to be only active in presence of the both effector molecules. The rate enhancement of the ribozyme in the presence of both molecules is 300-fold relative to the basic activity (dynamic range).[99] It is supposed, that the binding information is mediated by a slipping of the small stem structures linking the various aptamers to the hammerhead ribozymes.[100, 101] These findings were the basis for the later emerging computationally design of functional communication modules.[102, 103]

2.3.1 RNA Aptamers for a Modular Aptazyme for TNFα

Based on known RNA aptamers toward TNFα, four modular aptazymes were designed.[104, 105] (Figure 4 A, B, C) Each potential aptazyme consists of the hammerhead ribozyme,[106] a communication module,[101] and an aptamer sequence.

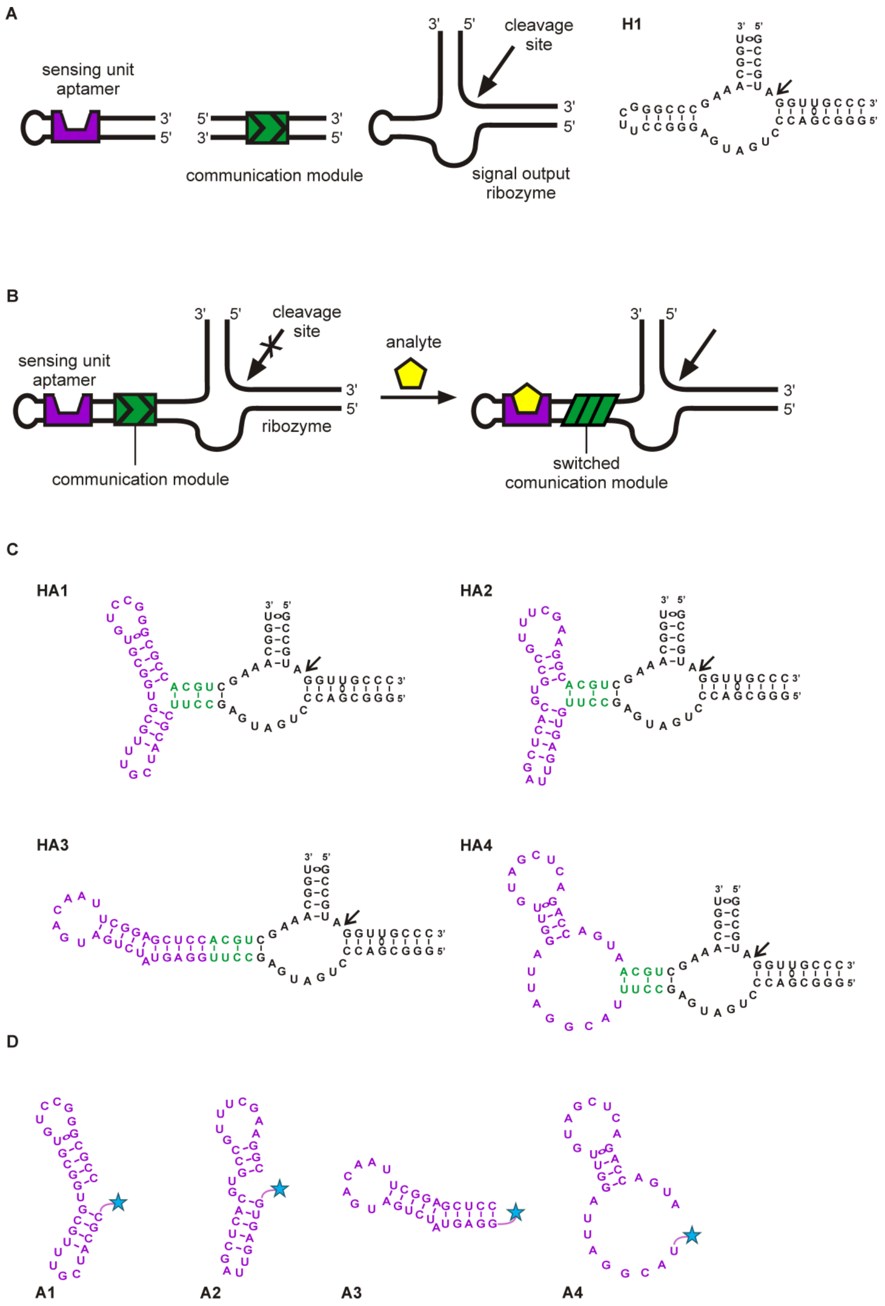
A
sensing unit
aptamer
3'
5'
5'
3'
3'
5'
communication module
3'
5'
cleavage
site
3'
5'
signal output
ribozyme
H1
B
sensing unit
aptamer
communication module
3'
5'
cleavage
site
3'
5'
ribozyme
analyte
3'
5'
3'
5'
switched
comunication module
C
HA1
HA2
HA3
HA4
D
A1
A2
A3
A4

Figure 4. The individual parts of a modular, allosteric ribozyme. A) Schematic illustration of the allosteric ribozyme. Additionally, the secondary structure and sequence of the reference ribozyme used in this work are shown.

The arrows indicate the cleavage sites. B) Modular assembly of the individual parts results in an aptazyme. Its cleavage activity is regulated by an analyte. The binding event of the analyte to the sensing unit (aptamer) causes a switch of secondary structure in the communication module, which in turn, stabilizes the ribozyme active structure. C) The sequences of the aptazymes HA1 to HA4. Black: ribozyme part; green: communication module; violet: aptamer domain. The secondary structure was modeled separately for ribozyme part and aptamer domain with RNA structure 4.5. Software. D) Aptamers A1 to A4. The asterisk located at the 5'-end symbolizes biotin or thiol modification, respectively. With permission of Springer from reference [107].

The aptazymes that are shown Figure 4 were designed in a previous work (diploma thesis) in cooperation with an industrial partner, who aimed for a biosensor for TNFα.[105] Unfortunately, none of the constructs significantly responded to the cytokine. Possibly, the modular assembly wasn't suitable. But on the other hand, the aptamers weren't well characterized. Therefore, the first goal of the present work was to investigate them more closely.

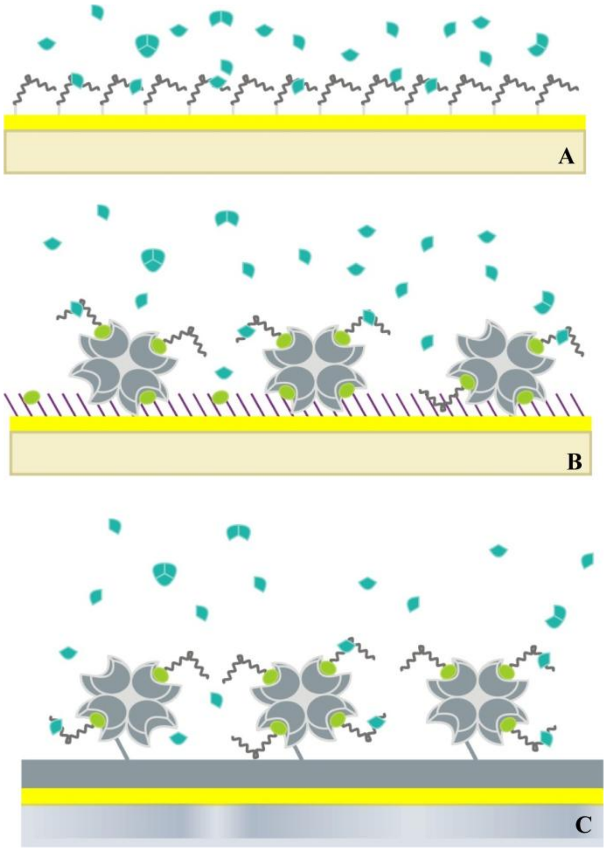

Figure 5. Scheme of systems used for the measurement of the interaction of aptamers and TNFα. The cytokine is shown in all possible quaternary structures, as mono-, di-, and trimer. It is assumed that it binds monomeric TNFα. A) RNA is immobilized by a C12-thiol linker on a gold-coated quartz crystal. B) Biotinylated RNA binds to streptavidin, which is immobilized on a biotin/PEG-modified gold-coated quartz crystal. C) A typical Biacore chip, consisting of a gold coated glass support, covered with a carboxy methyl dextran layer carrying activated carboxyl groups for streptavidin immobilization and subsequently capturing biotinylated RNA. With permission of Springer from [107].

Initially, only A1, A3, and A4 were chosen to be analyzed. The aptazyme with A2 showed hardly any cleavage acticity in the previously performed cleavage assays.[105] Using the BIACORE instrument that is based on surface plasmon resonance (SPR) technology, the binding characteristics of the aptamers toward TNFα were investigated. For this purpose, the aptamers A1, A3, and A4 were modified with a biotin moiety allowing their immobilization on a streptavidin coated gold chip (BIACORE, Figure 4 D; Figure 5 C). The three aptamers were immobilized in three of the four cells of the chip, the fourth cell served as reference. The results of this experiment can be seen in Figure 6. During a flow of freshly suspended TNFα, an increase in the resonance was recorded for all aptamers (Figure 6A). The resonance units decreased again during buffer flow. A control experiment with BSA was negative. As it can be taken from Figure 6A, the aptamer A3 exhibits the highest affinity toward TNFα, followed by aptamers A1 and than A4 with the lowest affinity. The plot in this figure also demonstrates that the change in resonance units during the association and dissociation differs from a typical sensorgram, which is described by a hyperbolic increase of resonance units during analyte flow and a hyperbolic decrease when this flow is stopped. However, the increase in resonance units during binding of TNFα was more sigmoidal than hyperbolic, which can be seen in Figure 6. Furthermore, there was a sharp decline in resonance units immediately after stopping the analyte flow. Both observations were less pronounced with decreasing protein concentration, as shown in Figure 6 B for the aptamer A3. The regeneration of the aptamer-modified surface was successful with 2 M NaCl. Thus, it is assumed that the interaction of RNA and protein in majority relies on ionic interactions.

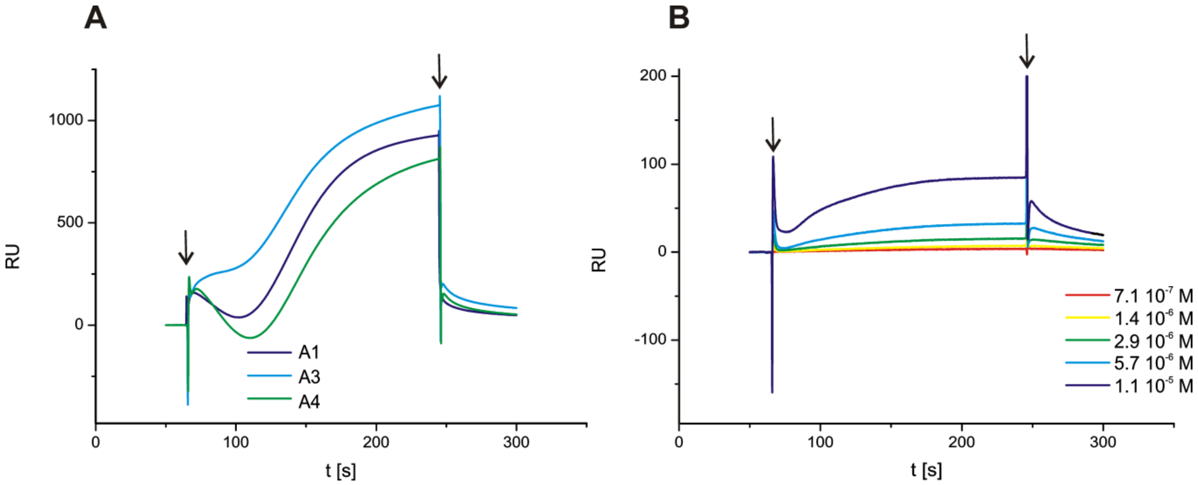

Figure 6. Sensorgram of SPR experiments with TNFalpha. A) Measurements with aptamers A1, A3, and A4 at high concentration of TNFα (2.3 · 10-5 M). The arrows indicate start or stop of the analyte flow, respectively. Curve shape demonstrates the disaggregation of the homotrimer after stopping the analyte flow. B) Sensorgram of SPR experiments with aptamer A3 at different lower concentrations of TNFα. With permission of Springer modified from reference [107].

The quaternary structure of TNFα in solution is driven by its concentration. At high concentration, a homotrimeric form is favored (90 % trimers at 10^{-5} M), and at low concentration, the protein is present in its monomeric form (10 % trimers at 10^{-10} M) [108-111]. Therefore, a possible explanation for the sharp decline of resonance units beginning with the flow of buffer is that homotrimers, which were bound to the aptamers, dissociated very fast. The following hyperbolic decrease of the curve can be caused by the slow dissociation of the monomer unit of the aptamer.

By manual data extraction of the hyperbolic curves at lower concentrations of TNFα, dissociation constants were calculated for A1 and A3 aptamers as 2.92 ± 1.69 µM and 12.79 ± 5.37 µM respectively. However, it wasn't possible to analyze the entire data using the software of the Biacore instrument possibly due to complex homotrimeric to monomeric equilibrium of TNFα. Therefore another method, namely quartz crystal microbalance, was employed for the further investigation of the aptamers. For measurements with a quartz crystal microbalance, the biotinylated aptamers were immobilized on streptavidin coated quartz crystals (Figure 5 B). Similar to the experiment with the Biacore instrument, in the Q-sense device, the measurement was carried out in a flow cell.

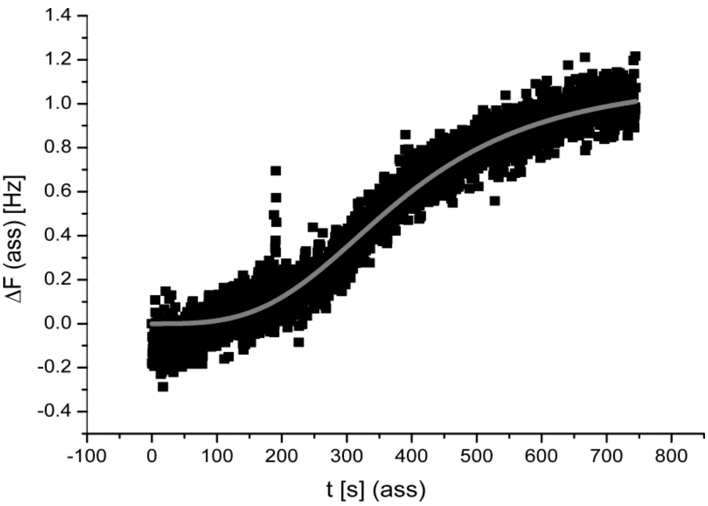

Figure 7. The absolute value of the frequency shift due to binding of TNFα to biotin-labeled aptamer 4 that was immobilized onto a streptavidin coated quartz crystal. The curve shape of a standard association curve is hyperbolic. Sigmoidal curves indicate a cooperative binding mode. Black squares: data points; gray line: Fit to the Hill-equation ($\Delta F = F_{max}\frac{t^n}{t^n+k^n}$; $k^n = {F_{max}}/{2}$). With permission of Springer from reference [107].

A sigmoidal association curve was observed in the QCM measurements (Figure 7). A positive cooperative binding mode results in sigmoidal association curves. A positive cooperative binding is described in the literature for streptavidin.[112-115] This binding mode, which is caused by a ligand-induced reduction in motion of the streptavidin protein, causes the extremely strong binding to biotin (K_D = $10^{-13,4}$ M). Moreover, the cooperativeness is supposed to be transmitted to the next binding partner.[114] This aspect goes together with the interpretation that in SPR measurements, the aptamer was bound to the homotrimeric form of TNFα at high protein concentrations and to the monomeric protein at lower concentrations. It was concluded that the immobilizing strategy distorted the results. Finally, it was necessary to choose a different immobilization method. Therefore, a protein-free immobilization method based on thiol-gold interaction was used as the next step. Aptamers A4 and A3 (high and low-affinity candidates), were synthesized with a thiol moiety and immobilized directly on gold coated quartz crystals (Figure 5). This time, TNFα was applied at low concentrations, to ensure monomer binding. However, no binding was observed with the aptamer A4 immobilized on the quartz crystal. In the case of the aptamer A3, a dissociation constant of about 200 nM could be determined. Yan and colleagues,[104] who selected the aptamers, used thawed TNFα, stored at -18 °C in PBS for their studies. In the present study, freshly suspended protein was always applied. Actually, using a thawed solution of TNFα in QCM measurements with the thiol-gold immobilized RNAs, the affinity towards the aptamers was increased. A4, which didn't bind to the freshly suspended protein, exhibits a dissociation constant of 50 nM towards thawed TNFα and the dissociation constant of the aptamer A3 was lowered to 40 nM.

QCM and SPR are both suitable methods to determine dissociation constants. However, due to their different measurement principles, the results have to be interpreted differently. Using the BIACORE, changes in the refractive index at the surface are recorded. The quartz crystal microbalance is more sensitive to changes in the surface structure where bound water also plays a role and will effect on the mass that is detected.[116, 117] Even more information can be obtained from the energy dissipation that is recorded by the Q-SENSE device used in this study. Rigid surfaces show lower energy dissipation than soft surfaces.[117-119] Therefore, the quotient of the maximum shift in energy dissipation and the maximum frequency shift $\Delta D_{max}/\Delta F_{max}$ is lower for more rigid surfaces.[119] Information about the rigidity of the surface can also be taken from the resonance overtones, n = 3,5,7,... Higher overtones have lower penetration depths, but by normalizing them, the frequency shift is equal to all frequencies in case of rigid surfaces.[118] Figure 8 A and B show the binding event of biotinylated RNA to the streptavidin coated quartz crystal (A) or that of thiolated RNA to the gold coated one (B), respectively. It is obvious that the binding modes and the resulting surfaces are totally different. The overall frequency shift due to binding of RNA is higher for the streptavidin coated crystal. Most probably, this was caused to a large extent by the application of a higher concentrated RNA solution and the more efficient immobilization strategy (biotin-streptavidin). More remarkably, and more importantly, the binding dynamics are different. In case of the streptavidin coated quartz, the RNA was bound very fast and the resonance frequency reached a constant value nearly immediately. When the thiolated RNA was bound to the gold surface, after an initial relatively strong frequency shift, which was similar for all overtones, the frequency shifted slightly in the opposite direction, then back again to become constant after a few minutes. Moreover, the overtones drifted away from each other. The energy dissipation for the different overtones behaved similarly and the change is up to two-fold higher compared to the streptavidin-coated surface.

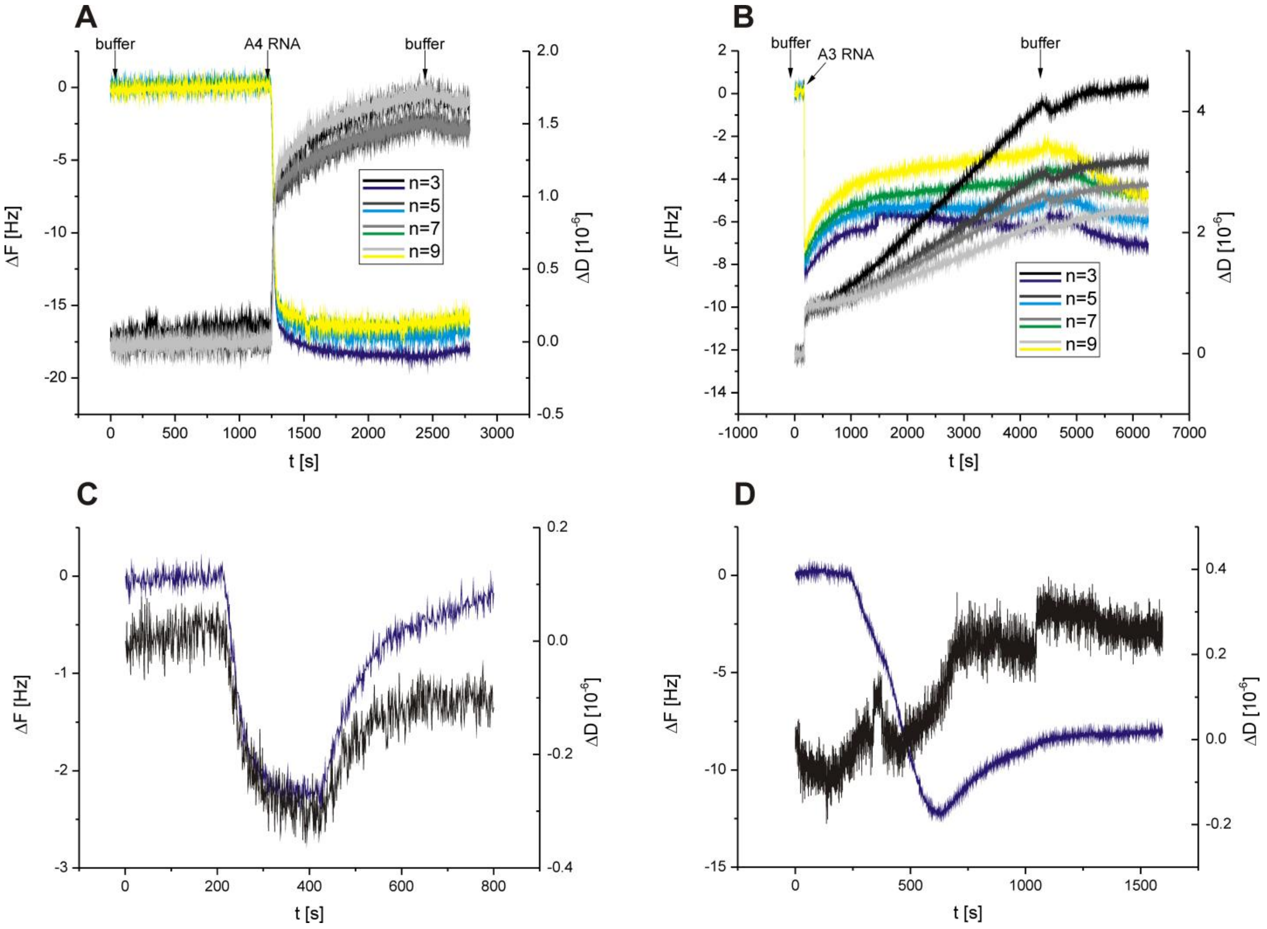

Figure 8. Various plots of frequency changes and energy dissipation during binding events on quartz crystals. A) The plot of frequency changes (colored curves) and energy dissipation (gray curves) during adsorption of biotinylated RNA to the streptavidin modified surface of the quartz crystal. B) An exemplary plot of changes of frequency (colored curves) and dissipation (gray curves) during adsorption of thiolated RNA to the gold-coated quartz crystal. C) An exemplary plot of frequency shift (purple curve) and dissipation (black curve) of the binding and dissociation process of TNFα to aptamer 3 (immobilized by a thiol moiety on a gold-coated quartz crystal). D) The plot of frequency shift (purple curve) and dissipation (black curve) of the binding and dissociation process of TNFα to aptamer 4 (immobilized by biotin on a streptavidin coated quartz crystal). With permission of Springer modified from reference [107].

Furthermore, in the diagram in Figure 8 B, a negative frequency shift was observed during buffer flow before stabilization. This suggests that additional water was bound to the RNA layer during buffer flow. For the layer formed by biotin-streptavidin immobilization of the RNA it resulted $\Delta D_{max}/\Delta F_{max} = 0.62$, for the one based on thiol-gold interaction it was $\Delta D_{max}/\Delta F_{max} = 0.09$. In sum, the results suggest that the RNA layer on the gold-coated quartz crystal is more disordered. It became more ordered and rigid during binding of freshly suspended TNFα (Figure 8 C) and returns to the initial state after the protein had dissociated. If thawed TNFα was applied, no shift in energy dissipation was observed. For the binding of freshly suspended protein, this behavior of the surface can be interpreted as the folding of the aptamers into an appropriate conformation to bind the protein, which caused a more ordered and thus more rigid surface. For thawed TNFα, it is probably bound to all aptamers present in random conformation. For the streptavidin-biotin immobilized aptamers that bound to the relatively high mass of the freshly suspended trimeric protein, the shift of energy dissipation was small as well, but positive (Figure 8 D). The energy dissipation remained positive also during dissociation. These considerations underline the assumptions made above concerning both, the affinity of the aptamers towards TNFα and the method of immobilization.

The previous experiments suggest that the low binding affinity of the aptamers toward TNFα might be caused by the quality or the quaternary structure of the protein. As a control, an ELISA was carried out; applying either freshly suspended TNFα or a PBS buffered solution of the protein (1 $\mu g \cdot ml^{-1}$), which was stored at -20 °C or 4 °C for one month, respectively. The ELISA was very sensitive to TNFα, the limit of detection (LOD) for the freshly suspended protein was 4.55 $pg \cdot ml^{-1}$. The LOD increased two-fold if frozen protein solution was applied (10.35 $pg \cdot ml^{-1}$), and increased to 75.27 $pg \cdot ml^{-1}$ for the protein solution stored at 4 °C. This result indicated for a structural change of the protein due to storage in solution.

2.3.2 Significance of the Results for the Construction of a Modular Aptazyme for TNFα

As mentioned previously, the quaternary structure of TNFα depends on its concentration where the physiological concentration of TNFα is in the picomolar range. At this concentration a considerable fraction of TNFα is in its monomeric form. The monomeric form is physiologically inactive, but, the receptor molecules force the protein into its trimeric and thus, biologically active structure. It is known that monomers of TNFα clump to high molecular mass aggregates *in vitro*. The aggregation process depends on temperature and time and is irreversible.[108-111]

The most obvious consequence of this information is that the investigated aptamers would only be useful for a biosensor applied in medicinal diagnostics if the amplification of the binding signal reached by the catalytic activity of aptazyme would be at least 1000-fold.[107] Second, it explains, why the aptamers in the work of Yan et al. who selected them, were able to inhibit TNFα-mediated cytotoxicity in L929 cells.[104] In their experimental design, they applied either TNFα or TNFα mixed with aptamers to the cells. They observed an inhibited cytotoxicity that was specific for the aptamers. It is highly probable that the protein was possibly slightly damaged, for example, clumped in aggregates, and its cytotoxicity wasn't present to its full extent which would not have an effect on the result in this experimental design. The aptamers were selected to have an affinity towards the thawed structure of TNFα and therefore were able to reduce the concentration of free monomers which are recruited by the TNFα-receptors.

In the cleavage assays with the rationally designed aptazymes (Figure 4), the concentration of TNFα varied from 100 to 5000 nM in the presence of 100 nM of the aptazyme. This means that at least the aptazyme built of aptamer A3, which showed a dissociation constant of ~200 nM in the QCM measurement, could have been able to bind the protein in the cleavage assay. However, no significant alteration of the aptazyme's cleavage activity could be proven by the addition of the protein. In sum, both, the design of the aptazyme and the aptamers itself, were proven to be not suitable to present a reliable biosensor for TNFα.

Therefore, as a different strategy to tackle the task, the method of *in vitro* selection was chosen.

3 Simultaneous *In Vitro* Selection of Aptamer and Catalytic Function

3.1 *In Vitro* Selection of Functional Nucleic Acids

In vitro selection enables the direct evolution of molecules like nucleic acids or peptides. In the preceding chapter, the concept of SELEX was already introduced. Originally, this term was strictly related to the process of aptamer selection. But the possibility to select affinity tools from a pool of nucleic acid inspired the research community for the selection of catalytic activity. Thus, the same principle is used for the *in vitro* selection of every desired function: ligands, catalytic activity or aptazymes that combine both functions. The process is unnatural and differs from natural evolution. A pool of molecules, which sequences are randomized, is exposed to conditions that allow selecting molecules with the desired function. Functional molecules are collected and amplified. Then, they again are exposed to the selection conditions for another round. This way, several rounds of selection are carried out in succession (Figure 9). The selection pressure (time, temperature, concentrations etc.) is successively elevated in each round. This way, after several rounds of selection, an enriched pool is obtained from the initial pool which is composed of only a few sequence families. *In vitro* selection may be carried out with natural or unnatural building blocks. In the case of nucleic acids, this means that the library can be composed of the four canonical nucleosides or modified nucleosides, e.g. carrying a 2'-fluoro group or base modifications or locked nucleic acids (LNA).[44, 120] Modifications are not only to increase stability but to expand the space of potential binding partners by increased variability and function.

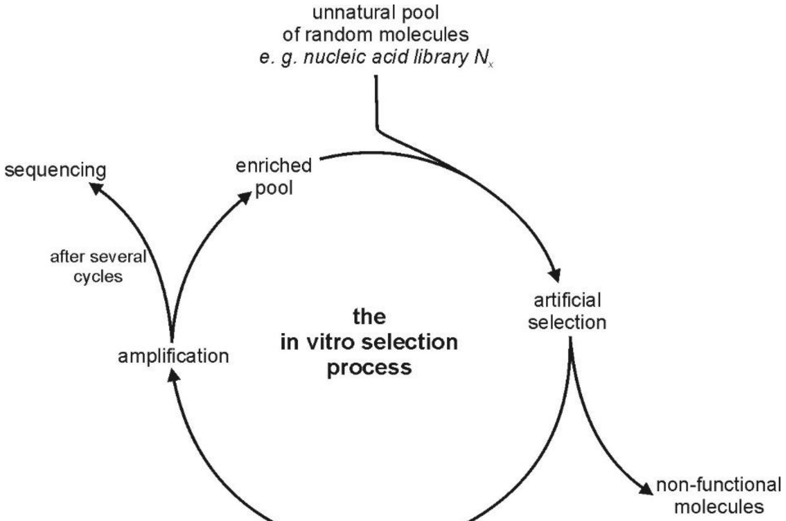
unnatural pool
of random molecules
e. g. nucleic acid library N_x
sequencing
enriched pool
after several cycles
artificial selection
the in vitro selection process
amplification
non-functional molecules
functional molecules

Figure 9. Illustration of the *in vitro* selection process.

The major advantage of SELEX is that theoretically a specific binder or catalyst can be created for any desired target or reaction. The major drawback of SELEX is the enormous laboratory effort and that it bears the high risk to fail successful selection because the target is inadequate. Additionally, the method itself is delicate. The amplification steps are especially difficult. PCR is hampered by the high sequence variability in the reaction mixture. It is frequently told about PCR products of higher than the expected length. For a selection of functional RNA, a reverse transcription is indispensable after a selection round and *in vitro* transcription is necessary after the amplification step. In the case of functional DNA, ssDNA has to be prepared from dsDNA after amplification. This can be realized by asymmetric PCR, a chemically modified antisense primer and the following size-separation by gel electrophoresis (polyethylene glycol-modified), the use of biotinylated primers and the following separation on streptavidin surfaces, λ-exonuclease digestion or even rolling circle mechanism.[16, 121-125] Several efforts have been made to optimize the labor-intensive SELEX,[126] However, it can be generalized that optimal SELEX conditions vary per target. The easiest way is to develop aptamers for *in vitro* applications, where it is easy to work in the absence of nucleases. Of course, it is possible to add modifications to the nucleic acids after the *in vitro* selection process in order to elevate stability against nucleases but sometimes it will be difficult to maintain the activity after modification. Therefore, modifications may be used during SELEX, too. Then, strategies for performing the amplification steps with the modifications have to be developed.

Irvine et al.[127] examined the parameters to be set in *in vitro* selection based on mathematical analysis and computational simulation: If it is aimed to select high-affinity binders, it is important to increase stringency in each selection round. In the early rounds, the high-affinity binders have to compete with the bulge of low-affinity or intermediate-affinity binders. To ensure the survival of these sequences, it is necessary to give it a chance to bind in competition. Therefore, enough target molecules have to be present in the earlier rounds. Furthermore, a high background in the separation step leads to false positives (i.e. agarose-specific binder, nitrocellulose filter-specific binder). Therefore, counter-selection steps have to be performed. The common experience indicates that a number of about 10 selection rounds is enough to find high-affinity sequences.[51] Experience also revealed that the success is often higher with larger random ranges. However, with increasing length of the random range, the number of possible sequences increases (4^N possibilities). A library with $N = 50$, for instance, has approximately 9×10^{84} possible sequences. This corresponds to 1.5×10^{61} mol of nucleic acids if every sequence exists once only. In the laboratory, an initial amount of 10^{14}-10^{15} molecules (10^{-12} to 10^{-9} M) is manageable. This corresponds to 25 fully randomized positions. However, it is more important that the length of the randomized sequence bears capacity for structure elements which are able to bind to the target. A hairpin structure, for example, spans at least 10 nucleotides.

The *in vitro* selection of catalytic function began with alterations of natural ribozymes. For instance, the conversion of shortened variants of the *Tetrahymena* ribozyme (group I intron) into ribozymes that cleave and ligate ssDNA revealed a 93 nt deletion form that cleaves ssDNA more efficient than the wild-type cleaved RNA.[128] The same ribozyme was also converted by *in vitro* selection from a Mg^{2+}-depending ribozyme to a Ca^{2+} depending species.[129] Furthermore, *in vitro* selection was used to study characteristics and sequence requirements of the hairpin ribozyme.[130-132] Extensive work was also done on the development of new nucleic acid enzymes catalyzing natural reactions of ribo-/enzymes like aminoacylation, [133, 134] hydrolysis and ligation [135], their modification [136] or non-natural reactions (i.e. Diels-Alder-reaction, alcohol oxidation [137-139]). At this point, it is referred to the various reviews concerning this field.[129, 140-142] A high number of DNAzymes were developed as well. Detailed information about the 8-17 DNAzyme family is given in section 4 (Combination of *In Vitro* Selection and Rational Design). For others, again it is referred to reviews.[140, 143-148]

3.2 The *In Vitro* Selection of an Aptazyme for TNFalpha

In parallel to the investigation of RNA-aptamers, the aim was to develop a DNA-biosensor for TNFα obtained by means of *in vitro* selection. The selection of an aptazyme by simultaneous *in vitro* selection of an aptamer domain and the desired catalytic function was chosen as a straightforward method for this purpose. In the case of successful *in vitro selection* rounds, this strategy could yield specific and sensitive biosensors in relatively short time. For the selection of an aptazyme for TNFα, a library was designed and the *in vitro* selection strategy was developed. Furthermore, chemical synthesis of DNA is cheaper than RNA. Therefore, in terms of stability and economy of the future biosensor, a DNA-based system was preferred instead of an RNA-based one.

3.2.1 Design and Synthesis of the DNA Library for TNFα

A nucleic acid library for *in vitro* selection has to be framed by defined sequences that enable primer binding for the amplification reactions. These sequences can be used to incorporate additional information or functions into the library. It was aimed to design a library for the *in vitro* selection of a ligand-dependent trans-self-cleaving DNAzyme. Self-cleaving DNAzymes (trans or cis) bind their substrate by Watson-Crick base pairing (see chapter 4). The substrate binding domain is characterized by two helices (generally containing at least 4 nucleotides) which surround the cleavage site. Therefore, libraries for the present work were designed to possess a fixed substrate binding domain. This domain also contained the ribonucleotide that was supposed to be the cleavage site (Figure 2). The ribonucleotide was going to be introduced by PCR with a primer. The first and very extensively investigated library A (Figure 10), was based on a sequence that was selected by Breaker and Joyce for a Pb^{2+}- and a Mg^{2+}-dependent DNAzyme, respectively.[91, 149] The cleavage site was set to be an internal adenosine ribonucleotide (rA).

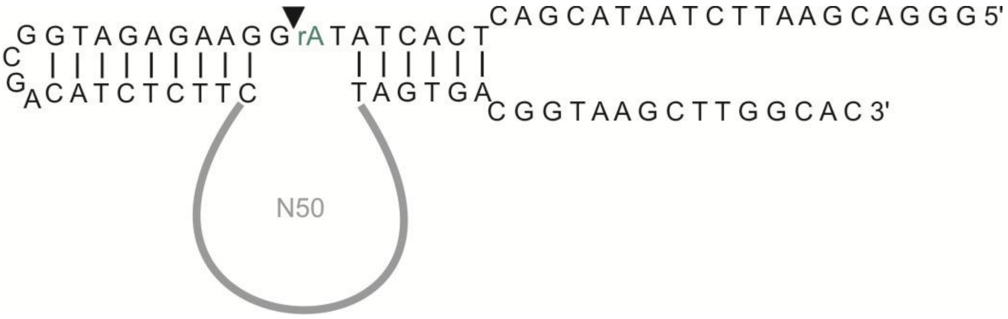

Figure 10. Scheme of the initial DNA library for the selection of a DNAzyme which responses to TNF*α*. Green: ribonucleotide; gray: randomized domain; arrow: cleavage site.

The primer binding sites and the fixed domains were designed following the *in vitro* selection protocol of the Mg^{2+}-dependent DNAzyme.[149] Independent of these specifications, the length of the randomized domain had to be decided. A large randomized domain could be useful for large analytes and is more variable than a smaller one. For the biosensor to be developed, the randomized domain, moreover, has to develop the ability to transform the binding information into allosteric information. However, the sequence number is by far higher than the manageable amount of molecules. Due to the lack of empirical value, it was decided arbitrarily to start with a library with 50 randomized nucleotides. The dsDNA library was generated by extension of primer PA2 (5'- Biotin-GGGACGAATTCTAATACGACTCA CTAT**rA**) in the presence of the antisense template (5'-GTGCCAAGCTTACCGTCACTA-N50-GAAGAGATGTCGCCA TCTCTTCCTATAGTGAGTCGTATTAG). The biotin modification was part of the applied *in vitro* selection strategy (see below). The oligonucleotides were purchased from Biomers. The extension protocol that was adopted from the literature[149] was slightly modified towards higher yield and then used to synthesize a library of 150 – 250 pmol DNA which corresponds to 10^{13} – 10^{14} different sequences.

3.2.2 *In Vitro* Selection Strategy

The *in vitro* selection strategy is illustrated in Figure 11. The scheme shows the *in vitro* selection process from the beginning with the antisense strand to the course of single *in* *vitro* selection rounds. After the extension of the antisense strand, the library was bound to streptavidin magnetic beads (SMBs; S1420S, NEB) by its biotin moiety at the 5'-end of the sense strand. The antisense strand was eliminated by alkaline treatment and removing of the supernatant.

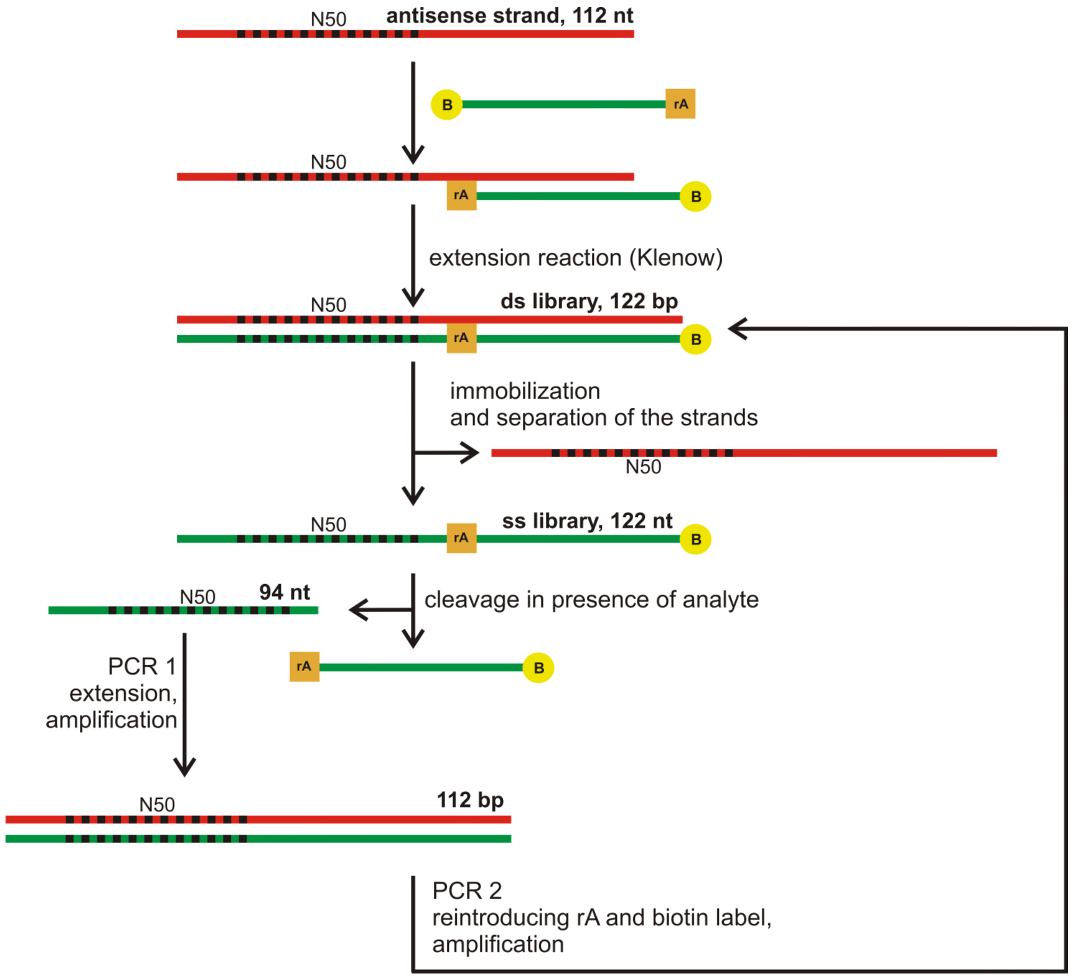
N50
antisense strand, 112 nt
B
rA
N50
rA
B
extension reaction (Klenow)
N50
ds library, 122 bp
rA
B
immobilization
and separation of the strands
N50
N50
ss library, 122 nt
rA
B
N50
94 nt
cleavage in presence of analyte
rA
B
PCR 1
extension,
amplification
N50
112 bp
PCR 2
reintroducing rA and biotin label,
amplification

Figure 11. Scheme of the *in vitro* selection strategy for simultaneous selection of aptamer and catalysis. The green strands represent the DNA carrying the information of the pool. The antisense strand was extended by a biotinylated primer. After immobilization of the dsDNA, the antisense strand was removed by alkaline treatment. In presence of the analyte (i.e. TNFα), a cleavage of the capable sequences was expected. Subsequently, the mutational active sequences were removed, extended and amplified by two consecutive PCRs. Then, the pool was prepared for a new round of *in vitro* selection.

Active sequences, that means, those, which were cleaved during a selection round, were collected and precipitated with ethanol and subsequently extended to their original length and amplified by PCR. The active sequences are then introduced in the next round by PA1a (5'-GTGCCAAGCTTACCGTCAC) and PA1b (5'-GGGACGAATTCTAATACGA CTCACTATAGGAAGAGATGGCGACATCT) primers. In a subsequent PCR, the ribonucleotide and the biotin modification were reintroduced by adding primer PA1a and PA2 to the former PCR product. Initially, the immobilization procedure had to be set up and it had to be proven that the ribonucleotide cleavage site remained stable during alkaline treatment for strand separation.

Evaluation of Immobilization and Strand Separation

Evaluation of DNA binding to SMBs was done with the biotinylated primer PA2. The parameters to improve binding of a biotin-labeled DNA to the SMBs were salt concentration and buffer type, reaction volumes, reaction time, the concentration of DNA and the number of beads. It was important to find a suitable buffer without chloride, in order to prevent precipitation with lead ions because these were intended to be applied in *in vitro* selection experiments. The best condition was found by the determination of the remaining fraction of DNA in the supernatant using the NanoDrop (UV/Vis-spectroscopy). For efficient binding, the salt concentration has to be high. No or insufficient binding was observed below 1 M NaCl. Furthermore, it was found, that the addition of Tween 20 did not have a significant effect on binding. It may be added to prevent biomolecules from sticking to the walls of reaction tubes or other tools. The most critical parameter is the concentration of DNA. The optimum concentration was 8 µM in HEPES buffer; below and above of this concentration, the binding efficiency was lower. 8 µM PA2 in binding buffer (buffer BA; 20 mM HEPES (pH 7.5), 1 M NaCl, 1 mM EDTA, 0.05 % Tween 20) resulted in 96 % binding of PA2. At least 90 % binding was achieved when the dsDNA library or a pool was bound to the beads. Subsequently, when dsDNA was bound to the beads, alkaline treatment for separation of the strands was carried out by washing 5 times with 0.2 M NaOH.[91, 149] Following the alkaline treatment, the beads were washed 3 times with equilibration buffer (EA; 20 mM HEPES (pH 7.5), 0.05 % Tween 20). Additionally, the stability of the biotin-streptavidin linkage was proven by immobilizing a biotinylated primer. The incubation time of alkaline treatment was elevated to 4 minutes. In this experiment, 20 % of the primer strands loosened. Afterward, the beads were incubated in selection buffer (20 mM HEPES (pH 7.5), 0.05% Tween 20, 5 mM $MgCl_2$) for 30 min, 90 min or overnight. During incubation in selection buffer (20 mM HEPES (pH 7.5), 0.05 % Tween 20, 5 mM $MgCl_2$) the bonds remained intact: no DNA could be detected in the supernatant even after incubation overnight, neither by UV/Vis-spectroscopy nor by analysis of the precipitate of the supernatant by PAGE.

The resulting protocol to prepare an *in vitro* selection round is shown in Table 1.

Table 1. Protocol for the binding of biotin labeled DNA to streptavidin magnetic beads (preparation for an *in vitro* selection round).

1)	Washing 160 µl beads (640 µg) + 130 µl binding buffer BA
2)	Binding add 150-170 pmol DNA (8 pmol/µl in binding buffer BA) leave react at RT for 15 min
3)	Washing 2 times with 130 µl washing buffer WA
4)	Separation of strands wash 5 times with 130 µl 0.2 N NaOH
5)	Equilibration wash 3 times with 130 µl equilibration buffer EA

3.2.3 The *In Vitro* Selection Process

To start with the *in vitro* selection the library was immobilized onto the beads following the optimized protocol (Table 1), immediately after ethanol precipitation of the extension reaction. However, the concentration of dsDNA was overestimated by UV/Vis measurement after ethanol precipitation of the extension reaction, because of the co-precipitated nucleotides. The extension reaction was purified by PAGE (section 6.6.10 Gel elution A), however the yield was very low (6 %). Therefore, the extension reaction was applied to the beads directly after ethanol precipitation. By determination of the amount of eluted ssDNA after alkaline treatment it was shown that 60 – 70 % of the library were bound (related to the amount of antisense template introduced in the extension reaction). Three pools were bound on beads (170 – 200 pmol, each; corresponding to 10^{14} sequences). Three different selection conditions were apllied to reduce the risk of failure due to unsuitable conditions. In the first condition, only TNFα in HEPES-buffer was used for *in vitro* selection. In the second and third conditions, lead acetate and magnesium chloride was added respectively (Table 2). In general, the cleavage reaction of DNAzymes of the 8-17 type happens in the presence of divalent cations. Transition metal cations can be used in considerable lower concentrations and they promote faster cleavage (see section 3.2). However, in solutions containing TNFα and lead ions, a precipitate was formed. The *in vitro* selection experiment was carried out as described briefly below, in Table 2 and more in detail in section 6.6.

Table 2. Scheme of selection procedure up to selection round 5. SA buffer (selection buffer): 20 mM HEPES, pH 7.5, 0.05% Tween 20, with the indicated additives. EA buffer (equilibration buffer): 20 mM HEPES pH 7.5, 0.05% Tween 20.

Pool 1: Pb^{2+}/**TNFα dependent**	**Pool 2:** Mg^{2+}/**TNFα dependent**	**Pool 3:** **TNFα dependent**
Immobilized as described in Table 1.		
Table 1 (20 µl immobilization volume); the introduced amount was calculated by the absorption of united supernatants of denaturation reaction with NaOH		
180 pmol	170 pmol	200 pmol
Negative selection 1		
+ 20 µl SA buffer 1 mM Pb^{2+}	+ 20 µl SA buffer 10 mM Mg^{2+}	+ 20 µl EA buffer
45 min, 37 °C, 550 rpm		
Washed 3 times with 130 µl EA buffer		
Negative selection 2		
+ 20 µl SA buffer 1 mM Pb^{2+}	+ 20 µl SA buffer 10 mM Mg^{2+}	+ 20 µl EA buffer
2 h, 37 °C, 550 rpm		
Washed 3 times with 130 µl EA buffer		
Selection round 1		
+ 20 µl SA buffer 1 mM Pb^{2+}, **10 µg/ml TNFα**	+ 20 µl SA buffer 10 mM Mg^{2+}, **10 µg/ml TNFα**	+ 20 µl EA buffer, **10 µg/ml TNFα**
2.5 h, 37 °C, 550 rpm		
Washed with 15 µl H_2O		
United supernatants used directly for PCR		
1. step: PCR 1; 2. step: ethanol precipitation; 3. step: PCR 2, 4. step ethanol precipitation		
Immobilized as described in Table 1.		
Table 1 (11.6 µl immobilization volume – 0.9 µl kept for later amplification); the introduced amount was calculated by the absorption of united supernatants of denaturation reaction with NaOH		
75 pmol	73 pmol	37 pmol
Selection round 2		
+ 12.5 µl SA buffer 1 mM Pb^{2+}, **10 µg/ml TNFα**	+ 12.5 µl SA buffer 10 mM Mg^{2+}, **10 µg/ml TNFα**	+ 12.5 µl EA buffer, **10 µg/ml TNFα**
2 h, 37 °C, 550 rpm		
Washed with 17.5 µl H_2O		
Pool 1: Pb^{2+}/**TNFα dependent**	**Pool 2:** Mg^{2+}/**TNFα dependent**	**Pool 3:** **TNFα dependent**
United supernatants used directly for nested PCR		
1. step: PCR 1; 2. step: ethanol precipitation; 3. step: PCR 2, 4. step ethanol precipitation		
Immobilized as described in Table 1.		

Table 1 (11.6 µl immobilization volume – 0.9 µl kept back); the introduced amount was calculated by the absorption of united supernatants of denaturation reaction with NaOH		
54 pmol	52 pmol	48 pmol
Selection round 3		
+ 12.5 µl SA buffer 1 mM Pb^{2+}, **10 µg/ml TNFα**	+ 12.5 µl SA buffer 10 mM Mg^{2+}, **10 µg/ml TNFα**	+ 12.5 µl EA buffer, **10 µg/ml TNFα**
1 h, 37 °C, 550 rpm		
Washed with 17.5 µl H_2O		
United supernatants used directly for nested PCR		
1. step: PCR 1; 2. step: ethanol precipitation; 3. step: PCR 2, 4. step ethanol precipitation		
Immobilized as described in Table 1.		
Table 1 (11.6 µl immobilization volume – 0.9 µl kept back); the introduced amount was calculated by the absorption of united supernatants of denaturation reaction with NaOH		
> 100 pmol*	> 100 pmol*	> 100 pmol*
Selection round 4		
+ 12.5 µl SA buffer 1 mM Pb^{2+}, **10 µg/ml TNFα**	+ 12.5 µl SA buffer 10 mM Mg^{2+}, **10 µg/ml TNFα**	+ 12.5 µl EA buffer, **10 µg/ml TNFα**
1 h, 23 °C, 550 rpm		
Washed with 17.5 µl H_2O		
United supernatants used directly for nested PCR		
1. step: PCR 1; 2. step: ethanol precipitation; 3. step: PCR 2, 4. step ethanol precipitation		
Immobilized as described in Table 1.		
Table 1 (11.6 µl immobilization volume – 0.9 µl kept back); the introduced amount was calculated by the absorption of united supernatants of denaturation reaction with NaOH		
>>100 pmol*	>> 100 pmol*	>> 100 pmol*
Selection round 5		
+ 12.5 µl SA buffer 1 mM Pb^{2+}, **5 µg/ml TNFα**	+ 12.5 µl SA buffer 10 mM Mg^{2+}, **5 µg/ml TNFα**	+ 12.5 µl EA buffer, **5 µg/ml TNFα**
1 h, 23 °C, 550 rpm		
Pool 1: **Pb^{2+}/TNFα dependent**	**Pool 2:** **Mg^{2+}/TNFα dependent**	**Pool 3:** **TNFα dependent**
Washed with 17.5 µl H_2O		
United supernatants used directly for nested PCR		
1. step: PCR 1; 2. step: ethanol precipitation; 3. step: PCR 2, 4. step ethanol precipitation		

* more than 100 pmol are not possible, because in PCR 2 only 100 pmol of primer 1aA and 2A are used, respectively

Starting with the third selection round, UV/VIS measurements of the supernatants of the alkaline treatment resulted in unrealistic high absorption. This kick-off process was carried out 'blind', without the control of PCR products by PAGE or agarose gel electrophoresis. It should be tested if the method was applicable in the way it had been built up at this stage.

PAGE Analysis of the extension reaction and the PCR

The analysis of the sequences was difficult by PAGE. In general, for the analysis of nucleic acids with about 100 bp, a 10 % PAGE is appropriate. Sequences of this length even migrate in 20 % PAGE. In this case, they didn't. A large part of the pool DNA was retained in the pocket or migrated considerably more slowly in comparison with a commercial DNA ladder. The problem was assigned to be caused by the large randomized domain (50 nt), i.e. diverse strong secondary structures. Therefore, some experiments were carried out with an equally constructed library with only 30 randomized nucleotides. However, this library behaved similarly concerning its electrophoretic mobility. The Figure 12 shows that when a 3 % agarose gel was used, the product of an extension reaction (102 bp) with the template N30 (92 nt) for the simultaneous in vitro selection of aptamer and catalytic function and Primer PA2, migrates as expected compared to a size standard. However, on a 10 % denaturing PAGE, the sequences migrate considerably slower, even, when they were eluted from the band in the agarose gel.

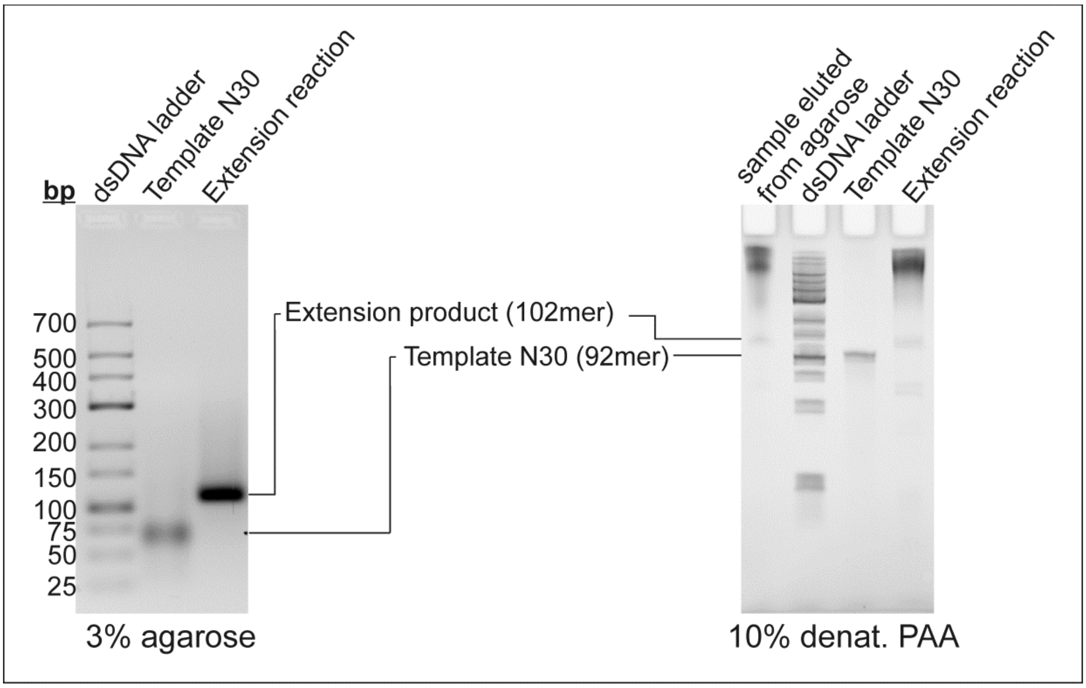
bp
dsDNA ladder
Template N30
Extension reaction
700
500
400
300
200
150
100
75
50
25
3% agarose
Extension product (102mer)
Template N30 (92mer)
sample eluted from agarose
dsDNA ladder
Template N30
Extension reaction
10% denat. PAA

Figure 12. Gel analysis of an extension reaction with the template N30 and PA2. The gels were post-stained with ethidium bromide.

Troubleshooting was performed, particularly with respect to sample purity (i.e. gel filtration, phenol/chloroform extraction) and running conditions. However, no improvements were achieved.

Re-Investigation of the Extension Reaction and Optimization of the PCR

The analysis of the pools of the first *in vitro* selection round revealed that a large amount of longer sequences were side products of PCR (cf. Figure 13, page 43). However, as early as in the extension reaction, longer sequences appeared as side products. Therefore, initially, the extension reaction was re-investigated and further optimized. Briefly, different conditions were evaluated with the use of *Taq* Polymerase and additives such as DMSO, BSA, or spermidine. Additionally, the concentration of $MgCl_2$ and the buffer composition was screened. The annealing temperature was evaluated for every condition. However, no improvement was achieved; moreover, it became clear, that the reaction was not controllable, the results were not reproducible and strongly depended on the sequences, which inherently varied with every reaction performed because the pool of sequences was very large. Replacement of *Taq* Polymerase with Klenow Fragment 5’→3’ exo- did not improve the result significantly.

With respect to generally satisfying results of immobilization, it was decided to focus on optimizing the amplification reactions instead of the extension reaction. A large number of PCR experiments were carried out in order to improve performance and the yield of PCR. For this purpose, a 50 nt randomized antisense library was used as a template and PA1A and PA2 (see section 3.2.2) were used as primers. Additionally, the gel purified dsDNA of the extension reaction or of the Klenow reaction was used as a template. Some experiments were done with a 30 nt randomized library, otherwise equal to the 50 nt randomized one. To simulate the reaction conditions after an *in vitro* selection round, the ssDNA bound to SMBs was subjected to a single *in vitro* selection round and then introduced as a template in PCR. A summary of the screened parameters is given in Table 3. Furthermore, touchdown PCR [150] was carried out, where the annealing temperature dropped from cycle to cycle about 1 °C to 3 °C. The working range was between 60 °C and 50 °C. Additionally, control experiments without template DNA and other DNA samples were carried out.

Table 3. Summary of parameters screened for optimization of PCR with DNA libraries.

Parameter	Variation
annealing temperature	52 °C – 72.5 °C
denaturation, annealing and elongation time	20 – 60 s
cycle number	5 – 30
DMSO	2 % – 15 %
Mg^{2+}	0.5 – 5 mM
K^+	4 – 100 mM
primer	0.2–2 µM
DNA template (ss or ds)	10^{-1} – 10^{-3} µM
DNA polymerase	*Taq* (self-made or ROBOKLON), $Vent_R$ (NEB), Opti*Taq* (ROBOKLON), *Pfu*/*Psp* (GENEON) • at different concentrations and in the buffer supplied with the enzyme • for self-made *Taq* polymerase: Pol buffer (ROBOKLON) or Tris-HCl, pH 8.5 plus salts and additives

A representative image of agarose gel electrophoresis for analysis of the PCR is shown in Figure 13 (page 43). PCR was most specific, at high annealing temperatures up to 72 °C; the temperature could be lowered by the addition of DMSO. Best results were achieved with low cycle numbers below 15. But, these conditions had a strong negative impact on the yield. Touchdown PCR and variations in denaturing, annealing and elongation period had no effect on the outcome of the reaction. Furthermore, the effect of the concentration of KCl in PCR was investigated. Higher concentrations of the monovalent salt (standard: 10 mM) can improve amplification of shorter fragments (that means < 500 bp). In the present experiments, it was observed that higher KCl concentrations (> 10 mM) forced the accumulation of artifacts. For Mg^{2+}, depending on the enzyme used, optimum concentrations were found. The biggest hurdle, concerning reaction composition and conditions, was that the results were not reproducible, which was most likely due to the different sequence composition in each template pool. Referring to the types of DNA polymerase investigated, the clear result was that *Taq* DNA polymerase is the most suitable enzyme for the present purpose. There was no difference observed between commercial and self-made enzyme. $Vent_R$ (NEB), Opti*Taq* (ROBOKLON), *Pfu*/*Psp* (GENEON) tend to produce even more PCR products that are longer than the product aimed for.

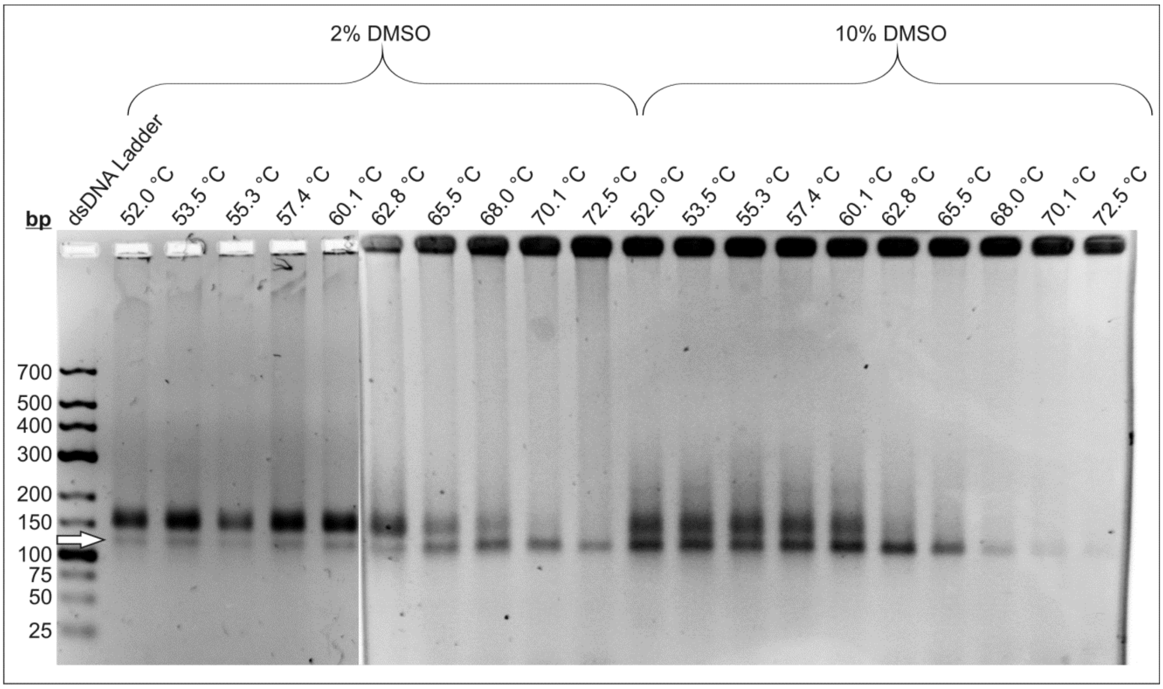

Figure 13. PCR of 50 nt library with 2% and 10% DMSO and at different annealing temperatures. The desired product is 122 bp in length (white arrow). 3% Agarose-EtBr; 120 V, 2h; pockets of the gel on the right are black because it was additionally stained with EtBR after the run.

Gel elution

If a reaction does not yield the desired product at a desired grade of purity, post-synthetic purification is the method of choice. Gel elution is a method to yield very pure nucleic acid-product. A nucleic acid sequence excised and eluted from a gel is free of side products (longer and shorter sequences) and compounds of preceding reactions, like dNTPs/NTPs, proteins, and primers. Moreover, depending on the resolution of the gel, it has a high integrity. However, if large amounts of nucleic acid product are needed or a high yield is aimed, gel elution is a critical step. In the present process, gel elution was applied to purify the extension reaction product (page 37), but the yield was insufficient. Nevertheless, an efficient gel elution procedure would have been helpful to overcome the difficulties in PCR (by post-synthetic purification) and therefore this method was re-evaluated. There are several gel extraction kits commercially available and various gel extraction protocols can be found in the literature.[151-155] This small selection of references was published between 1979 to 2013, which demonstrates that gel elution still is a hot topic. Different methods were tested for both PAA (5–20 %) and agarose gels (2–3 %). Some successful methods are presented in the following paragraph.

Electroelution of nucleic acids of 74 kDa was successful using the Spectra/Por Float-A-Lyzer, MWCO 100-500 Da, volume 1 ml. The gel slice was put in the dialysis tube, then it was positioned into a horizontal electrophoresis chamber. After 1,5 h at 160 V, the solution in the dialysis tube was reduced in a vacuum centrifuge and nucleic acids were ethanol precipitated. The yield was about 20 %.

Another method for agarose gels is the digestion of the gel with agarose. This procedure is relatively fast and according to THERMO SCIENTIFIC, recovers up to 90% of nucleic acid. This yield was not reached. For this method, special low melting point agarose has to be used since agarase is not able to digest solid agarose. By the use of agarose with low melting point, the digestion can take place at 42 °C in liquid agarose. The general procedure is, to cut off the desired band of the gel and subsequently let it melt at 70 °C for 10 min. After equilibration to 42 °C (10 min), 1 u agarase/100 µg of 1 % gel is added. After digestion (42 °C, 30 min) ammonium acetate is added to 2.5 M final concentration, in order to precipitate undigested agarose (with sodium acetate the sugars will be precipitated, too). The mixture is chilled on ice for 5 min and afterward centrifuged at 10,000 rpm for 10 min. The supernatant is transferred to a clean tube in which ethanol precipitation takes place. The precipitation should take place at room temperature, to prevent precipitation of sugars. This was shown to be a problem if small nucleic acids and small concentrations of nucleic acids have to be recovered. Furthermore, working with high concentrated agarose gels, high amounts of enzyme are needed and the digestion time has to be prolonged to 1 h. However, yields up to 40 % were reached for a 120 bp DNA.

For the QIAGEN Gel extraction kit (70 bp to 10 kbp, for agarose gel) it was found that the yield is very low if the DNA is smaller than 200 bp (5–10 %)

Finally, always variants of the classical crush and soak method were applied.[153] The reasons were that the other methods didn't outclass this classical method concerning cost, time and yield In this method, the gel slice is always crushed or cut into small pieces and soaked in the gel elution buffer. This buffer can be adjusted to the specific needs. In the present work 0.3 M NaOAc, pH 5.5 was applied for elution of RNA and 20 mM Tris-HCl, pH 8.2–8.5, 0.25 M NaOAc, 1 mM EDTA for elution of DNA. The yield can be elevated by elevating the duration and temperature of the elution step, freezing, and thawing of the gel slice, as well as elution in an ultrasonic bath. It was observed, that the yield also depends on the individual DNA or RNA sequence, and in general, it ranged from 5–40 %. For the sequences used in the present work, it was found that in most of the cases, the yield was maximal with three to four elution steps for one or two hours (see section 6.6.11 Gel elution B). However, for the present application, to purify the PCR, the performance of the method was not satisfying.

Emulsion PCR

As an alternative to the approaches described above, emulsion PCR (ePCR) was tested. In ePCR, amplification takes place in inverse micelles. At the best, every micelle contains only one template molecule. That means ePCR virtually reduces the diversity of the pool. This strategy had to be established in our lab first because the exact size and number of micelles strongly depends on the mixing device, the materials (vials, pipette tips) and the ambient temperature. The general procedure can be taken from chapter 6.16, (p.121). Additionally, for ePCR it is necessary to determine an optimum amount of BSA ($0-1$ mg ml^{-1}). BSA has to be added to prevent denaturation of DNA polymerase at the micelle-wall but it is also an efficient PCR-inhibitor. The resulting PCR-composition was: 1 µM primer PA2 and PA1a, Pol buffer (ROBOKLON), 0.2 mM dNTPs, 0.025 mg ml^{-1} BSA, 1.2 µl 50 µl^{-1} *Taq* DNA polymerase. The amount of DNA template varied between 10^{-2} and 10^{-6} µM. The initial denaturing took place at 92 °C for 3 min. Then 15 or 20 cycles of strand separation (30 s, 92 °C), primer annealing (30 s, 54 °C) and extension (30 s, 72 °C) followed. The reaction was ended by 3 min final extension at 72 °C and holding at 4 °C until further use. Purification of DNA is carried out by opening the emulsion with butanol and silica columns. As an alternative for the use of commercial silica columns and the required washing buffers, it was exploited that nucleic acids precipitate in butanol. After breaking the emulsion with butanol, no high-salt buffer was added for resolving the DNA and binding to silica-columns and the mixture was centrifuged. The DNA pellet was then purified by phenol-chloroform-extraction (PCE). However, this method is considerably more time-consuming. Control reactions without DNA template and, for comparison, a standard PCR without BSA were carried out. Emulsion PCR was very successful as impressively shown in Figure 14. In 'open' PCR ($3 \cdot 10^{-4}$ µM template DNA), large amounts of artifacts emerged. Artifacts were present in ePCR with $3 \cdot 10^{-4}$ µM template DNA, too, but strongly reduced. The artifacts were further reduced by lowering the amount of template; however, consecutively yield was also lowered. The low yield is a significant drawback of this method. That means, ePCR can help in handling difficult templates or template-primer combinations but the method is not a guarantee for success of the amplification reaction.

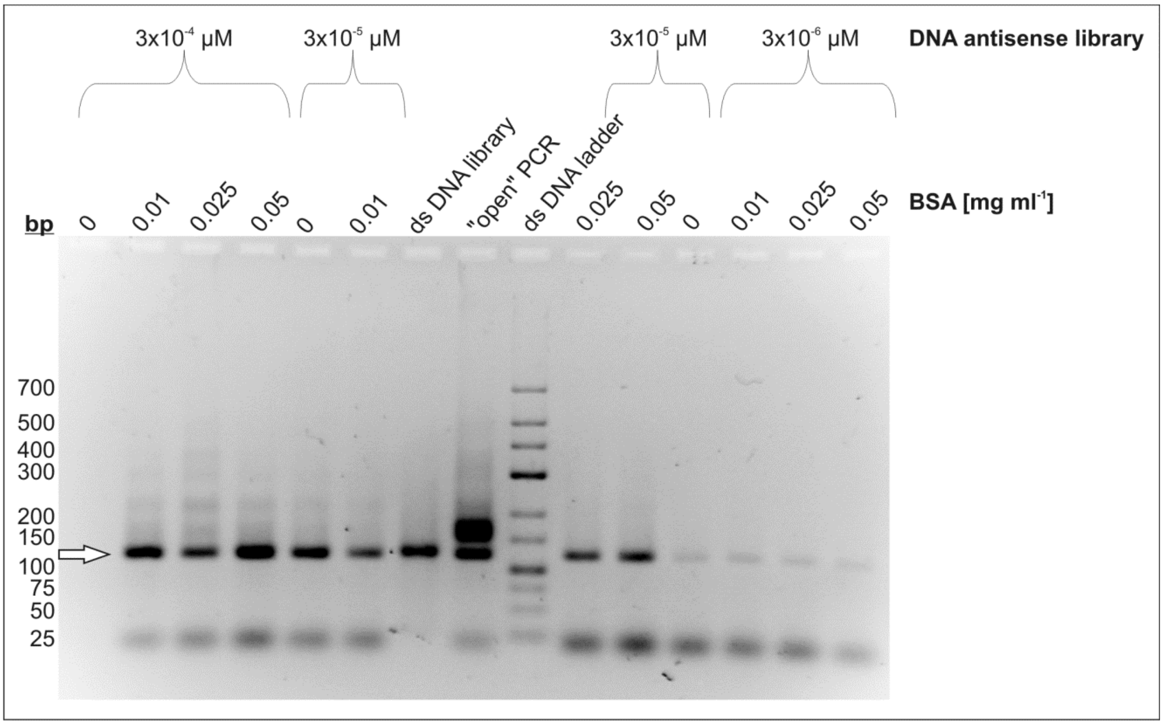

Figure 14. ePCR with different concentrations of template DNA antisense library and BSA. The desired Product is 122 bp in length (white arrow). "Open" PCR was done with $3x10^{-4}$ µM template DNA. 3% Agarose-EtBr; 120 V, 2h.

3.2.4 *In Vitro* Selection of an Aptazyme for Creatinine

At this point, the target analyte was changed. The experiments described in the section above were conducted in parallel to the investigation of the RNA aptamers for TNFα (section 2.3.1). This work revealed that applying TNFα as analyte is a complex task and that its use as a model-analyte is not straightforward. The initial decision for TNFα was made by the industrial cooperation partner. However, the cooperation ended and the *in vitro* selection did not succeed. Therefore, it was obvious to choose another molecule as a model-analyte to approach a general method to construct biosensors. The choice was made in favour of creatinine. Like TNFα, creatinine is an interesting biomarker and until now, no aptamers exist for both of them. However, as it is a small molecule, no difficulties arising from the tertiary or secondary structure and no dependence on concentration-dependent behaviour were expected. Furthermore, it is considerably cheaper, which in the development of a method is favourable.

Based on the aforementioned results, several new *in vitro* selection rounds were started for an creatinine aptazyme. Creatinine was added from 22 to 2.2 mM to an *in vitro* selection round. The performance of the rounds otherwise was equivalent to the performance with TNFα (section 6.15). The experiments were not successful. In general, concerning the amplification steps, the first and second round was manageable, but higher rounds were problematic. However, this would be expected to behave inverse because of reduced diversity of the pool. Both, ePCR and standard PCR were applied. The practicability of ePCR was found to be restricted in the present *in vitro* selection. For example 36 ePCRs had to be performed to amplify 1.5 % of the material of a single selection round in PCR 1. Then, for PCR2, a standard PCR with 5 cycles in a total volume of 1200 µl was applied. The final yield was about 120 pmol, as determined by immobilization on the streptavidin magnetic beads. Of course, a lot of work was done concerning other possibly critical steps (selection pressure, purification of nucleic acids), but always, progress was hampered by the amplification steps.

A New Library for Creatinine

Until this point, while working with TNFα and creatinine as analytes, a considerable effort was made to improve the PCR. The only parameter, which was always the same, was the library itself. Therefore, a slightly modified library was designed (Figure 15).

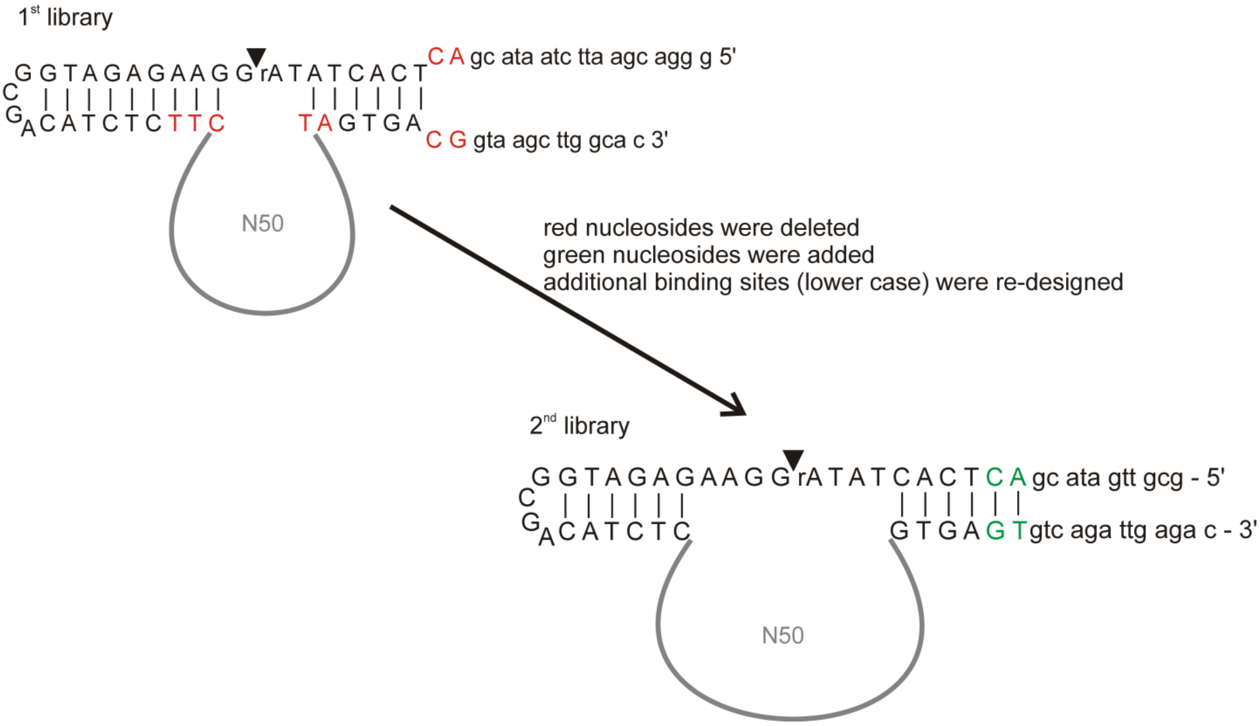
1st library
GGTAGAGAAGGrATATCACTCA gc ata atc tta agc agg g 5'
C
G
ACATCTCTTC
TAGTGACG gta agc ttg gca c 3'
N50
2nd library
GGTAGAGAAGGrATATCACTCA gc ata gtt gcg - 5'
C
G
ACATCTC
GTGAGT gtc aga ttg aga c - 3'
N50

red nucleosides were deleted
green nucleosides were added
additional binding sites (lower case) were re-designed

Figure 15. Adaption of the library's sequence. The sequence of the first library is based on the work on *in vitro* selection of Breaker and Joyce [91, 149], whereas the sequence of the second library is based on the 17E DNAzyme [92]. Furthermore, the fixed range was shortened. The additional primer binding sites were re-designed based on those of the first library.

In the first approach a fixed sequence and primer binding sites adopted from literature was used as library.[91, 149] For the second library, primer binding sites were re-designed concerning melting points, GC-content, primer secondary structure (self-dimers, cross dimers, hairpin structures) and structures possible with the different template-species (these are changing due to the nested PCR procedure). The fixed sequence of the DNAzyme part of the second library was based on the 17E DNAzyme,[92] that meanwhile was investigated (see chapter 4 'Combination of *In Vitro* Selection and Rational Design'; library: 5' GCGTTGATACGACTCACTATAGGAAGAGATGGCGA CATCTC-N50-GTGAGTGTCAGATTGAGAC). Instead of buying the oligonucleotide library, this time, it was synthesized in our own laboratory by the help of a Synthesizer (APPLIED BIOSYSTEMS). For every N in the sequence of the library, a mixture of A,G,C,T-phosphoramidites (CHEMGENES) was used. For this mixture, the same amounts (moles) of phosphoramidites were weighted and solved in 2.5 ml acetonitrile. Subsequently, these solutions were merged. The support was 2000 Å, 5'-DMT-deoxy cytidine (n-acetyl)-3'-Icaa CPG (CHEMGENES). The DNA was cleaved from the support and deprotected. Finally, it was purified by 8 % denaturing PAGE. The procedure was similar to the one described in section 6.7 'Synthesis of Aptamer Sequences'. The new primers (PC1a: 5' GTCTCAATCTGACACTCAC, PC1b: 5' GCGTTGATGCGACTCA CTATAGGAAGA GATGGCGACATC, PC2 5' Biotin-GCGTTGATACGACTCACTAT**rA**) were tested for the formation of false positives or artefacts in 'open' PCR; separately and in every possible combination. The result was that the combinations PC1b-PC1a and PC1a-PC2 were giving undesired products after 40 cycles of amplification, however, no false positives. Furthermore, P1bC itself produces unspecific PCR product. This problem would not be overcome with the given sequence of the DNAzyme: every possible dimer structure of P1bC and P1aC, P1aC and P2C, and P1bC and P1bC is caused by an intrinsic sequence motif. However, no products higher than 75 bp and none after 20 cycles arise. This qualified these primers for usage in the planned *in vitro* selection by applying the desired sequence of the DNAzyme library. In the following, various trials of *in vitro* selection were done. In addition to the process described above, the precipitated ssDNA from *in vitro* selection rounds was purified further by size exclusion chromatography before it was introduced in PCR. In general, ePCR was applied. However, sometimes it was made use of a standard PCR with very few cycles (≤ 5). This was necessary because of the low yield of ePCR. *In vitro* selection was started with the second library and creatinine as the analyte, but similar problems as known from the first library arose. Although, a positive influence of the new primer sequences was noticed, it wasn't possible to conduct the experiment to the end, which was to select an aptazyme.

3.3 The Simultaneous *In Vitro* Selection – Discussion

It was found that the designed method of *in vitro* selection did not have the potential to be proceeded successfully. The method was chosen because it presents several advantages. Above all, it would have been a fast method. This is important because the overarching goal of this work was to develop a method to present biosensors for various proteins in a fast manner. Provided that all steps were successful, a single *in vitro* selection round would have been taken one day to perform. Gel elution, which delays the procedure and additionally may exclude a considerable amount of active sequences, was supposed to be avoided. Immobilization by streptavidin–biotin interaction is fast and reliable. Nevertheless, it did not succeed to handle the amplification steps. The sequence variability, the intrinsic characteristic of a library, was identified as major challenge in PCR. Considering that the research community was able to perform a lot of successful *in vitro* selection experiments that were performed similar to the experiments in the present work, there has to be another reason for the failure. The second library, slightly modified especially at the primer binding sites, was somewhat easier to amplify, but the process again broke down due to unmanageable complications in PCR. But, due to the severe problems with amplification steps, other possible hurdles were not able to be detected. Respectively, this could be discussed another way round: other hurdles might have been reflected as complications in PCR. It has to be mentioned that despite the large number reports of successfully performed *in vitro* selections in literature, until now, there is no functional nucleic acid reported to be sensitive for TNFα or creatinine. In 2013 a short DNA aptamer for TNFα was developed.[156] However, since then, no further work with this aptamer was reported until now. From discussion with other scientists, I know that there have been efforts to develop an aptamer for creatinine in other working groups. It is possible, that nucleic acid is not able to represent an appropriate catalytically active ligand for either TNFα or creatinine. Moreover, in the present work, it was aimed to select affinity and catalytic activity in one step. This was clearly very demanding.

Nevertheless, important information on *in vitro* selections was gained for the future work and is summarized in the following. Most likely, it is not useful to spend more effort on detailed optimization of the PCR. It is quite possible that the most important aspect in PCR with DNA libraries is the concentration of the library template. This is underlined by the positive results with ePCR, in which the sequence variability is virtually reduced. However, ePCR is not always the method of choice, because of the strongly reduced yield. Every starting position has to be individually evaluated. Furthermore, the primers should be designed to have relatively high melting temperatures, in order to prevent undesired binding to the randomized domain. Another important fact is that Vent$_R$, Opti*Taq*, and *Pfu*/*Psp* DNA polymerases are not suitable for *in vitro* selections with libraries about 100 nucleotides in length. *Taq* DNA polymerase was shown to be the most appropriate enzyme for this purpose. Additionally, the relatively high error rate of *Taq* DNA polymerase (1/3000–1/10000 errors per bases)[157-159] might be useful in *in vitro* selection because it ensures a few mutations in the pool that are in general known to improve evolution.

4 Combination of *In Vitro* Selection and Rational Design

4.1 A New Approach for the Development of a Biosensor

Two different methods were shown to be inapplicable for the development of an aptazyme-biosensor. The first approach based on the RNA-aptazymes discussed in the first part of this work, failed because the aptamers weren't suitable for the analyte without restrictions. This result is an example of the general drawback of this method that is based on the modular, rationally designed composition of an aptazyme of preselected compounds. At least without further investigation of the compatibility of the building blocks, they may just don't work together as desired. In order to avoid this risk, it was decided to use *in vitro* selection. This method wasn't successful either. Although the true reason for failure wasn't identified, it seems reasonable, that the demand on *in vitro* selection with the chosen library was too high. As a result of these experiences, a method was developed, which makes use of a real combination of *in vitro* selection and rational design.

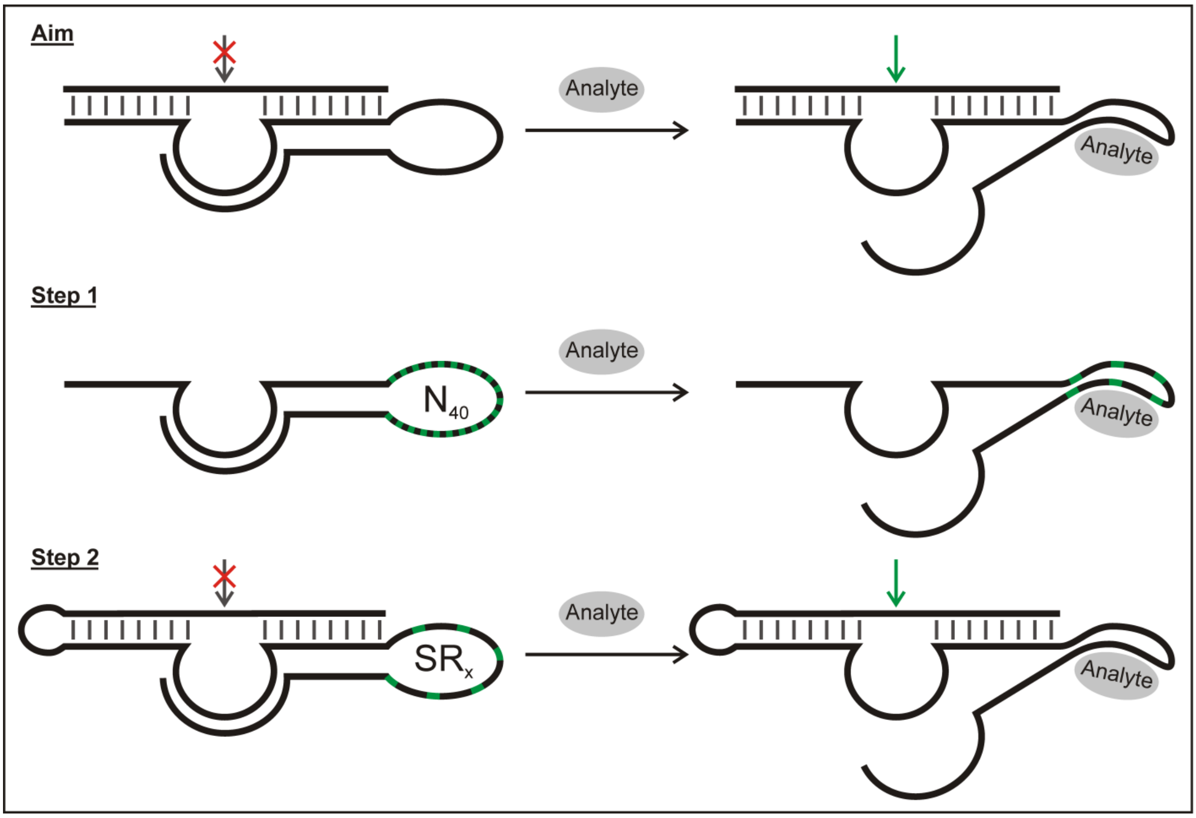

Figure 16. Schematic illustration of the approach for the development of an aptazyme based on rational design and *in vitro selection*. In the upper part, the targeted aptazyme reaction is shown: The analyte binds to the aptamer domain of a DNAzyme construct, which therefore undergoes a conformational change and is able to cleave its (trans-) substrate. The first step towards this aim is the *in vitro* selection of an aptamer with a rationally designed, substrate-free DNAzyme construct that has a randomized domain (N_{40}) positioned in between of the enzyme part of the DNAzyme and an inhibitory sequence. After a given selection round (SR_X) the second step follows, that implies the extension of the library to a cis-cleaving DNAzyme construct. Subsequent *in vitro* selection of cleavage activity yields the aptazyme.

The aptamer domain should be created by SELEX. A known DNAzyme should be modified by rational design to be suitable for allosteric regulation. Then, it should be carried through the SELEX procedure as an invariant sequence. Finally, catalyst and aptamer should be undergone additional *in vitro* selection to make them work together as an aptazyme (Figure 16). The design of the stepwise method required to decide how to deal with the cleavage site. There are two possibilities. The first one is to insert a non-cleavable substrate site (for example by the substitution of rA bei A, or 2'O-Me-A). The second one is to insert the substrate domain not earlier than in the second step of *in vitro* selection. It was decided for the latter technique. The inhibitor and the enzyme part form a duplex structure. It is known from the literature that a structurally constrained library can represent a good starting point for an *in vitro* selection.[160-162].

Streptavidin as a model analyte

Streptavidin was chosen as a model analyte for the development of this method because aptamers were already selected for this protein. This made sure that streptavidin is an appropriate analyte for SELEX. The first aptamer that was developed for streptavidin was identified from an RNA pool.[163] The aptamer S1 can be dissociated by biotin and has a dissociation constant of $7 \cdot 10^{-8}$ M. Based on this aptamer, a modified one was designed which resembles the original secondary structure after circularization.[164] This circularized aptamer is also dissociated by biotin like its parental linear aptamer. However, no dissociation constants were reported. Furthermore, a 2'-fluoro-2'-deoxypyrimidine RNA aptamer was developed.[165] This aptamer's (SA19) dissociation constant is $7 \pm 1.8 \cdot 10^{-9}$ M and in contrast to the aptamer S1, it is not dissociated by biotin. Aptamer S1 and SA 19 are both members of sequence groups that display an at least partially conserved loop. However, there is no sequence similarity between the differently *in vitro* selected aptamers. Moreover, it is interesting, that the 2'fluoro modified aptamer totally lost its affinity towards streptavidin if normal ribonucleotides were used for its transcription. Beside the RNA aptamers, DNA aptamers were identified during the development of a new *in vitro* selection method (FluMag-SELEX)[166] The dissociation constants of the four aptamers with the highest affinity were in the nanomolar range. All of them were released from streptavidin even at low concentrations of biotin. By pairs, they belong to sequence groups that share a mostly conserved loop domain. This is what they have in common with the RNA aptamers for streptavidin. For comparison, the K_D of the streptavidin-biotin interaction is $10^{-13.4}$ M and thus this binding is the strongest non-covalent interaction known. The measured affinity is 1000 fold higher than it would be by simple addition of the single contributions (the energy requirement for the association of two molecules and reducing internal rotations, the energy gain from hydrophobic effects, neutral and ionic hydrogen bridges). This circumstance is explained by the positive cooperativeness of the binding that is caused by a ligand-induced reduction in motion of the streptavidin protein, which causes stronger binding (see section 2.3.1).[114]

The catalytically active part – the 17E DNAzyme

The choice for the DNAzyme catalyst felt on the 17E DNAzyme, a catalyst of the 8-17 DNAzyme family. The 8-17 DNAzyme was first reported in 1997 together with the 10-23 DNAzyme.[167] It is a small synthetic oligonucleotide that was identified by *in vitro* selection in presence of 10 mM $MgCl_2$. Its small catalytic core catalyzes the hydrolysis of a ribonucleotide bond either located in an RNA strand or inserted in a DNA strand. Interestingly, this DNAzyme was found several times by different working groups that applied varying strategies and different bivalent and/or monovalent cations.[92, 168-173] The substrate strand is bound through Watson-Crick base pairing to the substrate binding domain of the DNAzyme. The sequences of the substrate and of the corresponding binding arms do not influence the cleavage activity of both, 8-17 and 10-23 DNAzyme (Figure 17). But, the 8-17 DNAzyme has a characteristic (r)G-T wobble pair next to the cleavage site, which is strictly required for activity. Its k_{cat} is about 10^{-2} min^{-1} under simulated physiological conditions (2 mM $MgCl_2$, 150 mM KCl, pH 7.5, 37 °C). The cleavage products are a 2' or 3' phosphate or a 2',3'-cyclic phosphate and a 5' hydroxyl group. The initial product is always the cyclic phosphate (Figure 20). Further *in vitro* selection analysis revealed that the consensus sequence of the single-stranded bulge, which connects the stem in the catalytic domain to the substrate binding domain, is WCGAA or WCGR (W = A or T; R = A or G).

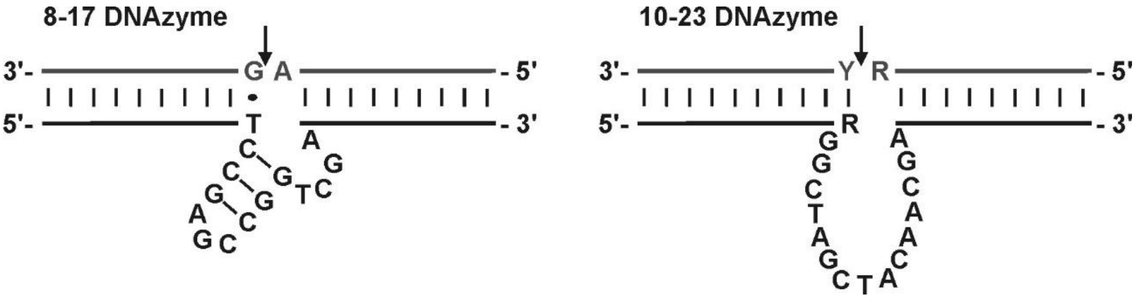

Figure 17. The composition of the original 8-17 and 10-23 catalytic motifs. [167] The substrate shown is an all-RNA strand and the arrows indicate the cleavage sites.

Four years after its publication the consensus sequence was analyzed more in detail by mutational studies.[168] The different mutants were tested for activity (single turnover) in the presence of 3 mM Mg^{2+}, Ca^{2+}, and Mn^{2+}. The k_{obs} values varied between $<10^{-4}$ min^{-1} up to 10^{-1} min^{-1} (0.5 – 10 µM DNAzyme, 1 nM substrate). Each mutant's activity was increased with the size of the divalent cation and the activity was in general 50-150-fold higher with Mn^{2+} than with Mg^{2+}. The manganese ion is the better Lewis acid and therefore may support the nucleophilic attack or the leaving group easier. Although, Ca^{2+}

is a weaker Lewis acid than Mg^{2+} and the activity increases in most cases. Activity was strongly reduced in the mutant A15G (Figure 18) and mutations in the stem II. The best activity was observed for the double mutant A12T/A15.0 with Mg^{2+} and Mn^{2+} though this mutant's activity is lower with Ca^{2+}. The results suggest a specific affinity for Ca^{2+}, which is given by A^{12} and A^{15}.

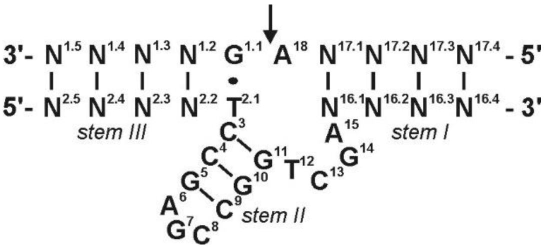
3'- N1.5 N1.4 N1.3 N1.2 G1.1 A18 N17.1 N17.2 N17.3 N17.4 - 5'
5'- N2.5 N2.4 N2.3 N2.2 T2.1 N16.1 N16.2 N16.3 N16.4 - 3'
stem III
stem I
C3 C4 G5 A6 G7 C8 C9 G10 G11 T12 C13 G14 A15
stem II

Figure 18. The canonical sequence of the 8-17 DNAzyme.[168]

The 17E DNAzyme (Figure 19) derives from *in vitro* selection in the presence of Zn^{2+}.[92] Its sequence is, except for the substrate binding arms, precisely the same as that of the A12T/A15.0 mutant and was published by Li et al. just a few months after the mutational studies mentioned above.

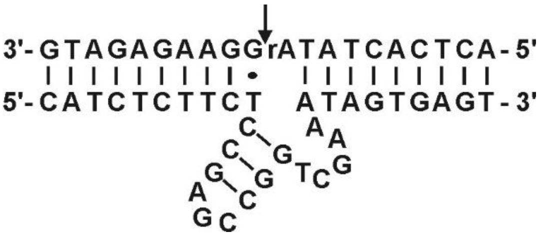
3'-GTAGAGAAGGrATATCACTCA-5'
5'-CATCTCTTCT ATAGTGAGT-3'
C C G A G C C G G T C G A A

Figure 19. Sequence and a proposed secondary structure of the 17E DNAzyme. The enzyme strand is complexed to the substrate strand, where the position of cleavage is indicated by an arrow.

In the above-mentioned work, the features of hydrated divalent cations were also taken into account. It became clear yet in the mutational studies of the 8-17 DNAzyme [168] that the effect of divalent cations on catalysis is important and varies among the different species. Therefore, in the following, the divalent cations are given a particular account. The researchers measured the activity of the DNAzyme in the presence of different metal ions and observed that it increases its catalytic activity with the decreasing pK_a of the hydrated metal ion species. Cleavage activity decreases stringently following this row: $Zn^{2+} >> Mn^{2+} \approx Co^{2+} > Cd^{2+} > Ni^{2+} > Mg^{2+} \approx Ca^{2+} > Sr^{2+} \approx Ba^{2+}$ (Table 4). This suggests that other characteristics of the cations effect on the activity.

Table 4. The trans-cleavage activity of 17E DNAzyme (sto) with different divalent cations at 100 µM , at pH=7 or 10 mM, at pH=6. Adapted from [92].

Cofactor	k_{obs} [min^{-1}]		pK_a
	100 µM, pH 7	10 mM, pH 6	
Ba^{2+}	-	0.0003	13.82
Sr^{2+}	0.0058	0.0005	13.18
Mg^{2+}	0.011	0.017	11.42
Ca^{2+}	0.012	0.015	12.70
Ni^{2+}	0.029	0.008	9.86
Cd^{2+}	0.095	-	10.08
Co^{2+}	0.20	0.25	9.65
Mn^{2+}	0.28	0.24	10.60
Zn^{2+}	1.7	1.35	8.96

Chemical modification experiments revealed the catalytic need for the N7 of A12 and A15 (original 8-17 sequence; Figure 18). An 8-17 DNAzyme with this sequence is active in the presence of transition metal ions and calcium. For activity in the presence of Mg^{2+}, A15.0 and T12 are required. Calcium ions are (like transition metal ions) able to coordinate A12 and A15 through coordination of one or two N7s and therefore build a bridge.[174] However, Mg^{2+} cannot manage the formation of such a bridge but this may be compensated with A15.0 and T12. Interestingly, in mutant A12T/A15.0 activity is reduced with Pb^{2+} and Zn^{2+}, and Ca^{2+}.[168, 175] The specific characteristics of the various cations result in different strategies of catalysis of DNAzymes of the 8-17-type. So, as mentioned above, yet, in presence of lead ions, a completely different cleavage mechanism happens. This was firstly announced by Li and Lu who studied the activity of the 17E DNAzyme with lead ions.[176] An extremely high cleavage activity (k_{obs} = 6.5 min^{-1}) is observed at a concentration of 500 nM of Pb^{2+}, the same concentration of Co^{2+}, Zn^{2+}, Mn^{2+}, Ni^{2+}, Cd^{2+}, Cu^{2+}, Mg^{2+}, Ca^{2+} just promotes cleavage about 400-fold less.

By mass spectrometry, it was disclosed that the mechanism in the presence of lead ions is a two-step mechanism and yields a 3'-end-monophosphate, whereas all other divalent cations yield the 3'-end-cyclic phosphate, as in the case of transesterification of RNA by ribozymes (Figure 20).[175]

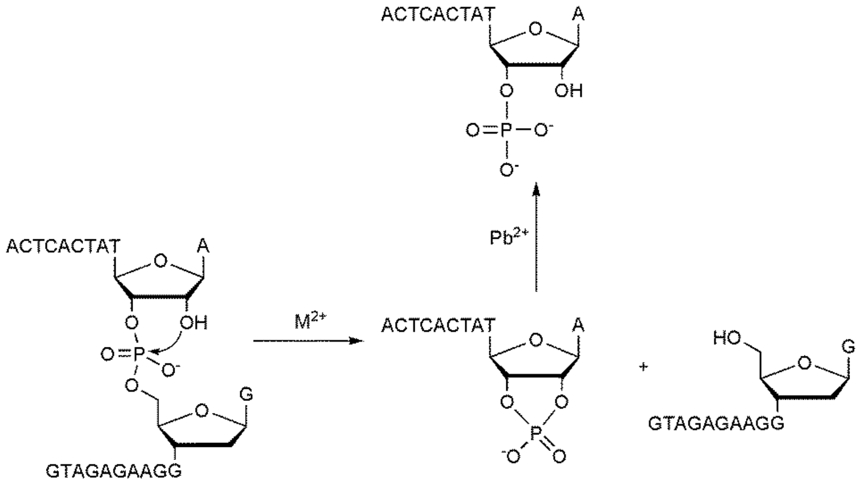

Figure 20. A possible mechanism for the catalysis of the 8-17 DNAzymes. The 3'-end monophosphate can be a 2'- or 3'-monophosphate.

Another aspect of catalysis is brought in by monovalent cations and is worth to have a closer look into. The general affinity of monovalent cations towards DNA is NH_4^+ >Cs^+ >K^+> Li^+>Na^+.[177] A possible influence was firstly discussed by Li et al., who found that monovalent cations, which are added to 17E DNAzyme cleavage reaction in the presence of zinc ions, reduce k_{obs} by half in each case (Table 5).[92] In 2009, an extensive study was published wherein the effect of monovalent cations on activity and folding was studied.[178] This study also refers to the hammerhead ribozyme, because it has similar size and secondary structure. The cleavage activity of the hammerhead ribozyme is higher with monovalent ions than divalent ion-dependent cleavage but for the 17E DNAzyme, this relation is inverted. The power of 4 mM monovalent salt to induce cleavage decreases in the following order: NH_4^+ > Li^+ > Na^+; K^+, Ru^+, and Cs^+. These cations do not induce cleavage of the DNAzyme but of the hammerhead ribozyme. Although, the last mentioned cations bind very weakly to the DNAzyme, global folding into the catalytically active structure is also observed in its presence of these cations. An overall correlation of cleavage activity, binding affinity and charge density was found. The K_D values of the monovalent cations are in the M^1 range, those of the earth alkaline metal cations in the M^{-3} range, and those of the transition metals cations zinc and strontium are in the M^{-6} range. Only the K_D value of the Ca^{2+} ion is not fitting into the order (see above). Its K_D is higher than that for Mg^{2+}. Whereas it has to be mentioned, that the dependence of cleavage activity on the dissociation constants and the binding affinity is not significant in the case of NH_4^+, Li^+, Na^+. To summarize, the effect of monovalent cations depends on their concentration and the combination with divalent cations. They can support cleavage but impede it if they replace divalent cations in a significant manner. In respect to Pb^{2+}, their role remains unclear.

Table 5. Effect of 150 mM monovalent salt on the cleavage rate of the trans-cleaving 17E DNAzyme in presence of 100 µM Zn^{2+} and 50 mM MES buffer (pH 6.0).

Type of salt	k_{obs} [min^{-1}]
Buffer only	0.2
LiCl	0.089
NaCl	0.12
KCl	0.10
NH_4Cl	0.097
RbCl	0.18
NaN_3	0.065
NaF	0.082
$NaNO_3$	0.11
NaBr	0.12
NaI	0.12
$NaClO_4$	0.13

The exact tertiary structure of the 8-17 DNAzyme family isn't known. Several studies revealed global folding of the 8-17 DNAzyme. Until now, there is no crystal structure but some FRET,[179, 180] single-molecule FRET (smFRET),[180-182] Tb^{III} luminescence spectroscopy[183] and cross-linking studies [181, 184] were carried out and are consistent with each other. Little folding happens independently from divalent metal cations. In Na-HEPES-buffer it was observed that stem I and III move slightly together but don't reach coaxially arrangement. However, this was only observed at 50 mM buffer (Na-HEPES), at 10 mM the effect was not noticed.[179, 181] The subsequent addition of Zn^{2+} or Mg^{2+} makes stem III moving towards stems I and II, whereas the metal-dependent folding affinity is higher for Zn^{2+}. 100 µM Zn^{2+}, 10 or 100 mM Mg^{2+} are adequate to saturate the folding, respectively. With 50 mM Mg^{2+} the duration of the folded state is shorter but the cleaved and unfolded state were shown to be more stable than with 10 mM Mg^{2+}. Most probably, the release of the product is slower at higher concentrations of Mg^{2+}, due to the stabilization of base pairs, whereas the cleavage is faster because the folded state is reached faster. Furthermore, Zn^{2+} and Mg^{2+} (as well as monovalent cations) are responsible for the beginning of conversion to Z-DNA in the stem II.

Plotting the FRET signal and k_{obs} against the concentration of the cations revealed that, in case of Mg^{2+} and Zn^{2+}, the activity depends on global folding. At the point of saturation of folding, the activity has not reached saturation and higher concentrations of Mg^{2+} and Zn^{2+} increase activity. Interestingly, global folding or Z-DNA formation was not observed in the presence of Pb^{2+}.[179] In the case of Pb^{2+}, neither saturation of the FRET signal nor saturation of cleavage activity (max. measured $k_{obs} \approx 4$ min^{-1}) was reached. Whereas, it is discussed, that global folding happens but the time resolution of FRET technique (100 ms) combined with manual pipetting does not allow measurement. Therefore, a reaction pathway (Figure 21) [182] was proposed by Lee and Koh et al. concerning the folding. This pathway is coherent with the earlier observation that cleavage in the presence of lead ions yields a different cleavage product (3'-monophosphate) than in presence of other ions.[178-180]

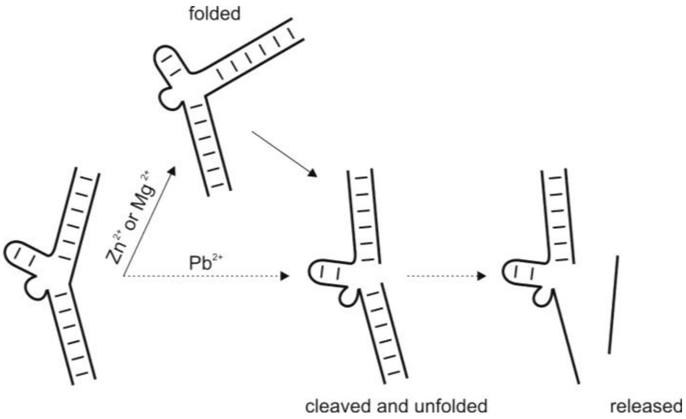

Figure 21. Folding states of the 8-17 DNAzyme in the cleavage reaction in presence of either Zn^{2+} or Mg^{2+} or Pb^{2+}, as it could be proven by FRET studies with the dyes at the 5'- ends of substrate strand and DNAzyme.

A and G of the triad loop (Figure 18 and Figure 19) are crucial for folding in the presence of Mg^{2+}. This was proven by cross-linking studies and smFRET measurements.[182, 184] There are no intra-DNAzyme cross-links but notably cross-linking of the substrate and DNAzyme involving the G·T wobble pair, the nucleotides of the bulge and the stem-loop of stem II. This results in a sandwich structure that cramps the scissile phosphate (Figure 22).[184] It is quite conceivable that the divalent cations are placed as a bridge between sites 15/15.0 and 12 (see above). This way they may stabilize the tertiary loop formed by the triade loop and the surrounding of the scissile phosphate. Another work postulated even the arrangement of nucleobases near to the scissile phosphate: Cross-linking studies with an uncleavable deoxy-thio-nucleotide at the cleavage position suggests that C13 and C3 are very close to the phosphate group.[185] The proximity of C13 is coherent with the sandwich structure as shown in Figure 22. However, a neighborhood of C3 is not directly seen from this illustration. Furthermore, C3 is proposed to act as base/acid in the cleavage mechanism. In another study, it was found that 7N or 8N of G11 may be involved in the cleavage reaction.

Although global folding couldn't be proven in the presence of Pb^{2+}, it was found that one binding site of lead may be the bulge with the scissile phosphate, especially at low buffer concentration, when stem I and III are not pre-orientated.[181, 183]. At 10 mM Na-HEPES-buffer spiked with 50 µM lead-cations cleavage activity is relatively low ($k_{obs} \approx 0.1\ \text{min}^{-1}$) and the plot of k_{obs} vs. $[Pb^{2+}]$ appears as a hyperbolic curve, which indicates monophasic cleavage. At higher concentrations of Na-HEPES (50 mM) cleavage kinetic with lead is biphasic. Concentrations of Pb^{2+} below 2 µM result in extremely low k_{obs}

values but velocity rises between 2 µM and 4 µM in a nearly exponential manner towards immeasurable values (≈ 4 min^{-1}). The role of the buffer is not clear. Maybe, the ionic strength influences the Pb^{2+} induced cleavage; however, the monovalent sodium ions obviously play a larger role as it was intended to them in the above-mentioned studies.[181]

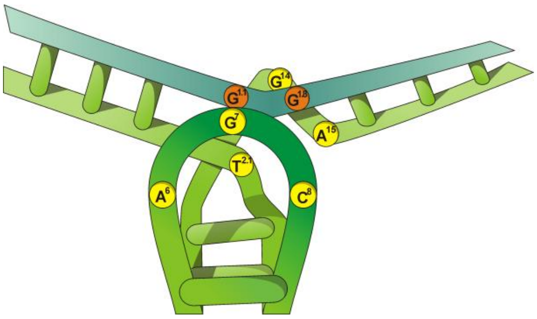

Figure 22. A model for the 8-17 DNAzyme-subtstrate complex. The substrate strand is shown in blue-green, the DNAzyme part in green. The folded structure was modeled according to crosslinking studies.[184]

It was demonstrated that the 8-17 DNAzymes are reliable self-cleaving molecules under various conditions. But, although there are widely used and a lot of research work was done with them, it is not possible to define the best conditions for a specific type, i.e. the 17E-DNAzyme. It is difficult to compare the present studies. The studies were done in various buffers, with or without sodium (Na-HEPES). Moreover, different concentrations of DNAzyme and substrate were applied. In some of the studies, an all RNA substrate strand was used (originally DNAzyme); however in most of the cases a DNA strand with a single ribonucleotide presented the substrate. To go into this in detail would go too far afield at this point. Finally, it should only be briefly announced that there is also selectivity towards the dinucleotide junction rN18-N1.1. The overall selectivity of the 8-17 DNAzyme: NG >NA >NC >NT.[186]

Of special interest for the present work is the activity of the 17E DNAzyme with a DNA–RNA hybrid substrate in the presence of Mg^{2+}–ions. Table 6 gives an overview about the cleavage assays with 17E and Mg^{2+} or exclusively monovalent salt (M^{+}) that were reported in the literature.

Table 6. k_{obs}-values for different single turnover (sto) experiments with 17E DNAzymes from literature. All cleavage assays were carried out at room temperature. Li et al. and Brown et al. did not mention if their MES or HEPES buffer contained Na^+, respectively, which concentration of Na^+ it contained. All references have the same corresponding author (Yi Lu).

Reference	*Li et al.[92]*		*Brown et al. [175]*		*Kim et al. [179]*	*Mazdumar et al. [178]*		
c_{Mg2+}	**10 mM**	**0.1 mM**	**10 mM**		**10 – 50 mM**	-		
M^+	-		-		-	**4 M NH_4^+**	**4 M Li^+**	**4 M Na^+**
buffer	50 mM MES	50 mM HEPES	50 mM MES	50 mM HEPES	50 mM Na- HEPES	50 mM Na-HEPES 25 mM EDTA		
pH	6.0	7.0	6.0	7.0	7.0	7.5		
$c_{17E\ enzyme}$	5 µM		5 µM		5 µM	5 µM		
$c_{17E\ substrate}$	0.5 nM		0.5 nM		4 µM	1 nM		
k_{obs} (sto) [min^{-1}]	**$1.7 \cdot 10^{-2}$**	**$1.1 \cdot 10^{-2}$**	**see [92]**	**$9 \cdot 10^{-1}$**	**$9 \cdot 10^{-2} – 1.2 \cdot 10^{-1}$**	**$1 \pm 0.1 \cdot 10^{-3}$**	**$0.7 \pm 0.1 \cdot 10^{-4}$**	**$\approx 10^{-5}$**

4.2 Investigation of the 17E-DNAzyme's Catalytic Activity

It was reasonable to investigate the 17E's cleavage activity before starting the *in vitro* selection assay based on this DNAzyme. For comparison of the performances of different DNAzymes or the performance of a single DNAzyme under various conditions, the kinetics of self-cleaving nucleic acids are of importance. Usually, in the case of nucleic acid enzymes, the reaction kinetic is measured for single turnover (the nucleic acid enzyme in excess) and multiple turnover (the substrate in excess) reactions. The cis-cleaving nucleic acid enzymes hold a special position. They are only capable of single-turnover but the reaction doesn't take place in excess of nucleic acid enzyme.

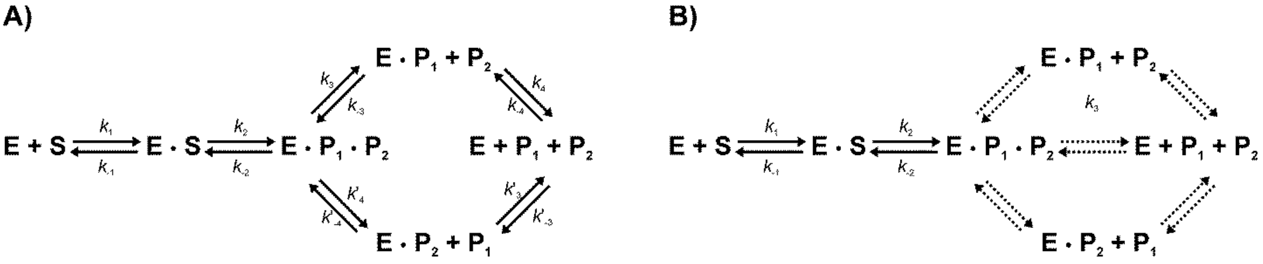

Figure 23. Minimal reaction-kinetic schemes of A) the small nucleolytic ribozymes and B) DNAzymes of the 8-17 type. The reaction course is not yet definitely clarified for 8-17 DNAzymes, as indicated by the dashed arrows and a unique velocity constant k_3, summarizing every possible step.

In the past, extensive kinetic studies with the small nucleolytic ribozymes were done.[106, 187] The minimal kinetic scheme includes (for a trans-cleaving ribozyme) substrate binding (k_1), cleavage (k_2), dissociation of cleavage products (k_3 and k_4), and the corresponding reverse steps (Figure 23 A). As described above the reaction mechanism of DNAzymes of the 8-17 types depends on the type of divalent cation and it has not definitely solved yet. The scheme in Figure 23 B doesn't display that two different 5'-products can be formed; that are 2'-3'-cyclic phosphate or the 3'-end-phosphates (Figure

20). For the cis-cleaving ribozymes and DNAzymes, again excluding the different products of the 5’-strand, the scheme can be further reduced as shown in Figure 24 because, only one product strand can leave the DNAzyme.

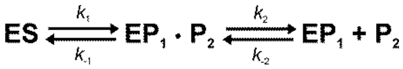

$$ES \underset{k_{-1}}{\overset{k_1}{\rightleftharpoons}} EP_1 \cdot P_2 \underset{k_{-2}}{\overset{k_2}{\rightleftharpoons}} EP_1 + P_2$$

Figure 24. Minimal reaction-kinetic scheme of cis-cleaving small nucleolytic ribozymes and DNAzymes of the 8-17 type.

A very common approach for the determination of comparable kinetic data for single turnover reactions is to apply Equation 1 to obtain k_{obs} (observed velocity constant at a given substrate concentration, a given ribozyme concentration or at the saturation concentration of nucleic acid enzyme; pseudo first order rate constant).[106, 187] k_{obs} includes k_1, k_{-1}, k_2 and k_{-2}.

The equation describes the product formation in a single turnover experiment and can be fitted to the data. P_0 is the initial fraction of cleavage product, P_t the fraction at a given point of time and P_∞ is the fraction of product at the equilibrium of the cleavage reaction.

Equation 1

$$P_t = P_0 + P_\infty(1 - e^{-k_{obs}t})$$

At saturating concentration of the ribozyme, k_{obs} is the sum of k_2 and k_{-2} (Figure 23 A). If the ligation reaction is negligible, Equation 2 can be used.

Equation 2

$$k_{obs} = k_2 = k_{obs,cleav}$$

For multiple turnover cleavage reactions, a hyperbolic curve is obtained by plotting the fraction of the product against the time. Then, the constant of Equation 1 describes the sum of all velocity constants shown in Figure 23. This approach is useful to make a fast comparison of various reaction conditions influencing the velocity of the reaction. At the beginning of the reaction, when practically no product is present, very fast, a stage is reached where the number of nucleic acid enzyme/substrate complexes is constant (steady-state phase, Equation 3) and the cleavage reaction is described by k_2 and k_3 (Figure 24). However, concerning that the dissociation of products of DNAzymes of the 8-17 type is significantly faster than the cleavage reaction ($k_3 >> k_2$),[188] the reaction is described as shown in Figure 25. The steady-state phase is described as a linear function of the time (Equation 4). In the course of time, the [ES] reduces and the velocity approaches zero. v_0 increases with increasing concentration of substrate. At the point of saturation with substrate $[ES] = [E]_{\text{total}}$. This means, the velocity depends only on the concentration of the enzyme and is described by Equation 5. k_{cat} is known as the turnover number and its reciprocal value is the time, which the enzyme needs for a single enzymatic turnover.

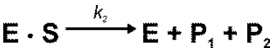

$$E \cdot S \xrightarrow{k_2} E + P_1 + P_2$$

Figure 25. Kinetic scheme of the initial reaction of a nucleic acid enzyme multiple turnover cleavage.

Equation 3

$$d[ES]/dt = 0$$

Equation 4

$$d[P]/dt = k_2\ [ES] = v_0$$

Equation 5

$$d[P]/dt = k_{cat}\ [E]_{total} = v_{max}$$

Plotting v_0 against [S] and applying the Michaelis-Menten equation, the Michalis-Menten constant (K_M) and the maximum velocity constant (v_{max}) as well as the turnover number (k_{cat}) can be determined (Equation 6). K_M is the sum of k_{-1} and k_2 divided by k_1. k_2 is mostly very small compared to k_{-1} and k_1 and K_M might be described by the quotient of k_{-1} and k_1. Therefore the K_M presents a dissociation constant and a value for the affinity of the enzyme towards the substrate.

Equation 6

$$v_0 = \frac{v_{max}[S]}{K_M + [S]}$$

4.2.1 Cleavage Assays with the 17E-DNAzyme

The 17E DNAzyme was selected by Yi et al in presence of Zn^{2+} but was found to cleave with Mg^{2+} as cofactor too.[92] Until now, this 17E DNAzyme cleaving a DNA/RNA hybrid substrate was investigated exclusively by the working group of Yi Lu.[175, 178, 180]. In our laboratory, DNAzymes were not established. Furthermore, it was aimed to work with Mg^{2+} as a cofactor, preferably, and the experimental conditions (concentration of DNAzyme and substrate, buffer-type) were supposed to be different to those in the literature. Therefore this DNAzyme was closely examined. The 17E DNAzyme (5'-CATCTCTTCTCCGAGCCGGTCGAAATAGTG AGT) was used for cleavage of a 5'-ATTO680-labeled RNA substrate. Prior to use the commercially provided substrate (5'-ACTCACTATrAGGAAGAGATG) containing a 5'-amino linker was reacted with a suitably activated ATTO680 derivative to generate the fluorescent RNA. The labeling reaction was purified by IP-RP-HPLC, ethanol precipitation and size exclusion chromatography. Single and multiple turnover experiments were carried out. The reaction temperature was set to 20 or 37 °C. Samples were taken and immediately, at indicated points of time, added to denaturing gel loading buffer. Afterwards, the reactions were analyzed by PAGE with the LI-COR sequencer.

First, the background cleavage without divalent cations was investigated. The result can be taken from Table 7. Catalytic activity or nonspecific cleavage was not observed after 18 h at 37 °C, except with 1 M NaCl (catalytic activity).

Table 7. Control of background cleavage without divalent cations. Samples were taken after 18 h incubation at 37 °C in 50 mM Tris-HCl. Hyphen: a combination that was not tested.

	Compositions of test mixtures			
pH	**20 nM substrate**	**20 nM substrate and 100 nM enzyme**	**20 nM substrate, 1 M NaCl**	**20 nM substrate and 100 nM enzyme, 1 M NaCl**
7.0	no cleavage	no cleavage	-	-
7.5	no cleavage	no cleavage	no cleavage	cleavage (≈ 50%)
8.0	no cleavage	no cleavage	-	-
8.3	no cleavage	no cleavage	-	-
8.5	no cleavage	no cleavage	-	-
9.0	no cleavage	no cleavage	-	-

An initial single turnover cleavage experiment (Figure 26) was carried out, where 100 mM Mg^{2+}, 100 µM Zn^{2+} and 20 µM Pb^{2+} were used as a cofactor (20 nM substrate, 100 nM DNAzyme). The different concentrations were used because according to literature, cleavage activity and the dissociation constants follow the row $Mg^{2+} << Zn^{2+} <$ µM Pb^{2+}.[175] Additionally, the DNAzymes were brought to reaction at 20 °C or 37 °C in three different buffers. Tris-HCl was applied at pH 7.5 or 8.3 and HEPES-Na at pH 7.5. For the reaction with lead, only HEPES-Na was used, because of precipitation with chloride in Tris-HCl. The overall trend was that at 37 °C the reaction proceeded faster. In every case, at the point of saturation 85–100 % of the substrate strands were cleaved. Reaction with Mg^{2+} was faster at higher pH-value and by the addition of NaCl, the reaction was slowed down. Obviously, even 50 mM HEPES-Na had a speed reducing effect, due to the low amount of sodium ions. With Zn^{2+} and Pb^{2+}, the trends were not as obvious as they were in the reaction with Mg^{2+}. In sum, these reactions were faster at 20 °C as at 37 °C and 1 M NaCl helped to restore higher cleavage activity at the higher temperature.

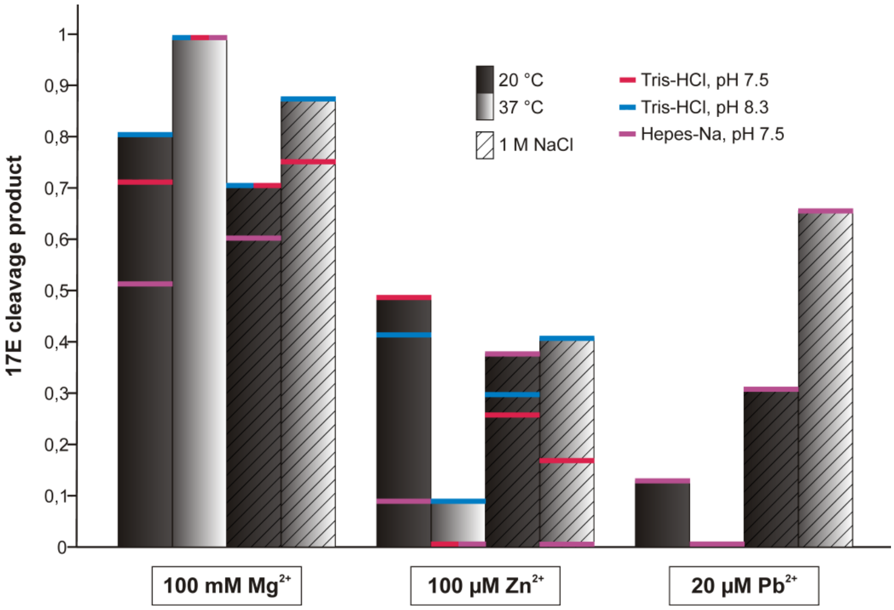

Figure 26. Comparison of 17E cleavage product with different divalent cations under various conditions after 5 minutes.

Additional experiments with 17E DNAzyme and Zn^{2+} as cofactor confirmed that activity was higher at 20 °C without NaCl and at 37 °C with NaCl.

Then, single turnover experiments with Mg^{2+} were carried out, to take a closer look at the cleavage activity of the 17E DNAzyme with this cation. The data obtained at 37 °C, with 10 or 100 mM Mg^{2+} and with a five-fold excess of DNAzyme are shown in Table 8. The five-fold excess of DNAzyme was not sufficient to reach saturation of the substrates. However, increasing the excess strongly fastened the reaction. The cleavage reaction turned out to be considerably fast, too fast, to be measured with the method applied, which includes manual pipetting. The presented data was obtained from measurements at 37 °C, the reaction proceeded slower at lower temperatures. Nevertheless, even at 4 °C, it was not possible to determine the saturation concentration of the DNAzyme because still, the reaction was too fast to be measured by the applied method. Therefore, no $k_{obs,cleav}$ could be determined.

Table 8. k_{obs} of 17E DNAzyme single turnover cleavage reaction at 37 °C (20 nM substrate, 100 nM enzyme; 50 mM Tris-HCl)**.**

pH	**k_{obs} (sto) [min^{-1}] 10 mM $MgCl_2$**	**k_{obs} (sto) [min^{-1}] 100 mM $MgCl_2$**
6.0		0.02 ± 0.00
7.0	0.13 ± 0.03	0.31 ± 0.07
7.5	0.45 ± 0.08	0.72 ± 0.20
8.0	0.65 ± 0.27	0.63 ± 0.19
8.3	0.62 ± 0.15	1.07 ± 0.11
8.5	0.63 ± 0.06	0.94 ± 0.10
9.0	0.87 ± 0.11	1.03 ± 0.20

The sensor system that was aimed to be developed, should amplify the signal through multiple turnover cleavage reactions. Therefore, the influence of Mg^{2+} and various monovalent cations, as well as the temperature on multiple turnover reactions with 100-fold excess of substrate (0.2 nM enzyme, 20 nM substrate), was tested. It was tried to evaluate the effect of Ca^{2+}, too, but it quenched the fluorescence of ATTO680, which was used to detect the substrate and product in a time-dependent manner. The monovalent cations were used as an additive in 100 mM Mg^{2+}-containing solutions. Li^{2+} and NH^{4+} were applied from 0.4 to 2 M (higher concentrations quenched the fluorescence signal), and Na^+ was added from 0.05 to 2 M.

Table 9.k_{obs} of 17E DNAzyme multiple turnover cleavage reaction at 37 °C (0.2 nM enzyme, 20 nM substrate; 50 mM Tris-HCl, pH = 7.5) **and different concentrations of Mg^{2+}(Left). The relative k_{obs} in reactions with 100 mM Mg^{2+} and monovalent cations referred to the reaction without monovalent cations (Right).**

$c(Mg^{2+})$ [mM]	**k_{obs} (mto) [min^{-1}]**
10	$5.12 \cdot 10^{-3}$
50	$9.22 \cdot 10^{-3}$
100	**$1.38 \cdot 10^{-2} \pm 3{,}54 \cdot 10^{-3}$**
125	$2{,}19 \cdot 10^{-2}$
150	$1.76 \cdot 10^{-2}$
200	$1.23 \cdot 10^{-2}$
300	$6{,}16 \cdot 10^{-3}$

$c(M^+)$ [M]	**relative k_{obs} (mto)**		
	Li^+	**NH_4^+**	**Na^+**
0.05			0.420
0.4	0.721	0.506	0.368
0.6	0.550	0.487	0.649
0.8	0.595	0.520	0.646
1	0.413	0.282	0.705
2	0.391	0.391	0.632

The maximum cleavage activity at pH 7.5 is reached with 125 mM $MgCl_2$ without the addition of any other cations. However, for *in vitro* selection with a supporting regulatory unit, a buffer containing 20 mM Tris-HCl (pH 7.6), 100 mM NaCl, 5 mM KCl, 1 mM $CaCl_2$, and 2 mM $MgCl_2$ was chosen (selection buffer SB, see below). This buffer was adopted from literature because it was used for successful *in vitro* selection of a streptavidin aptamer.[166] According to the findings of the investigation of the 17E-DNazyes's cleavage activity, the composition of this buffer was not supposed to be the best choice to support high catalytic activity. However, concerning that the earlier attempts of *in vitro* selection failed, it was decided, to choose a buffer that supports the *in vitro* selection of the aptamer functionality; provided that, the DNAzyme was active in this buffer. Therefore, the cleavage activity of the 17 E DNAzyme in this buffer was assayed at single and multiple turnover conditions. For single turnover, again a five-fold excess of ribozyme was chosen and the reaction was carried out at 37 °C. Two additional tests were carried out, where the final concentration of $MgCl_2$ was 10 mM or 100 mM. Multiple turnover assays were performed according to single turnover assays but at 100-fold excess of the substrate. At this point it should be kept in mind that Ca^{2+}, which is a component of the buffer, quenches the fluorescence of the ATTO680-dye. The kinetic parameters shown in Table 10 nevertheless reveal that the DNAzyme is active in the buffer that was desired for *in vitro* selection.

Table 10. k_{obs} of 17E DNAzyme sto cleavage reaction and v_0 of 17E DNAzyme mto cleavage reaction at 37 °C (20 nM substrate, 100 nM enzyme or 0.2 nM enzyme, 20 nM substrate; in SB) **and different concentrations of Mg^{2+}.**

	100 mM $MgCl_2$ in SB	10 mM $MgCl_2$ in SB	2 mM $MgCl_2$ in SB
k_{obs} sto [min^{-1}]	0.40 ± 0.01	0.35 ± 0.06	0.09 ± 0.01
v_0 mto [nM min^{-1}]	0.46 ± 0.16	0.14 ± 0.01	0.03 ± 0.00

4.2.2 Identification of Cleavage Products of the 17E DNAzyme

The cleavage products of the 17E DNAzyme are supposed to be a 2'-3'-cyclophosphate at the 5'-part of the cleaved substrate strand and a free 5'-OH-group at the 3'-part. Only in the case of Pb^{2+}-catalyzed cleavage, hydrolysis of the cyclophosphate and formation of 3'-phosphate was observed (Figure 20).[178-180] However, in this work, when the cleavage reaction was analyzed on 7.5 % LICOR PAGE, two cleavage products with slightly different electrophoretic mobility were observed. For LICOR-analysis, a sample of the substrate strand was treated with NaOH and used as a reference for the size of the cleavage product. On 15 %–PAGE, which was the standard for analysis of short (10–30 nt) oligos by fluorescence using the LICOR sequencer, no difference in electrophoretic mobility of the 5'-DNAzyme-product and the 5'-product of alkaline hydrolysis was observed. But, on 7.5 or 10 % PAGE, the product of alkaline hydrolysis (and following neutralization with HCl) migrated slightly faster and, occasionally, the band of the reaction product was resolved as two bands (Figure 27).

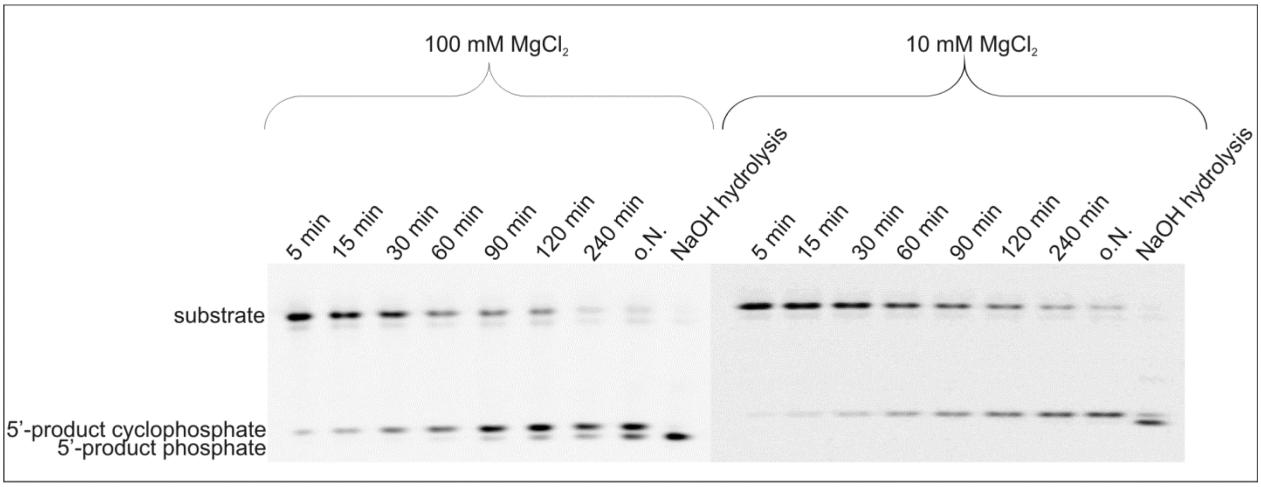
100 mM MgCl₂
10 mM MgCl₂
5 min
15 min
30 min
60 min
90 min
120 min
240 min
o.N.
NaOH hydrolysis
5 min
15 min
30 min
60 min
90 min
120 min
240 min
o.N.
NaOH hydrolysis
substrate
5'-product cyclophosphate
5'-product phosphate

Figure 27. 7 % denaturing LICOR PAGE of 17 E DNAzyme cleavage reactions with $MgCl_2$. Reaction conditions: 0.2 nM enzyme, 20 nM substrate, 50 mM Tris-HCl pH 7.5, 100 mM or 10 mM $MgCl_2$, 37 °C.

It was supposed, that the lower band, the one occurring from alkaline hydrolysis was the cleavage product with a phosphate at the 3'-end, whereas the higher band was the product with a 3'-cyclophosphate, that is, carrying one charge less, migrating slower in PAGE (pH 8.0). In order to demonstrate this assumption, the DNAzyme reaction and the alkaline hydrolysis of the substrate strand were analyzed by MALDI-TOF (Table 11). The analysis was carried out with the substrate strand carrying a 5'-aminohexyl linker. The result confirmed the interpretation of the gel analysis.

Table 11. Molecular weights and mass-to-charge ratio of the 17 E substrate and its cleavage products.

	MW [g/mol]	m/z found		deviation from expected m/z	
17 E substrate	6369.25	6375.47 3184.44		5.21 1.19	
		DNAzyme-reaction	alkaline hydrolysis	DNAzyme-reaction	alkaline hydrolysis
17 E 5'-product with cyclophosphate	3228.09	3229.90	-	0.80	
17 E 5'-product with phosphate	3246.1	-	3249.46		2.35
17 E 3'-product	3141	3142.87	3143.36	0.88	1.35

Applicability of the 17E-DNAzyme for the planned in vitro selection approach

The analysis of the 17E-DNAzyme's cleavage activity and reaction products revealed that it is a nucleic acid enzyme reliable catalyzing the transesterification reaction of its DNA/RNA - hybrid substrate. In a variety of conditions the reaction is very fast, even too fast to be analyzed with the applied methods. The desired buffer for *in vitro* selection contains cations that reduce the reaction rate and Ca^{2+}, which impedes the analysis of cleavage by fluorescence detection of the ATTO-680 labelled substrate. Nevertheless, activity was observed. Therefore, it was concluded that the 17E-DNAzyme was suitable for the planned *in vitro* selection approach.

4.3 Rational Design and Validation of the 17E-DNAzyme Inhibitor

Being familiar with the 17E DNAzyme, a model system was designed for the development of an *in vitro* selection method that combines SELEX and rational design. In the final (selected) system, the 17E DNAzyme was aimed to be to be linked to an aptamer domain, which inhibits the cleavage activity by Watson-Crick base pairing to catalytically indispensable parts of the DNAzyme. The inhibitory effect was aimed to be removed by binding of the analyte, streptavidin, to the aptamer domain. The DNAzyme-construct for proof of principle included an inhibitory sequence linked to the cis-DNAzyme (Figure 28). The library for *in vitro* selection should finally be constructed analogously to this setup. Then, the ten adenosine nucleotides linking the inhibitor strand to the DNAzyme were designed to be substituted by a longer stretch of randomized nucleotides. The inhibitor is a DNA sequence partially complementary to stem II. For proving the switching ability, a DNA oligomer complementary to the sequence of the inhibitor was applied. Using the software RNAstructure 5.7, this construct was designed to be the most stable in the active state ($\Delta G = 14.2$ kcal mol^{-1}). However, a mismatch was included to ensure certain flexibility (Figure 28).

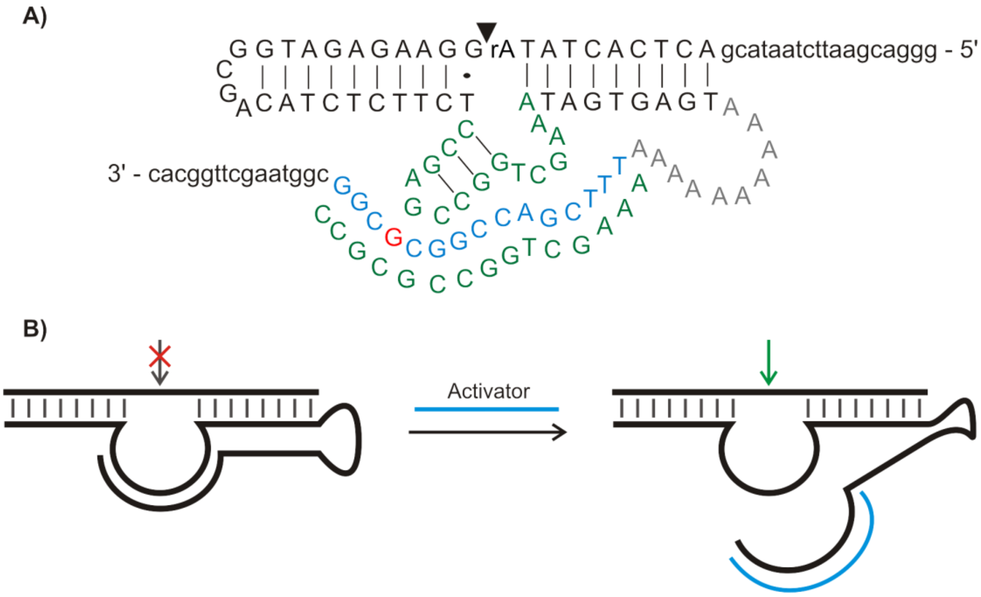
A)
G G T A G A G A A G G rA T A T C A C T C A gcataatcttaagcaggg - 5'
3' - cacggttcgaatggc
B)
Activator

Figure 28. Initial DNAzyme-construct for switchable catalysis. A) Lowercase letters are primer binding regions. Blue and green deoxynucleotides are complementary. The red colored guanosine represents a mismatch. B) Schematic illustration of the switching mechanism, that leads to an active DNAzyme.

This relatively long construct was prepared enzymatically by extension (Klenow-reaction) of two primers (5'-ATTO680-GGGACGAATTCTAATACGACTCACTATrA and 5'-AAAAAAAAAAAAAAAAAAAA-triethylene glycol phosphate-triethylene glycol phosphate-GTGCCAAGCTTACCGCCGCGCCGGTCGAAATTTTTTTTTTACTCACTATTTCGACCGGCTCGGAGAAGAGATGTCGCCATCTCTTCCTATAGTGAGTCGTATTAG) As the product of the Klenow-reaction is double-stranded DNA, one of the primers was modified with triethylene glycol units and lengthening nucleotides (oligo A). The DNA polymerase is able to extend the complementary strand as far as the triethylene glycol units and therefore this method yields mostly complementary DNA strands of unequal length. By denaturing PAGE the shorter sequence can be eluted and this way single-stranded DNA is yielded.[125] The construct showed low cleavage activity and was not switchable by the oligo effector EA-C1 (5'-CCGCGCCGGTCGAAA; Figure 28). However, it was not clear, if the inhibiting/activating strategy itself was not appropriate or if the ten adenosine nucleotides linking the DNAzyme to the inhibitor strand impeded the function. Additionally, the single strand production was not totally successful. The strands of different lengths that were obtained by the Klenow-reaction could not be quantitatively separated by PAGE. ssDNA preparation is a crucial step for the enzymatic synthesis of functional DNA and therefore, in the following, the results are reported more in detail.

The separation of strands by denaturing gel electrophoresis

The method for the separation of strands by denaturing gel electrophoresis was published as early as in 1995 by Williams et al.[125] This method promises to be a simple and economic strategy for the synthesis of ssDNA (Figure 29). The method is described for two DNA pools of different length (91 nt with a 20 nt lengthener segment and 247 nt with a 35 nt lengthener sequence). The quantitative separation of the strands was proven by 5'-[^{32}P]-labeling of the strands and detection with a phosphor imager.

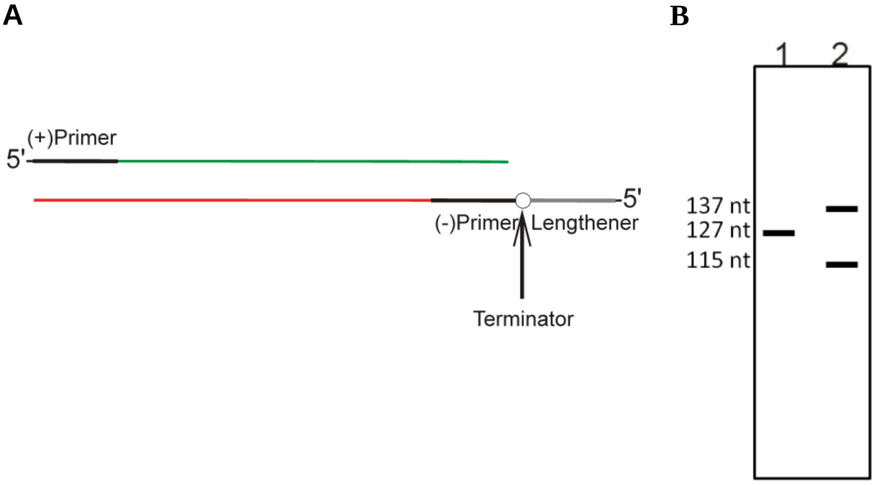

Figure 29. The principle (A) and the expected result (B) of the separation of strands by denaturing gel electrophoresis. The number of nucleotides refers to the sequences applied in the present work: 3'-antisense-Klenow primer: 127 nt; strand with the lengthener segment: 137 nt; shorter product strand (extended on the antisense-Klenow primer with the lengthener segment).

In the present work, with the specific sequences, it didn't succeed to separate the strands quantitatively. Several denaturing conditions and electrophoresis buffers were tested on PAGE and agarose gel electrophoresis. For PAGE in TBE buffer 5, 6, 7, 8, 9, and 10 % acrylamide was tested, with 7 and 8.3 M urea, or 10, 20, and 30 % formamide. Agarose gel electrophoresis was carried out with 2, 2.5, 3.5 % agarose, in TAE or MOPS, with 7M urea or 18 % formaldehyde. Additionally, alkaline agarose electrophoresis was tested. The most successful method was 10 % PAGE with 8.3 M urea, 10 % formamide, and heating of the gel electrophoresis device to 45 °C (water heating circuit). The result is shown in Figure 39 A. For preparative separation, a larger gel with longer migration distance was chosen. The bands were eluted and analyzed on the LICOR plate sequencer.

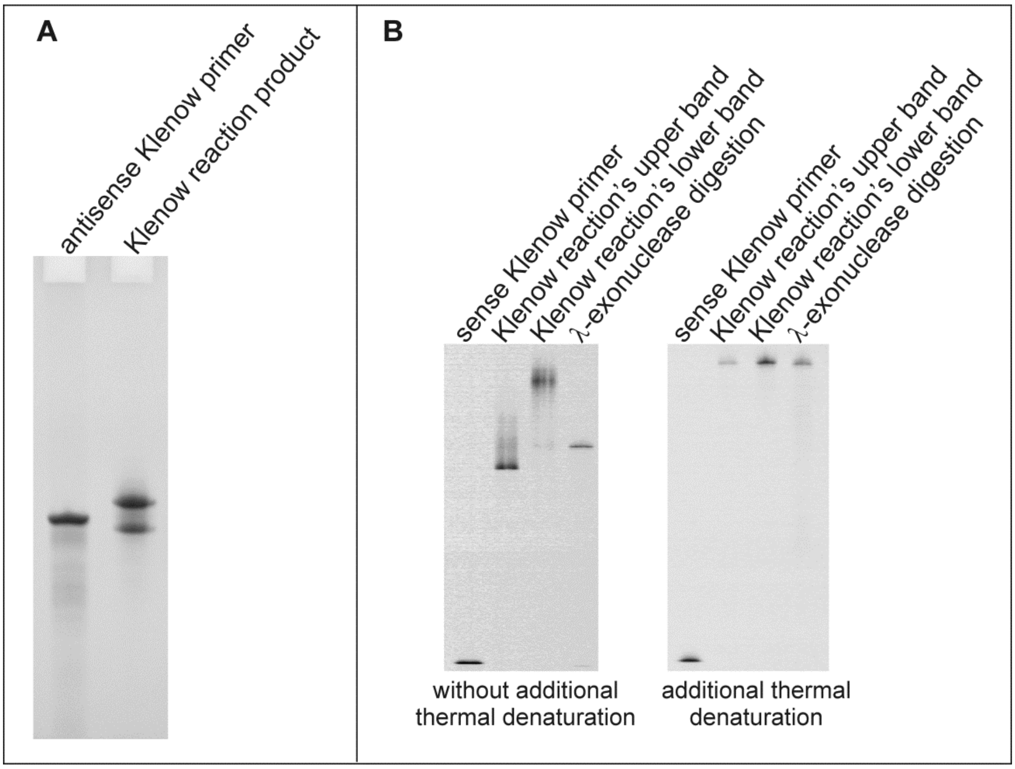
A
antisense Klenow primer
Klenow reaction product
B
sense Klenow primer
Klenow reaction's upper band
Klenow reaction's lower band
λ-exonuclease digestion
sense Klenow primer
Klenow reaction's upper band
Klenow reaction's lower band
λ-exonuclease digestion
without additional thermal denaturation
additional thermal denaturation

Figure 30. Separation of strands of unequal length by 10 % denat. PAGE. A) Separation of the Klenow reaction product by 10 % PAGE, 10 % formamide, 8.3 M urea, 45 °C. B) Analysis of the separation on 7.5 denat. (7 M urea) PAGE with the LICOR plate sequencer by fluorescence detection of the strands.

From the gels shown in Figure 30 B, it becomes clear that the separation was not successful. It resulted that both bands were contaminated with strands of the longer or shorter sequence, respectively. In the case of a quantitative separation, no signal would have been detected for the longer sequence, which wasn't labeled with the ATTO680-fluorescence dye. For comparison, a sample of the same ssDNA sequence, which was yielded by λ-exonuclease digestion, is shown. The analysis was done with different grades of denaturation. If the sample was applied without the usual thermal denaturation immediately before loading on the gel, arbitrary running behavior was detected. The results indicate for a strong duplex that was not separated by gel electrophoresis.

4.3.1 Proof of Principle with a Trans-Cleaving System

Digestion with λ-exonuclease was suitable to separate the strands, but the adenosine-linker was supposed to be another hurdle as well. Therefore, in order to eliminate the mentioned problems for the analysis of the inhibitor strategy, it was decided to test the setup with the trans-cleaving DNAzyme system. The inhibitor was added separately. In addition to the inhibitor sequence used in the initial design (5’-TTTCGACCGGCGCGG) named EI-C1 (enzyme inhibitor catalytic domain), two other inhibitor strands were designed. EI-C2 features two nucleotides less than EI-C1 at the 5’-end (5’-TCGACCGGCGCGG), and EI-S1 (enzyme inhibitor substrate domain) was supposed to block the substrate binding site instead of the catalytic core. (5’-ACTCACTATAAGAAGAGATG). As effector strands, EA-C1 (enzyme activator catalytic domain, 5’-CCGCGCCGGTCGAAA) and EA-S1 (enzyme activator substrate domain, 5’-CATCTCTTCTTATAGTGAGT) were applied. The enzyme and the substrate strand were the same as in section 4.2 'Investigation of the 17E-DNAzyme's Catalytic Activity'.

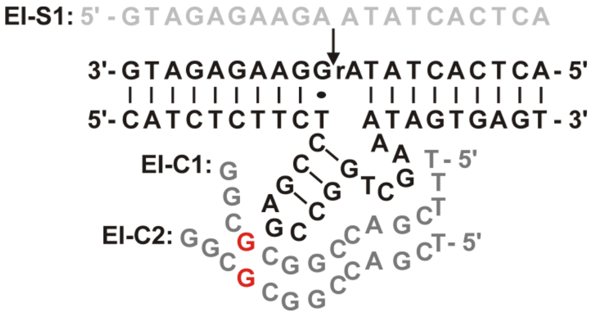
EI-S1: 5' - GTAGAGAAGA ATATCACTCA
3'- GTAGAGAAGGrATATCACTCA - 5'
5'- CATCTCTTCT ATAGTGAGT - 3'
EI-C1:
EI-C2:
T - 5'
T - 5'

Figure 31. Inhibitor sequences in proximity to their binding region at the 17E DNAzyme. The red letters indicate mismatches.

The cleavage reactions were performed at 37 °C and analyzed as described above. The procedure is described in section 6.19. At first, cleavage assays (sto) with a five-fold excess of DNAzyme over substrate were carried out (20 nM substrate, 100 nM enzyme). The inhibitors were added at five- or ten-fold excess (500 nM or 1000 nM). Figure 32 illustrates the cleavage product after 30 minutes. The reference reaction without inhibitors yielded 90.5 % cleavage product after 30 minutes. The diagram clearly shows that the inhibitory potential of EI-S1 was very low. EI-S1 was present as a competitive inhibitor in 25- or 50-fold excess of the substrate and the cleavage yield was only reduced by about the half. EI-C1 reduced the product formation by 98.2 % (500 nM) up to 99.4 % (1000 nM). EI-C1 was also shown to be a very potent inhibitor: its presence reduced the yield by 90.5 % (500 nM) to 95.1 % (1000 nM).

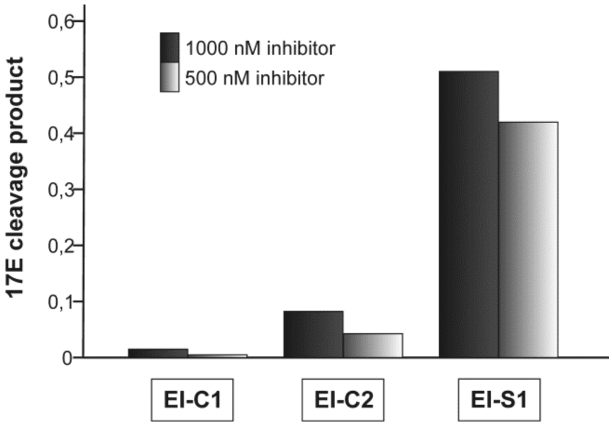

Figure 32. 17E cleavage product after 30 minutes with EI-C1, EI-C2 or EI-S1 (cleavage reaction with 20 nM substrate and 100 nM DNAzyme). The reference cleavage reaction without inhibitors yielded 90.5 % cleavage product after 30 minutes.

Next, the inhibitory effect of EI-C1, the most potent inhibitor, at different concentrations was tested. 250 nM, which corresponds to a 2.5-fold excess over DNAzyme was enough to reduce the cleavage yield after 60 minutes by about 93 %. Higher concentrations of EI-C1 up to 1000 nM inhibited the activity by maximal 98 % yield after 60 min. 1.2-fold excess of EI-C1 (120 nM) could reduce the yield only by 30 %. (Figure 33 A) By the addition of the oligo effector EA-C1, that is complementary to EI-C1, the cleavage activity was able to be restored.(Figure 34 B) With only 375 nM EA-C1 in presence of 500 nM EI-C1 again over 90 % cleavage product was yielded after 60 min. In presence of 120 nM inhibitor and with only 300 nM activator cleavage activity was completely restored.

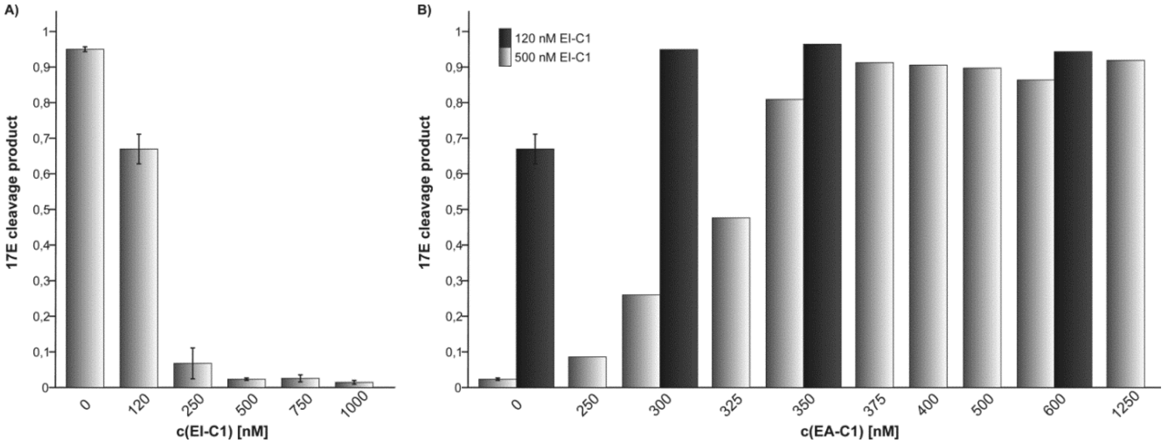

Figure 33. 17E cleavage product after 60 minutes with inhibitors and activators. (60 min = saturation of cleavage reaction with 20 nM substrate and 100 nM DNAzyme). **A) Without or with various concentrations of inhibitor EI-C1. B) With 120 or 500 nM EI-C1 and without or with various concentrations of activator EA-C1.**

Figure 34 A shows the time course of these reactions in the presence of the inhibitor EI-C1 and various concentrations of the activator EA-C1. The diagram illustrates that the inhibition and activation depended on the affinity of the inhibitor to the DNAzyme and the affinity of the activator to the inhibitor. The inhibition reflected not on the cleavage rate constant but on the cleavage yield. Additionally, the effect of the activator EA-C1 on inhibition with 500 nM EI-C2 (two nucleotides less than EI-C1 at the 3'-end) was analyzed. The result was similar to that with EI-C1 (Figure 34 C). However, the effect of reactivation was stronger. Furthermore, several tests were carried out to confirm the reliability of the experimental setup. In general, DNAzyme and substrate solutions were prepared separately, the DNAzyme solution with or without inhibitors and activators. To start the reaction, these solutions were mixed. Some cleavage reactions were carried out, where inhibitor and activator were added after starting the reaction or added to the substrate solution and where all components except magnesium chloride were prepared together and the reaction was started by addition of the salt. No difference in cleavage rate or yield was observed. Moreover, cleavage assays with only activator EA-C1 were

performed, to make sure, that its presence does not effect on cleavage activity. This was affirmed as shown in Figure 34 B.

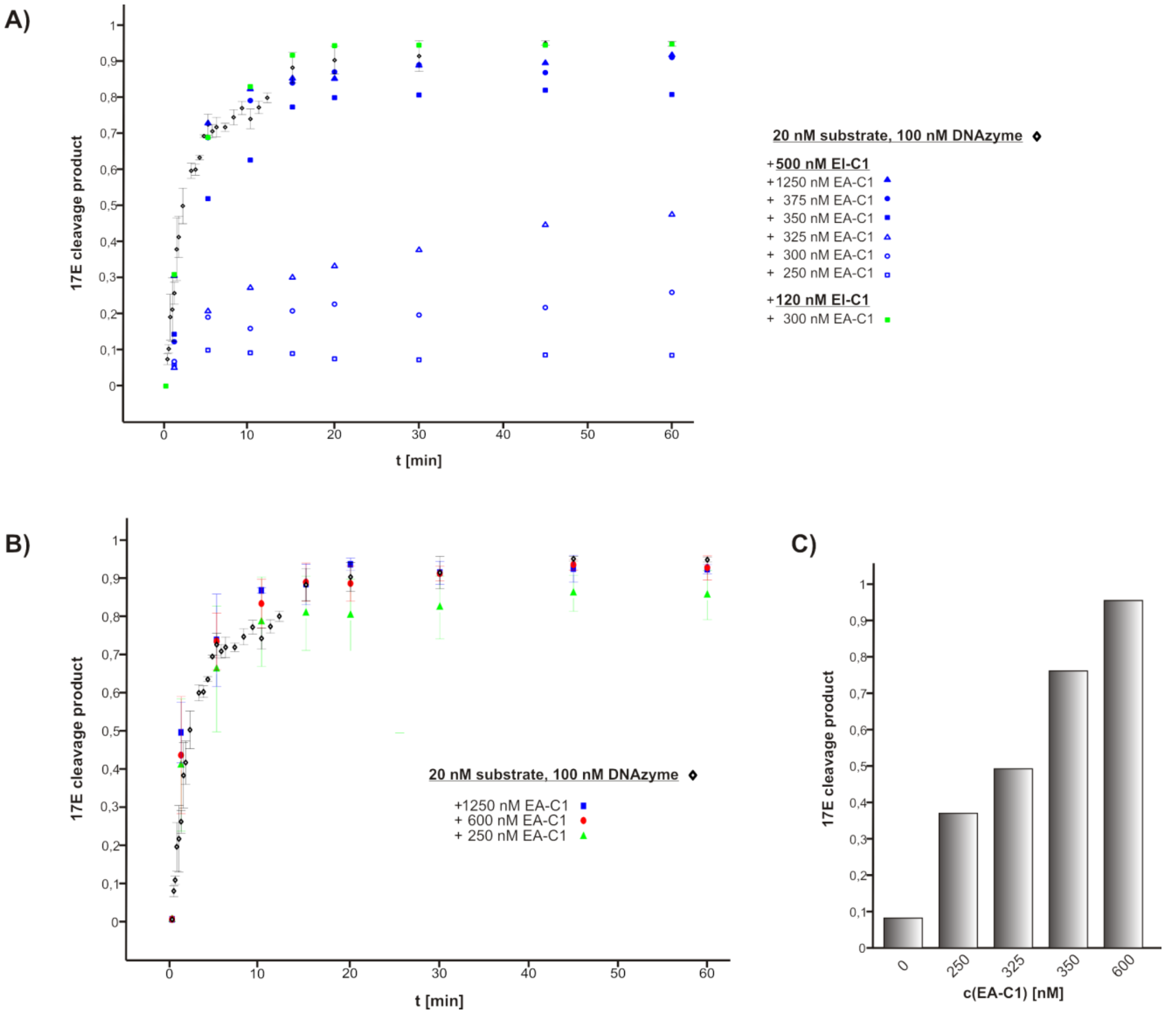

Figure 34. The cleavage reaction of the 17E-DNAzyme in presence of various inhibitor-activator combinations and in presence of activator, only. A) Time course of 17E cleavage (20 nM substrate, 100 nM DNAzyme; small black diamonds) with 120 nM inhibitor EI-C1 and 300 nM activator EA-C1 (green squares) or with 500 nM EI-C1 (blue symbols) and 250 nM (open squares), 300 nM (open circles), 325 nM (open triangles), 350 nM (closed squares), 375 nM (closed circles), 1250 nM (closed triangles) EA-C1. For reasons of simplicity results of experiments with 120 nM EI-C1 and 350 nM or 600 nM EA-C1 are not shown; the curves are equal to that for the experiment with 300 nM EA-C1. For the same reasons curves at 500 nM EI-C1 with 400 nM, 500 nM and 600 nM EA-C1 are not shown. B) Time course of 17E cleavage (20 nM substrate, 100 nM DNAzyme; small black diamonds) with 250 nM activator EA-C1 (green triangles), 600 nM EA-C1 (red circles) or 1250 nM EA-C1 (blue squares). C) 17E cleavage product after 60 minutes (saturation of cleavage reaction with 20 nM substrate and 100 nM DNAzyme) with 500 nM inhibitor EI-C2 and without or with various concentrations of activator EA-C1.

4.4 *In Vitro* Selection with a Supporting Regulatory Unit

4.4.1 Step 1: *In Vitro* Selection of the Aptamer Part

Based on the experiments and considerations that are described above, it was decided to use the inhibitor EI-C1 for the DNAzyme scaffold for *in vitro* selection. This decision was made as a result of two different considerations. The first was related to the extent of inhibition and the potential for release. The DNAzyme was inhibited by EI-C1 stronger than by EI-C2 but was released easier by EA-C1. It was decided that the power of inhibition is more important because it is a quality of the basic system i.e. the inhibited aptazyme. The ability to switch conformation to an active aptazyme was supposed to be selected. However, most likely, fewer sequences exist that are functional with EI-C1 than with EI-C2. The second consideration concerned the design of primers. It was not reasonable to add an additional primer binding site to the 3'-end inhibitory sequence. The additional nucleotides were possibly going to offset the inhibitory potential. As the inhibitory sequence was directly joined to the randomized domain, it defines the primer sequence and length. Using E1-C1, the resulting reverse primer was able to be two nucleotides longer and this, in the process of primer design for the whole planned *in vitro selection* process, showed to be more applicable (PD1: 5' CCGCGCCGGTCGAAA, PD2: 5' CATCTCTTC TCCGAGCCG GTC).

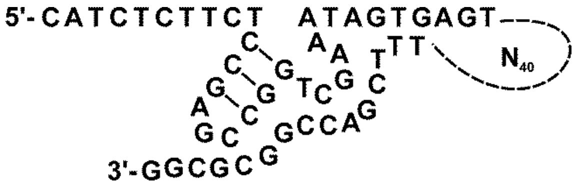

Figure 35. The sequence of the library for the first step in *in vitro* selection with a supporting regulatory unit. The secondary structure shown here is unlikely and only set by means of clarity.

Activity test of the library

To start with, it was analyzed if the library (5' CATCTCTTCTCCGAGCCGGTCGAA ATAGTGAGT**N40**TTTCGACCGGCGCGG, BIOTEZ), has cleavage activity and if it is controllable by the activator oligo EA-C1. Therefore, activity tests were performed at single turnover (sto) or at equimolar concentrations of DNAzyme-library. ATTO680-labeled substrate 17ES was used in the validation experiments above. Both tests were conducted with and without EA-C1.

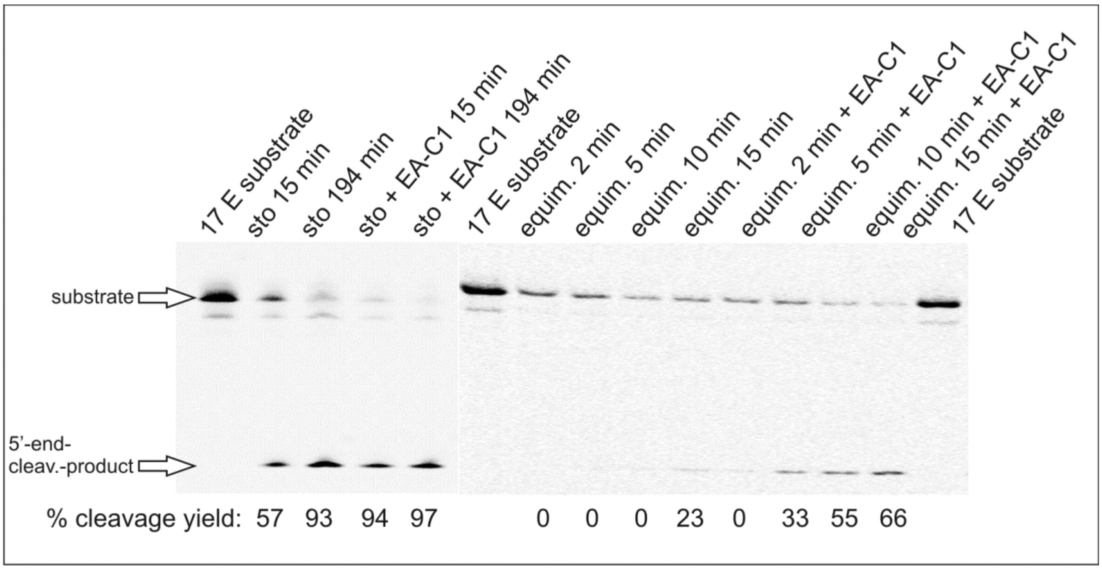

Figure 36. Activity tests of the library. The library is able to cleave the substrate, but cleavage activity is elevated by the activator. 7.5 denaturing PAGE, fluorescence detection.

The gel analysis of this cleavage experiment shown in Figure 36 demonstrated that the nucleic acid library contained some sequences that were able to cleave just in the presence of Mg^{2+} and others that aren't. Among these were some, whose cleavage activity was activated by the oligo EA-C1. This means the rationally designed inactivation strategy was applicable to the library chosen for this *in vitro* selection.

The in vitro selection strategy

The *in vitro* selection rounds were carried out on Dynabeads M280 SA, streptavidin coated magnetic beads, as it was done by Stoltenburg et al. for the DNA-aptamers and Tahiri-Alaoui for RNA-aptamers.[165, 166] The composition of the different buffers needed for the process is described in the methods. The buffer for *in vitro* selection was adapted from this *in vitro* selection for DNA aptamers as well (see chapter 4.2; 20 mM Tris-HCl, pH 7.6, 100 mM NaCl, 5 mM KCl, 1 mM $CaCl_2$, and 2 mM $MgCl_2$, +0.02% Tween20).[166] The composition of the elution buffer was 40 mM Tris-HCl, pH 8.0, 10 mM EDTA, 3.5 M urea. The pH of the buffer was adjusted to pH 8.0 at RT because of the strong temperature dependence of the pH-value of Tris-buffers.

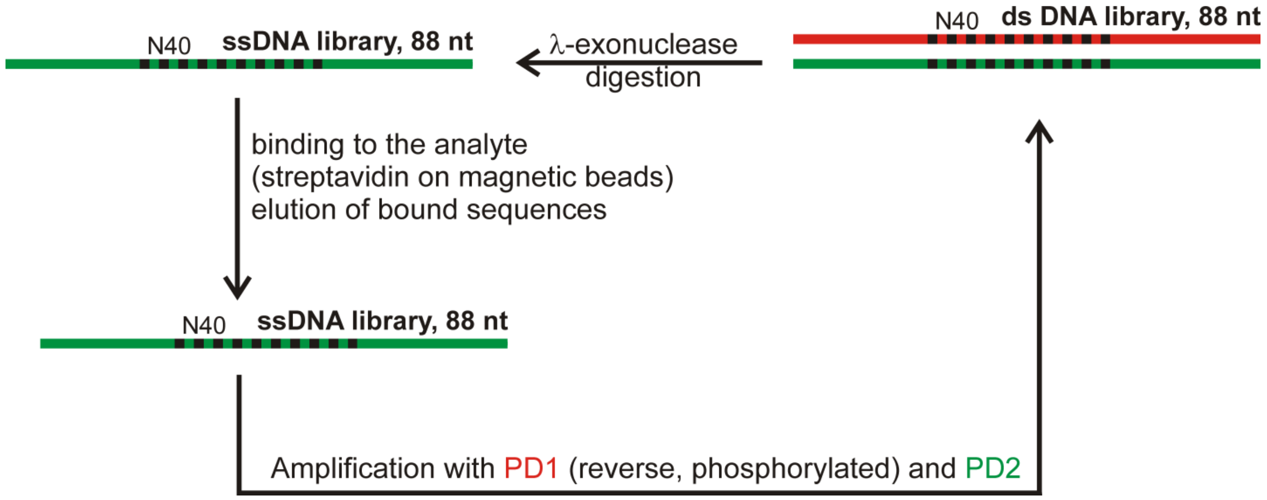
N40
ssDNA library, 88 nt
λ-exonuclease digestion
N40
ds DNA library, 88 nt
binding to the analyte
(streptavidin on magnetic beads)
elution of bound sequences
N40
ssDNA library, 88 nt
Amplification with PD1 (reverse, phosphorylated) and PD2

Figure 37. Scheme of the *in vitro* selection procedure for the aptamer selection (step 1). The green strands represent the DNA carrying the pool information . For the first *in vitro* selection round, it is applied as purchased to streptavidin magnetic beads. Sequences, which don't bind to the protein, are discarded. Subsequently, the active sequences are eluted and then amplified by PCR. The reverse primer is phosphorylated so that by λ-exonuclease digestion of the antisense strand, the pool is prepared for a new round of in vitro selection.

The scheme in Figure 37 is a rough outline of the *in vitro* selection procedure for the aptamer selection, showing only the core steps, namely, binding of the library to the analyte, amplification of active sequences and the synthesis of ssDNA.

Some reactions that were necessary for the performance of the *in vitro* selection, like the phosphorylation reaction of primer PD1 (for recognition by the λ-exonuclease), could be established independently from the *in vitro* selection itself. Others, like the production and purification of single-stranded DNA by λ-exonuclease digestion and the amplification steps had to be included in the process. The results for the phosphorylation and the digestion are presented in the following.

Phosphorylation of PD1

The phosphorylation of the antisense primer PD1 had to be optimized for reaction conditions and purification method. Since a large amount of PD1 is used for PCR reactions, lowest consumption of T4-polynucleotide kinase and highest yield after purification was targeted. (Figure 38 A). The product identity was proved by mass spectroscopy ($[M_{PD1\text{-}℗}+H^+]/z$ = 4644 Da, $[M_{PD1}+H^+]/z$ = 4563 Da, deviation$_{max}$ = 0.8 ‰, Figure 38 B). The yield varied between 60% and 100%.

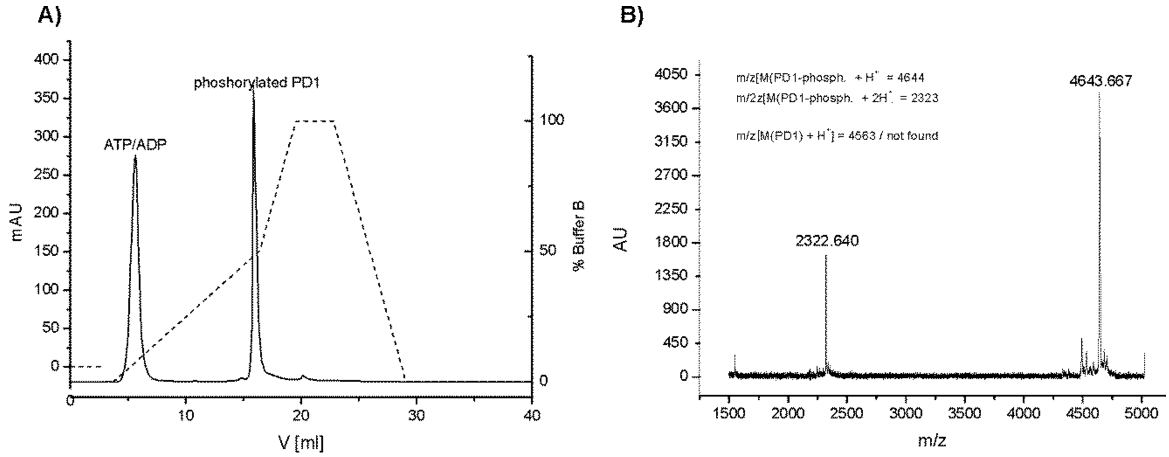

Figure 38. Analysis of the phosphorylation reaction. A) Chromatogramm of the HPLC-purification. B) Mass spectra of the phosphorylation reaction product.

Preparation of ssDNA by λ-exonuclease digestion of dsDNA

Following the amplification steps of the *in vitro* selection, the library is present as dsDNA. However, for *in vitro* selection, the sense strand has to be single stranded DNA. Digestion of the dsDNA, carrying 5'-phosphate at the antisense strand, was performed with λ-Exonuclease. It was found that the reaction works the best with the DNA purified on silica gel columns (see the manual of ePCR kit supplied by Roboklon). Another important aspect is the inactivation of the enzyme at 80 °C at the end of the reaction. If inactivation is missing, the enzyme stayed strongly bound at the DNA (first gel in Figure 39). Furthermore, the best ratio of DNA to λ-exonuclease was tested. For this application, the ratio was found to be 150 pmol DNA to 60 units of λ-exonuclease in a 120 µl reaction volume. This is the maximum reaction volume allowing efficient digestion (see 6.24). It is also possible to reduce the volume if needed.

In order to proof the success of the digestion, 5% native PAGE was performed. At this polyacrylamide concentration, the migration of dsDNA and ssDNA library is distinctly different and running time is just about 30 min. Denaturing gel conditions are not suitable since the migration behavior of both is nearly the same (Figure 39). Finally, it should be pointed out that thermal denaturation of the λ-exonuclease digestion sample before loading it on the native gel, was found to give the most reliable result.

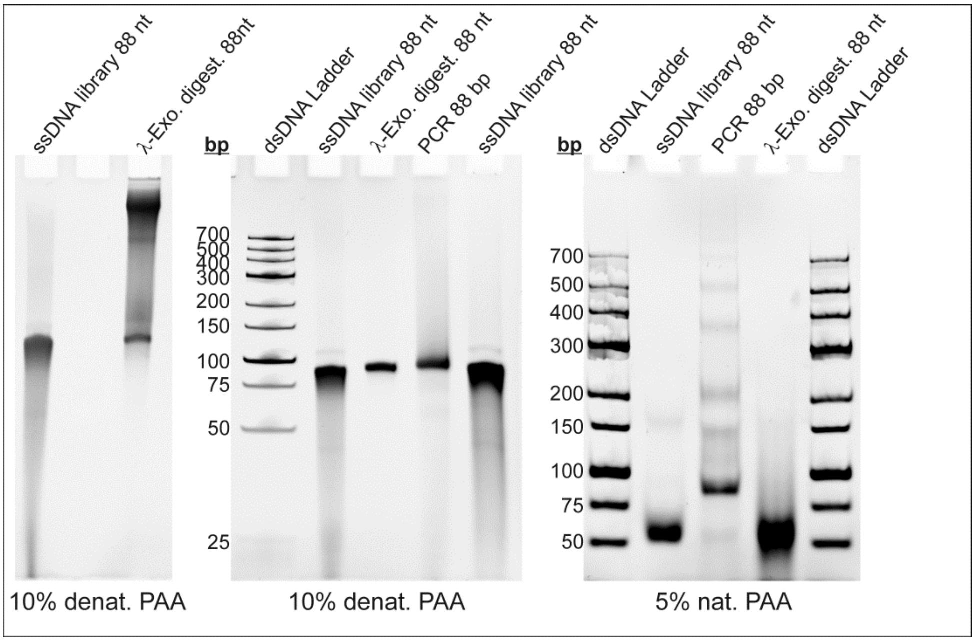
ssDNA library 88 nt
λ-Exo. digest. 88nt
bp
dsDNA Ladder
ssDNA library 88 nt
λ-Exo. digest. 88 nt
PCR 88 bp
ssDNA library 88 nt
bp
dsDNA Ladder
ssDNA library 88 nt
PCR 88 bp
λ-Exo. digest. 88 nt
dsDNA Ladder
700
500
400
300
200
150
100
75
50
25
700
500
400
300
200
150
100
75
50
10% denat. PAA
10% denat. PAA
5% nat. PAA

Figure 39. Exemplary PAGE images of the optimization of λ-exonuclease digestion (product: 88 nt). All gels were post-stained with EtBr. The first gel image shows that inactivation of the enzyme is indispensable. The other gel images were loaded with the same digestion and PCR reactions. Comparing both images it becomes clear that 5% nat. PAGE is the best to prove successful digestion.

Overview of the in vitro selection procedure

In the first rounds, the selection pressure was elevated by elevating the temperature and reducing the reaction time. Later on, washing steps were carried out more extensively. Additionally, bovine serum albumin (BSA) and herring sperm DNA (HS DNA) were added to the *in vitro* selection rounds to suppress non-specific binding. General procedures are described in the methods (see section 6.24 to 6.27, pp.123–125). The handling of the beads is also described in detail (section 6.13, p.118). The optimum PCR conditions (regular or emulsion PCR, cycle number) and compositions (amount/volume of template) were evaluated for each step. Sometimes, the amplification reactions had to be repeated because the outcome was not as desired or the PCR product had to be amplified again. These in-process-optimizations (PCR and other reactions) are the reason for not numbering of the selection rounds consecutively.

The process was started with a pool of three nmol ssDNA library ($1.8 \cdot 10^{15}$ molecules). In terms of variability, it wasn't necessary, after the first selection round, to introduce all the selected sequences in the next round. So this material served as the origin for several independent *in vitro* selections. Furthermore, after the amplification step of a given selection round, a proportion (at least 10 %) of the amplified DNA was stored and eventually was used for retrials, if problems emerged.

The in vitro selection procedure in detail

The material from the very first *in vitro* selection rounds with 3 nmol of the ssDNA library was consumed for establishing and optimizing. In order to prepare the first selection round with a second pool, 60 µl of 50 µM ssDNA library (3 nmol, $1.8 \cdot 10^{15}$ molecules) were denatured at 90 °C for 5 min and immediately chilled on ice for 10 min. Subsequently, the solution was held at RT for about 5 min. The process of denaturation was conducted before every *in vitro* selection round. Then, buffer components were added and the solution (total volume 500 µl) was proportioned in 50 µl aliquots to 10^7 SMBs. The mixture was incubated at 23 °C under mild shaking (300 rpm) for one hour and 15 minutes (SR2A1: *in vitro* selection round with pool 2 branch A round 1; Figure 40).

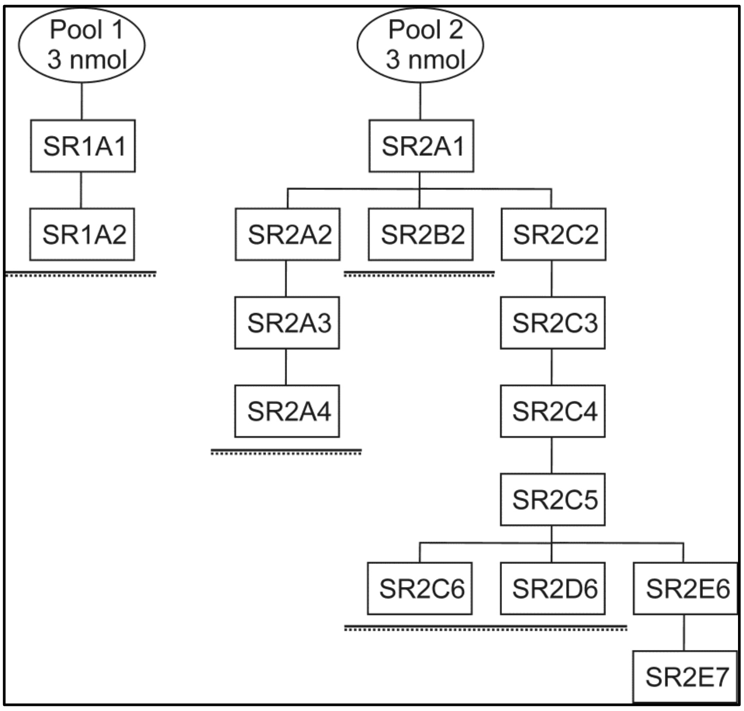

Figure 40. Chart of *in vitro* selection rounds starting with the second pool of ssDNA library. The nomenclature is: *in vitro* selection round with pool 2 branch A (or B–F)round 1 (or 2-7).

The material of the following *in vitro* selection rounds of branch A and B (Figure 40) were also consumed like the first pool for establishing and optimizing. The following section describes the procedure starting with the branch C. Figure 41 shows the gel analysis of the PCRs and no-template controls (NC) of oPCR1 2C3 (first open/regular PCR after *in vitro* selection round 2C3) and oPCR2 2C3 (second first open/regular PCR after *in vitro* selection round 2C3) and the λ-exonuclease reaction. This gel image is an example of an outcome that was judged as successful, that means, only little side products were detectable.

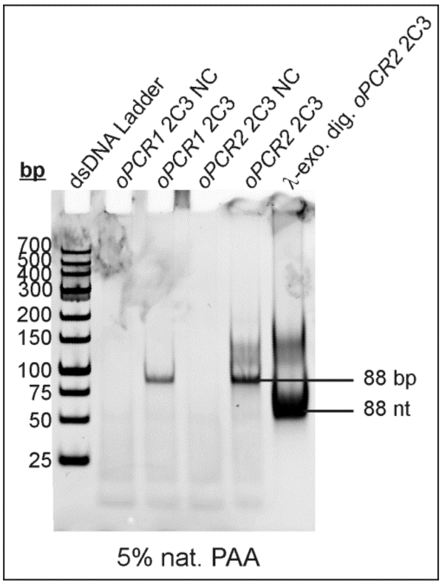
bp
dsDNA Ladder
oPCR1 2C3 NC
oPCR1 2C3
oPCR2 2C3 NC
oPCR2 2C3
λ-exo. dig. oPCR2 2C3
700
500
400
300
200
150
100
75
50
25
88 bp
88 nt
5% nat. PAA

Figure 41. PAGE (native) image of *oPCR1* 2C3, *oPCR2* 2C3 (product: 88 bp) and the corresponding λ-exonuclease digestion (product = 88 nt). The gel was post-stained with EtBr. NC = negative control reaction of the PCR.

Next, SR2C4, SR2C5, and SR2C6 were conducted. The gel analysis of the reaction steps of SR2C4 showed many and very strong higher bands than the desired one. Nevertheless, after λ-exonuclease digestion, mainly the desired product was visible on the gel (Figure 41). However, it was supposed that the variability of the pool was going to get smaller and that PCR was going to be more specific. But, after SR2C6 the yield of λ-exonuclease digestion was extremely low. From the image in Figure 42, it can be taken that the main PCR and λ-exonuclease digestion products after 2C6 weren't the desired one. Therefore, it was not possible to conclude, that the digestion reaction yielded the desired ssDNA as the main product.

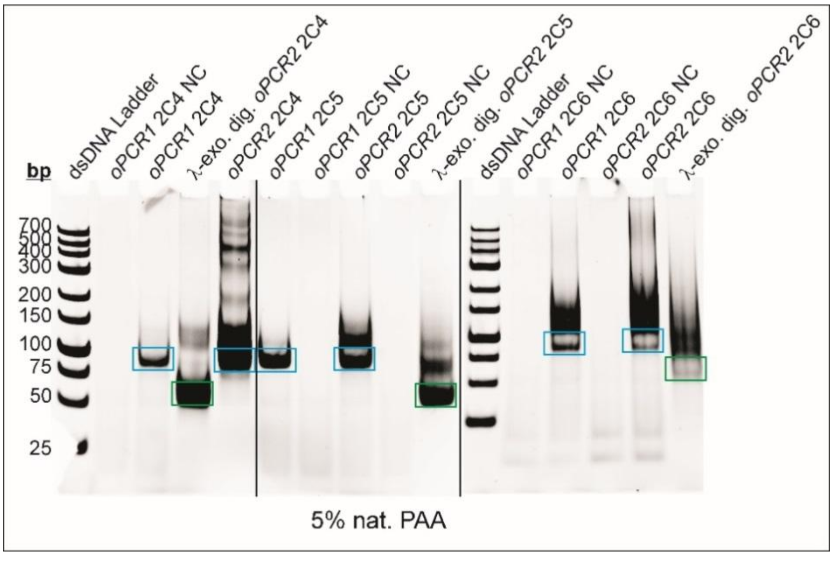
bp
dsDNA Ladder
oPCR1 2C4 NC
oPCR1 2C4
λ-exo. dig. oPCR2 2C4
oPCR2 2C4
oPCR1 2C5
oPCR1 2C5 NC
oPCR2 2C5
oPCR2 2C5 NC
λ-exo. dig. oPCR2 2C5
dsDNA Ladder
oPCR1 2C6 NC
oPCR1 2C6
oPCR2 2C6 NC
oPCR2 2C6
λ-exo. dig. oPCR2 2C6
700
500
400
300
200
150
100
75
50
25
5% nat. PAA

Figure 42. PAGE (native) images of all PCRs after SR 2C4 to 2C6 (product: 88 bp, blue boxes) and the corresponding λ-exonuclease digestions (product = 88 nt, green boxes). The gel was post-stained with EtBr. NC = negative control reaction of the PCR.

Additionally, a denaturing PAGE was performed (Figure 43). It is remarkable that the migration behavior of the samples of reactions after 2C4 and 2C5 is comparable at denaturing and native gel conditions but, the samples of oPCR2 2C6 didn’t or hardly migrate in denaturing PAGE, whereas in native PAGE only two bands at 88 bp and a smear about 100-200 bp is visible (Figure 41 and Figure 42). In oPCR2 2C6 variations from the standard PCR protocol were undertaken, in order to reduce the reaction volume and possibly increase the yield: template and primers were used at twice the standard concentration. This attempt wasn't successful but, the result is consistent with the observations made in the experiments for the simultaneous *in vitro* selection of aptamer and function (chapter 3.2) that the template concentration in PCR reactions during *in vitro* selection is critical.

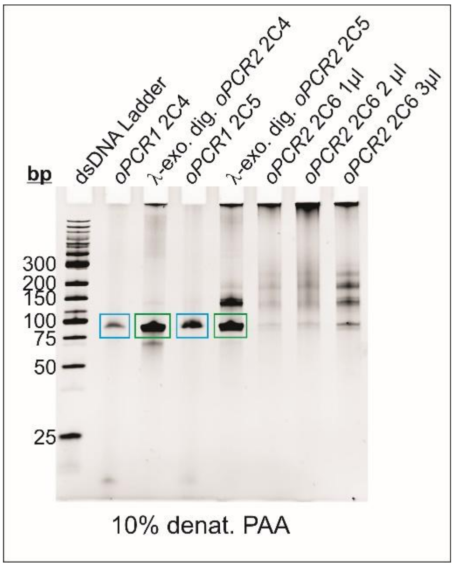

Figure 43. PAGE (denaturing) image of selected samples that were analyzed by native PAGE, yet (Figure 42). PCR product 88 bp: blue boxes; λ-exonuclease digestion 88 nt: green boxes. The higher bands of the dsDNA ladder cannot be allocated because they are denatured and the strands of a single marker band run differently. The gel was post-stained with EtBr.

However, it was decided to repeat oPCR2 after oPCR1 2C5 and purify the products by gel elution. In the following, for PCRs the amount of template was reduced by half or more and/or the PCR product was gel purified. Additionally, the amount of polymerase was varied, with no success. Eventually, good results were reached by a strong reduction of the amount of template and substantially elevation of the selection pressure, by the addition of an excess of the non-specific binders BSA (1 mg ml^{-1}) and herring sperm DNA (100 µg ml^{-1}) and extensive washing of the beads before elution of bound DNA sequences. In Table 12 the settings for selection pressure are summarized. Figure 44 shows a good example of the effect of the amount of template on the production of side products. In this case, after SR2F6, a preparative PCR was done with 0.8 µl of 200 µl selected material in a total volume of 1800 µl (corresponds to an estimated template concentration of 10^{-4} µM).

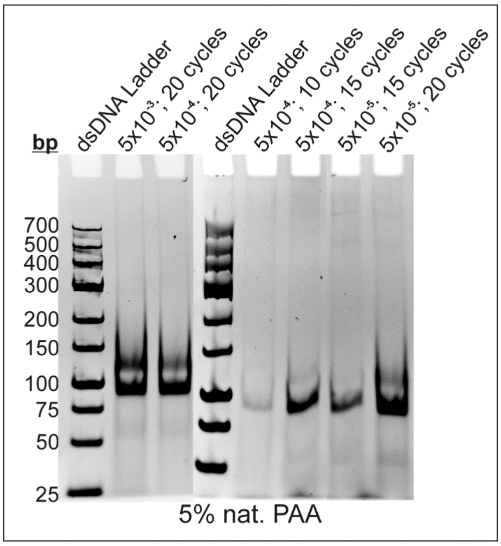
bp
dsDNA Ladder
5x10^{-3}, 20 cycles
5x10^{-4}, 20 cycles
dsDNA Ladder
5x10^{-4}, 10 cycles
5x10^{-4}, 15 cycles
5x10^{-5}, 15 cycles
5x10^{-5}, 20 cycles
700
500
400
300
200
150
100
75
50
25
5% nat. PAA

Figure 44. PAGE images of *test PCRs* after SR2F6 (product: 88 bp). Gels were post-stained with EtBr. The figures in exponential notation refer to the amount of template in µM (the concentration is estimated and 5x10^{-3} refers to 1 µl of total 200 µl selected material that was introduced in 100 µl PCR).

Table 12. Summary of the *in vitro* selection pressure's parameters of the final consecutive selection rounds.

***in vitro* selection round**	***in vitro* selection pressure**			
	additives	**reaction time**	**reaction temp.**	**washing**
SR2A1		75 min	23 °C	
SR2C2		30 min	23 °C	1 volume SB
SR2C3		10 min	23 °C	1 volume SB
SR2C4		10 min	25 °C	1 volume SB
SR2F5	BSA, h.s. DNA	10 min	25 °C	4 x 2 volumes SB
SR2F6	BSA, h.s. DNA	10 min	25 °C	6 x 2 volumes SB; 4th step: 5 min

4.4.2 Binding Assay

For the *in vitro* selection of the aptazyme, it was necessary to assay the binding activity of different pools of the aptamer selection rounds in order to choose the pool with highest catalytic activity. Initially, it was decided for a gel-shift assay (EMSA, electrophoretic mobility shift assay) with streptavidin. If the pool is mixed with streptavidin, the bound sequences would migrate slower than the non-bound ones. The method was validated by the application of biotinylated primer on TBE-buffer (tris/borate/EDTA) PAA gels. The result is shown in Figure 45. Whereas the biotinylated primer was strongly retained by the protein, initially, this was not observed with different pools of *in vitro* selection.

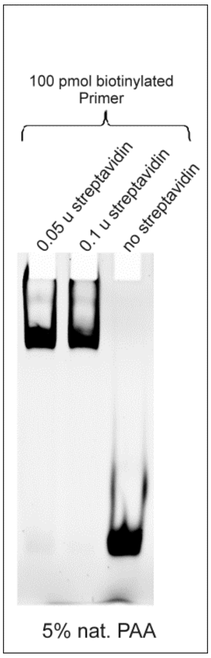

Figure 45. Validation of the EMSA for analysis of binding of any pool to streptavidin by 5% native PAGE. The biotinylated primer was mixed with streptavidin before sampling. Running and gel buffer was TBE. The gel was post-stained with EtBr.

In the following experiments gel concentration, temperature (as cooler the gel and the buffer, complexes may be more stable), running time, voltage, and the amount of streptavidin (or DNA) were varied. Starting with selection round SR2C4, often a considerable fraction of DNA remained in the pocket of the gel, which was a hint of DNA-streptavidin complexes. However, stained pockets are a frequently observed phenomenon; therefore, this could not be taken as a reliable result. EMSA also was performed on an agarose gel, to allow the suspected complexes to migrate into the gel (pores in agarose gel are larger than the ones in PAA gel). However, on the agarose gel, no difference in the running behavior between the sample with and without streptavidin was detected. Additionally, the samples were analyzed by reversed phase HPLC. An additional small peak was observed for the samples of higher selection rounds in the presence of streptavidin. This result again was not clear enough to prove the binding event, but, considering, that the stability of DNA/streptavidin complexes in acetonitrile might not be given and nevertheless, a signal was observed, the result motivated for repeating the EMSA with a buffer that resembles to the selection buffer. The selection buffer contains very high concentrations of salt and exhibits insufficient buffer capacity for gel electrophoresis. By reducing sodium chloride by half (50 mM instead if 100 mM), adding tris-borate and exchanging the buffer in short time intervals (1–3 min) during the run this problem could be overcome. The details of the procedure are described in the section 6.28. This way, it could be proven that the *in vitro* selection for an aptamer was successful and the affinity of the DNA pools for streptavidin increased with the selection rounds (Figure 46).

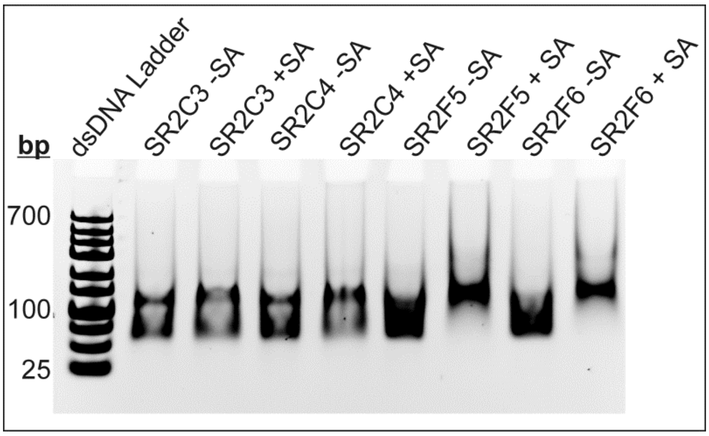

Figure 46. 5% PAA EMSA of different *in vitro* selection rounds. The gel was post-stained with EtBr.

The gel image in Figure 46 impressively shows that the sequences of SR2F6 and SR2F5 are totally retained by streptavidin under the given conditions. However, it was, because of the low buffering capacity of the running buffer, not possible to reach better separation of retained and non-retained sequences. As it can be seen from the lanes of selection rounds three and four (Figure 46, SR2C3 and SR2C4), the present resolution is not sufficient to quantify the bound sequences. Therefore the potency of binding could not be quantified, which would be a hint for the remaining variability of the pool. However, it was decided to start with SR6F2 into the *in vitro* selection part 2, the selection of the aptazyme. This decision was based on the various reports about *in vitro* selection in the literature. The most common number of rounds is about ten. This number, in general, refers to the round, whereupon no significant enhancement of binding capacity or catalytic activity was detected. For sure the number varied between the experiments. However, most researchers claim that five to 15 rounds are needed for a successful *in vitro* selection with nucleic acids.[144, 189, 190] This merely empirical statement is supported by a systematic investigation of 492 *in vitro* selection experiments, which demonstrated that the vast majority of SELEX experiments were carried out with ten rounds.[50]

A tabular summary of the finally successful *in vitro* selection steps that let to SR2F6 can be found on the next page.

Table 13. Summaray of *in vitro* selection rounds that let to SR2F6. oPCR = open (common) PCR, ePCR = emulsion PCR, eluate = sequences that bound to streptavidin in the selection round, RV = reaction volume of a single PCR reaction in µl, column pur. = PCR was purified on silica columns, precip. = PCR was ethanol precipitated. The second column shows the amount of ssDNA that was introduced in the designated round.

***in vitro* Sel. Round**	**ss DNA [pmol]**	**Composition**	**Conditions**	**Washing**	**Amplification steps**	
					PCR 1	***PCR 2 and following PCRs***
SR2A1	3000	20 µl beads/50 µl (10 x) 1xSB	23 °C 75 min 500 rpm	-	*ePCR1* 1/1 of eluate 25 cycles, 1 x RV 50, η = 10 pmol	*ePCR2* (1/1 column pur. *ePCR1*) 25 cycles, 4 x RV 50, η = 55 pmol *oPCR3* (1/4 column pur. *ePCR2*) 15 cycles, 30 x RV 50, η = 509 pmol
SR2C2	209	40 µl beads/100 µl	23 °C 30 min 500 rpm	1 x 100 µl	*oPCR1* 1/1 of eluate 15 cycles, 1 x RV 50	*oPCR2* (1/2 precip. o*PCR1*) 20 cycles, 20 x RV 100, η = 1054 pmol
SR2C3	200	40 µl beads/100 µl	23 °C 10 min 500 rpm	1 x 100 µl	*oPCR1* 1/1 of eluate 15 cycles, 4 x RV 50	*oPCR2* (1/1 column pur. o*PCR1*) 15 cycles, 20 x RV 100, η = 621 pmol
SR2C4	200	40 µl beads/100 µl	23 °C 10 min 500 rpm	1 x 100 µl	*oPCR1* 1/1 of eluate 15 cycles, 4 x RV 50	*oPCR2* (1/1 column pur. o*PCR1*) 15 cycles, 20 x RV 100, η = 613 pmol
SR2F5	32	30 µl beads/60 µl 1xSB 100 µg ml-1 h.-s.-DNA 1 mg ml-1 BSA	25 °C 10 min 500 rpm	4 x 120 µl	*oPCR1* 1/1 eluate 20 cycles, 8 x RV 100	
SR2F6	50	50 µl beads/100 µl 1xSB 100 µg ml-1 h.-s.-DNA 1 mg ml-1 BSA	25 °C 10 min 500 rpm	3 x 200 µl, 1 x 200 µl 5 min, 2 x 200 µl (total: 6 x 200 µl)	*oPCR1* 5/10,000 (5x10-4) eluate 15 cycles, 18 x RV 100 µl	

4.4.3 Step 2: *In Vitro* Selection of the Aptazyme

Based on the results of the binding assays and the above-mentioned considerations, the DNA pool of SR2F6 was assumed to be suitable to be converted into a cis-DNAzyme form to select for streptavidin-mediated cleavage activity (see Figure 16). For this conversion (Figure 47) a Klenow reaction (6.22) was performed, where the antisense Klenow Primer (5'-CACTATTTCGACCGGCTCGGAGAAGAGATGTCGCCATCTCTTCCTATAGTGAGT) and the ssDNA pool of SR2F6 (reamplification and digestion with λ-exonuclease) were extended on each other. The forward primer PD3 (ACTCACTAT**rA**GGAAGAGATGGCGACATC) for amplification reactions, was designed to have a melting point near to PD1, expecting that this way the PCR conditions could be the same as in part 1 (see section 6.27, p.125).

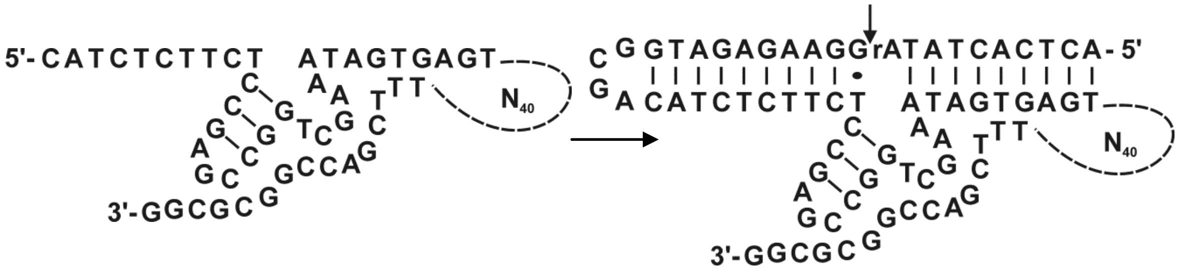

Figure 47. Conversion of the pool of Part 1 into the pool for *in vitro* selection Part 2.

Preparation of the pool and SRλ

The Klenow-reaction was not quantitative and the product was not pure. Therefore, it was purified by PAGE. Afterward, the sequences were amplified by PCR. Then, a digestion with λ-exonuclease was performed. This reaction is the first selection round of *the in vitro* selection of the aptazyme and it was named SRλ (selection round λ, Figure 51). During the λ-exonuclease digestion, every sequence that was not inhibited by the inhibitory sequence at the 3'-end (Figure 16, p.51), was going to be cleaved and therefore was going to be removed from the pool through gel purification. First, it was tried to separate the products on denaturing PAGE, but the sequences didn't migrate as expected (Figure 48 B) and therefore couldn't be located. In native PAGE, however, the bands could be located reliably and the separation was satisfactory (Figure 48 A and C). In order to prove the identity of cleaved and intact sequences, the product of gel elution was incubated in 0.5 N NaOH at 45 °C for 45 min. The correct product was supposed to be cleaved by this treatment at the single ribonucleotide junction, which was introduced by primer PD3. The reaction was supposed to yield a product, which was by 10 nucleotides shorter than the library and was of the same length as the unwanted active sequences of SRλ. As shown in Figure 48 C, this was proven. Moreover, this gel image shows that the ssDNA remained intact during the harsh elution procedure that involved freezing and heating up to 95 °C several times (6.6.11).

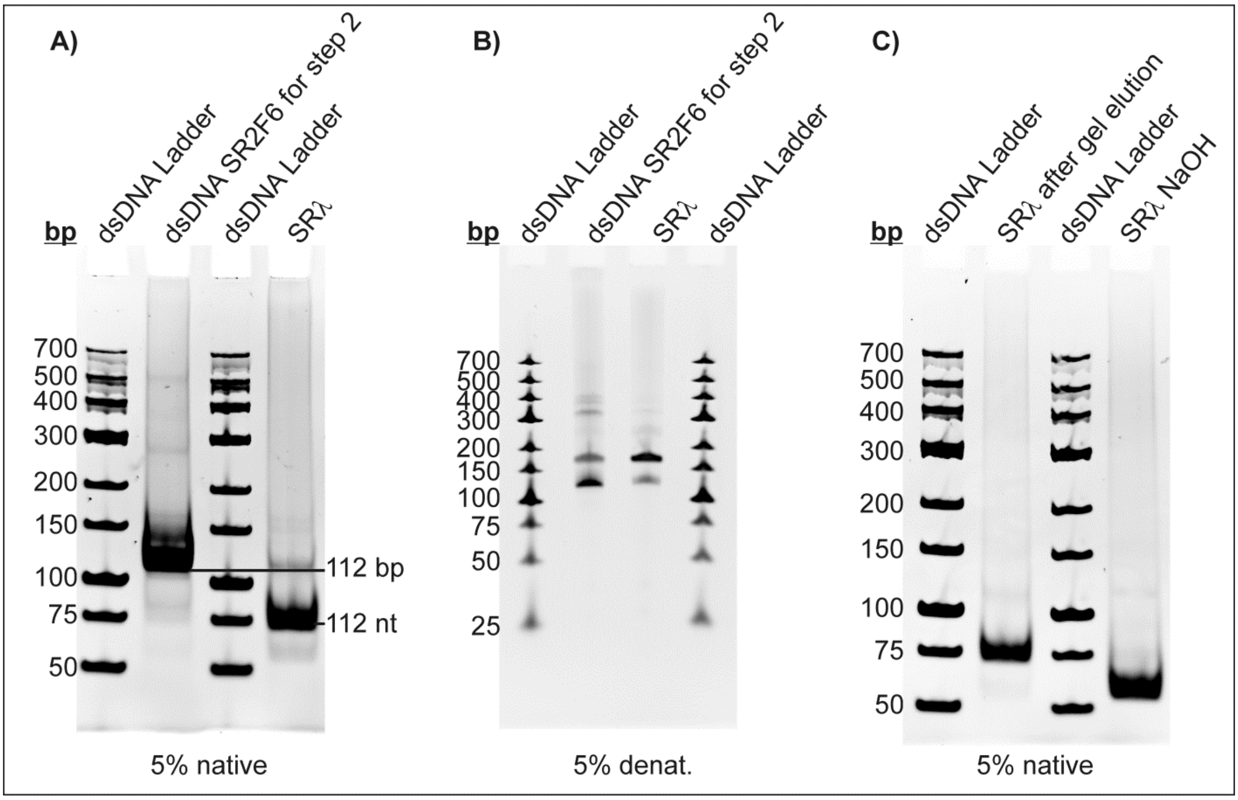
A)
bp
dsDNA Ladder
dsDNA SR2F6 for step 2
dsDNA Ladder
SRλ
700
500
400
300
200
150
100
75
50
112 bp
112 nt
5% native
B)
bp
dsDNA Ladder
dsDNA SR2F6 for step 2
SRλ
dsDNA Ladder
700
500
400
300
200
150
100
75
50
25
5% denat.
C)
bp
dsDNA Ladder
SRλ after gel elution
dsDNA Ladder
SRλ NaOH
700
500
400
300
200
150
100
75
50
5% native

Figure 48. 5% native and denaturing (7 M urea) PAGE of dsDNA (112 bp) and SRλ (112 nt) ; A and B. 5% native PAGE of purified SRλ (112 nt) and alkaline cleavage reaction of SRλ (102 nt); C. All gels were post-stained with ethidium bromide.

Binding activity of the extended pool

Additionally, it was investigated, if the extended pool had kept its binding activity toward streptavidin. An EMSA was conducted as described in the previous chapter (p.82). 3.6 pmol of ssDNA of SRl were incubated with 3.2 µg streptavidin (the same amount of streptavidin as in the assay carried out after the aptamer selection), 0.8 or 0.16 µg. In EMSA, streptavidin caused a noticeable retention of ssDNA (Figure 46). As it was proven that the aptamer function of the pool was maintained through transfer into the *cis*-cleaving system, step two of the *in vitro* selection could be tackled.

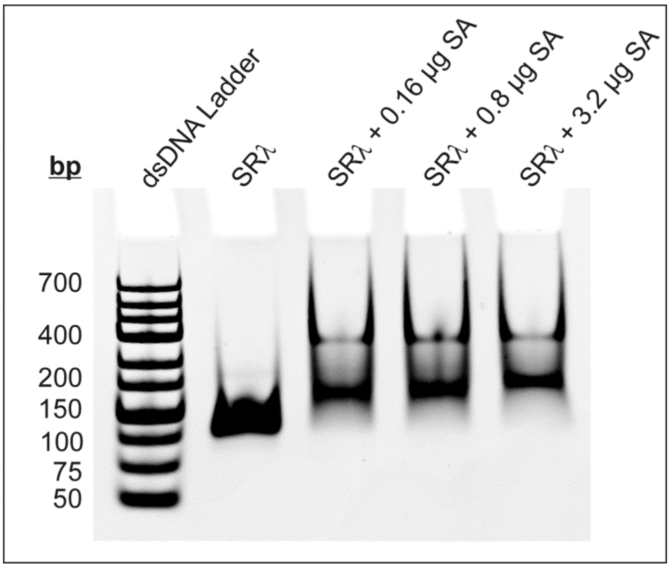

Figure 49. 5% PAA EMSA of different *in vitro* selection rounds. The gel was post-stained with EtBr.

The in vitro selection strategy

For the *in vitro* selection of cleavage activity, the streptavidin magnetic beads couldn't be used for separation of the active and inactive sequences anymore. The separation had to be based on the cleavage activity. In the simultaneous *in vitro* selection of aptamer and catalytic function (see section 3.2) streptavidin magnetic beads were used for this purpose. The DNA was modified with biotin and this way, cleaved sequences could be eluted. In a system like the present, where the analyte is streptavidin, of course, this method isn't appropriate. A simple alternative method is the gel separation of the sequences after an *in vitro* selection round. However, as discussed before, the yield in gel elution is low (page 41). Another possibility is to exploit other specific strong binding partners than streptavidin-biotin to perform the *in vitro* selection on a solid phase. In principle, the toolbox is large and well stocked. However, among the variety of different possibilities, immobilization of the library by Click chemistry was the method of choice. The term Click-reaction refers to reactions linking small molecules with heteroatoms (C-X-C) that meet several criteria, which include modularity, high yield, inoffensive byproducts, wide scope, stereospecificity, and the reactants being readily available.[191] One of these reactions is the 1,3-dipolar cycloaddition reaction, also known as Cu^I catalyzed [3+2] azide-alkyne cycloaddition (CuAAC-reaction).[192, 193] Although this reaction was used to modify nucleic acids,[194, 195], depending on the application, the so-called strain-promoted Click-reaction may be preferred for this purpose because no copper is needed as a catalyst to achieve short reaction times and a good yield.[196, 197] The copper ions possibly hamper ongoing reactions or induce damage to the nucleic acid. The reactions of ring-strained alkynes with azide derivatives are almost quantitatively and proceed in PBS or Tris-HCl buffers in 1 to 3 h. Furthermore, there are fewer parameters to optimize as in Cu(I)-involving reactions.[194, 198-200] For the present purpose, the use of DIBAC (aza-dibenzo cyclooctyne) for reaction with an azide seemed convenient (Figure 50). It is a relatively fast reacting and relatively hydrophilic alkine.[200] Additionally, primer oligonucleotides, which are modified with this molecule and azide magnetic beads are commercially available. The beads, however, at that stage were available from two manufacturers only. It is that using azide magnetic beads wasn't established in the research community. Some work was done using azide-modified surfaces, however, not to immobilize biomolecules, but small molecules like fluorescent dyes.[199, 201, 202]

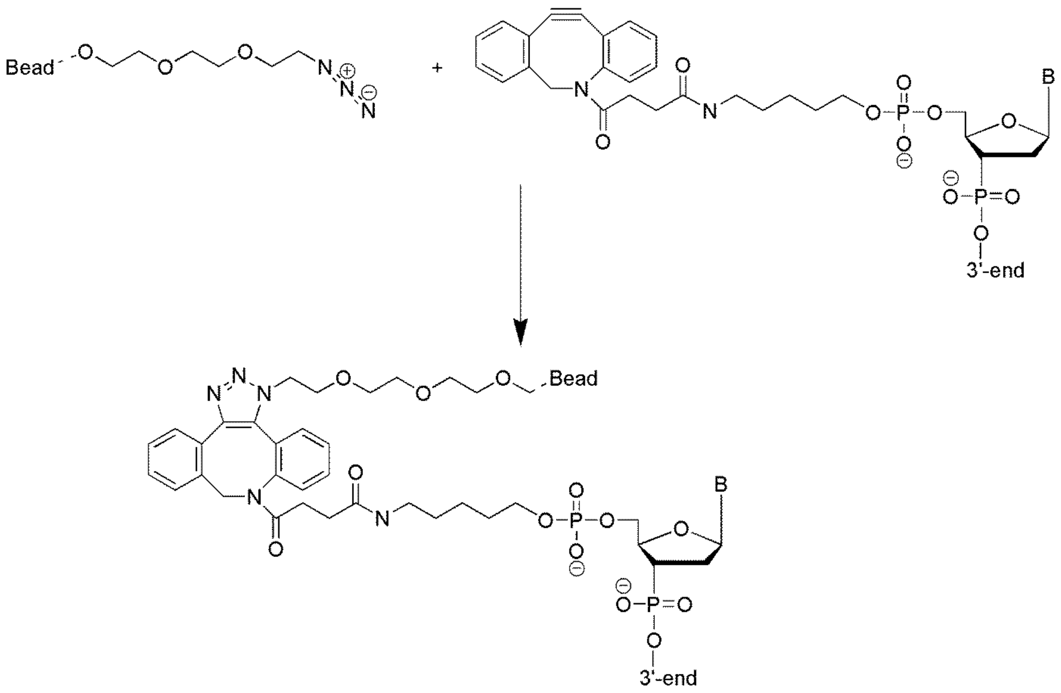

Figure 50. The reaction of 5'-DIBAC-labeled DNA with azide-modified magnetic beads.

It was obvious that a considerable development work had to be done, using the click-reaction for the performance of *in vitro* selection on magnetic beads. Therefore, it was started with an assay based on the separation of the active and inactive sequences on the gel, where the *in vitro* selection process itself proceeded in solution.

The in vitro selection for cleavage in solution

Following SRλ (see above), a negative selection round was carried out. That means the sequences were incubated without the ligand streptavidin, in order to remove sequences being active under the conditions of *in vitro* selection without streptavidin. Similar to the purification of SRλ, the non-cleaved sequences were eluted from the gel.

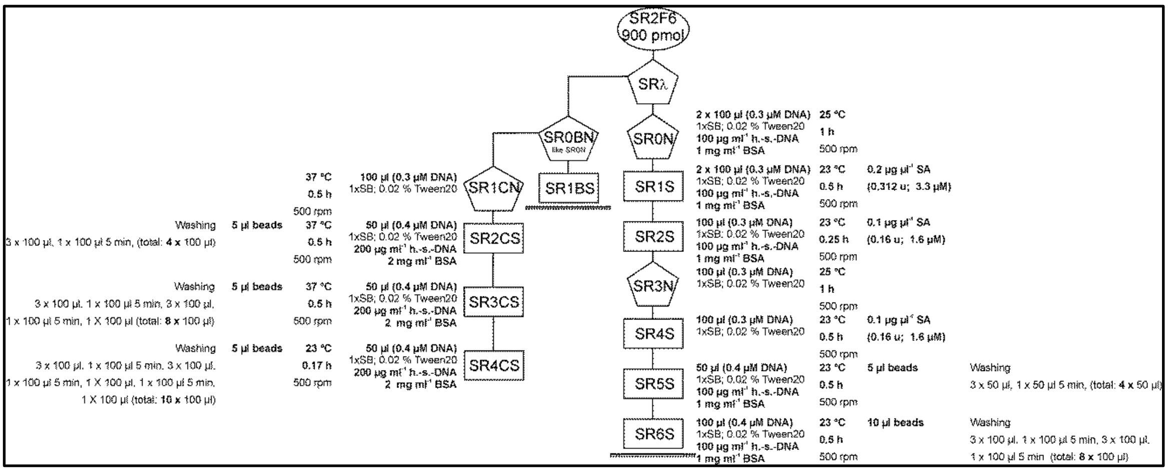
SR2F6
900 pmol
SRλ
SR0BN
like SR0N
SR0N
SR1CN
SR1BS
SR1S
SR2CS
SR2S
SR3CS
SR3N
SR4CS
SR4S
SR5S
SR6S
2 x 100 µl (0.3 µM DNA)
1xSB; 0.02 % Tween20
100 µg ml⁻¹ h.-s.-DNA
1 mg ml⁻¹ BSA
25 °C
1 h
500 rpm
2 x 100 µl (0.3 µM DNA)
1xSB; 0.02 % Tween20
100 µg ml⁻¹ h.-s.-DNA
1 mg ml⁻¹ BSA
23 °C
0.5 h
500 rpm
0.2 µg µl⁻¹ SA
(0.312 u; 3.3 µM)
100 µl (0.3 µM DNA)
1xSB; 0.02 % Tween20
100 µg ml⁻¹ h.-s.-DNA
1 mg ml⁻¹ BSA
23 °C
0.25 h
500 rpm
0.1 µg µl⁻¹ SA
(0.16 u; 1.6 µM)
100 µl (0.3 µM DNA)
1xSB; 0.02 % Tween20
25 °C
1 h
500 rpm
100 µl (0.3 µM DNA)
1xSB; 0.02 % Tween20
23 °C
0.5 h
500 rpm
0.1 µg µl⁻¹ SA
(0.16 u; 1.6 µM)
50 µl (0.4 µM DNA)
1xSB; 0.02 % Tween20
100 µg ml⁻¹ h.-s.-DNA
1 mg ml⁻¹ BSA
23 °C
0.5 h
500 rpm
5 µl beads
Washing
3 x 50 µl, 1 x 50 µl 5 min, (total: 4 x 50 µl)
100 µl (0.4 µM DNA)
1xSB; 0.02 % Tween20
100 µg ml⁻¹ h.-s.-DNA
1 mg ml⁻¹ BSA
23 °C
0.5 h
500 rpm
10 µl beads
Washing
3 x 100 µl, 1 x 100 µl 5 min, 3 x 100 µl,
1 x 100 µl 5 min (total: 8 x 100 µl)
37 °C
0.5 h
500 rpm
100 µl (0.3 µM DNA)
1xSB; 0.02 % Tween20
Washing
5 µl beads
3 x 100 µl, 1 x 100 µl 5 min, (total: 4 x 100 µl)
37 °C
0.5 h
500 rpm
50 µl (0.4 µM DNA)
1xSB; 0.02 % Tween20
200 µg ml⁻¹ h.-s.-DNA
2 mg ml⁻¹ BSA
Washing
5 µl beads
3 x 100 µl, 1 x 100 µl 5 min, 3 x 100 µl,
1 x 100 µl 5 min, 1 X 100 µl (total: 8 x 100 µl)
37 °C
0.5 h
500 rpm
50 µl (0.4 µM DNA)
1xSB; 0.02 % Tween20
200 µg ml⁻¹ h.-s.-DNA
2 mg ml⁻¹ BSA
Washing
5 µl beads
3 x 100 µl, 1 x 100 µl 5 min, 3 x 100 µl,
1 x 100 µl 5 min, 1 X 100 µl, 1 x 100 µl 5 min,
1 X 100 µl (total: 10 x 100 µl)
23 °C
0.17 h
500 rpm
50 µl (0.4 µM DNA)
1xSB; 0.02 % Tween20
200 µg ml⁻¹ h.-s.-DNA
2 mg ml⁻¹ BSA

Figure 51. Overview of *in vitro* selection rounds in solution for the selection of cleavage activity. Exemplary nomenclature of *in vitro* selection rounds: SR0BN: *in vitro* selection round number 0, pool B, negative *in vitro* selection round; SR1CS: *in vitro* selection round number 1, pool C, *in vitro* selection round for cleavage (S stands for *Spaltung* (*ger* cleavage). At the right and left side of the chart the conditions of the rounds are shown (incubation time, temperature, additives, concentration of the pool). Furthermore, the concentrations of streptavidin or the amount of beads, and in the letter case, the elution (washing) conditions with elution buffer are listed.

Subsequently, a number of *in vitro* selection rounds with streptavidin in solution were performed (Figure 51). The mixtures were incubated for different periods of time and then directly loaded on a PAA gel. The first problem of this strategy that occurred, was that BSA from the *in vitro* selection mixture superimposed the target band in the gel (cf. Figure 57, p.97). This could be overcome by size exclusion chromatography or purification on silica columns (ROBOKLON, small DNA purification Kit) before sampling on the gel or simply not adding this additive to the *in vitro* selection (both was tried). Other technical difficulties of the assay were relatively easily optimized. The product band was naturally always very thin and light, but using thin (0.75 mm) gels and if necessary, staining with ethidium bromide, it was easy to identify. Additionally, it was found that it was not necessary to purify the elution mixture (i.e. by ethanol precipitation or size exclusion chromatography) but that it could directly be introduced in PCR. Moreover, the supernatant of two or even a single elution step at 45 °C delivered enough material for a satisfying amplification reaction. Nevertheless, after four to six rounds, not enough cleavage products could be detected. *In vitro* selection was performed at 23 °C, however, 37 °C is the favored reaction temperature of the 17E DNAzyme (see above, section 4). Therefore, the temperature setting was changed too. Additionally, it was assumed that streptavidin in solution possibly restrained sequences on gel or in size exclusion chromatography and it was tried to circumvent this possible problem in different ways. So it was tried to use streptavidin magnetic beads as a supplier of the ligand followed by harsh denaturation steps, to perform denaturing gel electrophoresis or to add proteinase K after the *in vitro* selection. But, these interventions failed to success. It seemed that the *in vitro* selection wasn't operative. Finally, a cleavage assay was performed, in order to identify the progress of the *in vitro* selection.

Cleavage assay to monitor the progress of the in vitro selection in solution

The library and some selected pools from the *in vitro* selection were labeled with ATTO680 by using a modified primer PD3 in PCR reaction. The labeling of an amino-modified primer PD3 was performed as described in section 6.17. The fluorescence label was necessary because in a preceding experiment with unmodified nucleic acid no cleavage product was detected. The detection of low amounts of ATTO680 fluorescent dye-labeled nucleic acid in the present work was generally done by PAGE using the plate sequencer. Analysis of cleavage reactions by LICOR is well established; however, due to the difficulties with gel analysis in this *in vitro* selection process (possibly non-migrating sequences), this method was not supposed to be the method of choice. Consequently, a comparison with another separation method, like HPLC, seemed reasonable. Reversed phase and anion exchange technique were tested. For the separation of a 10mer ATTO680 labeled DNA from an 112 nt ATTO680 labeled DNA both separation methods are suitable. Some experiments were done with the "Nucleodur 250/4 100-5 C18 ec" column. However, spreading of material on the column was really high (one fifth of intensity of the labeled library or primer PD3 (p. 87) was reached after flow through the column in comparison to flow through the bypass). Therefore, the Mono-Q anion exchange column was chosen, of which the column volume is noticeable smaller (0.982 ml). The 10mer cleavage fragment eluted at 9.0 ml and the intact pool at 12.3 ml. The eluent was sodium perchlorate. The samples were prepared in 20 µl final volume with 5 pmol ssDNA, 1 x SB, 0.02% Tween, 0.05 µg µl^{-1} streptavidin, with or without BSA (2 mg ml^{-1}) and herring sperm DNA (200 µg ml^{-1}). 10 µl of a single cleavage reaction were mixed with the denaturing running buffer immediately after starting the reaction with streptavidin. The remaining fraction was incubated at 37 °C for 1 h. To calculate the percent of cleavage, the area under the curve was integrated using the software OriginLab. The results are shown in Table 14 and Figure 52. No increase in cleavage activity of the pool during *in vitro* selection could be proven in these experiments. It has to be admitted that the assignment of the 10mer cleavage product, could not be proven by a standard. It was tried to produce this standard by alkaline hydrolysis of PD3, but unfortunately this strongly reduced the fluorescence. However, the presence of the cleavage product was proven by PAGE (Figure 54).

Table 14. Cleavage yields of ssDNA of SR0BN and SR4CS (Mono-Q).

	t = 0 h		**t = 1 h**	
	impulse center	**% A (cleaved)**	impulse center	**% A (cleaved)**
SR0BN	8.95	**5.8**	8.93	**9.5**
SR4CS	8.93	**5.4**	8.93	**8.1**

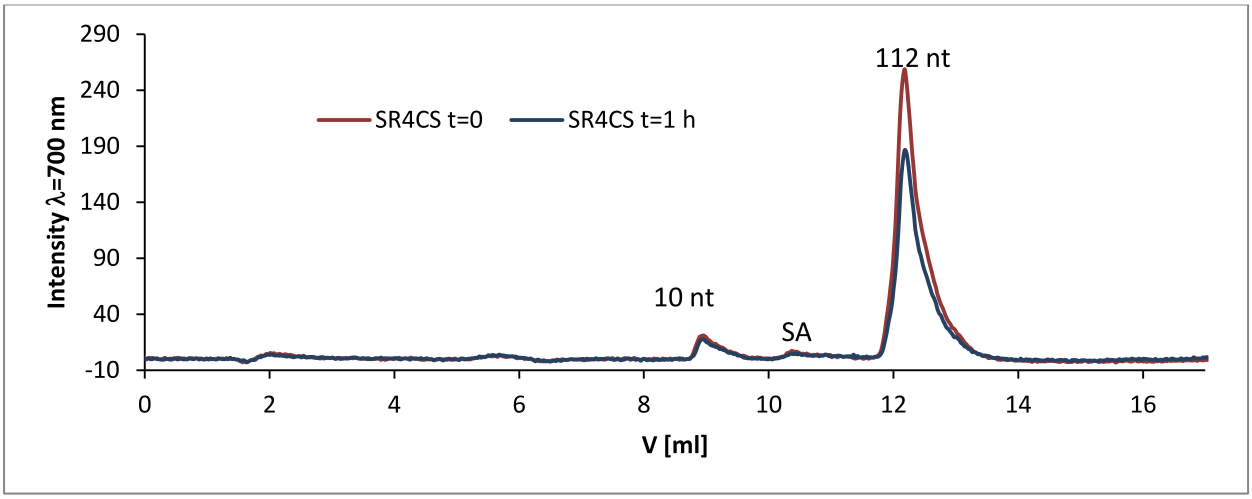

Figure 52. Chromatogram of the cleavage assays with SR4CS. Anion exchange chromatography (Mono-Q); flow: 1 ml/min; Gradient: 0% buffer B for 1 min, 20% buffer B in 4 min , 80% buffer B in 20 min.

In the experiments with BSA and herring sperm DNA quantification by the area under the curve, integration wasn't reasonable. Unfortunately, the proteins eluted between the 10mer and the intact sequences. The amount of streptavidin was low and did not overlay with the ATTO680 fluorescence signal, but the fluorescence peak of BSA interfered with the peak of the 10mer. However, comparison of a run without the DNAzyme and the two reaction mixtures show that the additives did not change the cleavage activity (Figure 53).

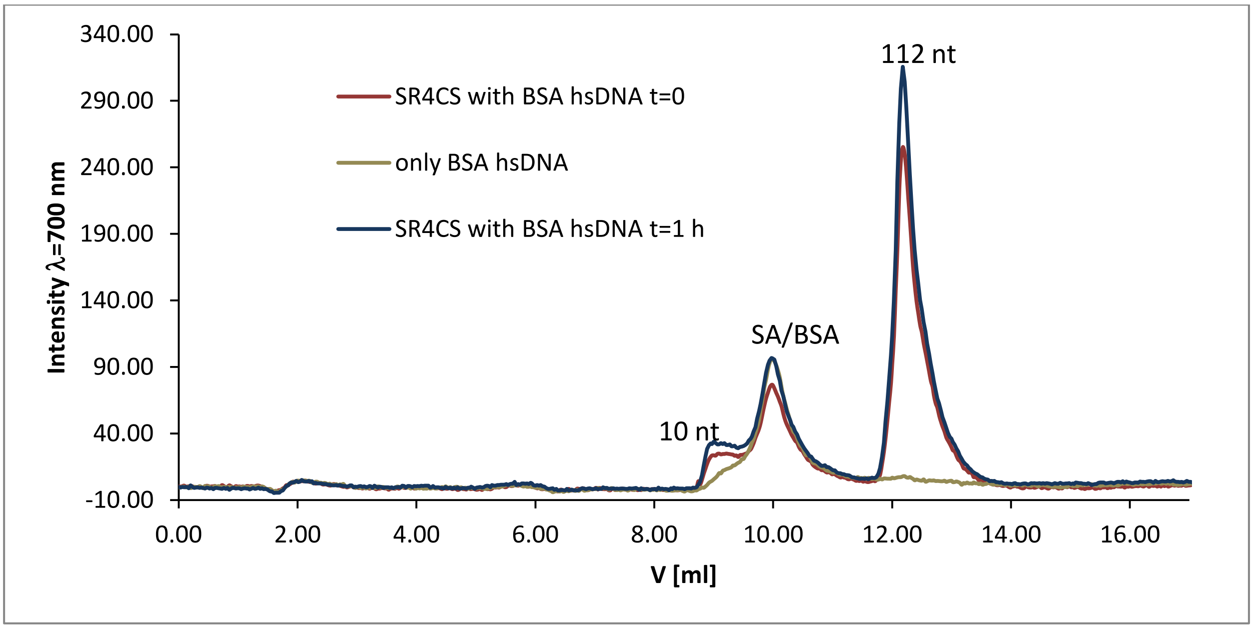

Figure 53. Chromatogram of cleavage assay with SR4CS and the additives BSA and herring sperm DNA. Anion exchange chromatography (Mono-Q); flow: 1 ml/min; Gradient: 0% buffer B for 1 min, 20% buffer B in 4 min , 80% buffer B in 20 min.

The experiment was then repeated for analysis by the plate sequencer (LICOR). The composition of a single reaction was: 20 nM ssDNA, 1 x SB, 0.02% Tween, 0.05 µg µl^{-1} streptavidin, with or without BSA (2 mg ml^{-1}) and hsDNA (200 µg ml^{-1}) in 20 µl total volume. 1 µl sample was mixed with 19 µl LB denat. or stop mix (see above). Results were similar to those in the HPLC-experiment (Figure 54). BSA (and herring sperm DNA) did not interfere with the nucleic acid bands. There is a high cleavage rate of SR0BN about 30% at t =0 and t = 1 h when no additives were present. This difference was not seen in samples of SR4CS, and moreover, this was not observed by this extend in an HPLC-experiment with SR0BN. However, there was no increase in cleaved sequences over the period of 1 h (Table 15, Figure 54). Therefore, the cleavage observed was not caused by streptavidin-mediated activity.

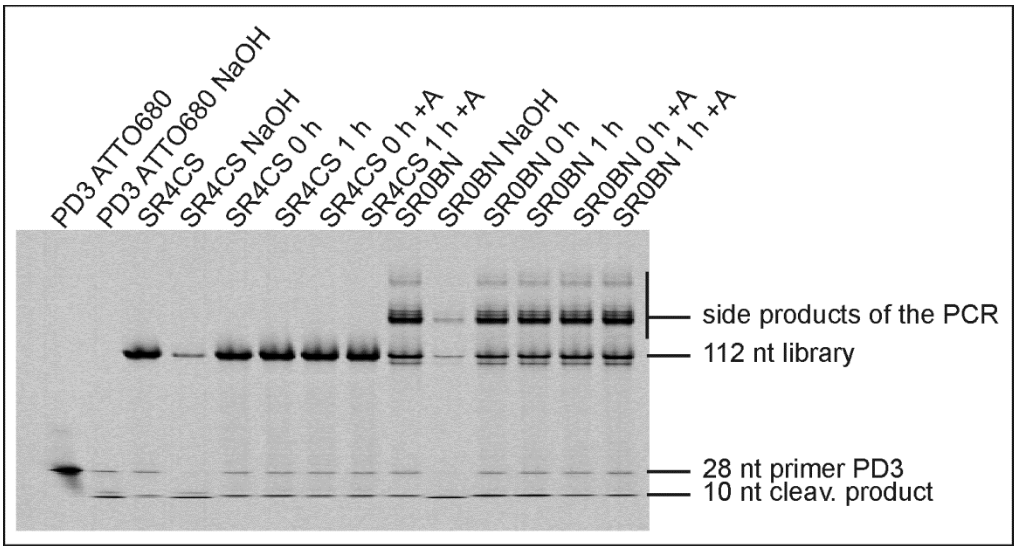
PD3 ATTO680
PD3 ATTO680 NaOH
SR4CS
SR4CS NaOH
SR4CS 0 h
SR4CS 1 h
SR4CS 0 h +A
SR4CS 1 h +A
SR0BN
SR0BN NaOH
SR0BN 0 h
SR0BN 1 h
SR0BN 0 h +A
SR0BN 1 h +A
side products of the PCR
112 nt library
28 nt primer PD3
10 nt cleav. product

Figure 54. 5% denat. LICOR-PAGE of the cleavage assay. A = additives (BSA and herring-sperm DNA); denaturing loading buffer.

Table 15. Cleavage yields of ssDNA of SR0BN and SR4CS in LB denat./Stopmix (LICOR). A = additives (BSA and hsDNA).

	t = 0 h	t = 1 h
	% A (cleaved)	% A (cleaved)
SR0BN	27.1/26.7	24.9/24.0
SR0BN + A	8.6/7.9	8.9/8.0
SR4CS	1.0/1.0	3.2/1.5
SR4CS + A	1.4/1.2	1.2/1.3

Both methods revealed a slightly higher cleavage activity of the pool of SR0BN. This is caused by the missing negative selection at 37 °C at this point of *in vitro* selection (Figure 51). However, positive selection failed. It was assumed, that the cleavage reaction is a reaction in equilibrium. That means, that even after SRλ some sequences were allowed to cleave in the digestion reaction, which had to be performed as preparation of every *in vitro* selection round. This way, always a few cleaved sequences would be present before starting the selection round.

The in vitro selection for cleavage on azide magnetic beads

With the present assay, it was not possible to remove these sequences reliably. Consequently, the assay was changed (Figure 55) and the library was modified with an azide by the use of an azide-modified primer PD3-DBCO-RIBO (5'-ACTCACTATrAGGAAAGAGATGGCGACAT;) that was applied in the PCR reaction.

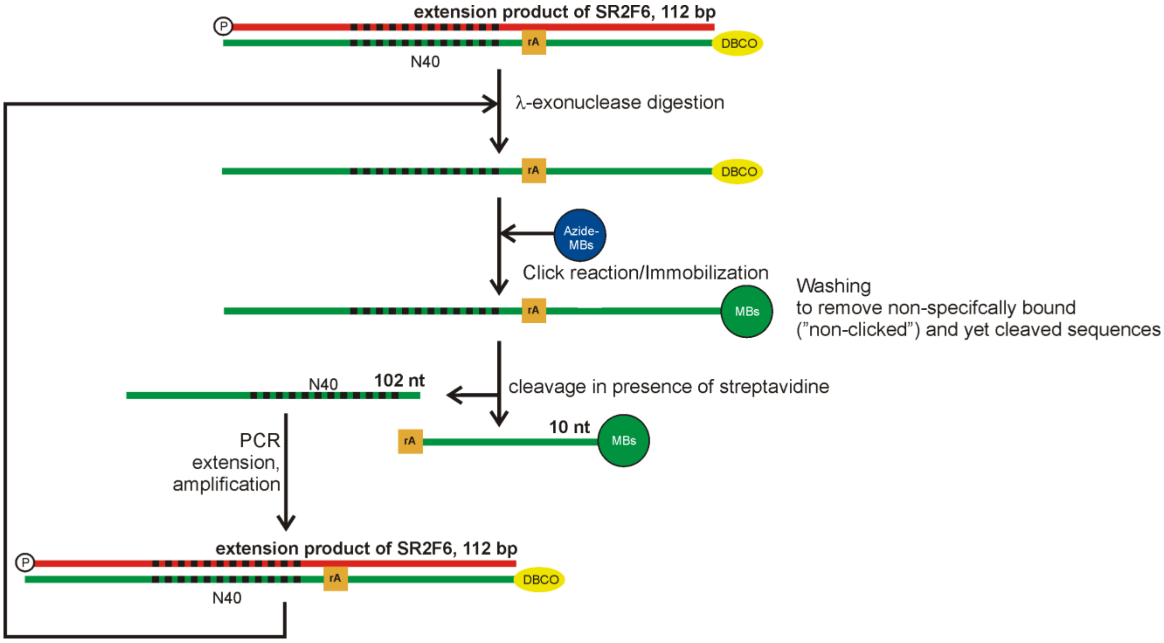
extension product of SR2F6, 112 bp
P
rA
DBCO
N40
λ-exonuclease digestion
rA
DBCO
Azide-MBs
Click reaction/Immobilization
rA
MBs
Washing
to remove non-specifcally bound
(”non-clicked”) and yet cleaved sequences
N40
102 nt
cleavage in presence of streptavidine
rA
10 nt
MBs
PCR
extension,
amplification
extension product of SR2F6, 112 bp
P
rA
DBCO
N40

Figure 55. Scheme of the *in vitro* selection strategy for the *in vitro* selection of cleavage on azide magnetic beads. The green strands represent the DNA carrying the information of the pool. After the digestion of the antisense strand (red) the library was immobilized on the magnetic beads by Click reaction. Non-specifically bound and non-specifically cleaved sequences were removed before streptavidin is added and the selection for active sequences started. Then, the pool was prepared for a new round of *in vitro* selection.

The click reaction was evaluated using the modified primer. Various concentrations of primer were applied to the beads in different buffer systems, and at different temperatures. After 0.5 h or 3 h, the supernatant was checked for remaining primer by UV-Vis spectroscopy. The primer was bound quantitatively in PBS, PBS/DMSO, and selection buffer. Additives like BSA and PEG strongly hampered the click reaction. The buffer type didn't effect on the reaction (in water only, the reaction didn't proceed). The reaction temperature had no detectable effect. Finally, it was decided to use the selection buffer for the binding reaction at 37 °C, gently shaking at 450 rpm. For proof of principle, the primer was immobilized and subsequently, the beads were washed twice with selection buffer SB containing 0.02 % Tween20 and incubated at 37 °C in SB with Tween20, BSA and herring sperm DNA for 1 h. None of the supernatants showed absorption at 260 nm. Then 1 M NaOH was added to the beads (37 °C, 15 min) to cleave the primer. This supernatant showed absorption comparable to the original primer solution. Following these preparations, the *in vitro* selection process for an aptazyme was started.

The process was conducted similarly to the previous *in vitro* selection assays. After the initial selection round SRλ (Figure 56), which was purified by PAGE, the DNA was bound to the beads. Following the washing steps, the incubation at increasing selection pressure was carried out. The supernatant was incubated with Proteinase K and then, strongly diluted, introduced in PCR. Afterward, the single stranded library was generated by digestion with λ-exonuclease and was bound to the beads, again. The detailed process for *in vitro* selection with azide magnetic beads is tabulated in the methods in section 6.31 (p.127).

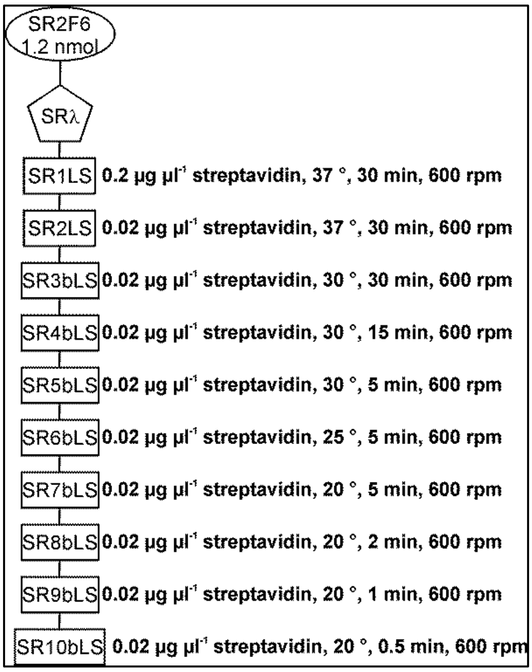
SR2F6
1.2 nmol
SRλ
SR1LS 0.2 µg µl^{-1} streptavidin, 37 °, 30 min, 600 rpm
SR2LS 0.02 µg µl^{-1} streptavidin, 37 °, 30 min, 600 rpm
SR3bLS 0.02 µg µl^{-1} streptavidin, 30 °, 30 min, 600 rpm
SR4bLS 0.02 µg µl^{-1} streptavidin, 30 °, 15 min, 600 rpm
SR5bLS 0.02 µg µl^{-1} streptavidin, 30 °, 5 min, 600 rpm
SR6bLS 0.02 µg µl^{-1} streptavidin, 25 °, 5 min, 600 rpm
SR7bLS 0.02 µg µl^{-1} streptavidin, 20 °, 5 min, 600 rpm
SR8bLS 0.02 µg µl^{-1} streptavidin, 20 °, 2 min, 600 rpm
SR9bLS 0.02 µg µl^{-1} streptavidin, 20 °, 1 min, 600 rpm
SR10bLS 0.02 µg µl^{-1} streptavidin, 20 °, 0.5 min, 600 rpm

Figure 56. Chart of *in vitro* selection rounds on azide magnetic beads starting with a pool of SR2F6. The nomenclature is: *in vitro* selection round number 1 (or 2; 3b–10b) branch L. Each round included a negative selection to remove sequence that cleaved non-specifically without streptavidin.

The most critical step was the washing of the beads after the click reaction to remove non-specifically bound and cleaved DNA-sequences (Figure 55). By UV-Vis spectroscopy, no nucleic acid was detectable in the supernatant. But, if the supernatant was concentrated by ethanol precipitation and analyzed by PAGE, using ethidium bromide for staining, a band with the length of the full-length product was detected. It was very thin, however, by PCR, these sequences were amplified just as well as the sequences that were yielded after the *in vitro* selection step. This can be taken from Figure 57 (compare with results of results of SR3bLS and SR7bLS). The washing after the click reaction was performed very extensively. In general to replace non-specific bound DNA sequences, 10 washing steps were carried out using selection buffer with 0.02% Tween, and with or without additional herring sperm DNA and BSA. The herring sperm DNA and the BSA is responsible for the strong smear in the lane of the eighth washing step in Figure 57. A lot of experiments were conducted concerning the washing.

Some washing steps were prolonged from 15 min up to more than 12 h overnight. However, it was found, that incubation in washing buffer for more than 30 minutes did not show any improvement. The non-specific bound DNA-sequences were most efficiently removed by frequent exchange of the washing solution.

In panel A of Figure 57, also a NaOH digestion is shown. This was always done after the *in vitro* selection step. By "cutting off" the 3' end of the remaining sequences after the selection, it could be proven, that the click reaction was successful.

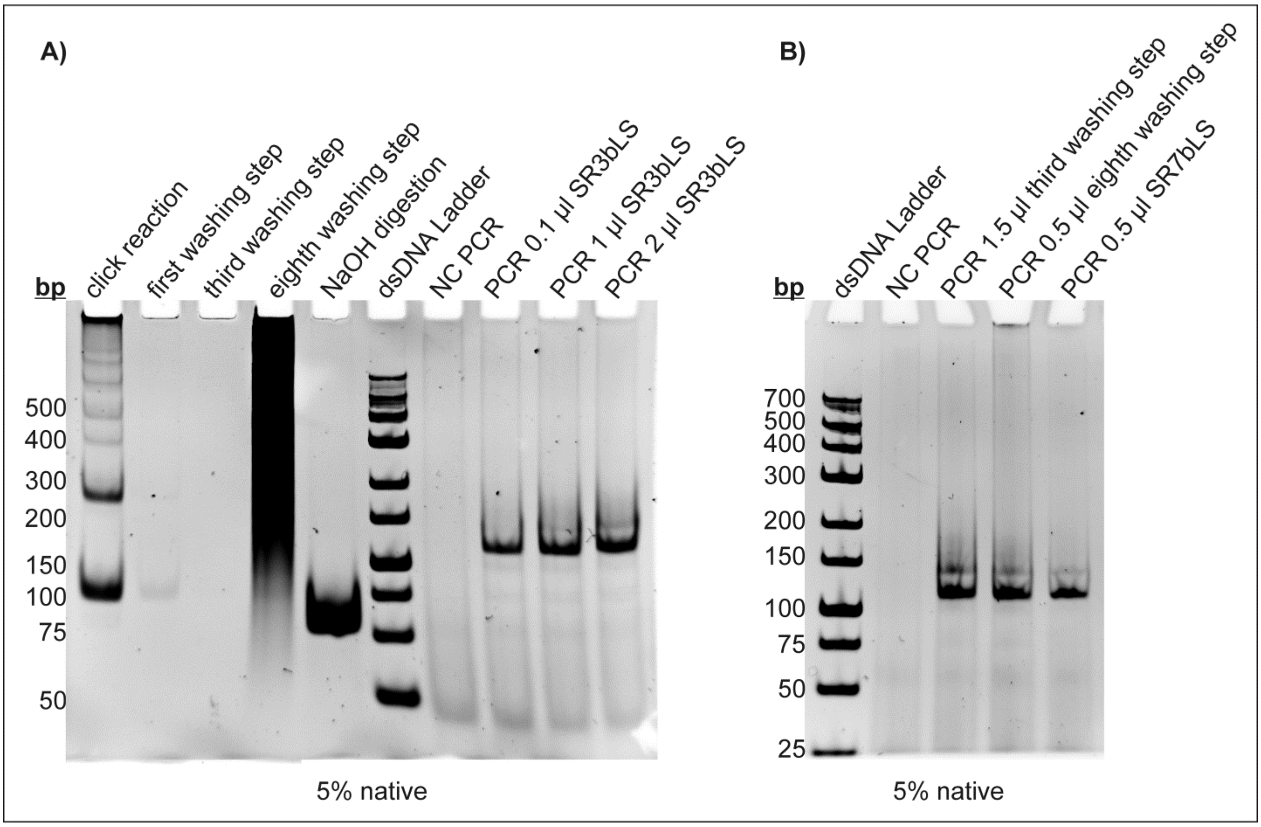
A)
bp
click reaction
first washing step
third washing step
eighth washing step
NaOH digestion
dsDNA Ladder
NC PCR
PCR 0.1 µl SR3bLS
PCR 1 µl SR3bLS
PCR 2 µl SR3bLS
500
400
300
200
150
100
75
50
5% native
B)
bp
dsDNA Ladder
NC PCR
PCR 1.5 µl third washing step
PCR 0.5 µl eighth washing step
PCR 0.5 µl SR7bLS
700
500
400
300
200
150
100
75
50
25
5% native

Figure 57. 5% native PAGE of various samples of *in vitro* selection after SR3bLS (A) and SR7bLS (B). A) Supernatant of click reaction: 20 µl, ethanol precipitated (112 nt); first washing step: 50 µl SB, ethanol precipitated; third washing step: 50 µl SB, 37 °C 5 min, ethanol precipitated (112 nt); eighth washing step: 50 µl SB, Tween, BSA, herring sperm DNA, 37 °C 30 min, ethanol precipitated (112 nt); NaOH digestion: 20 µl 1 M NaOH treatment after the in SR3bLS, ethanol precipitated (102 nt); NC PCR: no template control of PCR reaction; PCR with X µl of SR3bLS as template (112 bp). B) NC PCR: no template control of PCR reaction; PCR with X µl of different washing steps (third: 50 µl SB, Tween; eighth: 20 µl SB, Tween, BSA, herring sperm DNA) and SR3bLS as a template (112 bp). All gels were post-stained with ethidium bromide.

PCR is a very sensitive method, and in theory, a single molecule is enough to produce a detectable signal after the amplification. However, the results revealed that the present design of the assay wasn't able to specifically extract active sequences. With pool L finally, 10 *in vitro* selection rounds were performed. But, after selection round 10 (SR10bLS, Figure 56) the PCR that was performed with the supernatant of the selection round yielded less product, than that after the washing steps. The incubation of the library with the analyte streptavidin was extremely short in the last rounds, but functional

DNAzymes should cleave very fast. Therefore, in order to monitor the progress of the *in vitro* selection, cleavage assays were performed with material from SR1LS, SR2LS, SR4LS, SR6bLS, and SR8bLS by introducing an ATTO680 modification at the 5'-end as described above and in the section 6.17. No increase in cleavage activity was detected with the LICOR plate sequencer, with or without streptavidin. However, as it was observed in the first attempt of *in vitro* selection using gel separation, a basic cleavage about 1 % was detectable. Indeed, cleavage could be substantially triggered by addition of 100 mM $MgCl_2$. Therefore it was tried to perform the *in vitro* selection in presence of 10 mM $MgCl_2$. This experiment was stopped after the third round. Tracking of the washing steps, which then were performed with additional 10 mM $MgCl_2$ as well, clearly showed that in presence of the additional salt, always a large number of sequences was cleaved independent of the presence of the analyte streptavidine. A final cleavage experiment was done adding the activator EA-C1 (0) to material from SR6bLS. The activator oligo could not increase the cleavage activity with or without streptavidin.

4.4.4 Biacore (SPR) Measurements of the Potential Streptavidin Aptamers

Concerning the results and considerations of earlier *in vitro* selection experiments (section 3.3), it was supposed that the failure of *in vitro* selection for cleavage was a result of the impotency of the pool of SR2F6. Therefore, the binding reaction was additionally investigated by surface plasmon resonance (SPR). Using this method, the result of the EMSA (Figure 46, page 84) could be verified. For SPR measurements the Biacore T100 instrument was used. The DNA was prepared by PCR and λ-exonuclease digestion and for binding a commercially available streptavidin coated sensor chip was applied (Series S Sensor Chip SA, GE HEALTHCARE LIFE SCIENCES). The DNA was either applied directly after the enzymatic digestion or was previously purified by gel elution. In EMSA, the sequences of SR2F5 and SR2F6 pools appeared equal concerning their binding behavior. However, the low amount of template, which could be introduced in PCR after SR2F6, indicated for high variability of the pool after SR2F6. Therefore, it was decided to use sequences of SR2F6 only for the SPR measurements. From Table 16, it can be taken that the factor of enrichment of binding sequences through *in vitro* selection was at least about 300. Furthermore, the results suggest that the non-gel purified ssDNA is contaminated with 50% to 75 % dsDNA. The dissociation constant K_D was calculated from data of the measurement with 0.29 µM gel purified ssDNA. It is 35.8 ± 1.8 nM. Figure 58 shows the sensorgram of this measurement.

Table 16. Maximum resonance units (RUs) of different DNA samples at 10 µl min^{-1} flow for 300 s. The table shows the arithmetic mean value ($\bar{x}$) and the standard deviation (SD), which isn't strictly correct in some cases because the number of measurements was < 3. Therefore the number of measurements (#) is given, too.

Conc. [µM]	library			dsDNA SRF2F6			ssDNA SR2F6 (unpur.)			ssDNA SR2F6 (pure)		
	$\bar{x}$	SD	#	$\bar{x}$	SD	#	$\bar{x}$	SD	#	$\bar{x}$	SD	#
0.00	**-7.0**	3.3	5									
0.03										**24.7**	0.7	4
0.04										**34.6**	1.2	4
0.10	**-0.5**	1.2	4				**35.9**		1			
0.29										**366.9**	26.0	4
0.50							**125.6**	1.3	2			
1.00	**-0.9**	3.7	4	**53.5**	1.1	4	**264.1**	22.8	3			
2.00							**388.8**	26.1	3			
5.00							**559.9**	14.8	2			
10.00	**41.6**	4.7	4									

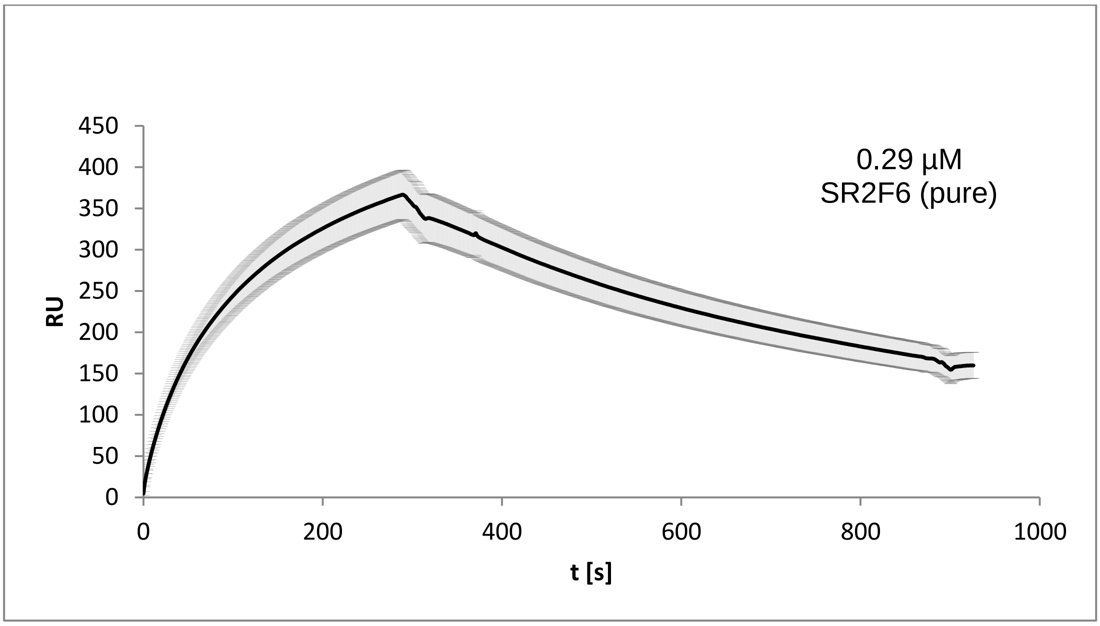

Figure 58. The sensorgram of the SPR experiment with 0.29 µM SR2F6. The black line shows the arithmetic mean value of the measurements and the gray shadow illustrates the standard deviation of the single data points.

4.4.5 Sanger-Sequencing of the Binding Pool

The relatively low dissociation constant of the pool SR2F6 with Streptavidin in the nanomolar range indicated that the *in vitro* selection for binders was already very advanced. That means, possibly, only a few sequences or sequence families were present. This could be a reason for the failure of the *in vitro* selection for cleavage activity. In order to confirm this assumption, it was decided, to analyze the sequences of the pool. Following the PCR, the DNA was cloned into *E.coli* TG1 cells, and the clones, which contained the insert, were used to isolate the plasmid DNA and to sequence the DNA.

The results which include the obtained sequences and the secondary structure predictions are shown in Figure 59 and Figure 60, respectively (these figures are also attached for folding out). The most stable secondary structure was calculated with mfold 4.7.[203-205] The temperature was set to 23 °C and the settings for the salt correction were 100 mM Na^+ and 3 mM Mg^{2+}. The sequences are very similar, the variability is extremely low. The secondary structure prediction reveals stem-loop structures for each of the clones that were forced by the interaction of the inhibitory strand and the catalytic domain (stem II). Only one of the six sequences found had the conserved stem II. In the majority of the sequences, an insertion mutation in stem II evolved during the *in vitro* selection. The additional guanosine nucleotide was inserted directly after the PD1 primer sequence. Taking a closer look at the sequences, the variability becomes even lower. The clone number 5.1 has the same sequence as the clones number 5_4, 5_6, n4_1, n4_3, except the duplication of the DNAzyme's sequence. Except a single base deletion in the N40-domain, this applies also for the clones number 4_3 and 4_5. The clone number n57_7 has a duplication of the inhibitory strand but the N40-domain has the same sequence as in clone numbers 5_3 and n52_5. Only clone number n42_4 exhibits more variations in the N40-domain. For the Sanger sequencing, the PCR wasn't gel purified and therefore longer sequences, than the desired one were sequenced as well. However, it is imaginable that the sequence of the N40 domain of clone number n42_4 is present in sequences of the correct length as well. This becomes even reasonable when the secondary structure of this sequence without the repetition-sequence is considered. The structure is very similar to the most stable structure of clone numbers 5_3 and n52_5 (Figure 61, additionally attached for folding out). For the clones, number 5_4, 5_6, n4_1, n4_3 in Figure 60 the structure with the minimum free energy (dG = -41.93 kcal mol^{-1}) is shown. Figure 61 displays an alternative structure prediction with dG = -40.28 kcal mol^{-1}. This figure compares three different sequences of the N40 domain that were found by sequencing and demonstrates striking structure similarities. Every sequence is predicted to form a large bulge following a long stem. The bulge formation is supported by the repetitive C-stretch at the 3'-end of the N40 domain. The structures continue with a stem-loop structure, which is extended with a further stem in a sharp angle. This stem again ends in a loop. Thus, the sequences share a stem-loop structure that resembles a clamp.

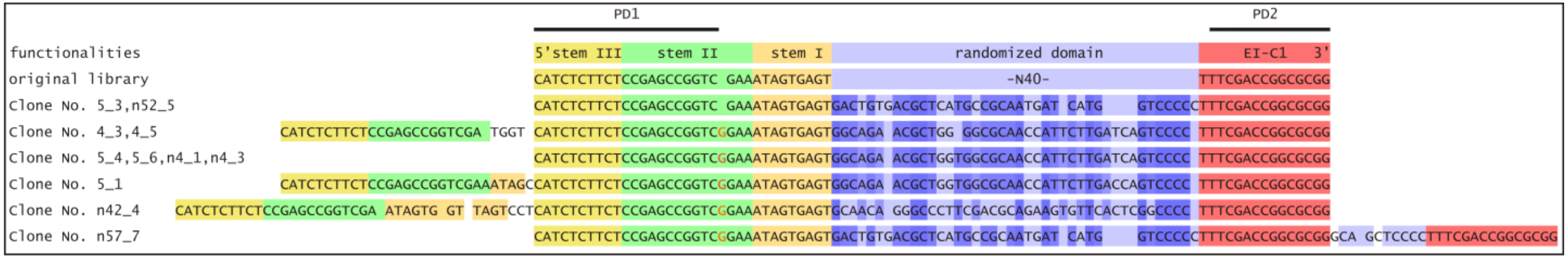

```
                                                                    PD1                                                               PD2
functionalities                                             5'stem III   stem II     stem I              randomized domain               EI-C1    3'
original library                                            CATCTCTTCTCCGAGCCGGTC GAAATAGTGAGT                  -N40-                    TTTCGACCGGCGCGG
Clone No. 5_3,n52_5                                         CATCTCTTCTCCGAGCCGGTC GAAATAGTGAGTGACTGTGACGCTCATGCCGCAATGAT CATG    GTCCCCCTTTCGACCGGCGCGG
Clone No. 4_3,4_5              CATCTCTTCTCCGAGCCGGTCGA TGGT CATCTCTTCTCCGAGCCGGTCGGAAATAGTGAGTGGCAGA ACGCTGG GGCGCAACCATTCTTGATCAGTCCCC TTTCGACCGGCGCGG
Clone No. 5_4,5_6,n4_1,n4_3                                 CATCTCTTCTCCGAGCCGGTCGGAAATAGTGAGTGGCAGA ACGCTGGTGGCGCAACCATTCTTGATCAGTCCCC TTTCGACCGGCGCGG
Clone No. 5_1                  CATCTCTTCTCCGAGCCGGTCGAAATAGCCATCTCTTCTCCGAGCCGGTCGGAAATAGTGAGTGGCAGA ACGCTGGTGGCGCAACCATTCTTGACCAGTCCCC TTTCGACCGGCGCGG
Clone No. n42_4      CATCTCTTCTCCGAGCCGGTCGA ATAGTG GT TAGTCCTCATCTCTTCTCCGAGCCGGTCGGAAATAGTGAGTGCAACA GGGCCCTTCGACGCAGAAGTGTTCACTCGGCCCC TTTCGACCGGCGCGG
Clone No. n57_7                                             CATCTCTTCTCCGAGCCGGTCGGAAATAGTGAGTGACTGTGACGCTCATGCCGCAATGAT CATG    GTCCCCCTTTCGACCGGCGCGGGCA GCTCCCCTTTCGACCGGCGCGG
```

Figure 59. Sequences of the pool SR2F6.

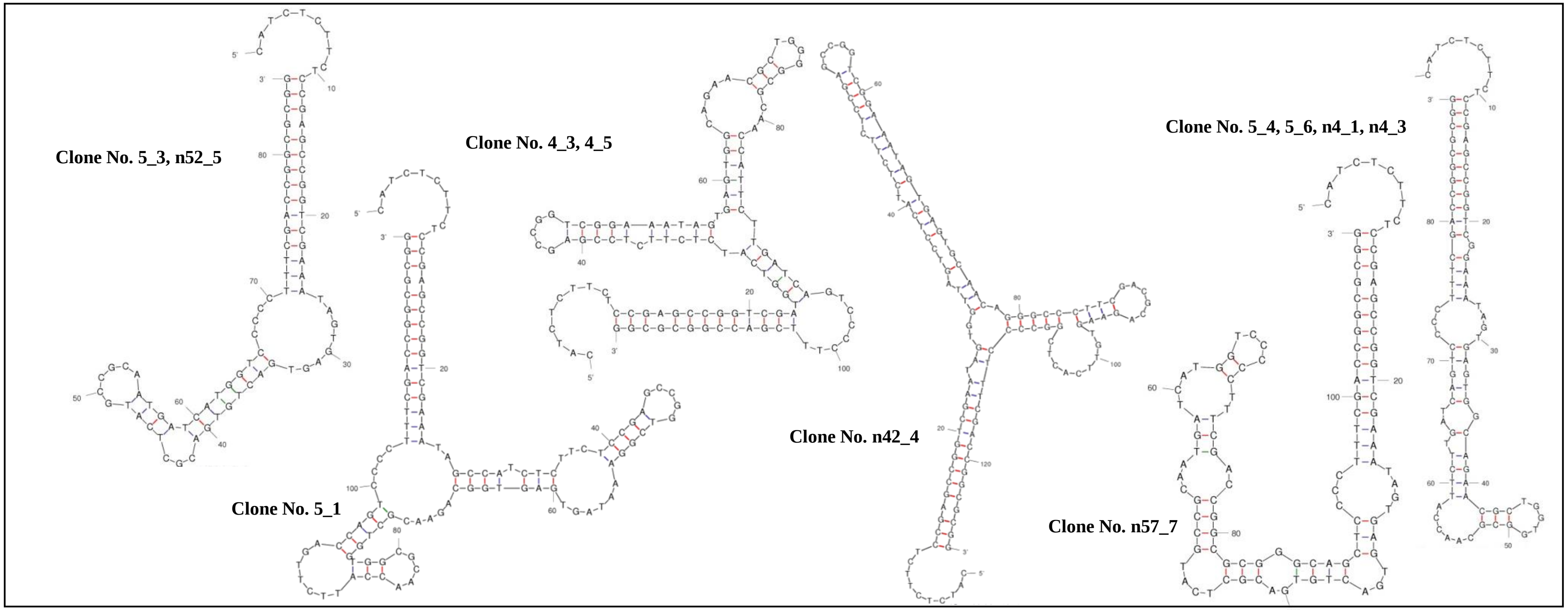

Figure 60. Secondary structure prediction for the sequences of the pool SR2F6.

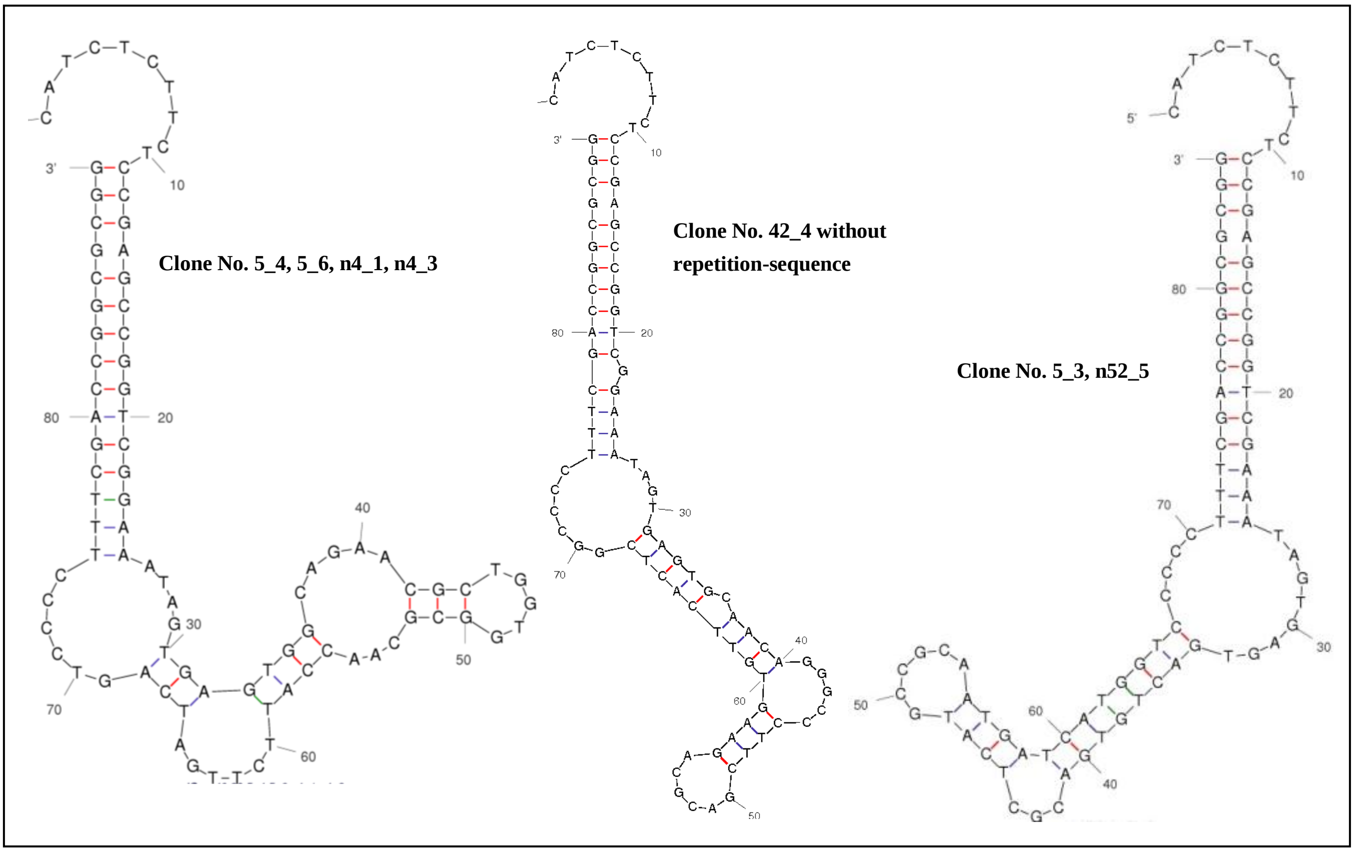
Clone No. 5_4, 5_6, n4_1, n4_3
Clone No. 42_4 without repetition-sequence
Clone No. 5_3, n52_5

Figure 61. Secondary structure prediction. Shown are the structures with the minimum free energy for the sequences of Clone No. 53, n52_5 and Clone No. 42_4 without repetition-sequence and an alternative secondary structure of clone No. 5_4, 5_6, n4_1, n4_3.

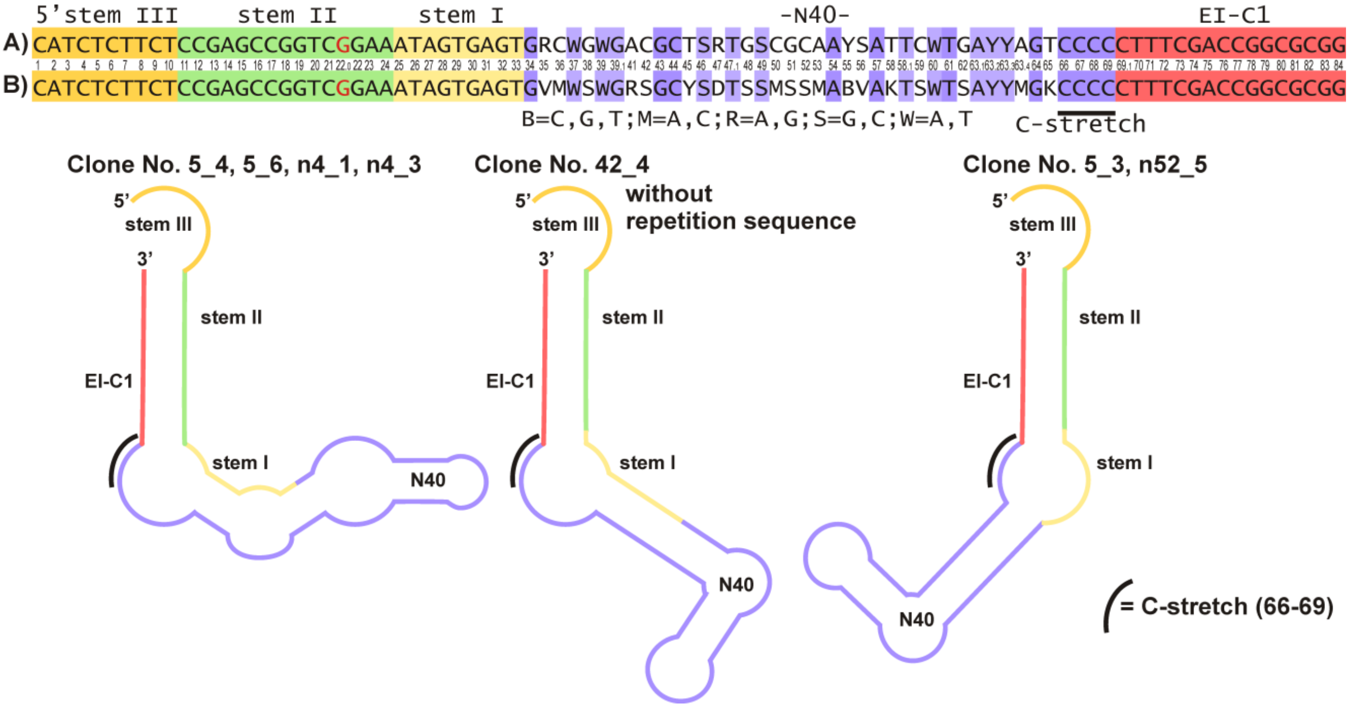
5'stem III
stem II
stem I
-N40-
EI-C1
A) CATCTCTTCTCCGAGCCGGTCGGAAATAGTGAGTGRCWGWGACGCTSRTGSCGCAAYSATTCWTGAYYAGTCCCCCTTTCGACCGGCGCGG
B) CATCTCTTCTCCGAGCCGGTCGGAAATAGTGAGTGVMWSWGRSGCYSDTSSMSSMABVAKTSWTSAYYMGKCCCCCTTTCGACCGGCGCGG
B=C,G,T;M=A,C;R=A,G;S=G,C;W=A,T
C-stretch
Clone No. 5_4, 5_6, n4_1, n4_3
Clone No. 42_4
without repetition sequence
Clone No. 5_3, n52_5
5'
3'
stem III
stem II
EI-C1
stem I
N40
= C-stretch (66-69)

Figure 62. Common sequence and schematic presentation of the probable secondary structures of the streptavidin aptamers. A) Common sequence without Clone No. 42_4. B) Common sequence including clone 42_4.

4.5 Concluding Discussion of the Combination of *In Vitro* Selection and Rational Design

4.5.1 Analysis of the 17E-DNAzyme's Cleavage Activity

The reason to investigate the 17E-DNAzyme's cleavage activity was mainly to become familiar with the system and to ensure that it would cleave under the conditions of *in vitro* selection, which was confirmed (Table 10, p.66). The cleavage activity was slightly lowered in the presence of additional cations (100 mM NaCl, 5 mM KCl, 1 mM $CaCl_2$) of the *in vitro* selection buffer ($k_{obs}\,\mathrm{sto} = 0.35\ \mathrm{min}^{-1}$ vs. $k_{obs}\,\mathrm{sto} = 0.45\ \mathrm{min}^{-1}$ at 10 mM $MgCl_2$). The reduced content of $MgCl_2$ (2 mM instead of 10 mM) caused an additional decrease in the rate of the cleavage reaction by one power of ten. However, all known *in vitro* selections of streptavidin aptamers used a mixture of various cations in the *in vitro* selection buffer and the presence of monovalent cations is of strong importance for the formation of tertiary structure.[163-166, 206, 207] It was indispensable to accept lower cleavage activity of the "mother-DNAzyme" as a compromise to select for binding activity.

Apart from this, some interesting insights into the cleavage activity of the 17E DNAzyme were obtained. However, it was a rudimentary analysis, not at least because the nucleic acid enzyme reaction is very fast and therefore is difficult to analyze by the help of manual pipetting. The concentration of enzyme for saturation of the single turnover reaction was not found, but at five-fold excess, an optimum concentration of Mg^{2+} cations about 125 mM was found. The influence of monovalent cations on the reaction was analyzed as well. The literature-known observation that these cations hamper the catalysis was confirmed. For Na^+, catalytic cleavage was observed without the addition of any divalent cation (Table 7, p.63). Moreover, increasing concentrations of NH_4^+ and Li^+ continuously reduce the activity of the DNAzyme, whereas, though the addition of Na^+ indeed reduces the activity, increasing its concentration was shown to support the reaction (Table 9, p.65). This is in particular interesting since the power to induce cleavage decreases in the following order: $NH_4^+ > Li^+ > Na^+$ (K^+, Ru^+, and Cs^+ do not induce cleavage of the DNAzyme).[178] The general affinity of these cations toward DNA follows the same order.[177]. That means the effect of sodium ions on 17E DNAzyme's cleavage in combination with divalent cations profits from its lower affinity towards the catalyst. The diminishing effects on activity caused by monovalent cations can be explained by substitution of divalent cations at the catalytically important sites, but not on their reduced power to catalyze the cleavage in comparison to divalent cations. However, an elevated concentration of salt stabilizes the secondary and tertiary structure. This generally stabilizing effect of sodium ions (Table 9) was already observed in the initial cleavage experiment with Mg^{2+}, Pb^{2+}, and Zn^{2+} (Figure 26, Figure 26, p.64). Na^{+} reduced the cleavage activity in presence of Mg^{2+} at 20 °C and 37 °C and in presence of Pb^{2+} and Zn^{2+} at 37 °C but it restored and elevated the strongly reduced cleavage activity in presence of Pb^{2+} and Zn^{2+} at 37 °C. At 37 °C, the spatial arrangement of the DNAzyme is less stable than at 20 °C and the obviously necessary structure cannot be stabilized by the low concentrations of Zn^{2+} and Pb^{2+} alone. The fact that this observation was made for Pb^{2+}, indicates that also in the case of Pb^{2+}-dependent catalysis, a folded state of the DNAzyme (Figure 21) is critical for catalysis, which isn't proven up to now. Another feature of Pb^{2+} that is documented in the literature as a unique one, is that the reaction product in its presence is the 2'-or 3'-phosphate instead of the 2',3'-cyclophosphate. It is not clear if the hydrolysis to the phosphate happens by the DNAzyme catalysis or is driven by the basicity of the metal hydrate. In the present work, hydrolysis of the cyclophosphate was observed in Mg^{2+}-catalyzed reactions. The hydrolysis was stronger at 100 mM $MgCl_2$ than at 10 mM $MgCl_2$ (Figure 27). At 10 mM Mg^{2+} the duration of the folded state of the DNAzyme is longer, but the cleaved and unfolded state are more stable with 50 mM Mg^{2+}.[180] The dissociation constant for Mg^{2+} as a cofactor is $K_D = 0.7$ mM.[178] That means, at 50 mM as well as at 10 mM, the DNAzyme should be saturated with the divalent cation. If excess of cations, stabilizes the cleaved and unfolded state electrostatically, the increase in k_{obs} that was observed in this work isn't caused by stabilizing the transition state, but by impeding the reverse reaction. This effect was enhanced by the formation of the phosphate, which makes the cleavage reaction irreversible. At concentrations above 125 mM $MgCl_2$, k_{obs} was reduced again, which could be reasoned by too strong stabilization of the unfolded state. Taken together, these results indicate non-enzymatic hydrolysis of the cyclophosphate that is promoted by a longer duration of the unfolded state (the folded state wasn't observed until now in presence of lead ions).

The metalloenzymes of the 8-17 family, on the one hand, represent a really potent and robust cleavage system and on the other its mechanism and the driving forces of cleavage are diverse and depending on each other. This may be the reason why members of the 8-17 were isolated in so many *in vitro* selection experiments and therefore it appeared particularly suitable as the catalytically active part in the present combination strategy for *in vitro* selection.

4.5.2 Rational Design and *In Vitro* Selection

Several oligo-based inhibitors and re-activators were rationally designed and its functionality was evaluated experimentally. The inhibition by an inhibitor oligo mostly complementary to stem II was shown to be very effective (EI-C1, EI-C2). A strand complementary to the substrate binding domain (EI-S1) was not as effective, though the resulting duplex was designed to be more stable than that formed with the substrate strand. Due to considerations concerning the primer design for the *in vitro* selection and the inhibitory potential of the inhibitor (see 4.3 Rational Design and Validation of the 17E-DNAzyme Inhibitor), EI-C1 was chosen as the inhibitory part of the library for the *in vitro* selection. A cleavage experiment with this library showed that the rationally designed inactivation strategy was applicable to the library chosen for this *in vitro* selection (Figure 36, p.75). The following *in vitro* selection of the aptamer proceeded relatively trouble-free, in comparison to earlier attempts in this work. During the process and establishment of the *in vitro* selection, the crucial factors for the success of this process were identified. One important aspect was the digestion of the dsDNA with λ-exonuclease (see section 4.4.1 Step 1: *In Vitro* Selection of the Aptamer Part). This "tool" had to be optimized, although, it represents no step that is specific for an *in vitro* selection. Not surprisingly, the most important steps are the amplification steps between the rounds and the *in vitro* selection pressure. The immense effect of elevated selection pressure is illustrated by the enrichment of streptavidin binders after SR2F5 (Figure 46, p.84), by introducing additional washing steps [190] and adding non-specific binders (herring sperm DNA and BSA). The impact of the (low) template concentration in the amplification steps became blatantly obvious in this work. However, in fact, the exact quantity of "low" is not easily determined. In this work, the amount of template that was introduced in a PCR reaction was given as parts of the selection volume or the amount of substance calculated from 100 % yield in the previous PCR. In reports of *in vitro* selection, the amount of template for the amplification sometimes as well is given in parts of the *in vitro* selection volume. More often, it isn't named at all. It is that *in vitro* selection experiments aren't always well documented and reported.[50] However, this is in the nature of this experiment: in principle, it is a very easy experiment with few, repetitive steps. It may be assumed, that the interested reader of a scientific journal isn't interested in reading detailed discourse about e.g. how much microliters were introduced in each step and if accidently, after a given selection round, the washing step took 1 min longer. But, the success of an *in vitro* selection is a complex interaction of multiple factors, of which not all are always disclosed; and it may be suspected that some are hidden only in the knowledge of experienced experimenters. To come back to the question of the amount of template: in a protocol found in the literature for *in vitro* selection of DNA aptamers, it is recommended to reduce the amount of template from the fifth round on (starting with the complete material in 100 µl in 1000 µl total volume of PCR).[190] Another possibility is, to perform test PCRs with various volumes of *in vitro* selection template, as it was often practiced in the present work. Additionally, the application of emulsion PCR was proven as well suitable to overcome difficulties in amplification.

Finally, the selection of an aptamer for streptavidin succeeded. After SR2F6 an EMSA was performed. The assay was rather qualitatively, but the binding of the pool to streptavidin and the enrichment of binders during the *in vitro* selection was proven (Figure 46, p.84). However, it was a challenge to find suitable conditions for this experiment. A control assay with biotinylated primer and streptavidin showed strong retention of the primer by streptavidin on a standard TBE-PAGE (Figure 45, p. 83). This was not observed for the library. The affinity of the selected sequences towards streptavidin was maintained during the EMSA in a high salt buffer that resembled the selection buffer and that required frequent buffer exchange steps. Based on the results of this assay, it was decided to proceed with the *in vitro* selection of cleavage activity. The question arose, which pool should be used. Neither in the lane of SR2F5 nor in that of SR2F6 non-retained sequences were detected on the gel. There was the risk that the sequence variability wasn't high enough for the next step. It was considered that the reports in literature state that the most SELEX experiments need about ten rounds to proceed and even then, more than one sequence family is found (see discussion in section 4.4.2).[50, 144, 189, 190] Therefore, the pool SR2F6 was extended with the substrate part of the 17E DNAzyme. It was judged as a success that the first *in vitro* selection round of the second part (SRλ), yielded enough intact sequences (Figure 48, p.88). This step was critical. If the inhibitor strand of the construct hadn't been able to inactivate the DNAzyme's cleavage ability during the digestion of the antisense strand, the experiment would have been failed at this point. Later it was found that the cleavage reaction under the conditions of the digestion was an equilibrium reaction. The equilibrium was strongly on the site of the none-cleaved sequences. Additionally, these sequences were relatively stable under extremely harsh conditions (gel-elution). Nevertheless, the *in vitro* selection did not proceed. It was supposed that not enough specificity was given in the *in vitro* selection rounds in solution. Therefore, a covalent attachment of the sequences on magnetic beads was chosen. By PCR analysis, it was found that even extremely extensive washing steps did not quantitatively remove non-specifically bound sequences. Magnetic beads are commercially available with different surface characteristics. The beads that were used in the initial *in vitro* selection experiment with TNFα (see section 3.2), S1420S, NEB, have a carboxylate modified surface where streptavidin was bound to. They show low non-specific binding for proteins. In order to prevent stacking of TNFα, which was introduced and was only available at low concentration, to the beads, they were chosen for this experiment. Possibly, non-specific adhesion of the nucleic acid to these beads hampered this *in vitro* selection. For the approach discussed in the present section, beads were chosen, that were modified with a streptavidin monolayer and that are additionally blocked with BSA, to prevent non-specific binding of nucleic acids (Dynabeads M280). The beads that were chosen for the *in vitro* selection of cleavage activity are composed of benzene, ethenhyl- and homopolymer with encapsulated magnetite and modified with azide and no additional information about the surface is available.[1] It is assumed that the beads, i.e. their ability to prevent non-specific binding of sequences to be selected, have an impact on the success of an *in vitro* selection. However, a PCR based assay, to detect non-specific binding is very sensitive. During an *in vitro* selection process, the selection pressure is elevated from round to round and always, some less active sequences are going over in the next round. Finally, it is crucial that the active sequences accumulate. Therefore, non-specific binding to the immobilization surface for sure hampers the *in vitro* selection but isn't necessarily the prerequisite for its failure. Unfortunately, it was finally shown, that the *in vitro* selection of aptamers was too advanced. Using the Biacore, it was possible to investigate the pool more quantitatively than by the EMSA. The dissociation constant of the gel purified pool is $K_D = 38$ nM (see section 4.4.4 Biacore (SPR) Measurements of the Potential Streptavidin Aptamers, Table 16, p.99), which is comparable to the SA19 2'-fluoro-2'-deoxypyrimidine RNA aptamer ($K_D = 7$ nM), the RNA aptamer S1 ($K_D = 70$ nM), and a group of 2'fluoro modified DNA aptamers with dissociation constants in the nanomolar range.[163-166] The Sanger sequencing of the pool revealed an extremely low sequence variability that only was elevated by sequences with primer repetitions. These repetitions represent the longer PCR products that were often discussed in this work. The formation of these by-products was the worst with the first library used in this work, but it could be handled to some extent with primer design and PCR modifications. Interestingly, the observation and an analysis of this phenomenon was published in December 2014.[208] The authors reported the "by-product formation in repetitive PCR amplification of DNA libraries during SELEX". As countermeasures against this problem are mentioned the same actions as they were implemented in the present work (primer design, library design, PCR setting, ePCR). Even more interesting is that the authors analyzed two different types of the by-product formation. They proposed two mechanisms, which they named: "ladder type" and "non-ladder type". The "ladder type" by-product is prolonged with every cycle of PCR, the non-ladder type isn't. The "ladder type" evolves by annealing of the 3'-end of the full-length construct to the 5'-end of the randomized domain. This causes extension of the 3'end with the sequence of the reverse primer. This leads to the theoretical unrestricted addition of the primer sequence. If the first error-priming event doesn't happen directly before the reverse primer sequence a gap consisting of nucleotides copied from the randomized domain evolves, which prevents unrestricted repetitions of the primer sequence. This way, by-products of the "non-ladder type" evolve. In the present *in vitro* selection of aptamers for streptavidin by-products of the non-ladder type evolved (Figure 59, p.99).Nevertheless, aptamers for streptavidin were selected. As it was discussed in section 4.4.5 (Sanger-Sequencing of the Binding Pool, p.99–100), the selected sequences share a cramp-like stem-loop structure (Figure 62, p.100). Stem-loop structures were found for the already existing streptavidin aptamers as well.[163, 165, 166] No striking sequence similarity with the known aptamers was found, anyway, two of them are RNA aptamers. All have in common, that they exhibit a final stem-loop and an internal larger loop, like the aptamers found in this work. It would be very interesting to compare the aptamers more extensively. But it would be necessary to investigate the structure of the present work experimentally, to create a less hypothetical and theoretical basis. Moreover, for the present work, it is more relevant, that the attempt to separate the selection of the aptamer and the cleavage activity failed. The influence of the pre-defined stem-loop structure clearly was underestimated. The structurally constrained library obviously represented an exceptionally good starting point for the *in vitro* selection.[160-162] Most possibly, it is because the stem-loop structure is a conserved structural motif for streptavidin aptamers. The libraries that were applied for two RNA aptamers and the DNA aptamer weren't structurally constrained. Nevertheless, all *in vitro* selections resulted in similar structural motifs. The formation of this motif was enforced by the design of the present library. Even if the sequence variability would have been higher after selection round SR2F6, the formation of the active DNAzyme structure would have destroyed the stem-loop structure that evolved during the first selection rounds and which seems to be indispensable for the binding of streptavidin. In sum, with the results of the Sanger sequencing, it became clear that the second part of *in vitro* selection couldn't be successful. Additionally, the power of structural restriction and rigidity in intermolecular interaction is emphasized. A fact that is often discussed when comparing antibodies and aptamers (see section 2.1) and that played a role in the context of streptavidin-based immobilization in the very first part of this work (see section 2.3.1).

---

[1] Meanwhile a number of suppliers sell azide magnetic beads, but at this point of time, Jena Bioscience and Turbobeads® were the only suppliers for azide magnetic beads.

5 Summary and Outlook

The overarching goal of this work was to develop a biosensor based on functional nucleic acids. The biosensor should be modular, such that by exchange of the recognition unit, tailored biosensors could be created, allowing detecting a variety of analytes on demand. In the context of the cooperation with a company, initially, TNFα was chosen as an analyte. In a previous work, it was tried to build a modular aptazyme for TNFα that was based on four aptamers that were developed by SELEX. Here, these aptamers were investigated more closely by different methods (SPR, QCM). In the present work, it was proven beyond doubt that this attempt was not feasible. The aptamers were not able to bind the biologically active form of TNFα.

An even more interesting finding was that a common tool to immobilize molecules to investigate their interactions with a binding partner, namely the streptavidin-biotin interaction, can strongly influence the result of the assay and causing false-positive results.

Afterwards, it was decided to continue the work with a DNAzyme and modular approach was strictly refrained. It was tried to build aptazymes for TNFa or creatinine by *in vitro* selection, which failed. Most likely, the crucial factors were the ligands itself and the high demand on *in vitro* selection to select two functionalities (aptamer and catalytic activity) in parallel. This was the reason, to develop a new and a different method with streptavidin as a model analyte. The new strategy was to combine *in vitro* selection and rational design. The 17E-DNAzyme was chosen as catalytically active module. In preparation of the *in vitro* selection work, its properties were analyzed. An oligo-based inhibitor of the 17E-DNAzyme was rationally designed and its functionality was experimentally evaluated. Then, a library was designed which contained the 17E-DNAzyme, a randomized domain, and the inhibitor and its functionality was experimentally proven. The *in vitro* selection for the aptamer and the catalytic function were separated in two steps where the substrate strand was introduced in the second step.

The knowledge about *in vitro* selection procedures, which was gained in the first trials with TNFα and creatinine was applied and could be substantially broadened. The crucial factors for the success of this process were identified. Most important steps are the amplification steps between the rounds and the *in vitro* selection pressure. The template concentration in the PCR has to be very low; the selection pressure has to be high. However, in fact, the exact quantity of "low" and "high" is difficult to determine exactly, it has to be individually evaluated for every amplification step, and this makes *in vitro* selection a method that requires a lot of experimental skills, optimization procedures, and experience.

An EMSA was established and performed to qualitatively prove the affinity of the library for streptavidin in the first step of the *in vitro* selection method. For the second step, the *in vitro* selection of the catalytic function, considerable effort was done, but the *in vitro* selection did not succeed. Using the Biacore, the dissociation constant of the pool, which was applied in the second step of *in vitro* selection, was determined to be $K_D = 38$ nM. This is very low, and by sequencing the pool it was found that the sequence variability was too low. The sequences share a cramp-like stem-loop structure, which hold the DNAzyme in an inactive conformation.

This work presents valuable results for the development of biosensors based on nucleic acids, applying *in vitro* selection and rational design. Aptamers for streptavidin were selected. The library, which was used for this *in vitro* selection was structurally constrained. This obviously, represented an exceptionally good starting point for the *in vitro* selection.

Slight variations of the strategy, i.e. to include the substrate strand of the DNAzyme in the first step and/or introduce the inhibitor strand not until the second step, very likely could lead to success. However, for streptavidin as a model system, another strategy becomes obvious: One could exploit the presumed cramped stem-loop structure to loosen the inhibitor strand in presence of streptavidin. Therefore the library has to be designed with two variable domains. One domain would be located in between the DNAzyme and the inhibitor strand, the other downstream of the inhibitor strand.

Finally, a lot of information about the development of *in vitro* selection systems was gained. Important work was done on establishing a click chemistry-based immobilization strategy. This work is going to fundamentally facilitate a new *in vitro* selection approach based on this immobilization strategy.

6 Materials and Methods

6.1 Buffers and Solutions

All solutions and compounds were molecular biology grade. Solutions and buffers containing inorganic salts (p.a.), alkali or mineral acids were filtered with a 0.45 µm filter. Demineralized water was filtered with a 0.2 µm filter before use.

10xPCR buffer	200 mM Tris-HCl, pH 8.3, 500 mM KCl, 15 mM $MgCl_2$
acrylamide gel solution	ROTH
BA, binding buffer	20 mM HEPES (pH 7.5), 1 M NaCl, 1 mM EDTA, 0.05% Tween 20
Denaturing gel loading buffer	98 vol% formamide, 2 vol% 0.5 M EDTA
denaturing gel loading buffer	98 V% formamide, 2 V% EDTA
EA, equilibration buffer	20 mM HEPES (pH 7.5), 0.05% Tween 20
EB elution buffer	40 mM Tris-HCl, pH 8.0, 10 mM EDTA, 3.5 M urea
EDTA for the preparation of buffers and solutions	0.5 M, pH 8
gel elution buffer DNA	20 mM Tris-HCl, pH 8.2–8.5, 0.25 M NaOAc, 1 mM EDTA
gel elution buffer RNA	0.5 M NaOAc, pH 5.5
gel loading buffer	10 mM Tris-HCl, 60 % glycerol, 60 mM EDTA
HEPES-buffer	HEPES, pH adjustment with NaOH
PBS	137 mM NaCl, 2.7 mM KCl, 12 mM phosphate, pH 7.4
phenol : chloroform : isoamyl alcohol 25 : 24 : 1	Roti®-Phenol/Chloroform/Isoamyl alcohol, ROTH
SB, selection buffer	20 mM Tris-HCl (pH 7.6), 100 mM NaCl, 5 mM KCl, 1 mM $CaCl_2$, and 2 mM $MgCl_2$, 0.02% Tween 20
stop mix	7 M urea, 50 mM EDTA
TAE Agarose buffer	40 mM Tris acetate, 1 mM EDTA, pH 8.0
TBE PAGE buffer	0.1 M Tris-HCl, 83 mM boric acid, 1 mM EDTA, pH 8.0
TE	20 mM Tris-HCl, 0.1 mM EDTA, pH 8.1
WA, washing buffer	20 mM HEPES (pH 7.5), 0.5 M NaCl, 1 mM EDTA, 0.05% Tween 20

6.2 Proteins and Reagents, Kits and Accessory

Agar Kobe I	AppliChem
agarose	high resolution, Roth
Ampicillin	AppliChem
ATP	10 mM, Thermo Fisher Scientific
ATTO680 NHS-ester	ATTO-TEC GmbH
azide magnetic beads	Jena Bioscience

BSA	acetylated, Roboklon
DNA-Spin Plasmid Purification Kit	iNtRON
dNTPs	10 mM, Thermo Fisher Scientific
dsDNA ladder	Thermo Fisher Scientific
E. coli TG1	Genotyp: *supE thi-1* Δ(*lac-proAB*) Δ(mcrB-hsdSM)5 (r_K^- m_K) [F’ traD36 proABlacqZΔM15]
ELISA kit (hTNFα, hIL-6)	Peprotech
emulsion PCR kit	Roboklon
glycogen	Thermo Fisher Scientific, 20 mg/ml
herring sperm DNA	Thermo Fisher Scientific
LB-Agar plates (Amp)	1% (w/v) tryptone, 0,5% (w/v) yeast extract, 1% (w/v) NaCl, 1,5% Agar Kobe I, 100 µg/ml ampicillin
LB-Medium	1% (w/v) tryptone, 0,5% (w/v) yeast extract, 1% (w/v) NaCl
low melting point agarose	Thermo Fisher Scientific
QiaQuick Gel extraction Kit	QUIAGEN
quartz crystals (gold-coated and streptavidin-coated)	Biolin scientific
Sensor Chip SA (for Biacore)	GE Lifescience
small DNA purification kit	Roboklon
spermidine	Thermo Fisher Scientific
Streptavidin	NEB
streptavidin magnetic beads SMB	S1420S, NEB or Dynabeads M280 SA, Invitrogen
TNFα	human, recombinant, lyophylised from Tris buffer; Peprotech
TOPO® TA Cloning®	Invitrogen
Tryptone	AppliChem
Tween 20	Applichem
X-Gal	AppliChem
X-Gal-Lösung	40 mg/ml X-Gal in DMF
Yeast extract	AppliChem

6.3 Enzymes

Taq DNA polymerase	if the concentration is indicated in units per volume:
	Thermo Fisher Scientifc or Roboklon
	if the concentration is indicated in volume per volume:
	prepared in the laboratory

Vent$_R$ DNA polymerase	New England Biolabs
Opti*Taq* DNA polymerase	Roboklon
Pfu/*Psp* DNA polymerase	GeneOn
Klenow Fragment 5’→3’ exo$^-$	Thermo Fisher Scientifc
agarase	Thermo Fisher Scientifc

λ-exonuclease	Roboklon or Thermo Scientific
T4-polynucleotide kinase (PNK)	Roboklon

6.4 Devices

Biacore T200	GE Healthcare
biological safety cabinet	Hera Safe, Thermo Scientific
centrifugation	centrifuge 5804 R, Eppendorf, Heraeus Multifuge X1R, Thermo Scientific; MIKRO 120 Microfuge, Hettich
gel analysis	Darkroom-CN-3000, Vilber Lourmat
gel electrophoresis	small gels: MIDGET 2050, Pharmacia, Power Supply PS 300-B, Hoefer, larger gel: self-made apparatus, plate sequencer: LICOR4200
HPLC	Äkta Purifier, Amersham Biosciences
mass spectrometry	microflex MALDI-TOF MS, Bruker Daltonics
Microplate Reader	PERKIN-ELMER
Oligo-Synthesis	Gene assembler Special, Pharmacia
pH-meter	Knick
quartz-crystal microbalance	Q-sense E4, Biolin Scientific
shaking incubator	MaxQ 8000, Thermo Scientific
thermoblocks	digital heatblock, VWR, ThermoMixer comfort, Eppendorf
Thermo-Cycler	T-3000, Biometra, Thermocycler Gradient, Eppendorf
UV/VIS spectroscopy	NanoDrop® ND-1000 spectrophotometer
water purification system	Barnstead Nanopure, Thermo Scientific
waterbath	WNB7-45, Memmert

6.5 Software

Analysis of gel images	Base ImageIR
Evaluation of HPLC data	Unicorn
Evaluation of mass spectra	flexAnaylsis Version 3.0
Evaluation software for Biacore	GE Healthcare
graphic software	ChemDraw Ultra 8.0 CorelDraw Graphics Suite X3
Oligo analyzing software	Oligo Anaylzer, www.idtdna.de RNA structure 4.5 Mfold web server for nucleic acid folding and hybridization prediction Nucleic Acids Res. 31 (13), 3406-15, (2003)
sequence analysis	GENEIOUS (Biomatters)
Q-sense software	Biolin Scientific
Software for calculations	MS Excel, Origin

6.6 Basic Methods

6.6.1 NanoDrop (UV/Vis-spectroscopy)

The concentration of nucleic acids was determined by using the NanoDrop ND-1000 UV/Vis-Spectrometer at 260 nm. The volume of the samples was always 1.5 µl. The blank measurement was done with the solution in which the nucleic acid was solved in. The concentration was calculated according to the Lambert-Beer-law. The extinction coefficients were calculated with the oligo analyzer tool at www.idtdna.com. For double stranded DNA, the value for single-stranded DNA was doubled and multiplicated with 0.66 because of the absorption-reducing effect of base stacking (Equation 7).

Equation 7

$$\varepsilon_{dsDNA} = \varepsilon_{ssDNA} \cdot 2 \cdot 0.66$$

To calculate the concentration of ATTO680 labelled nucleic acid corresponding to the data are given by the company (ATTO-TEC GMBH), a correction factor CF_{260} of 0.3 for the dye was used. The corrected adsorption was calculated as follows:

Equation 8

$$A_{labelled\ NA} = A_{260} - (A_{680} \cdot 0.3)$$

6.6.2 Ethanol Precipitation

Ethanol precipitation was carried out with 0.3 M NaOAc, pH 7 in the aqueous phase and 2.5 V% ethanol for dsDNA or 3 V% ethanol for ssDNA. After incubation at RT for 10 min, the solution was incubated at -18 °C between 30 min and O.N., depending on concentration. If very low concentrations of nucleic acids were present, e.g. after a selection round, 100 µg/ml glycogen were added to the aqueous phase. After centrifugation at 13.000 rpm for 20–30 min, the supernatant was removed and the pellet was washed with 70 % ice-cold ethanol. Subsequently, it was centrifuged again at 13.000 rpm for 5 min and after removing of the supernatant, it was dried in a vacuum centrifuge at 45 °C for 2 min. If the pellet was very large, for example, when precipitation was carried out in a 40 ml tube, the drying period was extended up to 20 min.

6.6.3 Butanol Precipitation

For butanol precipitation, the procedure was similar to the ethanol precipitation, but no salt was added and the alcohol was added in 20 fold excess of the volume.

6.6.4 Gel filtration/ Size Exclusion Chromatography

1.2 g Sephadex G25 were suspended in 10 ml water. For swelling, the suspension was incubated at 10 °C overnight or at RT for at least 2 h.

Recycled spin columns (cleaned CENTRI•Pure MINI Spin Columns Desalt Z-50; emp biotech) were filled with 1 ml of the suspension of the swollen Sephadex G25 (using a 1 ml pipette, carefully suspending the material) Then the column was placed into a wash tube and centrifuged at 1000 x g for 2 min. 400 µl water were added to the column and the former steps were repeated. Next, the column was placed into a collection tube and the sample (40-150 µl) was added to the center of the gel bed. The column was centrifuged at 1000 x g for 2 min, again. It was important, to maintain same column orientation in every centrifugation step.

Gravity columns were filled with 10 ml of swollen Sephadex G25 and DNA was eluted with water. 300–500 µl fractions were analyzed by UV-Vis spectroscopy (NanoDrop). The fractions containing nucleic acid were united and dried in a vacuum concentrator.

6.6.5 Purification on Silica Columns

PCRs for the Combination of *in vitro* selection and rational design were usually purified on spin columns. The PCR/DNA Purification Kit purchased from Roboklon was used. For purification of single-stranded DNA (e.g. λ-exonuclease digestion or DNA from *in vitro* selection rounds in Part 2 of *in vitro* selection) the Short DNA Clean-Up Kit was used. The nucleic acid was eluted with the supplied low salt buffer.

6.6.6 Native PAGE

For preparation of polyacrylamide (PAA) gels with a size of 60 x 80 x 1.5 mm or 60 x 80 x 0.75 mm, 200 µl of 10% APS solution and 20 µl TEMED were added to 20 ml of an acrylamide:bisacrylamide 19:1 solution with the desired concentration in TBE to initiate polymerisation. After 15–20 min the gel was poured into the vertical electrophoresis chamber that was filled with TBE running buffer. For gels with concentrations below 10 % a constant voltage of 100 V was applied, whereas for higher concentrations of gel, 120 V was applied. Immediately before loading the samples, the pockets were rinsed with buffer by the help of a syringe. Detection of nucleic acids was carried out by placing the gel on a fluorescing plate using UV light at 254 nm or at 365 nm after staining with ethidium bromide (0.5 µg/ml, incubation for 15 min; gels were rinsed with water before irradiation). The gels for the "Combination of *In Vitro* Selection and Rational Design" were thin gels (0.75 mm). Otherwise thicker gels (1.50 mm) were prepared.

6.6.7 Denaturing PAGE

For the small gels, the procedure was similar to the preparation of native PAA gels, but the acrylamide/bisacrylamide solution was prepared with 7 M urea. To purify the chemical synthesized RNA a larger gel with the dimensions 200x150x1.5 mm was used. The size of denaturing PAA gels for the LI-COR sequencer was 250x200x0.25 mm. For both, the volume of the PAA and APS solution was doubled, whereas the volume of TEMED as catalyst remained constant. Electrophoresis was employed in 1 x TBE buffer, for small gels at 120 V (pre-run 100 V, 20 min), for the larger gel at 350 V (pre-run 200 V, 30 min). For LI-COR gels a voltage of 1500 V was applied (pre-run 1500 V, 45 min) and 0.6 x TBE buffer was used. In this case, the detection of ATTO680 labeled nucleic acids was performed during the run by a laser at 700 nm.

6.6.8 Native Agarose Electrophoresis

Agarose gels were prepared by boiling the required amount of agarose in TAE buffer until the solution was clear. Then, the gel was cast on a 20 x 30 cm gel slide (thickness 0.5 mm). The running distance was 30 or 15 cm (two combs in the distance of 15 cm). In general 120 V were applied. Detection of nucleic acids was similar to PAGE. In some cases, ethidium bromide was added directly to the gel. This way, post-staining, in general, wasn't required.

6.6.9 Sample Preparation for Gel Electrophoresis

For native gels, samples were mixed with 1/6 of 6 x loading buffer (10 mM Tris-HCl, 60 % glycerol, 60 mM EDTA), the size marker (ladder) was mixed with 6 x loading dye (loading buffer plus 0.03 % bromophenol blue and xylene cyanol. Samples for denaturing gels were mixed 1:1 with denaturing gel loading buffer (98 V% formamide, 2 V% EDTA), heated at 90 °C for 2 min and immediately put on ice before sampling. Small and thin (0.75 mm) gels were loaded with maximum 10 µl, the thicker ones with maximum 20 µl. The pockets of the agarose gels held maximum 20 µl. LI-COR gels were loaded with 0.2–1.5 µl per sample.

6.6.10 Gel elution A

RNA or DNA was excised from the gel. The slice was cut in pieces and soaked in elution buffer. The buffer was exchanged twice, resulting in three elution steps: (1) 10 °C, shaking for 4 h, (2) 10 °C, shaking for 12 h, (3) 10 °C, shaking for 4 h. The united elution buffers were precipitated with ethanol.

6.6.11 Gel elution B

Elution of DNA was done in three to four steps. On single step included freezing (-18 °C, ≥ 10 min) of the gel pieces in elution buffer, thawing at 95 °C for 10 min and finally incubating at 45 °C ≥ 45 min. If the yield was too low for the downstream application, steps were repeated and elution time was prolonged (2–12 h). The DNA was recovered from the elution buffer by ethanol precipitation.

6.6.12 Phenol-Chloroform Extraction

For phenol-chloroform extraction of DNA, a TE-buffered (pH 8.1) DNA solution was used. For extraction of RNA a non-buffered, aqueous and therefore slightly acidic RNA solution was mixed with an equal volume of a mixture of phenol : chloroform : isoamyl alcohol 25 : 24 : 1 in a reaction tube of appropriate size. For DNA Roti®-Phenol/Chloroform/Isoamyl alcohol was applied. For RNA a mixture of the three solvents was saturated with water. The solution was mixed thoroughly and then centrifuged until the phases were separated. The aqueous phase, in general, was the upper one and was pipetted into a fresh tube. The extraction was repeated up to three times. The organic phases were then extracted a second time with TE or water. Finally, the united aqueous phases were washed with chloroform (equal volume) to remove residual phenol, by mixing, centrifuging and removing the aqueous phase by pipetting. Finally, the nucleic acid was precipitated with ethanol.

6.6.13 Reactions in Thermal Cycler: PCR and Other Enzymatic Reactions

For PCR reactions and enzymatic reactions with a volume below or equal to 120 µl, thermal cyclers with slots for 0.2 ml and 0.5 ml reaction tubes were used. The programs are described elsewhere. The lid temperature was set to 95 °C.

6.7 Synthesis of Aptamer Sequences

A1-, A2-, A3-, A4-RNAs were prepared by the phosphoramidite method on controlled pore glass (CPG) support. The 5’-end was modified either with biotin (biotin CED phosphoramidite) or with a thiol modification (DMT-hexane-diol phosphoramidite and 5' thiol modifier hexyl CE phosphoramidite). The RNA was cleaved from the support by treatment with a 1:1 mixture of 8 M ethanolic methylamine and 25% NH_3 at 65 °C for 40 min. After cooling down to room temperature, the supernatant was removed and the support was washed twice with water : ethanol 1 : 1. The supernatant and the washing solution were united and lyophilized. The 2'-*O*-TBDMS group was removed by treatment with triethylamine trihydrofluoride at 55 °C for 1.5 h. The deprotected RNA was concentrated by a butanol precipitation. All RNAs were purified by PAGE (6.6.7, 6.6.11). The trityl-moiety (a protecting group for thiol-modification) was removed directly before the RNA aptamers were immobilized in order to avoid oxidative dimerization of the thiols. Therefore, 5 nmol RNA was suspended in 50 µl PBS, pH 7.2, mixed with 7.5 µl 1 M $AgNO_3$, and incubated at room temperature for 30 min. Afterward, 10 µl of 1 M DTT was added and mixed thoroughly. Following 5 min incubation at room temperature, the suspension was centrifuged. The supernatant was removed by pipetting; the pellet was washed with 50 µl PBS, and again centrifuged. Finally, the resulting supernatants were combined.

6.8 QCM Experiments

For quartz crystal microbalance (QCM) experiments the Q-sense E4 device and Q-sense software (Biolin Scientific) were used. The gold coated (100 nm) quartz crystals were prepared for the immobilization of RNA by rinsing them with water and ethanol and drying with nitrogen. Then the crystal was cleaned with oxygen plasma and put into the measurement flow-cell of the Q-sense E4 device. The crystal was allowed to oscillate for 60 – 90 min in PBS buffer, PBS, containing 1 mM $MgCl_2$, 10 mM DTT, 0.05 % Tween 20 (same conditions as used in aptamer selection[104]) to reach a stable baseline. The flow was 150 µl min^{-1}, and the temperature was set to 20 °C. The TNFα protein and the thiolated RNA, which was applied in the nanomolar range, were applied PBS. After immobilization of the RNA, the quartz was blocked with mercaptoethanol. The association data was recorded during the flow of TNFα in PBS (0.574 µM, 10 µg ml^{-1} and 0.287 µM, 5 µg ml^{-1}). During the subsequent buffer rinse for 10 to 20 min, the dissociation data was recorded. Finally, the surface was regenerated with 2 M NaCl. The streptavidin coated quartz crystals were introduced in the measurements as they were supplied. The immobilization took place with a micromolar concentration of the biotinylated RNA.

6.8.1 QCM Data Evaluation

For the determination of dissociation constants, the rate constants of association (k_{ass}) and dissociation (k_{diss}) were calculated. As association data served the frequency shift beginning with the point of time of starting the analyte flow plus the delay time of frequency shifts after the sample injection. Similarly, the dissociation data was used beginning with the point of time of starting the buffer flow plus the delay time of frequency shifts after sample injection. The Equation 9 was fitted to the association data and k_{diss} was calculated. Then the Equation 10 was fitted to the dissociation data and k_{ass} was calculated (Equation 11). Finally, by dividing k_{diss} by k_{ass} the constant of dissociation K_D was calculated (Equation 12).

Equation 9

$$\Delta F = a \cdot exp^{k_{diss}\Delta t}$$

Equation 10

$$\Delta F = a(1 - exp^{-b\Delta t})$$

Equation 11

$$k_{ass} = \frac{b - k_{diss}}{c_{TNF\alpha}}$$

Equation 12

$$K_D = \frac{k_{diss}}{k_{ass}}$$

6.9 SPR Measurements of RNA Aptamers

Surface plasmon resonance (SPR) experiments were carried out with the Biacore T100 device. The 1 µM biotinylated RNA in PBS was applied to a streptavidin coated gold chip (Series S Sensor Chip SA, GE HEALTHCARE LIFE SCIENCES) with a flow rate of 10 µl min^{-1} until about 125 RU were reached. The protein TNFα was applied at various concentrations: 22.8 µM (397 µg ml^{-1}), 11.4 µM (198 µg ml^{-1}), 5.7 µM (99 µg ml^{-1}), 2.85 µM (50 µg ml^{-1}), 1.425 µM (25 µg ml^{-1}), 0.713 µM (12 µg ml^{-1}). As running buffer served PBS, containing 1 mM $MgCl_2$, 10 mM DTT, 0.05 % Tween 20 (same conditions as used in aptamer selection).[104] The flow rate was 20 µl min^{-1} and the temperature was set to 20 °C. The measurements with BSA for specificity control were carried out (1 µM and 5 µM or 69 µg ml^{-1} or 345 µg ml^{-1}). A solution of 2 M NaCl was used to regenerate the surface. Blank measurements with buffer only were also conducted. One of the four flow cells was always used as a reference cell.

6.9.1 SPR Data Evaluation

The determination of the dissociation constants was performed analogously to as described in QCM data evaluation.

6.10 ELISA of TNFalpha

TNFα concentration was adjusted to 1µg ml^{-1} in water. Three aliquots were prepared, one used directly for the ELISA assay, the other two aliquots were stored for a month at 4 °C and -20 °C respectively. The procedure was as described by the supplier of the kit. For the measurements, TNFα dilutions from 0-1000 pg ml^{-1} were prepared. As a specificity control, the cytokine hIL-6 (PEPROTECH) was applied. The color development was monitored at 405 nm with the microplate reader Victor^3 (PerkinElmer, Germany).

6.11 Extension Reaction of the Library (section 3.2.1)

The extension reaction was carried out in 50 µl aliquots of the reaction mixture composed of 10 mM Tris-HCl, pH 8.3, 1.5 mM $MgCl_2$, 50 mM KCl, 0.2 mM dNTPs, 0.1% glycerol, 0.5 µM of primer and template and 0.02 U $µl^{-1}$ *Taq* DNA polymerase. Initially, the mixture was heated to 95 °C for 1 min, then the primer annealing took place at 53 °C for 1 min and for the extension, the reaction was incubated at 72 °C for 5 min. The reaction was held at 4 °C until further use. The primers and the template were purchased from BIOMERS.

6.12 General Application of TNFα

The lyophilized (from Tris buffer) recombinant human TNFα was stored at 4 °C after delivery from PEPROTECH for not longer than one month according to the manufacturer information. Immediately before use, the protein was reconstituted in water and further transferred into Tris-HCl buffer (pH 7.5). The buffered protein solution was used for a maximum of five days. This protocol was applied if not otherwise mentioned.

6.13 Working with Magnetic Beads

Magnetic beads are delivered in suspension. The suspension was mixed by up- and down-pipetting immediately before use. The desired volume was transferred into a 1.5 ml reaction tube. A magnetic rack was used to retain the beads at the wall of the tube and to remove the supernatant. Depending on the solution, beads were removed from the suspension by the magnet after 30 to 60 s. Washing, elution or equilibration steps were performed by adding the desired solution and mixing with a Vortex mixer. For longer periods of time, like during selection rounds or binding processes, the beads were resuspended by mixing or up- and down-pipetting from time to time.

6.14 Binding of the Library to the Streptavidin Magnetic Beads (3.2.2)

Table 17. Protocol for the binding of biotin labeled DNA to streptavidin magnetic beads (preparation for an *in vitro* selection round).

1)	Washing 160 µl beads (640 µg) + 130 µl binding buffer BA
2)	Binding add 150-170 pmol DNA (8 pmol/µl in binding buffer BA) leave react at RT for 15 min
3)	Washing 2 times with 130 µl washing buffer WA
4)	Separation of strands wash 5 times with 130 µl 0.2 N NaOH
5)	Equilibration wash 3 times with 130 µl equilibration buffer EA

6.15 Process of the Initial *in Vitro* Selection Experiment (section 3.2.3)

In vitro selection was carried out with three independent pools of DNA. Initially, three extension reactions were carried out and independently bound to the beads (160 µl) immediately after ethanol precipitation. Then, two subsequent negative selection rounds were carried out. The reaction volume was 20 µl. The beads were incubated in buffer EA (pool 1), in buffer EA plus 1 mM $Pb(OAc)_2$, or in buffer EA plus 5 mM $MgCl_2$ at 37 °C (550 rpm) for 45 min and 2 h. The supernatants that contained the 3'-end of cleaved sequences, were discarded, and beads were washed three times with 130 µl buffer EA before starting a new round. Subsequently, the first *in vitro* selection round took place. Therefore, 10 µg ml^{-1} TNFα were added to the corresponding buffers. The pools were incubated at 37 °C (550 rpm) for 2.5 h. The supernatants were collected and beads were washed with 15 – 20 µl water. The united supernatants were precipitated with ethanol and directly introduced into PCR. This procedure was repeated for 5 subsequent selection rounds. The selection pressure was elevated by reducing temperature and time. The PCR reactions were done in 50 µl. In PCR 1 (Table 18, Table 19) the complete material precipitated from *in vitro* selection rounds and 0.2 µM primer PA1a and PA1b were introduced. Additional components were 10 mM Tris-HCl, pH 8.3, 1.5 mM $MgCl_2$, 50 mM KCl, 0.2 mM dNTPs, 0.1 % glycerol and 0.02 U μl^{-1} Taq DNA polymerase. The initial denaturing took place at 94 °C for 1 min. Then 30 cycles of strand separation (60 s, 94 °C), primer annealing (60 s, 54 °C) and extension (60 s, 74 °C) followed. The reaction was closed by 7 min final extension at 72 °C. The reaction was held at 4 °C until further use. It was precipitated with ethanol and subsequently introduced in PCR2 (Table 20, Table 21). The protocol was equal to that described above, but 0.5 µM primers were used (PA1a and PA2) and only 20 cycles were run.

6.15 Process of the Initial in Vitro Selection Experiment (section 3.2.3)

Table 18. PCR 1 reaction composition.

Component	$c_{Stocksol.}$	$c_{reaction}$
Tris-HCl, pH 8.3	100 mM	10 mM
$MgCl_2$	100 mM	1.5 mM
KCl	1000 mM	50 mM
dNTPs	25 mM	0.2 mM
glycerol	10 %	0.1 %
PA1a	10 µM	0.2 µM
PA1b	10 µM	0.2 µM
DNA Taq Pol.	5 U/µl	0.05 U/µl
DNA Matrix	?	?
Water		

Table 19. PCR 1 reaction conditions.

T [°C]	t [s]	cycles	step
94	60	1	initialization
94	10	30	strand separation
53	30		annealing
72	30		extension
72	420	1	final extension
8	∞	1	final hold

Lid temperature: 95 °C

Table 20. PCR 2 reaction composition.

Component	$c_{Stocksol.}$	$c_{reaction}$
Tris-HCl, pH 8.3	100 mM	10 mM
$MgCl_2$	100 mM	1.5 mM
KCl	1000 mM	50 mM
dNTPs	25 mM	0.2 mM
glycerol	10 %	0.1 %
PA1a	10 µM	0.5 µM
P2A	10 µM	0.5 µM
DNA Taq Pol.	5 U/µl	0.1 U/µl
DNA Matrix	?	?
Water		

Table 21. PCR 2 reaction conditions.

T [°C]	t [s]	cycles	step
94	60	1	initialization
94	60	20	strand separation
53	60		annealing
72	60		extension
72	420	1	final extension
8	∞	1	final hold

Lid temperature: 95 °C

6.16 Emulsion PCR

Every required component is delivered by the Micellula DNA Emulsion & Purification Kit supplied by ROBOKLON. The procedure was as described in the manufacturer's manual. The preparation was carried out in the cold-storage room at 4 °C. Briefly, three oil components were mixed and precooled to 4 °C (300 µl). Then the PCR water phase (50 µl) was added and the emulsion was prepared by vortexing at maximum speed at 4 °C for 5 min. This mixture was split in triplicates to fit in 250 µl reactions tubes suitable for the slots of the thermocycler. After finishing PCR, the emulsion was broken with butanol. 1000 µl are enough for one or maximum two ePCRs. Then, DNA was solved in high-salt buffer. After phase separation, the aqueous phase (and for higher yield also the interface) was applied on a silica column supplied by ROBOKLON. DNA was washed several times and finally eluted from the column with the supplied buffers. If more than one or two ePCRs were conducted in parallel, for the aqueous phase, a master mix was used. The oil components were always mixed separately for every single (triple) reaction.

6.17 Synthesis and Deprotection of the DNA-library

The DNA was prepared by the phosphoramidite method on controlled pore glass (CPG) support with the Oligo-Synthesizer (APPLIED BIOSYSTEMS). For every N in the sequence of the library, a mixture of A,G,C,T-phosphoramidites (CHEMGENES) was used. For this mixture, the same amounts (moles) of phosphoramidites were weighted and solved in 2.5 ml acetonitrile. Subsequently, these solutions were merged. The support was 2000 Å, 5'-DMT-deoxy cytidine (n-acetyl)-3'-Icaa CPG (CHEMGENES). The DNA was cleaved from the support and the base-labile protecting groups were removed by treatment with a 1:1 mixture of 40% aqueous methylamine and 32% NH_3 at 65 °C for 30 min. After cooling down to room temperature the supernatant was removed and the support washed twice with water : ethanol 1 : 1. The supernatant and the washing solution were united and reduced in a vacuum centrifuge. The deprotected DNA was purified and concentrated by a butanol precipitation. Finally, it was further purified by 8 % denaturing PAGE.

6.18 ATTO Labelling

The labeling reaction was carried out with 10 nmol of the substrate in 200 mM sodium carbonate buffer, pH 8, adding 100 µg ATTO680-NHS in DMF. The mixture was incubated at room temperature for 4 h. After ethanol precipitation, the labeled RNA was purified by IP-RP-HPLC (Nucleodur 100-5 C18 ec 250/4, column volume cv = 3.142 ml). Buffer A was 0.1 M TEAAc (triethylammonium acetate), 5 % acetonitrile, buffer B was 0.1 M TEAAc (triethylammonium acetate), 30 % acetonitrile. The labeled substrate strand eluted at 73 % buffer B (gradient: 0 – 85 % buffer B in 14 cv, 0.5 ml min^{-1}).

6.19 Cleavage Reactions with DNAzymes

The procedure of all experiments was always the same: 17E enzyme and 17E substrate (purchased from BIOMERS or BIOTEZ) were denaturated separately in a solution containing all other compounds (buffer, monovalent cations, divalent cations) at 90 °C for 2 min. If inhibiting oligos were added to the reaction, they were added to the enzyme's solution. The mixtures were equilibrated at the designated reaction temperature for 15 min. Then, the reaction was started by mixing the separately prepared enzyme and substrate solutions. Samples (1 µl) were taken at indicated time points and immediately, at indicated points of time, added to 19 µl denaturing gel loading buffer. Afterward, reactions were analyzed on 15 % denaturing PAGE by detection of the fluorophore ATTO680 (LI-COR sequencer). The ratio of the substrate and product bands was calculated using the software Gene ImagIR.

6.20 Alkaline Lysis of DNAzymes or Substrate Strands

For alkaline lysis of DNA strands with a single ribonucleotide, an aqueous solution of the hybrid oligo was incubated with the same volume of 2 M NaOH, for 36 min–2 h at 37 °C. Then, an equal volume of 1 M HCl was added. Depending on the downstream application, the nucleic acid was precipitated with ethanol or/and desalted by size-exclusion chromatography.

6.21 MALDI-TOF Analysis of Nucleic Acids

For mass analysis 2 µl (100 – 1000 pmol) nucleic acid were mixed with a tip of a spatula of cation exchange resin (Dowex-NH^{4+}) in a reaction tube. The resin was stored swollen in water, and 7 µl were taken with a truncated, therefore wider, pipette-tip. The water was taken away with a pipette and the nucleic acid solution was added. After 5–15 min incubation, 1 µl was pipette on a ground steel MALDI target plate. The droplet was mixed with 1,5 µl of the matrix-solution by pipetting directly on the plate.

The matrix was always prepared freshly. A saturated solution of trihydroxy acetophenone (THAP) in acetonitrile was prepared (60 mg THAP, 500 µl acetonitrile). This mixture was mixed with an equal volume of 11.4 mg/ml diammonium citrate in water. The matrix was mixed thoroughly for several minutes.

6.22 Klenow Reaction

The composition of the reaction is shown in Table 22. First, buffer, water, primers and template were mixed, denatured at 90 °C for 2 min and ongoing, incubated at 37 °C for 15 min. Then, dNTPs and Klenow fragment, exo$^-$ were added. The reaction took place for maximum 30 min at 37 °C. The reaction was stopped by ethanol precipitation.

Table 22. Composition of Klenow reaction. 10 x Klenow buffer (THERMO): 500 mM Tris-HCl (pH8.0), 50 mM $MgCl_2$, 10 mM DTT.

Component	C_{stock}	$c_{reaction}$
Klenow buffer	10 x	1 x
Primer *rev*	10 µM	2 µM
Primer *fw*	10 µM	2 µM
dNTPs	25 mM	0.5 mM
Klenow frg., exo$^-$	5 U/µl	0.04 U/µl

6.23 Cleavage Activity of the Library (4.4.1)

To test the cleavage activity, 100 nM DNAzyme were incubated in 50 mM Tris-HCl (pH 7.5) at 37 °C after an initial denaturation step at 90 °C for 2 min. Then, $MgCl_2$ was added to a final concentration of 10 mM. The reaction was done without or with 1 µM or 10 µM oligo effector.

6.24 Phosphorylation of PD1

A single 50 µl reaction contained 1.5 nmol PD1 and 40 units of T4-PNK. The solutions were incubated at 37 °C for 30 min. Subsequently, the enzyme was inactivated at 75 °C for 10 min. The reactions were ethanol precipitated. 10 of these reactions were purified together by IP-RP-HPLC (Nucleodur 100-5 C18 ec 250/4, column volume cv = 3.142 ml). Buffer A was 0.1 M TEAAc (triethylammonium acetate), 5 % acetonitrile, buffer B was

0.1 M TEAAc (triethylammonium acetate), 30 % acetonitrile. The labeled substrate strand eluted at 46 % buffer B (gradient: 0 – 50 % buffer B in 4 cv, 0.5 ml min^{-1}).

6.25 Lamda-Exonuclease Digestion

After purification of dsDNA on silica columns, the DNA concentration was in general about 1.5 µM in the elution buffer of the delivering company. This solution was directly introduced in λ-exonuclease digestion. The reaction tolerates 20 % deviation from the concentrations of DNA indicated in Table 23. The reaction took place for 60 min at 37 °C. The enzyme was inactivated at 80 °C for 10 min. The total reaction volume was sometimes reduced but never elevated.

Table 23. The composition of 120 µl λ-exonuclease digestion reaction.

Component	c_{stock}	$c_{reaction}$	V [µl]
λ-exonuclease buffer	10 x	1 x	12
dsDNA (antisense strand is 5'-phosphorylated)	1.5 µM	1.25 µM	100
λ-exonuclease	25 U/µl	0.5 U/µl	2.4
Water			5.6

The reaction was purified by gel filtration (6.6.4) or on silica columns (6.6.5).

6.26 Process of the *In Vitro* Selection Part 1 (4.4.1)

Table 24 shows the general procedure of a single *in vitro* step. Volumes and amount of the substance were adjusted as indicated for the specific experiments. The buffer for *in vitro* selection was: 20 mM Tris-HCl, pH 7.6, 100 mM NaCl, 5 mM KCl, 1 mM $CaCl_2$, 2 mM $MgCl_2$, 0.02 % Tween20; modified from Stoltenburg et al. [166] For elution of bound sequences that took place at 80 °C, the same buffer was adapted from the literature , except for the pH, which was adjusted to pH 8.0 at RT, because of the strong temperature dependence of the pH-value of Tris-buffers. The composition of the elution buffer was 40 mM Tris-HCl, pH 8.0, 10 mM EDTA, 3.5 M urea.

Before binding to the beads (Dynabeads M280 SA, INVITROGEN), the ssDNA was incubated at 90 °C for 5 min. Then it was incubated on ice for 5 min and subsequently, at the temperature, the selection takes place for 5 min. Not until then, the buffer components were added (pre-tempered).

Table 24. Protocol for a single *in vitro* selection step on streptavidin magnetic beads.

1)	**Washing (three times)** 40 µl beads (Dynabeads M280) + 100 µl Sel-buffer vortex and add magnet for 30–60 s; remove and discard supernatant
2)	***In vitro* selection** add about 200 pmol ssDNA in 1 x Sel-buffer plus 0,02% Tween 20, final volume: 100 µl vortex and leave react at X °C for Y min, agitation (400-500 rpm); add magnet for 30–60 s; remove supernatant, wash with SB
3)	**Elution of selected sequences** wash 2 times with 100 µl Elu-buffer, at 80 °C, 500 rpm for 7 min
4)	**Isolation of selected sequences** precipitate with 0,3 M NaOAc, pH 7, 100 µg ml^{-1} glycogen and 3 V% ethanol

6.27 General PCR Composition and Programs

Table 25. The general composition of ePCR.

Components	**Concentration**		
	stock	**reaction**	**unit**
Pol buffer (Roboklon or 10xPCR buffer) (1.5 mM $MgCl_2$)	10	1	x
BSA	0.25	0.025	mg/ml
dNTPs	2.5	0.2	mM
5'-Primer	100	0.5	µM
3'-Primer	100	0.5	µM
DNA Template		max. 0.05	µM
***Taq* DNA Pol. (Rosetta)**		0.5	µl/50 µl

For ePCR, first, the oil components are mixed and precooled to 4 °C. Then the water phase (

Table 25) is added and the emulsion is prepared by vortexing at 4 °C for 5 min (see 6.15)

Table 26. General ePCR program.

Temperature [°C]	Time [s]	No. of cycles	PCR step
92	120	1	Intitial denaturation
92	20	25	Denaturation
65	30		Annealing
72	20		Extension
72	120	1	Terminal Extension
4	∞	1	Hold

Table 27. General composition of oPCR.

Components	Concentration		
	stock	**reaction**	**unit**
10xPCR buffer	10	1	x
dNTPs	25	0.25	mM
5'-Primer	100	0.5	µM
3'-Primer	100	0.5	µM
DNA Template		max. 0.05	µM
***Taq* DNA Pol. (Rosetta)**		0.5	µl/50 µl

Table 28. General oPCR program.

Temperature [°C]	Time [s]	No. of cycles	PCR step
92	120	1	Intitial denaturation
92	20	15	Denaturation
65	30		Annealing
72	20		Extension
72	120	1	Terminal Extension
4	∞	1	Hold

In some cases, conditions varied from the general compositions and programs given above. If it is relevant, it is pointed out in the main text.

In most cases, PCR1 is precipitated. The concentration of template for PCR2 is then calculated from 100 % yield in PCR 1 that, for sure, is not reached. But this method guarantees a consequent and comparable calculation of experiments.

6.28 Electrophoretic Mobility Shift Assay (EMSA)

The buffer for the EMSA was the selection buffer with the half of the NaCl concentration and additional tris/borate (SB 0.5 x NaCl 0.5 x TB; 45 mM tris base, 45 mM borate, 50 mM NaCl, 2 mM $MgCl_2$, 5 mM KCl, 1 mM $CaCl_2$). The acrylamide : bisacrylamide ratio was chosen to be 29 : 1 instead of 19 : 1 as in general for PAGE. 5%. The samples were loaded with SB 0.5 x TB containing 5 % glycerol. 3.6 pmol DNA were denaturated at 90 °C for 4 min. Then the sample was adjusted to 8 µl to a final concentration of 1 x SB with or without 3.2 µg streptavidin. Subsequently, the samples were incubated at 23 °C for 10 min. Finally, 1.3 µl LB EMSA were added. The gels were run at a constant voltage of 80 V and the current was kept constant at 40 mA by regular buffer exchange. With a syringe, the buffer was sucked from the buffer reservoirs and fresh buffer was added. The first buffer exchange was done after 8 min, then every 2–4 min. The electrophoresis was run for 30 min. The EMSA was performed under a hood because of the considerable formation of chlorine gas.

6.29 NaOH Digestion after SRλ

5 µl 1 N NaOH was added to about 70 pmol (5 µl) DNA and incubated at 45 °C for 45 min. Subsequently, 5 µl 1 N HCl and water (to get 4 µM DNA) were added and the sample was analyzed by PAGE.

6.30 Anion exchange chromatography for Cleavage Assay

Anion exchange chromatography was performed on a Mono-Q column (cv 0.982 ml). The detection of ATTO680 took place at 700 nm and the excitation wavelength was 690 nm. The denaturing buffer system was 2 mM Tris-HCl, 6 M Urea, and 20% acetonitrile, pH 7.4. Sodium perchlorate served as eluent (buffer A: 10 mM, buffer B: 400 mM). The gradient was: 0% buffer B for 1 min, 20% buffer B in 4 min, 80% buffer B in 20 min. Samples (5 pmol ssDNA) were mixed with buffer A, denatured at 90 °C for 5 in and immediately chilled on ice before loading on the column.

6.31 Process of the *In Vitro* Selection on Beads Part 2 (4.4.3)

Table 29 shows the general procedure of a single *in vitro* step. Before binding on the beads, the ssDNA was incubated at 90 °C for 5 min. Then it was incubated on ice for 5 min. The selection pressure was applied by reduction of the reaction time and the amount of streptavidin. In the last selection rounds, 0.02 µg μl^{-1} of streptavidin was present. The temperature varied between 23 °C and 37 °C. Following step 4b (digestion with proteinase K) the DNA was diluted and introduced in PCR.

Table 29. Protocol for a single *in vitro* selection step on azide magnetic beads.

1)	**Binding of the pool to azide magnetic beads** 0.5–1.2 µM ssDNA in 20 µl 1 x SB + 5 µl beads incubate at 37 °C, 600 rpm, 60 min vortex and add magnet for 60 s; remove supernatant
2)	**Washing** · 2 x 50 µl 1 x SB · 1 x 50 µl 1 x SB, incubate at 37 °C, 600 rpm, 15 min · 2 x 50 µl 1 x SB · 2 x 50 µl 1 x SB/1 mg ml^{-1} BSA, 0.1 mg ml^{-1} h.s.-DNA, incubate at 37 °C, 600 rpm, 3 min · 1 x 50 µl 1 x SB/1 mg ml^{-1} BSA, 0.1 mg ml^{-1} h.s.-DNA, incubate at 37 °C, 600 rpm, 30 min · 2 x 50 µl 1 x SB/1 mg ml^{-1} BSA, 0.1 mg ml^{-1} h.s.-DNA, incubate at 37 °C, 600 rpm, 3 min · 1 x 50 µl 1 x SB After each washing step: vortex and add magnet for 60 s; remove supernatant
3)	***In vitro* selection** Add 20 µl X µg µl-1 streptavidin in 1 x SB (tempered) mix and leave react at Y °C for Z min (600 rpm) add magnet for 30–60 s; remove supernatant, wash with 20 µl SB, unite both supernatants
4a)	**Digestion with proteinase K** add 1 µl enzyme to the united supernatants of step3, incubate at 37 °C for 1–2 h; inactivation of the enzyme: 95 °C, 10 min
4b)	**alkaline cleavage of remaining sequences** add 20 µl NaOH and incubate at 37 °C for 15–30 min

6.32 SPR measurements of Streptavidin Aptamers

Surface plasmon resonance (SPR) experiments were carried out with a Biacore T100 device. The DNA of *in vitro* selection round 2F6 was applied to a streptavidin coated gold chip (Series S Sensor Chip SA, GE Healthcare Life Sciences) either directly after the enzymatic digestion or after gel elution. The digestion reaction was purified by silica columns (Small DNA Purification Kit, Roboklon). The measurements were performed with 0.029 µM, 0.044 µM, 0.1 µM, 0.289 µM, 0.5 µM, 1 µM, 2 µM, and 10 µM DNA of SR2F6 and the original library. In case of unpurified DNA, the extinction coefficient for pure DNA was used to calculate the molar concentration. That means the real concentration was lower. Running buffer was *in vitro* selection buffer SB without Tween 20 (20 mM Tris-HCl (pH 7.6), 100 mM NaCl, 5 mM KCl, 1 mM $CaCl_2$, and 2 mM $MgCl_2$). Additionally, the original library was applied to the streptavidin coated chip at 1 µM, 5 µM, 10 µM and 50 µM. Furthermore, a measurement with 1 µM double-stranded PCR product was performed that was purified by silica columns (PCR purification kit, ROBOKLON). Blank measurements with buffer only were also conducted. The flow was 10 µl min^{-1} and the temperature was set to 20 °C. Association data was collected for 300 s and dissociation data for 500 s during buffer flow. The bound sequences were eluted with 50 mM NaOH for 60 s and the surface was equilibrated with buffer SB for 120 s before starting a new measurement. One of the four flow cells was always used as a reference cell.

6.32.1 SPR Data Evaluation

The determination of the dissociation constants was performed analogously to QCM data evaluation as described in 6.8.1.

6.33 Cloning, Expression, and Sequencing

6.33.1 Overnight Culture

5 ml of autoclaved LB medium in a test tube were mixed with ampicillin (100 µg ml^{-1}). Then the media was inoculated with *E. coli* TG1 cells. The culture was incubated at 37 °C and 200 rpm overnight.

6.33.2 Preparation of Chemically-Competent E. coli TG1 Cells

The overnight culture of *E. coli* TG1 cells was used to inoculate 500 ml LB-medium. This culture was incubated at 37 °C and 220 rpm until the optical density reached $OD_{600} = 0,9$. Then, the culture was incubated on ice for 1 h and afterwards centrifuged at 4 °C and 2500 x g for 15 min. The pellet was suspended in 50 ml ice-cold TSS solution. The suspension was frozen in liquid nitrogen in aliquots and stored at -80 °C.

6.33.3 Transformation of Plasmid DNA in Chemically-Competent E. coli TG1 Cells

Chemically-competent *E. coli* TG1 cells were thawed on ice. 1-2 µl plasmid DNA (about 5 ng) were added to 50 µl of the cell suspension. The mixture was incubated on ice for 30 min. The heat shock was executed at 42 °C for 45 s. The cells were colled down on ice for 1 min and 500 µl pre-warmed LB medium was added. After the following incubation at 37 °C and 230 rpm for 1 h, the suspension was centrifuged at 5200 rpm for 1 min. 300 µl of the supernatant were removed. The cell pellet was resuspended in the remaining media and plated on agar (with ampicillin). The plates were incubated overnight at 37 °C.

6.33.4 TOPO-TA Cloning

To prepare the DNA for sequencing, it was amplificated by PCR and then subcloned with the help of the TOPO® TA Cloning® Kit. 4 µl of the PCR product were mixed with 1 µl of the salt solution (1.2 M NaCl, 0.06 M $MgCl_2$) and added to 1 µl of the pCRII TOPO® vector. After incubation at room temperature for 8 min, 2 µl of the cloning product were transformed in chemically-competent *E. coli* TG1 cells. The identification of clones that contained the desired insert took place by blue-white screening. The blue clones were cultivated overnight.

6.33.5 Isolation of the Plasmid-DNA

The overnight culture was centrifuged at 5000 rpm for 5 min and the DNA was isolated with the help of the DNA-spin Plasmid DNA Purification Kit following the supplier's manual.

6.33.6 Sequencing

The Sanger-sequencing was outsourced to the company GATC.

Table of Figures

Figure 1. The proportion of aptamers by their target that were selected for binding to different targets by SELEX from 1997 to 2013. 17
Figure 2. Mechanism of hydrolytic cleavage of a phosphodiester bond in RNA. 20
Figure 3. Schematic illustration of an aptazyme. 21
Figure 4. The individual parts of a modular, allosteric ribozyme. 22
Figure 5. Scheme of systems used for the measurement of the interaction of aptamers and TNFα. 23
Figure 6. Sensorgram of SPR experiments with TNFalpha. 24
Figure 7. The absolute value of the frequency shift due to binding of TNFα to biotin-labeled aptamer 4 25
Figure 8. Various plots of frequency changes and energy dissipation during binding events on quartz crystals. 27
Figure 9. Illustration of the *in vitro* selection process. 31
Figure 10. Scheme of the initial DNA library for the selection of a DNAzyme which responses to TNFα. 34
Figure 11. Scheme of the *in vitro* selection strategy for simultaneous selection of aptamer and catalysis. 35
Figure 12. Gel analysis of an extension reaction with the template N30 and PA2 40
Figure 13. PCR of 50 nt library with 2% and 10% DMSO and at different annealing temperatures. 43
Figure 14. ePCR with different concentrations of template DNA antisense library and BSA. 46
Figure 15. Adaption of the library's sequence. 47
Figure 16. Schematic illustration of the approach for the development of an aptazyme based on rational design and *in vitro selection*. 51
Figure 17. The composition of the original 8-17 and 10-23 catalytic motifs. 53
Figure 18. The canonical sequence of the 8-17 DNAzyme.[168] 54
Figure 19. Sequence and a proposed secondary structure of the 17E DNAzyme. 54
Figure 20. A possible mechanism for the catalysis of the 8-17 DNAzymes. 56
Figure 21. Folding states of the 8-17 DNAzyme 58
Figure 22. A model for the 8-17 DNAzyme-subtstrate complex 59
Figure 23. Minimal reaction-kinetic schemes of A) the small nucleolytic ribozymes and B) DNAzymes of the 8-17 type. 60
Figure 24. Minimal reaction-kinetic scheme of cis-cleaving small nucleolytic ribozymes and DNAzymes of the 8-17 type. 61

Figure 25. Kinetic scheme of the initial reaction of a nucleic acid enzyme multiple turnover cleavage. 62
Figure 26. Comparison of 17E cleavage product with different divalent cations under various conditions after 5 minutes. 64
Figure 27. 7 % denaturing LICOR PAGE of 17 E DNAzyme cleavage reactions with $MgCl_2$. 66
Figure 28. Initial DNAzyme-construct for switchable catalysis. 68
Figure 29. The principle (A) and the expected result (B) of the separation of strands by denaturing gel electrophoresis. 69
Figure 30. Separation of strands of unequal length by 10 % denat. PAGE. 70
Figure 31. Inhibitor sequences in proximity to their binding region at the 17E DNAzyme. 71
Figure 32. 17E cleavage product after 30 minutes with EI-C1, EI-C2 or EI-S1 71
Figure 33. 17E cleavage product after 60 minutes with inhibitors and activators. 72
Figure 34. The cleavage reaction of the 17E-DNAzyme in presence of various inhibitor-activator combinations and in presence of activator, only. 73
Figure 35. The sequence of the library for the first step in *in vitro* selection with a supporting regulatory unit. 74
Figure 36. Activity tests of the library. 75
Figure 37. Scheme of the *in vitro* selection procedure for the aptamer selection (step 1). 76
Figure 38. Analysis of the phosphorylation reaction. 77
Figure 39. Exemplary PAGE images of the optimization of λ-exonuclease digestion (product: 88 nt). 78
Figure 40. Chart of *in vitro* selection rounds starting with the second pool of ssDNA library. 79
Figure 41. PAGE (native) image of *oPCR1* 2C3, *oPCR2* 2C3 (product: 88 bp) and the corresponding λ-exonuclease digestion (product = 88 nt). 80
Figure 42. PAGE (native) images of all PCRs after SR 2C4 to 2C6 80
Figure 43. PAGE (denaturing) image of selected samples that were analyzed by native PAGE, yet (Figure 42). 81
Figure 44. PAGE images of *test PCRs* after SR2F6 (product: 88 bp). 82
Figure 45. Validation of the EMSA for analysis of binding of any pool to streptavidin by 5% native PAGE. 83
Figure 46. 5% PAA EMSA of different *in vitro* selection rounds. 84
Figure 47. Conversion of the pool of Part 1 into the pool for *in vitro* selection Part 2. 87
Figure 48. 5% native and denaturing (7 M urea) PAGE of dsDNA (112 bp) and SRλ (112 nt) 88

Figure 49. 5% PAA EMSA of different *in vitro* selection rounds. The gel was post-stained with EtBr. 89
Figure 50. The reaction of 5'-DIBAC-labeled DNA with azide-modified magnetic beads. 90
Figure 51. Overview of *in vitro* selection rounds in solution for the selection of cleavage activity..91
Figure 52. Chromatogram of the cleavage assays with SR4CS..93
Figure 53. Chromatogram of cleavage assay with SR4CS and the additives BSA and herring sperm DNA. Anion exchange chromatography (Mono-Q); flow: 1 ml/min; Gradient: 0% buffer B for 1 min, 20% buffer B in 4 min , 80% buffer B in 20 min.........93
Figure 54. 5% denat. LICOR-PAGE of the cleavage assay. 94
Figure 55. Scheme of the *in vitro* selection strategy for the *in vitro* selection of cleavage on azide magnetic beads. 95
Figure 56. Chart of *in vitro* selection rounds on azide magnetic beads starting with a pool of SR2F6. 96
Figure 57. 5% native PAGE of various samples of *in vitro* selection after SR3bLS (A) and SR7bLS (B)..97
Figure 58. The sensorgram of the SPR experiment with 0.29 µM SR2F6. 99
Figure 59. Sequences of the pool SR2F6. 99
Figure 60. Secondary structure prediction for the sequences of the pool SR2F6. 99
Figure 62. Common sequence and schematic presentation of the probable secondary structures of the streptavidin aptamers. 100
Figure 61. Secondary structure prediction. Shown are the structures with the minimum free energy for the sequences of Clone No. 53, n52_5 and Clone No. 42_4 without repetition-sequence and an alternative secondary structure of clone No. 5_4, 5_6, n4_1, n4_3..100

Table of Tables

Table 1. Protocol for the binding of biotin labeled DNA to streptavidin magnetic beads............ 37

Table 2. Scheme of selection procedure up to selection round 5.. 38

Table 3. Summary of parameters screened for optimization of PCR with DNA libraries. 42

Table 4. The trans-cleavage activity of 17E DNAzyme (sto) with different divalent cations at 100 µM.. 55

Table 5. Effect of 150 mM monovalent salt on the cleavage rate of the trans-cleaving 17E DNAzyme 57

Table 6. k_{obs}-values for different single turnover (sto) experiments with 17E DNAzymes from literature. 60

Table 7. Control of background cleavage without divalent cations.. 63

Table 8. k_{obs} of 17E DNAzyme single turnover cleavage reaction at 37 °C................................ 64

Table 9.k_{obs} of 17E DNAzyme multiple turnover cleavage reaction at 37 °C 65

Table 10. k_{obs} of 17E DNAzyme sto cleavage reaction and v_0 of 17E DNAzyme mto cleavage reaction at 37 °C... 66

Table 11. Molecular weights and mass-to-charge ratio of the 17 E substrate and its cleavage products... 67

Table 12. Summary of the *in vitro* selection pressure's parameters of the final consecutive selection rounds.. 82

Table 13. Summaray of *in vitro* selection rounds that let to SR2F6... 85

Table 14. Cleavage yields of ssDNA of SR0BN and SR4CS (Mono-Q)................................... 92

Table 15. Cleavage yields of ssDNA of SR0BN and SR4CS in LB denat./Stopmix (LICOR). .. 94

Table 16. Maximum resonance units (RUs) of different DNA samples at 10 µl min^{-1} flow for 300 s. 99

Table 17. Protocol for the binding of biotin labeled DNA to streptavidin magnetic beads (preparation for an *in vitro* selection round)... 119

Table 18. PCR 1 reaction composition. 120

Table 19. PCR 1 reaction conditions. 120

Table 20. PCR 2 reaction composition. 120

Table 21. PCR 2 reaction conditions. 121

Table 22. Composition of Klenow reaction.. 123

Table 23. The composition of 120 µl λ-exonuclease digestion reaction.................................. 124

Table 24. Protocol for a single *in vitro* selection step on streptavidin magnetic beads............. 125

Table 25. The general composition of ePCR... 125

Table 26. General ePCR program.. 126

Table 27. General composition of oPCR.. 126

Table 28. General oPCR program.. 126

Table 29. Protocol for a single *in vitro* selection step on azide magnetic beads.........................128

References

1. Jijakli, K., et al., *The in vitro selection world.* Methods, 2016. **106**: p. 3-13.
2. Cech, T.R., A.J. Zaug, and P.J. Grabowski, *In vitro splicing of the ribosomal RNA precursor of tetrahymena: Involvement of a guanosine nucleotide in the excision of the intervening sequence.* Cell, 1981. **27**(3): p. 487-496.
3. Guerrier-Takada, C., et al., *The RNA moiety of ribonuclease P is the catalytic subunit of the enzyme.* Cell, 1983. **35**(3): p. 849-857.
4. Fire, A., et al., *Potent and specific genetic interference by double-stranded RNA in Caenorhabditis elegans.* Nature, 1998. **391**(6669): p. 806-811.
5. Sashital, D.G. and S.E. Butcher, *Flipping Off the Riboswitch: RNA Structures That Control Gene Expression.* ACS Chem Biol, 2006. **1**(6): p. 341-345.
6. Prody, G.A., et al., *Autolytic processing of dimeric plant virus satellite RNA.* Science, 1986. **231**(4745): p. 1577-80.
7. Rich, A., et al., *The molecular structure of polyadenylic acid.* J Mol Biol, 1961. **3**(1): p. 71-IN19.
8. Hoogsteen, K., *Hydrogen Bonding between Purines and Pyrimidines A2 - PULLMAN, BERNARD*, in *Molecular Associations in Biology*. 1968, Academic Press. p. 21-38.
9. Crick, F.H.C., *Codon—anticodon pairing: The wobble hypothesis.* J Mol Biol, 1966. **19**(2): p. 548-555.
10. Silverman, S.K., *Rube Goldberg goes (ribo)nuclear? Molecular switches and sensors made from RNA.* RNA, 2003. **9**(4): p. 377-383.
11. Yuce, M., N. Ullah, and H. Budak, *Trends in Aptamer Selection Methods and Applications.* Analyst, 2015. **140**(16): p. 5379-99.
12. Mann, D., et al., *In vitro selection of DNA aptamers binding ethanolamine.* Biochem Biophys Res Commun, 2005. **338**(4): p. 1928-34.
13. Bruno, J.G., et al., *Development of DNA aptamers for cytochemical detection of acetylcholine.* In Vitro Cell Dev Biol Anim, 2008. **44**(3-4): p. 63-72.
14. Bock, L.C., et al., *Selection of single-stranded DNA molecules that bind and inhibit human thrombin.* Nature, 1992. **355**(6360): p. 564-6.

15. Tang, Z., et al., *Selection of aptamers for molecular recognition and characterization of cancer cells.* Anal Chem, 2007. **79**(13): p. 4900-7.
16. Cao, X., et al., *Combining use of a panel of ssDNA aptamers in the detection of Staphylococcus aureus.* Nucleic Acids Res, 2009. **37**(14): p. 4621-8.
17. Tram, K., et al., *Translating Bacterial Detection by DNAzymes into a Litmus Test.* Angew Chem Int Edit, 2014. **53**(47): p. 12799-12802.
18. Stojanovic, M.N. and D.W. Landry, *Aptamer-Based Colorimetric Probe for Cocaine.* J Am Chem Soc, 2002. **124**(33): p. 9678-9679.
19. Aguirre, S., et al., *A Sensitive DNA Enzyme-Based Fluorescent Assay for Bacterial Detection.* Biomolecules, 2013. **3**(3): p. 563-577.
20. Ali, M.M., et al., *Fluorogenic DNAzyme Probes as Bacterial Indicators.* Angew Chem Int Edit, 2011. **50**(16): p. 3751-3754.
21. Xia, X., X. Piao, and D. Bong, *Bifacial Peptide Nucleic Acid as an Allosteric Switch for Aptamer and Ribozyme Function.* J Am Chem Soc, 2014. **136**(20): p. 7265-7268.
22. Kellenberger, C.A., et al., *RNA-Based Fluorescent Biosensors for Live Cell Imaging of Second Messenger Cyclic di-AMP.* J Am Chem Soc, 2015. **137**(20): p. 6432-6435.
23. Liu, L.-h., X.-h. Zhou, and H.-c. Shi, *Portable optical aptasensor for rapid detection of mycotoxin with a reversible ligand-grafted biosensing surface.* Biosens Bioelectron, 2015. **72**(0): p. 300-305.
24. Diba, F.S., S. Kim, and H.J. Lee, *Amperometric bioaffinity sensing platform for avian influenza virus proteins with aptamer modified gold nanoparticles on carbon chips.* Biosens Bioelectron, 2015. **72**(0): p. 355-361.
25. Baker, B.R., et al., *An electronic, aptamer-based small-molecule sensor for the rapid, label-free detection of cocaine in adulterated samples and biological fluids.* J Am Chem Soc, 2006. **128**(10): p. 3138-9.
26. Cruz-Aguado, J.A. and G. Penner, *Determination of Ochratoxin A with a DNA Aptamer.* J Agr Food Chem, 2008. **56**(22): p. 10456-10461.
27. Peeters, M., et al., *Label-free Protein Detection Based on the Heat-Transfer Method—A Case Study with the Peanut Allergen*

Ara h 1 and Aptamer-Based Synthetic Receptors. ACS Appl Mat Interf, 2015. **7**(19): p. 10316-10323.

28. Kim, M., et al., *Arsenic Removal from Vietnamese Groundwater Using the Arsenic-Binding DNA Aptamer.* Environ Sci Technol, 2009. **43**(24): p. 9335-9340.
29. Piganeau, N., et al., *An Allosteric Ribozyme Regulated by Doxycyline.* Angew Chem Int Edit, 2000. **39**(23): p. 4369-4373.
30. Liao, W. and X.T. Cui, *Reagentless aptamer based impedance biosensor for monitoring a neuro-inflammatory cytokine PDGF.* Biosens Bioelectron, 2007. **23**(2): p. 218-224.
31. Tuleuova, N., et al., *Development of an aptamer beacon for detection of interferon-gamma.* Anal Chem, 2010. **82**(5): p. 1851-7.
32. Katilius, E., Z. Katiliene, and N.W. Woodbury, *Signaling aptamers created using fluorescent nucleotide analogues.* Anal Chem, 2006. **78**(18): p. 6484-9.
33. Yamamoto, R., T. Baba, and P.K. Kumar, *Molecular beacon aptamer fluoresces in the presence of Tat protein of HIV-1.* Genes Cells, 2000. **5**(5): p. 389-96.
34. Ho, H.A. and M. Leclerc, *Optical sensors based on hybrid aptamer/conjugated polymer complexes.* J Am Chem Soc, 2004. **126**(5): p. 1384-7.
35. Wei, H., et al., *Simple and sensitive aptamer-based colorimetric sensing of protein using unmodified gold nanoparticle probes.* Chem Commun (Camb), 2007(36): p. 3735-7.
36. Maehashi, K., et al., *Label-free protein biosensor based on aptamer-modified carbon nanotube field-effect transistors.* Anal Chem, 2007. **79**(2): p. 782-7.
37. Xiao, Y., et al., *Label-free electronic detection of thrombin in blood serum by using an aptamer-based sensor.* Angew Chem Int Ed Engl, 2005. **44**(34): p. 5456-9.
38. Ocaña, C., M. Pacios, and M. del Valle, *A Reusable Impedimetric Aptasensor for Detection of Thrombin Employing a Graphite-Epoxy Composite Electrode.* Sensors, 2012. **12**(3): p. 3037-3048.
39. Tombelli, S., et al., *Aptamer-based biosensors for the detection of HIV-1 Tat protein.* Bioelectrochemistry, 2005. **67**(2): p. 135-41.
40. Schlensog, M.D., et al., *A Love-wave biosensor using nucleic acids as ligands.* Sensor Actuator B Chem, 2004. **101**(3): p. 308-315.

41. Fredriksson, S., et al., *Protein detection using proximity-dependent DNA ligation assays.* Nat Biotechnol, 2002. **20**(5): p. 473-7.
42. Xiang, Y., et al., *Ultrasensitive Label-Free Aptamer-Based Electronic Detection.* Angewandte Chemie (International ed. in English), 2007. **46**(47): p. 9054-9056.
43. Teller, C., S. Shimron, and I. Willner, *Aptamer-DNAzyme hairpins for amplified biosensing.* Anal Chem, 2009. **81**(21): p. 9114-9.
44. Gold, L., et al., *Aptamer-based multiplexed proteomic technology for biomarker discovery.* PLoS One, 2010. **5**(12): p. e15004.
45. Malerich, P. and D. Elston, *Introduction to TNF/pathophysiology of TNF*, in *TNF-alpha Inhibitors*, J. Weinberg and R. Buchholz, Editors. 2006, Birkhäuser Basel. p. 1-8.
46. Russel, C.B.S., S.; Robson, K.M.; Kerkof, K.; Kivman, L.D.; Notari, K.H.; Rees, W.H.; Leshinsky, N.; Patterson, S.D., *Biomarker sample collection and handling in the clinical setting to support early-phase drug development*, in *Biomarker methods in drug discovery and development*, F. Wang, Editor. 2008, Humana Press: Totawa. p. 1-26.
47. Han, W.K., et al., *Urinary biomarkers in the early detection of acute kidney injury after cardiac surgery.* ChemMedChem, 2009. **4**(5): p. 873-82.
48. Ellington, A.D. and J.W. Szostak, *In vitro selection of RNA molecules that bind specific ligands.* Nature, 1990. **346**(6287): p. 818-22.
49. Tuerk, C. and L. Gold, *Systematic evolution of ligands by exponential enrichment: RNA ligands to bacteriophage T4 DNA polymerase.* Science, 1990. **249**(4968): p. 505-10.
50. McKeague, M., et al., *Analysis of In Vitro Aptamer Selection Parameters.* J Mol Evol, 2015: p. 1-12.
51. Gold, L., et al., *Diversity of Oligonucleotide Functions.* Annu Rev Biochem, 1995. **64**(1): p. 763-797.
52. Nomura, Y., et al., *Conformational plasticity of RNA for target recognition as revealed by the 2.15 Å crystal structure of a human IgG–aptamer complex.* Nucleic Acids Res, 2010. **38**(21): p. 7822-7829.
53. Burgstaller, P. and M. Famulok, *Structural characterization of a flavin-specific RNA aptamer by chemical probing.* Bioorg Med Chem Lett, 1996. **6**(10): p. 1157-1162.

54. Lee, J.-H., F. Jucker, and A. Pardi, *Imino proton exchange rates imply an induced-fit binding mechanism for the VEGF165-targeting aptamer, Macugen.* FEBS Lett, 2008. **582**(13): p. 1835-1839.
55. Tyagi, S. and F.R. Kramer, *Molecular beacons: probes that fluoresce upon hybridization.* Nat Biotechnol, 1996. **14**(3): p. 303-8.
56. Javaherian, S., et al., *Selection of aptamers for a protein target in cell lysate and their application to protein purification.* Nucleic Acids Res, 2009. **37**(8): p. e62.
57. Ruta, J., et al., *Covalently bonded DNA aptamer chiral stationary phase for the chromatographic resolution of adenosine.* Anal Bioanal Chem, 2008. **390**(4): p. 1051-7.
58. Gragoudas, E.S., et al., *Pegaptanib for Neovascular Age-Related Macular Degeneration.* New Engl J Med, 2004. **351**(27): p. 2805-2816.
59. McNamara, J.O., 2nd, et al., *Cell type-specific delivery of siRNAs with aptamer-siRNA chimeras.* Nat Biotechnol, 2006. **24**(8): p. 1005-15.
60. Dassie, J.P., et al., *Systemic administration of optimized aptamer-siRNA chimeras promotes regression of PSMA-expressing tumors.* Nat Biotechnol, 2009. **27**(9): p. 839-49.
61. Zhou, J., et al., *Selection, characterization and application of new RNA HIV gp 120 aptamers for facile delivery of Dicer substrate siRNAs into HIV infected cells.* Nucleic Acids Res, 2009. **37**(9): p. 3094-109.
62. Branson, B.M., *FDA approves OraQuick for use in saliva. On March 25, the FDA approved the first rapid test for HIV in oral fluids.* AIDS Clin Care, 2004. **16**(5): p. 39.
63. Ruigrok, V.J.B., et al., *Alternative affinity tools: more attractive than antibodies?* Biochem J, 2011. **436**(1): p. 1-13.
64. *Lucentis® (ranibizumab injection).* [cited 2017 12 March]; Available from: https://www.gene.com/media/product-information/lucentis
65. Hoogenboom, H.R., *Selecting and screening recombinant antibody libraries.* Nat Biotechnol, 2005. **23**(9): p. 1105-16.
66. Dickey, F.H., *The Preparation of Specific Adsorbents.* Proc Natl Acad Sci USA, 1949. **35**(5): p. 227-9.

67. Spivak, D.A., *Optimization, evaluation, and characterization of molecularly imprinted polymers.* Adv Drug Deliver Rev, 2005. **57**(12): p. 1779-1794.
68. Sidhu, S.S. and S. Koide, *Phage display for engineering and analyzing protein interaction interfaces.* Curr Opin Struct Biol, 2007. **17**(4): p. 481-7.
69. Koide, A., et al., *The fibronectin type III domain as a scaffold for novel binding proteins.* J Mol Biol, 1998. **284**(4): p. 1141-51.
70. Binz, H.K., et al., *High-affinity binders selected from designed ankyrin repeat protein libraries.* Nat Biotechnol, 2004. **22**(5): p. 575-82.
71. Vogel, M., et al., *Designed ankyrin repeat proteins as anti-idiotypic-binding molecules.* Ann N Y Acad Sci, 2007. **1109**: p. 9-18.
72. Drolet, D.W., L. Moon-McDermott, and T.S. Romig, *An enzyme-linked oligonucleotide assay.* Nat Biotechnol, 1996. **14**(8): p. 1021-5.
73. Storz, U., *IP Issues in the Therapeutic Antibody Industry*, in *Antibody Engineering*, R. Kontermann and S. Dübel, Editors. 2010, Springer Berlin Heidelberg. p. 517-581.
74. Missailidis, S. and A. Hardy, *Aptamers as inhibitors of target proteins.* Expert Opin Ther Pat, 2009. **19**(8): p. 1073-82.
75. Thiel, K., *Oligo oligarchy-the surprisingly small world of aptamers.* Nat Biotechnol, 2004. **22**(6): p. 649-51.
76. Li, Y. and R.R. Breaker, *Kinetics of RNA Degradation by Specific Base Catalysis of Transesterification Involving the 2‘-Hydroxyl Group.* J Am Chem Soc, 1999. **121**(23): p. 5364-5372.
77. delCardayre, S.B. and R.T. Raines, *Structural determinants of enzymatic processivity.* Biochemistry, 1994. **33**(20): p. 6031-7.
78. Soukup, G.A. and R.R. Breaker, *Relationship between internucleotide linkage geometry and the stability of RNA.* RNA, 1999. **5**(10): p. 1308-25.
79. Emilsson, G.M., et al., *Ribozyme speed limits.* RNA, 2003. **9**(8): p. 907-18.
80. Breaker, R.R., et al., *A common speed limit for RNA-cleaving ribozymes and deoxyribozymes.* RNA, 2003. **9**(8): p. 949-57.
81. Kath-Schorr, S., et al., *General Acid–Base Catalysis Mediated by Nucleobases in the Hairpin Ribozyme.* J Am Chem Soc, 2012. **134**(40): p. 16717-16724.

82. McCown, P.J., W.C. Winkler, and R.R. Breaker, *Mechanism and Distribution of glmS Ribozymes.* Methods Mol Biol, 2012. **848**: p. 113-129.
83. Torres, R.A. and T.C. Bruice, *The Mechanism of Phosphodiester Hydrolysis: Near In-line Attack Conformations in the Hammerhead Ribozyme.* J Am Chem Soc, 2000. **122**(5): p. 781-791.
84. Wilson, T.J., et al., *Nucleobase-mediated general acid-base catalysis in the Varkud satellite ribozyme.* Proc Natl Acad Sci U S A, 2010. **107**(26): p. 11751-6.
85. Wilson, T.J., et al., *The Novel Chemical Mechanism of the Twister Ribozyme.* J Am Chem Soc, 2016.
86. Wilson, T.J., A.C. McLeod, and D.M. Lilley, *A guanine nucleobase important for catalysis by the VS ribozyme.* Embo J, 2007. **26**(10): p. 2489-500.
87. Scott, E.C. and O.C. Uhlenbeck, *A re-investigation of the thio effect at the hammerhead cleavage site.* Nucleic Acids Res, 1999. **27**(2): p. 479-84.
88. Derrick, W.B., et al., *Hammerhead cleavage of the phosphorodithioate linkage.* Biochemistry, 2000. **39**(16): p. 4947-54.
89. Steitz, T.A. and J.A. Steitz, *A general two-metal-ion mechanism for catalytic RNA.* Proc Natl Acad Sci U S A, 1993. **90**(14): p. 6498-502.
90. Nakano, S., D.M. Chadalavada, and P.C. Bevilacqua, *General acid-base catalysis in the mechanism of a hepatitis delta virus ribozyme.* Science, 2000. **287**(5457): p. 1493-7.
91. Breaker, R.R. and G.F. Joyce, *A DNA enzyme that cleaves RNA.* Chem Biol, 1994. **1**(4): p. 223-9.
92. Li, J., et al., *In vitro selection and characterization of a highly efficient Zn(II)-dependent RNA-cleaving deoxyribozyme.* Nucleic Acids Res, 2000. **28**(2): p. 481-488.
93. Carmi, N., L.A. Shultz, and R.R. Breaker, *In vitro selection of self-cleaving DNAs.* Chem Biol. **3**(12): p. 1039-1046.
94. Gu, H., et al., *Small, highly active DNAs that hydrolyze DNA.* J Am Chem Soc, 2013. **135**(24): p. 9121-9.
95. Porta, H. and P.M. Lizardi, *An allosteric hammerhead ribozyme.* Biotechnology (N Y), 1995. **13**(2): p. 161-4.
96. Tang, J. and R.R. Breaker, *Rational design of allosteric ribozymes.* Chem Biol, 1997. **4**(6): p. 453-459.

97. Soukup, G.A. and R.R. Breaker, *Engineering precision RNA molecular switches.* Proc Natl Acad Sci USA, 1999. **96**(7): p. 3584-3589.
98. Araki, M., et al., *Allosteric regulation of a ribozyme activity through ligand-induced conformational change.* Nucleic Acids Res, 1998. **26**(14): p. 3379-3384.
99. Jose, A.M., G.A. Soukup, and R.R. Breaker, *Cooperative binding of effectors by an allosteric ribozyme.* Nucleic Acids Res, 2001. **29**(7): p. 1631-7.
100. Tang, J. and R.R. Breaker, *Mechanism for allosteric inhibition of an ATP-sensitive ribozyme.* Nucleic Acids Res, 1998. **26**(18): p. 4214-4221.
101. Soukup, G.A. and R.R. Breaker, *Engineering precision RNA molecular switches.* P Natl A Sci, 1999. **96**(7): p. 3584-3589.
102. Penchovsky, R. and R.R. Breaker, *Computational design and experimental validation of oligonucleotide-sensing allosteric ribozymes.* Nat Biotech, 2005. **23**(11): p. 1424-1433.
103. Hall, B., J.R. Hesselberth, and A.D. Ellington, *Computational selection of nucleic acid biosensors via a slip structure model.* Biosens Bioelectron, 2007. **22**(9–10): p. 1939-1947.
104. Yan, X., X. Gao, and Z. Zhang, *Isolation and characterization of 2'-amino-modified RNA aptamers for human TNFalpha.* Genomics Proteomics Bioinformatics, 2004. **2**(1): p. 32-42.
105. Nübel, C., *Development of a reporter ribozyme for the detection of TNFalpha*. 2011, Universität Greifswald: Greifswald.
106. Fedor, M.J. and O.C. Uhlenbeck, *Kinetics of intermolecular cleavage by hammerhead ribozymes.* Biochemistry, 1992. **31**(48): p. 12042-12054.
107. Nübel, C., et al., *Challenges and Opportunities in the Development of Aptamers for TNFalpha.* Appl. Biochem. Biotechnol., 2016. **179**(3): p. 398-414.
108. Aderka, D., et al., *Stabilization of the bioactivity of tumor necrosis factor by its soluble receptors.* J Exp Med, 1992. **175**(2): p. 323-9.
109. Corti, A., et al., *Oligomeric tumour necrosis factor alpha slowly converts into inactive forms at bioactive levels.* Biochem J, 1992. **284**(Pt 3): p. 905-910.
110. Alzani, R., et al., *Mechanism of suramin-induced deoligomerization of tumor necrosis factor alpha.* Biochemistry, 1995. **34**(19): p. 6344-50.

111. Marusic, J., et al., *Recognition of human tumor necrosis factor alpha (TNF-alpha) by therapeutic antibody fragment: energetics and structural features.* J Biol Chem, 2012. **287**(11): p. 8613-20.
112. Sano, T. and C.R. Cantor, *Cooperative biotin binding by streptavidin. Electrophoretic behavior and subunit association of streptavidin in the presence of 6 M urea.* J Biol Chem, 1990. **265**(6): p. 3369-73.
113. Hyre, D.E., et al., *Cooperative hydrogen bond interactions in the streptavidin-biotin system.* Protein Sci, 2006. **15**(3): p. 459-67.
114. Williams, D.H., et al., *Understanding Noncovalent Interactions: Ligand Binding Energy and Catalytic Efficiency from Ligand-Induced Reductions in Motion within Receptors and Enzymes.* Angew Chem Int Edit, 2004. **43**(48): p. 6596-6616.
115. Weber, P.C., et al., *Structural origins of high-affinity biotin binding to streptavidin.* Science, 1989. **243**(4887): p. 85-8.
116. Caruso, F., D.N. Furlong, and P. Kingshott, *Characterization of Ferritin Adsorption onto Gold.* J Colloid Interf Sci, 1997. **186**(1): p. 129-140.
117. Höök, F., et al., *A comparative study of protein adsorption on titanium oxide surfaces using in situ ellipsometry, optical waveguide lightmode spectroscopy, and quartz crystal microbalance/dissipation.* Colloid Surface B, 2002. **24**(2): p. 155-170.
118. Feiler, A.A., et al., *Adsorption and viscoelastic properties of fractionated mucin (BSM) and bovine serum albumin (BSA) studied with quartz crystal microbalance (QCM-D).* J Colloid Interf Sci, 2007. **315**(2): p. 475-481.
119. Hianik, T., I. Grman, and I. Karpisova, *The effect of DNA aptamer configuration on the sensitivity of detection thrombin at surface by acoustic method.* Chem Commun (Camb), 2009(41): p. 6303-5.
120. Uzawa, T., et al., *Expansion of the aptamer library from a "natural soup" to an "unnatural soup".* Chem Commun, 2013. **49**(18): p. 1786-1795.
121. Flynn-Charlebois, A., et al., *Deoxyribozymes with 2'-5' RNA ligase activity.* J Am Chem Soc, 2003. **125**(9): p. 2444-54.
122. Gu, H. and R.R. Breaker, *Production of single-stranded DNAs by self-cleavage of rolling-circle amplification products.* Biotechniques, 2013. **54**(6): p. 337-43.

123. Marimuthu, C., et al., *Single-stranded DNA (ssDNA) production in DNA aptamer generation.* Analyst, 2012. **137**(6): p. 1307-15.
124. Pagratis, N.C., *Rapid preparation of single stranded DNA from PCR products by streptavidin induced electrophoretic mobility shift.* Nucleic Acids Res, 1996. **24**(18): p. 3645-6.
125. Williams, K.P. and D.P. Bartel, *PCR product with strands of unequal length.* Nucleic Acids Res, 1995. **23**(20): p. 4220-1.
126. Cox, J.C., et al., *Automated selection of aptamers against protein targets translated in vitro: from gene to aptamer.* Nucleic Acids Res, 2002. **30**(20): p. e108.
127. Irvine, D., C. Tuerk, and L. Gold, *Selexion: Systematic evolution of ligands by exponential enrichment with integrated optimization by non-linear analysis.* J Mol Biol, 1991. **222**(3): p. 739-761.
128. Robertson, D.L. and G.F. Joyce, *Selection in vitro of an RNA enzyme that specifically cleaves single-stranded DNA.* Nature, 1990. **344**(6265): p. 467-8.
129. Lehman, N. and G.F. Joyce, *Evolution in vitro of an RNA enzyme with altered metal dependence.* Nature, 1993. **361**(6408): p. 182-5.
130. Berzal-Herranz, A., S. Joseph, and J.M. Burke, *In vitro selection of active hairpin ribozymes by sequential RNA-catalyzed cleavage and ligation reactions.* Genes Dev, 1992. **6**(1): p. 129-34.
131. Joseph, S., et al., *Substrate selection rules for the hairpin ribozyme determined by in vitro selection, mutation, and analysis of mismatched substrates.* Genes Dev, 1993. **7**(1): p. 130-8.
132. Berzal-Herranz, A., et al., *Essential nucleotide sequences and secondary structure elements of the hairpin ribozyme.* Embo J, 1993. **12**(6): p. 2567-73.
133. Illangasekare, M., et al., *Aminoacyl-RNA synthesis catalyzed by an RNA.* Science, 1995. **267**(5198): p. 643-7.
134. Xu, J., et al., *RNA aminoacylation mediated by sequential action of two ribozymes and a nonactivated amino acid.* Chembiochem, 2014. **15**(8): p. 1200-9.
135. Bartel, D.P. and J.W. Szostak, *Isolation of new ribozymes from a large pool of random sequences [see comment].* Science, 1993. **261**(5127): p. 1411-8.
136. Pan, T. and O.C. Uhlenbeck, *In vitro selection of RNAs that undergo autolytic cleavage with lead(2+).* Biochemistry, 1992. **31**(16): p. 3887-3895.

137. Seelig, B. and A. Jaschke, *A small catalytic RNA motif with Diels-Alderase activity.* Chem Biol, 1999. **6**(3): p. 167-76.
138. Tarasow, T.M., S.L. Tarasow, and B.E. Eaton, *RNA-catalysed carbon-carbon bond formation.* Nature, 1997. **389**(6646): p. 54-7.
139. Tsukiji, S., S.B. Pattnaik, and H. Suga, *An alcohol dehydrogenase ribozyme.* Nat Struct Mol Biol, 2003. **10**(9): p. 713-717.
140. Balke, D., et al., *Generation and selection of ribozyme variants with potential application in protein engineering and synthetic biology.* Appl Microbiol Biotechnol, 2014. **98**(8): p. 3389-3399.
141. Morimoto, J., et al., *Flexizymes: their evolutionary history and the origin of catalytic function.* Acc Chem Res, 2011. **44**(12): p. 1359-68.
142. Lehman, N., *Origin of life: Cold-hearted RNA heats up life.* Nat Chem, 2013. **5**(12): p. 987-9.
143. Silverman, S.K., *DNA as a Versatile Chemical Component for Catalysis, Encoding, and Stereocontrol.* Angew Chem Int Edit, 2010. **49**(40): p. 7180-7201.
144. Silverman, S.K., *Deoxyribozymes: Selection Design and Serendipity in the Development of DNA Catalysts†.* Acc Chem Res, 2009. **42**(10): p. 1521-1531.
145. Silverman, S.K., *In vitro selection, characterization, and application of deoxyribozymes that cleave RNA.* Nucleic Acids Res, 2005. **33**(19): p. 6151-6163.
146. McManus, S.A. and Y. Li, *The structural diversity of deoxyribozymes.* Molecules, 2010. **15**(9): p. 6269-84.
147. Schlosser, K. and Y. Li, *Biologically inspired synthetic enzymes made from DNA.* Chem Biol, 2009. **16**(3): p. 311-22.
148. Baum, D.A. and S.K. Silverman, *Deoxyribozymes: useful DNA catalysts in vitro and in vivo.* Cell Mol Life Sci, 2008. **65**(14): p. 2156-74.
149. Breaker, R.R. and G.F. Joyce, *A DNA enzyme with Mg2+-dependent RNA phosphoesterase activity.* Chem Biol, 1995. **2**(10): p. 655-660.
150. Korbie, D.J. and J.S. Mattick, *Touchdown PCR for increased specificity and sensitivity in PCR amplification.* Nat Protocols, 2008. **3**(9): p. 1452-1456.
151. He, M., et al., *Optimized centrifugation for rapid elution of DNA from agarose gels.* Genet Anal-Biomol E, 1992. **9**(1): p. 31-33.

152. Saha, B.K., S. Strelow, and D. Schlessinger, *Electrophoretic elution of nucleic acids from acrylamide and agarose gels.* J Biochem Biophys Methods, 1983. **7**(4): p. 277-84.
153. Sambrook, J. and D.W. Russell, *Isolation of DNA fragments from polyacrylamide gels by the crush and soak method.* CSH Protoc, 2006. **2006**(1).
154. Yang, R., J. Lis, and R. Wu, *Elution of DNA from agarose gels after electrophoresis.* Methods Enzymol, 1979. **68**: p. 176-82.
155. Lopez-Gomollon, S. and F.E. Nicolas, *Purification of DNA Oligos by denaturing polyacrylamide gel electrophoresis (PAGE).* Methods Enzymol, 2013. **529**: p. 65-83.
156. Orava, E.W., et al., *A short DNA aptamer that recognizes TNFalpha and blocks its activity in vitro.* ACS Chem Biol, 2013. **8**(1): p. 170-8.
157. Tindall, K.R. and T.A. Kunkel, *Fidelity of DNA synthesis by the Thermus aquaticus DNA polymerase.* Biochemistry, 1988. **27**(16): p. 6008-6013.
158. Eckert, K.A. and T.A. Kunkel, *DNA polymerase fidelity and the polymerase chain reaction.* Genome Res, 1991. **1**(1): p. 17-24.
159. Ling, L.L., et al., *Optimization of the polymerase chain reaction with regard to fidelity: modified T7, Taq, and vent DNA polymerases.* Genome Res, 1991. **1**(1): p. 63-69.
160. Davis, J.H. and J.W. Szostak, *Isolation of high-affinity GTP aptamers from partially structured RNA libraries.* P Natl A Sci, 2002. **99**(18): p. 11616-11621.
161. Hamm, J., *Characterisation of Antibody-Binding RNAs Selected from Structurally Constrained Libraries.* Nucleic Acids Res, 1996. **24**(12): p. 2220-2227.
162. Mayer, G., et al., *An RNA molecule that specifically inhibits G-protein-coupled receptor kinase 2 in vitro.* RNA, 2008. **14**(3): p. 524-534.
163. Srisawat, C. and D.R. Engelke, *Streptavidin aptamers: affinity tags for the study of RNAs and ribonucleoproteins.* RNA, 2001. **7**(4): p. 632-641.
164. Umekage, S. and Y. Kikuchi, *Production of circular form of streptavidin RNA aptamer in vitro.* Nucl Acid S, 2006. **50**(1): p. 323-324.
165. Tahiri-Alaoui, A., et al., *High affinity nucleic acid aptamers for streptavidin incorporated into bi-specific capture ligands.* Nucleic Acids Res, 2002. **30**(10): p. e45.

166. Stoltenburg, R., C. Reinemann, and B. Strehlitz, *FluMag-SELEX as an advantageous method for DNA aptamer selection.* Anal Bioanal Chem, 2005. **383**(1): p. 83-91.
167. Santoro, S.W. and G.F. Joyce, *A general purpose RNA-cleaving DNA enzyme.* Proc Natl Acad Sci U S A, 1997. **94**(9): p. 4262-6.
168. Peracchi, A., *Preferential activation of the 8-17 deoxyribozyme by Ca(2+) ions. Evidence for the identity of 8-17 with the catalytic domain of the Mg5 deoxyribozyme.* J Biol Chem, 2000. **275**(16): p. 11693-7.
169. Carrigan, M.A., et al., *Quantitative Analysis of a RNA-Cleaving DNA Catalyst Obtained via in Vitro Selection.* Biochemistry, 2004. **43**(36): p. 11446-11459.
170. Cruz, R.P., J.B. Withers, and Y. Li, *Dinucleotide junction cleavage versatility of 8-17 deoxyribozyme.* Chem Biol, 2004. **11**(1): p. 57-67.
171. Schlosser, K. and Y. Li, *Tracing Sequence Diversity Change of RNA-Cleaving Deoxyribozymes under Increasing Selection Pressure during in Vitro Selection.* Biochemistry, 2004. **43**(30): p. 9695-9707.
172. Schlosser, K., et al., *In vitro selection of small RNA-cleaving deoxyribozymes that cleave pyrimidine–pyrimidine junctions.* Nucleic Acids Res, 2008. **36**(14): p. 4768-4777.
173. Kasprowicz, A., et al., *In vitro selection of deoxyribozymes active with Cd2+ ions resulting in variants of DNAzyme 8-17.* Dalton T, 2015. **44**(17): p. 8138-8149.
174. Rong, W., et al., *8-17 DNAzyme modified with purine analogs in its catalytic core: the conservation of the five-membered moieties of purine residues.* Bioorg Med Chem Lett, 2012. **22**(13): p. 4238-41.
175. Brown, A.K., et al., *A lead-dependent DNAzyme with a two-step mechanism.* Biochemistry, 2003. **42**(23): p. 7152-61.
176. Li, J. and Y. Lu, *A Highly Sensitive and Selective Catalytic DNA Biosensor for Lead Ions.* J Am Chem Soc, 2000. **122**(42): p. 10466-10467.
177. Bleam, M.L., C.F. Anderson, and M.T. Record, *Relative binding affinities of monovalent cations for double-stranded DNA.* P Natl A Sci, 1980. **77**(6): p. 3085-3089.
178. Mazumdar, D., et al., *Activity, folding and Z-DNA formation of the 8-17 DNAzyme in the presence of monovalent ions.* J Am Chem Soc, 2009. **131**(15): p. 5506-15.

179. Kim, H.K., et al., *Metal-dependent global folding and activity of the 8-17 DNAzyme studied by fluorescence resonance energy transfer.* J Am Chem Soc, 2007. **129**(21): p. 6896-902.
180. Kim, H.K., et al., *Dissecting metal ion-dependent folding and catalysis of a single DNAzyme.* Nat Chem Biol, 2007. **3**(12): p. 763-8.
181. Liu, Y. and D. Sen, *Local rather than global folding enables the lead-dependent activity of the 8-17 deoxyribozyme: evidence from contact photo-crosslinking.* J Mol Biol, 2010. **395**(2): p. 234-41.
182. Lee, N.K., et al., *Folding of 8-17 deoxyribozyme studied by three-color alternating-laser excitation of single molecules.* J Am Chem Soc, 2007. **129**(50): p. 15526-34.
183. Kim, H.K., et al., *Probing metal binding in the 8-17 DNAzyme by TbIII luminescence spectroscopy.* Chemistry, 2008. **14**(28): p. 8696-703.
184. Liu, Y. and D. Sen, *A contact photo-cross-linking investigation of the active site of the 8-17 deoxyribozyme.* J Mol Biol, 2008. **381**(4): p. 845-59.
185. Sekhon, G.S. and D. Sen, *A Stereochemical Glimpse of the Active Site of the 8−17 Deoxyribozyme from Iodine-Mediated Cross-Links Formed with the Substrate's Scissile Site.* Biochemistry, 2010. **49**(42): p. 9072-9077.
186. Schlosser, K., et al., *Sequence-function relationships provide new insight into the cleavage site selectivity of the 8-17 RNA-cleaving deoxyribozyme.* Nucleic Acids Res, 2008. **36**(5): p. 1472-81.
187. Hegg, L.A. and M.J. Fedor, *Kinetics and Thermodynamics of Intermolecular Catalysis by Hairpin Ribozymes.* Biochemistry, 1995. **34**(48): p. 15813-15828.
188. Ferrari, D. and A. Peracchi, *A continuous kinetic assay for RNA-cleaving deoxyribozymes, exploiting ethidium bromide as an extrinsic fluorescent probe.* Nucleic Acids Res, 2002. **30**(20): p. e112.
189. Silverman, S.K. *Nucleic acid enzymes (ribozymes and deoxyribozymes): in vitro selection and application.* 2009. John Wiley & Sons, Inc.
190. Mayer, G. and T. Höver, *In Vitro Selection of ssDNA Aptamers Using Biotinylated Target Proteins*, in *Nucleic Acid and Peptide Aptamers*, G. Mayer, Editor. 2009, Humana Press. p. 19-32.

191. Kolb, H.C., M.G. Finn, and K.B. Sharpless, *Click Chemistry: Diverse Chemical Function from a Few Good Reactions.* Angew Chem Int Edit, 2001. **40**(11): p. 2004-2021.
192. Tornøe, C.W., C. Christensen, and M. Meldal, *Peptidotriazoles on Solid Phase: [1,2,3]-Triazoles by Regiospecific Copper(I)-Catalyzed 1,3-Dipolar Cycloadditions of Terminal Alkynes to Azides.* J Org Chem, 2002. **67**(9): p. 3057-3064.
193. Rostovtsev, V.V., et al., *A Stepwise Huisgen Cycloaddition Process: Copper(I)-Catalyzed Regioselective "Ligation" of Azides and Terminal Alkynes.* Angew Chem Int Edit, 2002. **41**(14): p. 2596-2599.
194. El-Sagheer, A.H. and T. Brown, *Click chemistry with DNA.* Chem Soc Rev, 2010. **39**(4): p. 1388-1405.
195. Gierlich, J., et al., *Click Chemistry as a Reliable Method for the High-Density Postsynthetic Functionalization of Alkyne-Modified DNA.* Org Lett, 2006. **8**(17): p. 3639-3642.
196. Agard, N.J., J.A. Prescher, and C.R. Bertozzi, *A Strain-Promoted [3 + 2] Azide−Alkyne Cycloaddition for Covalent Modification of Biomolecules in Living Systems.* J Am Chem Soc, 2004. **126**(46): p. 15046-15047.
197. Jewett, J.C. and C.R. Bertozzi, *Cu-free click cycloaddition reactions in chemical biology.* Chem Soc Rev, 2010. **39**(4): p. 1272-1279.
198. Rozkiewicz, D.I., et al., *Transfer Printing of DNA by "Click" Chemistry.* Chembiochem, 2007. **8**(16): p. 1997-2002.
199. Eeftens, J.M., et al., *Copper-free click chemistry for attachment of biomolecules in magnetic tweezers.* BMC Biophysics, 2015. **8**(1): p. 1-7.
200. Debets, M.F., et al., *Aza-dibenzocyclooctynes for fast and efficient enzyme PEGylation via copper-free (3+2) cycloaddition.* Chem Commun, 2010. **46**(1): p. 97-99.
201. Bharathi, M.V., M. Chhabra, and P. Paira, *Development of surface immobilized 3-azidocoumarin-based fluorogenic probe via strain promoted click chemistry.* Bioorg Med Chem Lett, 2015. **25**(24): p. 5737-5742.
202. Kuzmin, A., et al., *Surface Functionalization Using Catalyst-Free Azide−Alkyne Cycloaddition.* Bioconjugate Chem, 2010. **21**(11): p. 2076-2085.

203. Zuker, M., *Mfold web server for nucleic acid folding and hybridization prediction.* Nucleic Acids Res, 2003. **31**(13): p. 3406-15.
204. SantaLucia, J., Jr., *A unified view of polymer, dumbbell, and oligonucleotide DNA nearest-neighbor thermodynamics.* Proc Natl Acad Sci U S A, 1998. **95**(4): p. 1460-5.
205. N., P., *Prediction of nucleic acid hybridization: parameters and algorithms. PhD Dissertation.* Detroit, MI: Wayne State University, 2000.
206. Egli, M., *DNA-Cation Interactions.* Chem Biol. **9**(3): p. 277-286.
207. Williamson, J.R., M.K. Raghuraman, and T.R. Cech, *Monovalent cation-induced structure of telomeric DNA: The G-quartet model.* Cell, 1989. **59**(5): p. 871-880.
208. Tolle, F., et al., *By-Product Formation in Repetitive PCR Amplification of DNA Libraries during SELEX.* PLoS One, 2014. **9**(12): p. e114693.

Appendix

Sequences of the Oligonucleotides

Section 2

Aptamer A1	CGCAUCGUUUGCGUGGCGUGUCCGGGCGCC (RNA)
Aptamer A2	GUGAG UUAGCUCACGUGCCGUUUCGAAGGC (RNA)
Aptamer A3	GGAGUAUCUGAUGACAAUUCGGAGCUCC (RNA)
Aptamer A4	UACGGAUUAGGUUGUAGCUCAGACCAGUA (RNA)

Section 3

Primer PA2	Biotin-GGGACGAATTCTAATACGACTCA CTATrA
Antisense template	
Template N50 (TNFα)	GTGCCAAGCTTACCGTCACTA-N50-GAAGAGATGTCGCCATCTCTTCCTATAGTGAGTCGTATTAG
Template N30 (TNFα)	GTGCCAAGCTTACCGTCACTA-N30-GAAGAGATGTCGCCATCTCTTCCTATAGTGAGTCGTATTAG
Template N50 (creatinine)	GCGTTGATACGACTCACTATAGGAAGAGATGGCGACATCTC-N50-GTGAGTGTCAGATTGAGAC
PA1a	GTGCCAAGCTTACCGTCAC
PA1b	GGGACGAATTCTAATACGACTCACTATA GGAAGAGATGGCGACA TCT
PC1a	GTCTCAATCTGACACTCAC
PC1b	GCGTTGATGCGACTCACTATAGGAAGAGATGGCGACATC
PC2	Biotin-GCGTTGATACGACTCACTATrA

Section 4

17E enzyme part, trans	CATCTCTTCTCCGAGCCGGTCGAAATAGTGAGT
17E substrate part	ACTCACTATrAGGAAGAGATG NH_2-ACTCACTATrAGGAAGAGATG

	ATTO680-ACTCACTATrAGGAAGAGATG
5'-Klenow Primer	ATTO680-GGGACGAATTCTAATACGACTCACTATrA
3'-Klenow Primer	AAAAAAAAAAAAAAAAAAAA-triethyleneglycol phosphate-triethyleneglycol phosphate-GTGCCAAGCTTACCGCCGCG CCGGTCGAAATTTTTTTTTTACTCACTATTTCGACCGGCTCGGAGAAGAGATGTCGCCATCTCTTCCTATAGTGAG TCGTATTAG
EI-C1	TTTCGACCGGCGCGG
EI-C2	TCGACCGGCGCGG
EI-S1	ACTCACTATAAGAAGAGATG
EA-C1	CCGCGCCGGTCGAAA
EA-S1	CATCTCTTCTTATAGTGAGT
17E enzyme part, trans	CATCTCTTCTCCGAGCCGGTCGAAATAGTGAGT
17E substrate part	NH_2-ACTCACTATrAGGAAGAGATG ATTO680-ACTCACTATrAGGAAGAGATG
Library	CATCTCTTCTCCGAGCCGGTCGAAATAGTGAGT-N40-TTT CGACCGGCGCGG
PD1	CCGCGCCGGTCGAA
PD2	CATCTCTTCTCCGAGCCG GTC
antisense Klenow primer	CACTATTTCGACCGGCTCGGAGAAGAGATGTCGCCATCTCTTCCTATAGTGAGT
PD3	ACTCACTATrAGGAAGAGATGGCGACATC NH_2-ACTCACTATrAGGAAGAGATGGCGACATC DBCO- ACTCACTATrAGGAAAGAGATGGCGACAT

Zusammenfassung und Ausblick

Das übergeordnete Ziel dieser Arbeit war es, einen Biosensor basierend auf Nukleinsäuren zu entwickeln. Dieser Biosensor sollte modular aufgebaut sein, so dass die Erkennungseinheit ausgetauscht werden könnte. Dieses Design sollte ermöglichen, nach Bedarf maßgeschneiderte Biosensoren für verschiedene Analyten zu entwickeln. Im Rahmen einer Industriekooperation wurde zu Beginn TNFα als Analyt gewählt. In der dieser Arbeit vorangegangen Diplomarbeit wurden vier modulare Aptazyme mit TNFα-Aptameren als Erkennungseinheiten entwickelt und untersucht. Da nicht nachgewiesen werden konnte, dass diese Aptazyme auf ihren Analyten reagierten, wurden in der hier vorliegenden Arbeit die Bindungseigenschaften der Aptamere mittels SPR und QCM genauer untersucht. Es wurde zweifelsfrei gezeigt, dass die verwendeten Aptamere nicht in der Lage waren, die biologisch aktive Form von TNFα zu binden.

Im Zuge dieser Untersuchungen wurde die interessante Entdeckung gemacht, dass die Streptavidin-Biotin-Bindung, die ein weit verbreitetes Werkzeug zum Immobilisieren von Molekülen zur Untersuchung ihrer Wechselwirkung mit Bindungspartnern ist, die Ergebnisse dieser Untersuchungen beeinflussen und verfälschen kann.

Zur Entwicklung des Biosensors wurde im nächsten Schritt vom modularen Aufbau Abstand genommen. Außerdem wurde ein DNAzym anstelle eines Ribozyms als Basis des zu entwickelnden Aptazyms gewählt. Die Versuche mittels *in vitro* Selektion Aptazmye für TNFα oder Kreatinin zu entwickeln scheiterten. Es ist sehr wahrscheinlich, dass diese Analyten keine geeigneten Liganden für die *in vitro* Selektion darstellten. Vor allem ist aber davon auszugehen, dass die Anforderung, zwei Funktionalitäten in einem Schritt zu entwickeln, zu hohe Anforderungen an den *in vitro* Selektionsprozess gestellt hat. Aus diesem Grund wurde eine neue und andersartige Methode mit Streptavidin als Modellanalyt entwickelt, in der die *in vitro* Selektion und das rationale Design kombiniert angewandt wurden. Als katalytisch aktive Einheit wurde das 17E-DNAzym gewählt. Dessen Spalteigenschaften wurden in Vorbereitung auf die folgenden Arbeiten analysiert. Es wurde ein DNA-Oligo-Inhibitor für das DNAzyme rational designed und charakterisiert. Danach wurde die das 17E-DNAzym und den Inhibitor enthaltende Bibliothek designed und dessen Funktionalität experimentell nachgewiesen. Die *in vitro* Selektion des Aptazyms wurde in zwei Arbeitsschritte geteilt. Im zweiten Schritt, der auf die Selektion der Bindungseigenschaft folgte, wurde der 17E-Substratstrang in die Bibliothek eingeführt, um die katalytische Aktivität zu selektieren.

Im Verlauf dieser Arbeiten wurden die Kenntnisse über Selektionsprozesse, die in den ersten Versuchen mit TNFα und Kreatinin gewonnen wurden, erheblich ausgeweitet. Als entscheidende Faktoren des Prozesses wurden die Amplifikationsschritte und der Selektionsdruck identifiziert. Es ist notwendig, die Templatkonzentration in der PCR sehr gering zu halten, wobei die genaue Menge für jede Reaktion individuell zu definieren ist. Die *in vitro* Selektion ist eine Methode, die viel experimentelles Geschick, extensive Optimierungsarbeiten und vor allem Erfahrung bedarf.

Um den Erfolg des ersten *in vitro* Selektionsschritts der neu entwickelten Methode zu überprüfen, wurde ein EMSA etabliert, womit nachgewiesen werden konnte, dass Streptavidin-Binder selektiert wurden. Allerdings blieb der zweite Schritt, die Selektion der katalytischen Aktivität erfolglos. Biacore-Experimente ermöglichten die Dissoziationskonstante des Pools zu ermitteln, der für den zweiten Schritt der *in vitro* Selektion eingesetzt wurde. Das Ergebnis mit $K_D = 38$ nM belegt eine schon stark ausgeprägte Affinität der Bibliothek zu Streptavidin. Die Sequenzierung offenbarte eine sehr geringe Variabilität im verwendeten Pool. Alle identifizierten Sequenzen weisen eine klammerartige Sekundärstruktur auf, die das DNAzyme in seiner inaktiven Konformation einfriert.

In dieser Arbeit werden wichtige Ergebnisse für die Entwicklung von Biosensoren mittels *in vitro* Selektion und rationalem Design, die auf Nukleinsäuren basieren sollen, präsentiert. Es wurden Aptamere für Streptavidin selektiert, die klammerartig strukturiert sind und niedrige Dissoziationskonstanten aufweisen. Die Bibliothek, die für diesen Selektionsschritt eingesetzt wurde war strukturell eingeschränkt, was offensichtlich einen außergewöhnlich guten Ausgangspunkt für die *in vitro* Selektion darstellte.

Geringe Variationen in der Strategie, wie besipielsweise, das 17E-Substrat schon in der Bindungsselektion einzuführen, oder den Inhibitorstrang erst im zweiten Schritt zu verwenden, könnten die Erfogschancen, ein Aptazym für Streptavidin zu selektieren, erhöhen. Eine andere Möglichkeit wäre, die klammerartige Stammstruktur der Aptamere zu nutzen, um einen das DNAzym inhibierenden Inhibitorstrang in Anwesenheit von Streptavidin zu lösen. Dazu müsste die Bibliothek zwei variable Domänen enthalten; eine zwischen DNAzym und Inhibitorstrang und die zweite abwärts des Inhibitorstranges.

So wurden mit dieser Arbeit wertvolle Grundlagen zur Entwicklung von Aptazymen gelegt. Im zweiten *in vitro* Selektionsprozesschritt wurden außerdem wichtige Arbeiten zur Etablierung einer auf Click-Chemie basierenden Immobilisierung durchgeführt. Die Ergebnisse dieser Arbeit können für nachfolgende Arbeiten mit dieser Immobilisierungsstrategie verwendet werden.

Danksagung

Ich bedanke mich bei Frau Prof. Dr. Sabine Müller für die Möglichkeit, diese Arbeit anzufertigen. Das Projekt war eine große Herausforderung, die ich gerne und mit viel Freude angenommen habe. Ich habe gerne unter Frau Prof. Dr. Sabine Müllers Betreuung gearbeitet und bin ihr sehr dankbar für die offenen wissenschaftlichen Diskussionen, die Freiheiten in der Bearbeitung meines Themas und für ihre Unterstützung in allen Höhen und Tiefen während der Bearbeitungszeit.

Dr. Bettina Appel danke ich für klärende Diskussionen, ihren kritischen Blick auf meine Ergebnisse und ihre großzügige Hilfsbereitschaft.

Der Arbeitsgruppe von Prof. Dr. Sven Hammerschmidt, insbesondere Dr. Lothar Petruschka, möchte ich für die Möglichkeit, die Biacore-Experimente durchzuführen danken.

Ich bedanke mich auch bei Sony Europe Limited und dem Team aus Stuttgart. Im Rahmen der Zusammenarbeit in der ersten Phase dieser Arbeit, konnte ich die QCM-Messungen in Stuttgart durchführen.

Simone Turski möchte ich für die organisatorische Unterstützung im Labor danken, und dafür, dass sie auch auf kurzfristige Anfrage, oft noch den ein oder anderen Puffer für mich hergestellt hat.

Ece Gaffagorulari danke ich dafür, dass sie die Mühe auf sich genommen hat, meine Arbeit Korrektur zu lesen.

Mein herzlicher Dank gilt meinen Mitstreitern in der Arbeitsgruppe Darko Balke, Jennifer Frommer, Robert Hieronymus und Nico Rublack, die mir auch bei fachlichen Problemen immer mit gutem Rat zur Seite standen. Darko Balke und Kathleen Balke danke ich auch für die tatkräftige Unterstützung bei den Sequenzierungsarbeiten.

Fünf ereignisreiche Jahre sind mit der Bearbeitung dieses Projektes ins Land gegangen. Es war eine lehrreiche, wertvolle und schöne Zeit und ich bin allen Greifswalder Freunden, die mich in dieser Zeit begleitet, unterstützt und wenn nötig auch abgelenkt haben, unendlich dankbar. Meinen Eltern und meinen Geschwistern danke ich sehr für ihre Unterstützung und ihr Verständnis in diesen Jahren.

Fold-out: Figure 59 and Figure 60

Fold-out: Figure 62 and Figure 61

Lebenslauf

Claudia Nübel

geboren am 11. April 1984 in Soest

seit 07.2016

Wissenschaftlerin BioNTech RNA Pharmaceuticals GmbH

08.2011–06.2016

Universität Greifswald, Institut für Biochemie, Anfertigung einer Doktorarbeit

Thema der Doktorarbeit: *Development of biosensors for proteins based on functional nucleic acids*

Betreuer: Prof. Dr. Sabine Müller

10.2006–07.2011

Universität Greifswald, Diplom Biochemie

Thema der Diplomarbeit: *Development of a reporter ribozyme for the detection of TNF*α

10.2008–02.2009

Auslandsaufenthalt (Erasmus Stipendium), Universität Oviedo, Spanien

09.2003–06.2006

BASF AG, Ludwigshafen am Rhein, Ausbildung Chemielaborantin

1994–2003

Aldegrever-Gymnasium Soest, Abitur

Publikationen

Artikel

2016

S. Müller, B. Appel, D. Balke, R. Hieronymus, C. Nübel, **Thirty-five years of research into ribozymes and nucleic acid catalysis: where do we stand today?** *F1000Research* 2016, 5: F1000 Faculty Rev-1511.

C. Nübel, B. Appel, I. Hospach, M. Mai, N. Krasteva, G. Nelles, L. Petruschka, S. Müller. **Challenges and Opportunities in the Development of Aptamers for TNFα.** *Applied Biochemistry and Biotechnology* 2016, 179, 398-414.

2014

J. Xu, B. Appel, D. Balke, C. Wichert, S. Müller. **RNA aminoacylation mediated by sequential action of two ribozymes and a non-activated amino acid.** *ChemBioChem* 2014, 15, 1200-1209.

D. Balke,* C. Wichert,* B. Appel, S. Müller. **Generation and selection of ribozyme variants with potential application in protein engineering and synthetic biology**. *Appl. Microbiol. Biotechnol.* 2014, 98, 3389-3399.

2012

T. S. Arunachalam, C. Wichert, B. Appel, S. Müller. **Mixed oligonucleotides for random mutagenesis: best way of making them**. *Org. Biomol. Chem.* 2012, 10, 4641-4650.

Posterbeiträge

C. Wichert, H. Schmidt, S. Müller. **Development of protein sensors based on functional DNA**

2015: *Bioorthogonal Chemistry, Meeting of the Division of Biochemistry (GDCh) VI Nucleinsäurechemie-Treffen*

2014: *XXI Round table on Nucleosides, Nucleotides and Nucleic Acids*

C. Wichert, B. Appel, I. Hospach, M. Mai, N. Krasteva, G. Nelles, S. Müller. **Development of protein sensors based on nucleic acids**

2013: *V Nucleinsäurechemie-Treffen*

2012: *7th Meeting der GBM Study Group RNA Biochemistry*